UNIVERSITY OF
LIVERPOOL

Endoperoxides as Antimalarials and the Application of Singlet Oxygen to the Synthesis of Key Intermediates En Route to Synthetic 1,2,4-Trioxanes
and
Synthesis and Biological Activity of Minor Groove Binding-Artemisinin Conjugates

Thesis submitted in accordance with the requirements of the University of Liverpool for the degree of Doctor in Philosophy

by

Louise Josephine Ilse La Pensée

September 2009

Acknowledgements

Firstly I would like to thank my supervisor Professor Paul O'Neill for the opportunity to undertake this PhD and all his help, support and motivation throughout my work. I would also like to thank my co-supervisor Dr Nick Greeves, Dr Rick Cosstick and Dr Julie Fisher for their guidance and valuable input.

I would also like to show my appreciation for all the technical staff at the University of Liverpool for all their help, Dr Paul Leonard, Alan, Moya and Tony.

I am also very grateful to Sunil Sabbani, James Gaynor and Xiaofeng Wu for their help and expertise.

A massive thank you to all the members of the 4th floor past and present and a special mention to Chi, Zeyn, Bénè, Gibbo, Edite, Mike, Ally, Sarah, James, Tobo, Shane and Matt. I'm very lucky to have met such an amazing group of people. Thank you so much for all the wicked laughs/gossip/nights out/country retreats and of course all the support/shoulders/pieces of blue roll. A particular mention for my wing-man and lab-buddy Vicky who has helped me pick myself up and start again so many times, your focus when working and focus when partying is inspirational! I couldn't have done it without you!

I would like to say thank you to all the Bev massive and also to Carly who have given true encouragement and friendship out-side of chemistry.

I would also like to thank my Mum and Dad and Annie for their infinite wisdom, support and faith, you amaze me every day!!!!I love you very much! I'd also like to thank Tess who would make an excellent therapist!

Finally, a huge thank you to Paul for your love, patience and belief in me. I couldn't have got through the tough bits without you and the fun bits would never have been so much fun! Thank you so much for peeling me off the ceiling occasionally and reminding me there is life after!

Contents

Endoperoxides as Antimalarials and the Application of Singlet Oxygen to the Synthesis of Key Synthetic Intermediates en Route to Synthetic 1,2,4-Trioxanes and the Synthesis and Biological Activity of Minor Groove Binding-Artemisinin Conjugates

Artemisinin, is a naturally occurring sesquiterpene lactone with potent antimalarial activity imparted by a 1,2,4-trioxane pharmacophore. Artemisinin based combination therapies are currently considered the most effective treatment in advanced cases of malaria. Synthetic 1,2,4-trioxanes retain the pharmacophore of artemisinin and have demonstrated excellent antimalarial activity. Previous research has produced spirocyclic 1,2,4-trioxanes *via* dye-sensitised photooxygenation of allylic alcohols (ene reaction) to obtain β-hydroperoxy alcohols. The β-hydroperoxy alcohols then undergo condensation with a variety of cyclic ketones to generate the target 1,2,4-trioxane heterocycle.

We have developed a route to enantiomerically enriched 1,2,4-trioxanes *via* the diastereoselective ene reaction of enantiomers of chiral allylic alcohols. The use of phosphite ozonide adducts as a chemical source of singlet oxygen has also been explored as an alternative to traditional photochemical conditions.

Initially, we prepared a chiral *cis*-allylic alcohol (93% ee) *via* asymmetric transfer hydrogenation of a propargyl ketone. *threo*-selective photooxygenation to the β-hydroperoxy alcohol progressed in moderate yield (40-43% yield) and subsequent condensation with 2-adamantanone, provided opposing enantiomerically enriched, spirocyclic 1,2,4-trioxanes.

This was then adapted to a more facile route, whereby enantioenriched allylic alcohols were accessed *via* the enantioselective addition of dialkyl zinc reagents to an α,β-unsaturated aldehyde, catalysed by (+)- or (-)-exo-(morpholino)isoborneol (MIB). The resulting chiral disubstituted allylic alcohols (90-98% ee) were subjected to diastereoselective photooxygenation to give (*S*,*S*)- and (*R*,*R*)-*threo* β-hydroperoxy alcohols in excellent yields (86-100% yield). Peroxyacetalisation of the β-hydroperoxy alcohols with various cyclic ketones provided a series of optically active 1,2,4-trioxanes.

In addition to their well-known antimalarial activity, artemisinin and derivatives possess potent activity against cancer cells with DNA cleavage being implicated as a potential mode of cytotoxic action. Netropsin and distamycin are naturally occurring antibiotics, consisting of a chain of amide-linked *N*-methyl pyrrole units, demonstrating high affinity for the minor groove of DNA. Oligopyrrole derivatives of netropsin and distamycin have been exploited as DNA delivery agents, where coupling to cytotoxic moieties have provided hybrids with enhanced cytotoxic activity.

Herein, we have prepared novel artemisinin-oligopyrrole conjugates using amide coupling chemistry. Modification of artemisinin at the C-10 position provided a C-10 phenoxy carboxylic acid linker which underwent successful peptide coupling with a dipyrrole carboxamide chain to yield the desired conjugate. The chemistry was then extended to incorporate 3-carbon and 5-carbon spacers between artemisinin and the minor groove binding portion.

DNA binding studies of our conjugates with a synthetic dodecamer indicate a reduction in DNA binding affinity when compared to netropsin. However, work is ongoing to further evaluate the thermodynamic effect the conjugates have on double-strand DNA. The synthetic procedures developed in this project will pave the way for the synthesis of analogues with higher affinity for DNA than our current derivatives, defining the relationship between the binding affinity and cytotoxic properties of this novel class of DNA directed drug.

Publications

Sunil Sabbani, Louise La Pensée, Jill Davies, Erik Hedenström, Paul M. O'Neill, Diastereoselective Schenck Ene Reaction of Singlet Oxygen with Chiral Allylic Alcohols; Access to Enantiomerically Enriched 1,2,4-Trioxanes, *Tetrahedron*,**2009**, *65*, 8531-8537.

Michael Jones, Amy E. Mercer, Paul A. Stocks, Louise J. I.La Pensée, Rick Cosstick, Kevin Park, Miriam E. Kennedy, Ivo Piantanida, Stephen A. Ward, Jill Davies, Patrick G. Bray, Sarah L. Rawe, Jonathan Baird, Tafadzwa Charida, Omar Janneh, Paul M. O'Neill, Antitumour and antimalarial activity of artemisinin-acridine hybrids, *Bioorganic & Medicinal Chemistry Letters*, **2009**, *19*, 2033-2037.

Abbreviations

$AgClO_4$	silver perchlorate
Anal	analysis
approx.	approximately
aq.	aqueous
ATH	asymmetric transfer hydrogenation
AHA	anhydroartemisinin
$BF_3.Et_2O$	boron trifluoride etherate
Boc	*tert*-butoxycarbonyl
Boc_2O	di-*tert*-butyl dicarbonate
Bu	butyl
BzCl	benzoyl chloride
cat.	catalytic
CCR	carbon centred radical
CD	circular dichroism
$CDCl_3$	deuterated chloroform
$CHCl_3$	chloroform
CH_2Cl_2	dichloromethane
CI	chemical ionization
Cl_3CCOCl	trichloroacetyl chloride
CPI	cyclopropyl indole
d	doublet
DAIB	3-*exo*-(dimethylamino)isoborneol
DCE	1,2-dichloroethane
DHA	dihydroartemisinin
DMF	dimethyl formamide
DMSO	dimethyl sulphoxide
DPPA	diphenylphosphoryl azide
d.r.	diastereomeric ratio
EDC	*N*-ethyl-*N*'-(3-dimethylaminopropyl)carbodiimide
EDIPA	ethyl diisopropyl amine
ee	enantiomeric excess
eq.	molar equivalents
ES	electrospray ionization
EtO_2	diethyl ether
EtOAc	ethyl acetate
EtOH	ethanol
g	gram(s)
GC	gas chromatography
HBTU	*O*-(1*H*-benzotriazol-1-yl)-*N*,*N*,*N*',*N*'-tetramethyl uronium hexafluorophosphate
HNO_3	nitric acid
Hr	hour(s)
HOBt	1-hydroxybenzotriazole
HRMS	high resolution mass spectrometry
Hz	Hertz
i	iso
$LiAlH_4$	lithium aluminium hydride
m	multiplet
M	Molar
Me	methyl
MeCN	acetonitrile
MeOD	deuterated methanol
MeOH	methanol
MIB	3-*exo*-(morpholino)isoborneol

min	minute(s)
mL	millilitre(s)
µL	microlitre(s)
mmol	millimole(s)
µM	micromole(s)
mol	mole(s)
m.p.	melting point
MS	mass spectrometry
N	normal
$NaClO_2$	sodium chlorite
NaH_2PO_4	sodium dihydrogen phosphate
NaOOCH	sodium formate
NCI	National Cancer Institute, USA
NEt_3	triethylamine
Hexane	*n*-hexanes
nM	nanomolar
NMR	nuclear magnetic resonance
$^1O_2$	singlet oxygen
ORD	optical rotatory dispersion
P.	*Plasmodium*
PBD	benzodiazepine
$(PhO)_3PO_3$	triphenyl phosphite
POA	phosphite ozonide adduct
PPh_3	triphenyl phosphine
Pr	propyl
PtO_2	platinum (IV) oxide
Py	pyridine
q	quartet
quin	quintet
ROS	reactive oxygen species
r.t.	room temperature
s	singlet
SERCA	sarcoplasmic/endoplasmic reticulum Ca^{2+}-ATPase
$SOCl_2$	thionyl chloride
t	tertiary
t-BuOH	2-methylpropan-2-ol
tert	tertiary
TFA	trifluoroactetic acid
TfR	transferrin receptor
THF	tetrahydrofuran
t.l.c.	thin layer chromatography
T_m	thermal melting
TMSOTf	trimethylsilyl trifluoromethanesulfonate
TPP	tetraphenyl porphine
TsDPEN	*N*-(*p*-toluenesulfonyl)-1,2-diphenylethylenediamine
p-TsOH	tosic acid
WHO	World Health Organization
v	volume
w	weight
$ZnCl_2$	zinc chloride

1.0 Introduction - Endoperoxides as Antimalarials and the Application of Singlet Oxygen to the Synthesis of Key Synthetic Intermediates en Route to Synthetic 1,2,4-Trioxanes

1.1 Artemisinin and Malaria

Malaria is a disease responsible for millions of deaths every year and it is becoming an increasing problem as many parasite strains are developing resistance to established treatments such as the 4-aminoquinolines including chloroquine. Artemisinin, and its first generation derivatives, have emerged as a mainstay in the treatment of advanced cases of malaria. Their efficacy against chloroquine resistant malarial strains is attributed to an alternative mechanism of action, involving several different parasite targets.

1.1.1 The Discovery of Artemisinin

Artemisinin **1** is a natural product isolated from the plant *Artemisia annua*. Infusions of *Artemisia annua* were widely used as a remedy for fever in ancient China, being first recorded in *The Handbook for Emergency Treatments* by Ge Hang written 340AD.[1] In 1967, the Chinese government launched a program to find new malaria treatments including research into plants used traditionally in medicine. Artemisinin was successfully isolated and identified as the active component. The semi-synthetic derivatives sodium artesunate **2**, artemether **3** and arteether **4** have allowed for simple administration of the drug and have since been used clinically (Figure 1.2).

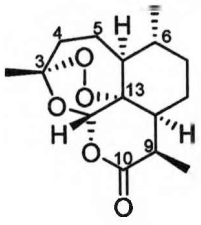

1

Figure 1.1 *Artemisinin*

1.1.2 Implications for the Clinical Administration of Artemisinin

The overall yield of artemisinin from the extraction process is poor being 0.01-0.80% of its dry weight and this has limited its commercialisation.[2] The poor solubility of artemisinin in oil and water has also previously posed a problem. The drug could be administered orally but this was impossible in advanced and comatose cases. The design and synthesis of first generation artemisinin derivatives sodium artesuneate[3] **2** (water soluble) and artemether **3**, arteether **4** (lipid soluble)[4] allow for parenteral and intrarectal routes.

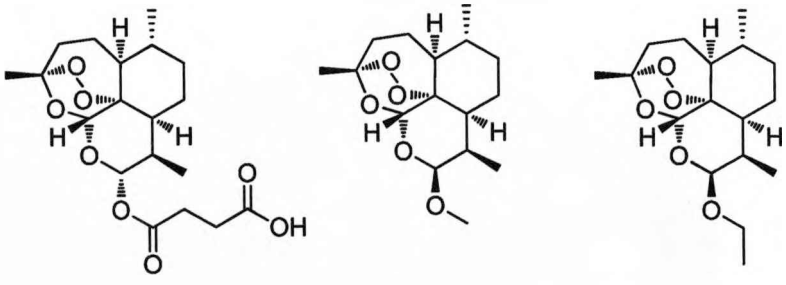

2 **3** **4**

Figure 1.2 *First generation artemisinin derivatives artesunate 2, artemether 3 and arteether 4.*

An important consideration in the utility of these compounds is their short half lives. The aforementioned ether derivatives are metabolised by cytochrome P450 mediated

dealkylation, to the clinically effective metabolite dihydroartemisinin (DHA). Likewise artesunate undergoes hydrolysis to DHA within 10 minutes of administering. DHA is metabolised by glucuronidation at the C-10 position and excretion.[5] As a result of this swift metabolism, artemisinin based treatments reduce parasite burden below detectable levels but without eliminating all the parasites.[6] This ultimately creates a risk of recrudescence: to circumvent these risks and maintain the high efficacy of artemisinin, the World Health Organisation (WHO) has advised administration of artemisinins in combination with other antimalarial agents (*e.g.* lumefantrine, amodiaquine, mefloquine, sulfadoxine-pyrimethamine).[7]

1.1.3 The Mechanism of Action of Artemisinin

1.1.3.1 The Malaria Parasite Life Cycle

After a person is initially bitten by the infected *Anopheles* mosquito vector, the parasites of genus *Plasmodium*, first accumulate in liver hepatocytes. They then invade the host erythrocytes, digesting host haemoglobin and replicating in an asexual manner. The erythrocyte will then burst releasing merozoites into the blood stream which infect more erythrocytes and continue replicating. A small proportion of merozoites will differentiate into male and female gametocytes which lie dormant in the host until taken up by the next mosquito to bite the infected person. The gametocytes will then reproduce sexually in the digestive tract of the mosquito to produce sporozoites which, residing in the mosquito saliva, wait for inoculation into the next host.

The mechanism by which artemisinin exerts its antimalarial activity has been the subject of extensive research and debate. The drug displays preferential accumulation

in parasite infected erythrocytes[8] and demonstrates a high efficacy against the erythrocytic stages of *Plasmodium* with activity against asexual stages and early gametocytes.[6] The endoperoxide bridge of artemisinin has been confirmed as crucial to its pharmacological mechanism, as removal results in loss of antimalarial activity.[9]

1.1.3.2 The Endoperoxide Bridge is Cleaved Forming Toxic Species

It is understood that the endoperoxide is activated by ferrous iron to form species capable of attacking biomacromolecules of the malaria parasite. This active species and the intermediates formed during its production have split artemisinin research into two main concepts: homolytic cleavage of the endoperoxide to form carbon centred radicals (CCRs) and heterolytic cleavage to form a hydroperoxide and reactive oxygen species (ROSs). These concepts shall be expanded upon in the following section and are summarised in Figures 1.3 and 1.4.

1.1.3.2.1 Homolytic Cleavage

Examination of the Fe(II) facilitated degradation of artemisinin led to the isolation of two major products: a THF acetate **7** and deoxoartemisinin **10** (Figure 1.3). The following homolytic mechanism was proposed accordingly.[10-12]

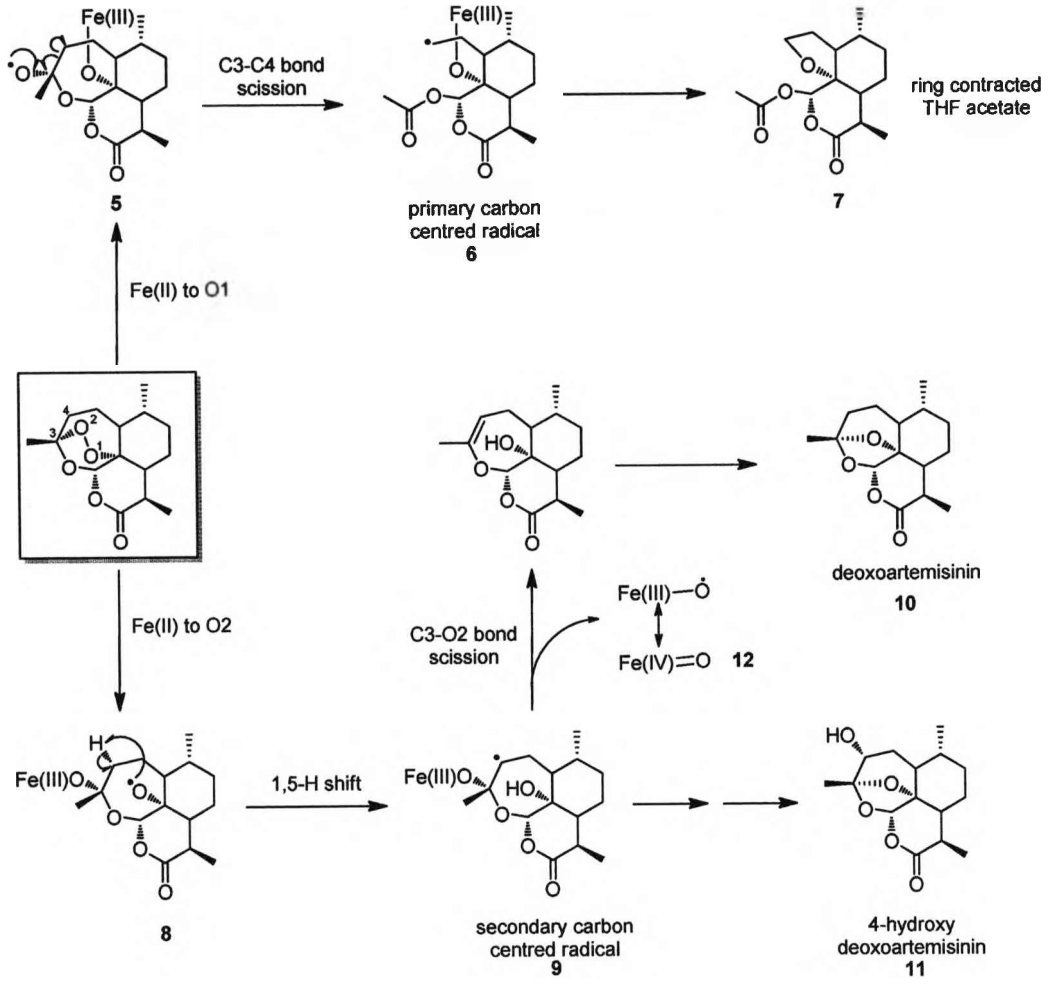

Figure 1.3 *Homolytic cleavage of the endoperoxide bridge and the resulting harmful species.*

Iron (II) acts as a catalyst where the initial step is the transfer of a single electron to the O-O σ* orbital cleaving the O-O bond and forming an oxy radical and an OFe^{3+} complex, **5** and **8**. This scission of the fused ring structure allows for two paths. In the first, scission of the C3-C4 bond generates a primary carbon centred radical on C4, **6**. Loss and regeneration of Fe(II) leaves two radical centres which combine to produce the furan acetate metabolite **7**. In the second, the production of the free oxy radical attracts H-atom migration and results in a 1,5-hydrogen shift to give **9**. Loss

of the $^{\cdot}OFe^{3+}$ complex allows for unsaturation of the C3-C4 bond and subsequent deoxoartemisinin formation, **10** and **11**.

Posner[13] sought to give further support to the hypothesis that the 1,5-hydrogen transfer is a crucial step in heme-promoted activation of artemisinin. Structurally modified 1,2,4-trioxanes, that would prevent such a 1,5-shift, were synthesised and displayed very poor activity *in vitro*. A number of these intermediates have also been confirmed by radical trapping experiments.[14-17]

However the interaction of these radical species with some of the proposed parasitic targets has never been directly observed. Wu *et al.* also highlights fundamental problems with proposing carbon centred radicals as causing fatal damage to parasite macromolecules: 1) carbon centred radicals should theoretically be eliminated by endogenous parasite radical-scavenging systems, 2) The structure of artemisinin means that intramolecular quenching of the formed primary and secondary radical centres would be a much more plausible path than any intermolecular attack, and 3) If artemisinin were able to attack *via* intermolecular radical attack; why is it more potent than simple organic peroxides that can potentially generate stoichiometric radical levels?[18] Wu proposes that artemisinin could form artemisinin-heme adducts or cysteine based S-Fe-artemisinin chelates that would allow for more plausible intramolecular attack and potentially produce irreversible binding to enzyme active sites.[19]

1.1.3.2.2 Heterolytic Cleavage

The formation of deoxoartemisinin as a by-product of iron(II) mediated cleavage has also been implicated in a heterolytic mechanism (Figure 1.4).

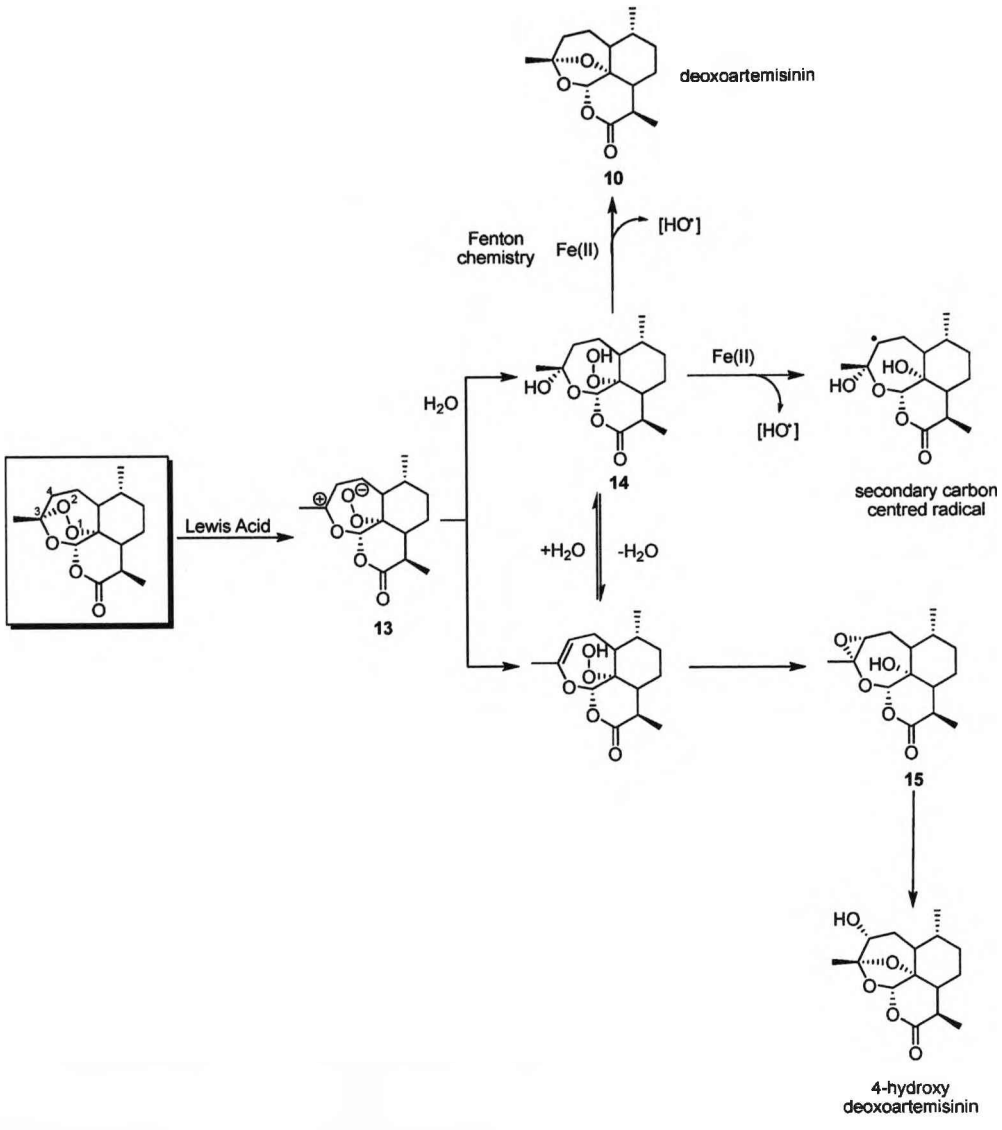

Figure 1.4 *Heterolytic cleavage of the endoperoxide bridge and the resulting harmful species.*

In the proposed path for heterolytic ring opening, artemisinin acts as a masked hydroperoxide, which is opened by Fe(II) behaving as a Lewis acid, to give **13**. Capture of the peroxide anion **13** by a nucleophile, such as H_2O, forms the hydroperoxide **14** which can then undergo reduction by Fe(II) (Fenton chemistry) to form hydroxyl radicals and a number of reactive oxygen species. Alternatively, loss

of the C3 hydroxyl group gives a saturated C3-C4 bond which can be oxidised to an epoxide **15**.

In 1996 Haynes confirmed Fe(II) and not Fe(III) as the peroxide activating species, presented evidence for a iron-artemisinin adduct and proposed that artemisinin interacts with hemin *via* a free hydroperoxide.[20,21] Further evidence for hydroperoxide formation was the observation that in the presence of artemisinin tertiary amines formed *N*-oxides. This transformation is reminiscent of *N*-oxide formation by peracids and hydroperoxides in the presence of a Lewis acid or protic acids. Additional support for a hydroperoxide intermediate is the non-endoperoxide oxygen of the trioxane ring. Hydroperoxide formation is proposed to be aided by this structural feature through stabilisation of the carbocation by resonance forms: lack thereof resulting in a reduction in potency.

1.1.3.3 Artemisinin is Implicated in Attacking a Number of Parasite Targets

It has been hypothesised that artemisinin may cause oxidative stress at non-specific lipid targets *via* the formation of reactive oxygen species[22] and may enhance the redox activity of heme.[23] The proposed mechanism (Figure 1.5) begins with cleavage of the peroxide bridge by lipid solubilised heme[24] to produce carbon centred radicals on artemisinin. These radicals facilitate the formation of a hydroperoxide moiety on the lipid bilayer. Fenton type chemistry results in cleavage of the hydroperoxide and the release of reactive oxygen species (hydroxyl radicals and superoxide anions). More recently these reactive oxygen species have been linked to the damage of the parasite food vacuole, vacuolar rupture and parasite autodigestion.[25]

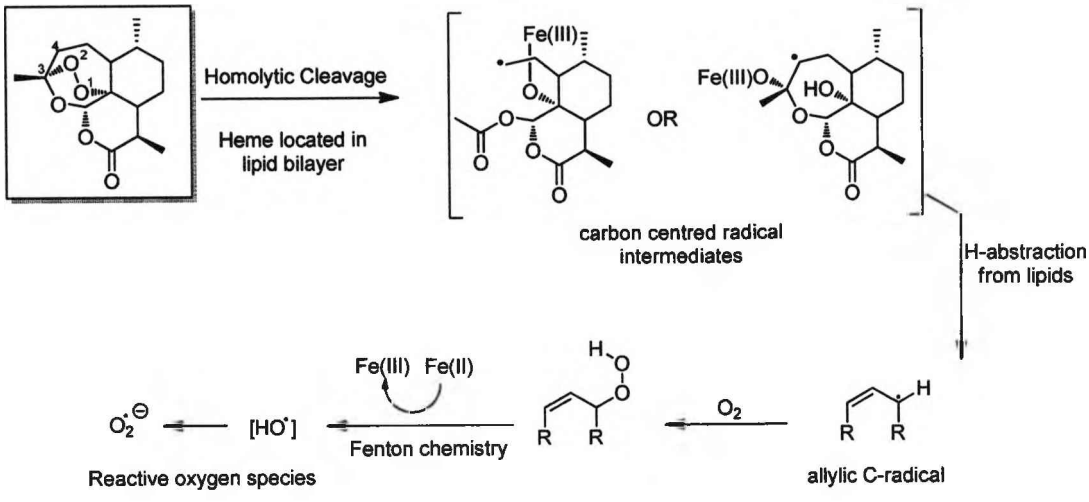

Figure 1.5 *Proposed mechanism for artemisinin mediated lipid peroxidation.*

Much evidence has gathered indicating that artemisinin and its analogues may exert their antimalarial effect *via* a similar mechanism to that of the quinoline class of antimalarial i.e. by the formation of heme adducts to block hemozoin formation.

Meshnick and co-workers identified that artemisinin can form adducts with heme and that during this process the peroxide bridge is cleaved, thereby activating artemisinin.[26,27] Robert, Meunier and co-workers characterised the heme-artemisinin adduct **16**, indicating that all four *meso* positions of heme were alkylated by the primary carbon centred radicals of activated artemisinin (Figure 1.6).[28-31]

Biological testing of various artemisinin derivatives has also shown a positive correlation between levels of heme alkylation and *in vitro* antimalarial activity adding support for this proposed mechanism of action.[32,33]

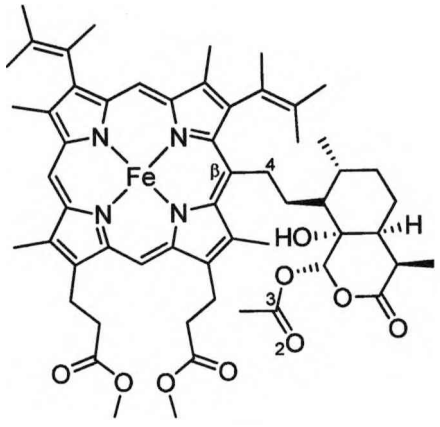

16

Figure 1.6 *Alkylation of heme by artemisinin. Only alkylation at the β-position is shown.*

Pandey *et al.* have demonstrated that artemisinin has the capacity to inhibit parasitic enzymes responsible for the digestion of haemoglobin (aspartic acid proteases and cysteine proteases) and a histidine rich protein (PfHRP II) shown to catalyse the polymerisation of heme.[34]

The structural similarity of artemisinin to thapsigargin **17** (Figure 1.7), a known sarcoplasmic/endoplasmic reticulum Ca^{2+}-ATPase (SERCA) inhibitor, has highlighted the SERCA of *P. falciparum* (*Pf*ATP6) as potential parasiticidal target.[35,36] The inhibition of *Pf*ATP6 by artemisinin was confirmed by the antagonistic relationship displayed by artemisinin and thapsigargin.[37] The endoperoxide bridge also appears to play a role in enzyme inhibition as desoxyartemisinin (lacking the endoperoxide bridge) had no inhibitory effect on *Pf*ATP6 and the iron-chelator, desferrioxamine, quenched inhibition of *Pf*ATP6 by artemisinin indicating cleavage of the peroxide bridge by Fe(II) is vital.

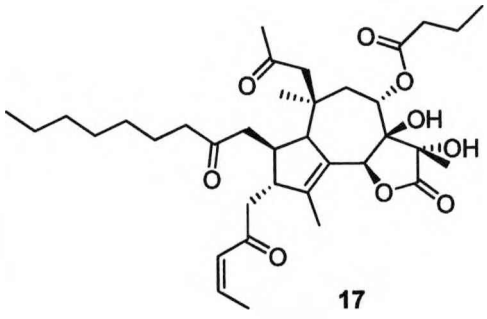

17

Figure 1.7 *Thapsigargin, a known SERCA inhibitor.*

However, arguments against this mode of activity are that the opposing enantiomers of trioxanes, structurally similar to artemisinin, have equal activity. This indicates that the mechanism of artemisinin does not in fact depend on stereospecific interactions with a protein. These studies will be discussed in more depth in Section 1.4.[38,39]

It has also been proposed that artemisinin may target NADH dehydrogenase enzymes of parasite mitochondria, thereby breaking down the mitochondrial electron transport chain, causing depolarisation of mitochondrial membrane potential and disruption of parasite respiration.[40]

It is unlikely that artemisinin acts at one, single biological target. This is supported by the wealth of evidence proposing a number of reactive intermediates and demonstrating that artemisinin has the potential to affect a wide variety of parasite structures and systems. Add to this the limited resistance to artemisinin observed, and it suggests a multi-targeted attack of the malaria parasite, the exact nature of which is yet to be confirmed.

1.2 Photooxygenation as a Route to 1,2,4-Trioxanes

As elucidated by Jefford,[41] the 1,2,4-trioxane moiety found on artemisinin has proved essential for antiparasitic activity. In an effort to provide more economic and readily available analogues of artemisinin, research has focused on the synthesis of simplified analogues incorporating the 1,2,4-trioxane pharmacophore (Figure 1.8).[38,42,43] A key step in the synthesis of 1,2,4-trioxanes is the introduction of the peroxide functionality. Singlet oxygen, generated *via* photooxygenation, is a popular reagent allowing the introduction of oxygen in a controlled manner. In the following sections we will discuss the origins of singlet oxygen as a synthetically useful species and the remarkable regio- and stereoselectivity many of its reactions display. We will then continue in Section 1.4 with an examination of the previous routes, employing singlet oxygen, used to realise the 1,2,4-trioxane target.

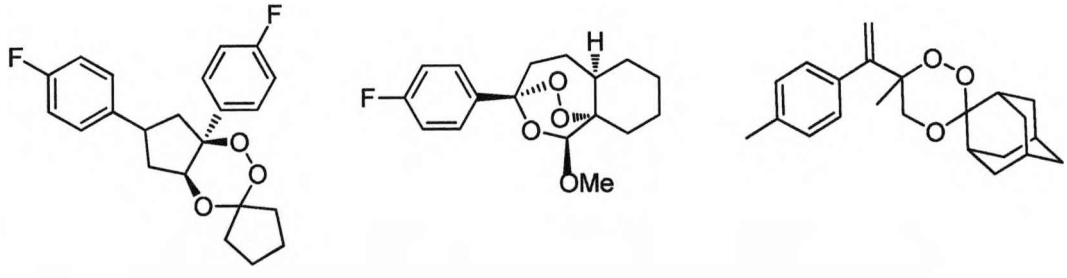

Figure 1.8 *1,2,4-Trioxane artemisinin analogues displaying antimalarial activity comparable to that of the parent compound.*

1.2.1 Elucidation of the Singlet Oxygen Intermediate ($^1O_2$)

Research into photooxidation processes dates back to the late 19th century when biologists discovered that a combination of dyes, oxygen and light were toxic to organisms such as paramecia and photochemical reactions involving oxygen resulted

in oxygenation of biological material.[44] In 1928 Mulliken proposed molecular orbital descriptions of triplet ground state ($^3\Sigma_g^-$), excited singlet delta ($^1\Delta_g$) and excited singlet sigma ($^1\Sigma_g^+$) oxygen (Figure 1.9).[45,46]

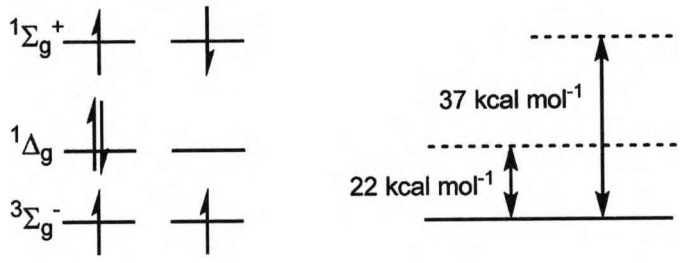

Figure 1.9 *Ground, first and second excited states of molecular oxygen.*

Work by Kautsky in the 1930s developed the theory that dye-sensitised photooxygenation reactions proceed *via* a singlet oxygen intermediate by demonstrating the diffusible nature of the reactive species, presumed to be $^1\Sigma_g^+$.[47] However, during the 1930s, and through to the mid-60s, there was considerable doubt that such a singlet oxygen intermediate was involved in the mechanism of photooxidation reactions. A large body of evidence amassed contrary to the intermediacy of singlet oxygen, arguing that energy transfer (37 kcal/mol) from a dye molecule to molecular oxygen required to form $^1\Sigma_g^+$ was not viable. In fact a sensitiser-oxygen complex was proposed by many as the reactive species.[48] Kautsky responded to this by indicating that formation of $^1\Delta_g$ (22 kcal/mol above ground state O_2) was a viable energy transfer from dyes (emitting at 820 nm).[49] However, this response from Kautsky was largely ignored in the subsequent literature produced by his peers.

Not until 1963 was the idea of singlet oxygen as a vital intermediate revived. Observations of solutions of NaOCl and H_2O_2 detected a red chemiluminescence attributed to the emission pairs of $^1O_2$ molecules.[50-52] Pathways where $^1O_2$ decays to triplet ground state O_2 and hv [1268nm (22kcal/mol)] were reported.[53-55] Foote and Wexler further confirmed $^1O_2$ to be the reactive intermediate in dye-sensitised photooxygenation.[56] Comparison of the H_2O_2/NaOCl reaction conditions, known to generate singlet oxygen, and dye-sensitised photooxygenation conditions demonstrated that 2,5-dimethylfuran underwent transformation to 2,5-dimethyl-2-hydroperoxy-5-methoxy dihydrofuran in both cases: thereby linking the mechanistic pathways and intermediates (Figure 1.10).

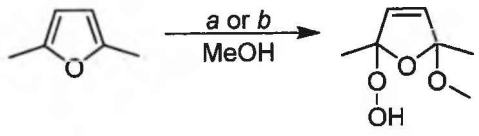

Figure 1.10 *Identical reaction pathway of a) the H_2O_2/NaOCl system and b) dye-sensitised photooxygenation.*

Arguments for an excited sensitiser-oxygen complex were finally quashed when it was shown that a) rates of photooxidation were independent of the sensitiser used, b) sensitisers exert no steric influence, and c) radical scavengers do not influence the reaction.[57,58]

1.2.2 The Synthetic use of Singlet Oxygen

In the following section we will discuss the nature of singlet oxygen in a qualitative fashion, however a discussion of the quantum mechanical aspects of this subject can be found in a review by Kearns.[59]

Synthetically useful singlet oxygen is the first excited state ($^1\Delta_g$) of molecular oxygen at 22 kcal mol^{-1} above the triplet ground state ($^3\Sigma_g^-$). The second excited singlet state ($^1\Sigma_g^+$), at 37 kcal mol^{-1} above the ground state, is not synthetically active as a result of its transient existence in solution (10^{-12} seconds). This transience and instability is due to the rapid spin allowed transition from the second excited state, $^1\Sigma_g^+$, to the first excited singlet state, $^1\Delta_g$. Correspondingly, the synthetic use of the first excited state is derived from its metastability in solution (10^{-3}-10^{-6} seconds) as a result of the spin disallowed transition to the ground state (Figure 1.11).

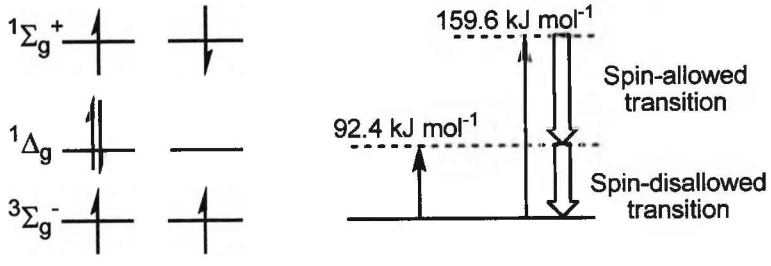

Figure 1.11 *Spin-disallowed transition from the singlet excited to the triplet ground state imparts stability to singlet oxygen.*

The triplet oxygen ground state is paramagnetic rendering capable of free radical reactions and processes. Conversely, singlet oxygen is diamagnetic denoting its restriction to two electron reactions in a similar manner to ethylene.

1.2.3 The Generation of Singlet Oxygen via Photooxygenation

There are a number of chemical sources of singlet oxygen reported in the literature, including the hydrogen peroxide/sodium hypochlorite system,[60] disproportionation of H_2O_2 by mineral compounds,[61,62] thermolysis of phosphite ozonide adducts,[63] base-

catalysed disproportionation of peracids[64] and from the thermolysis of naphthalenic endoperoxides.[65,66]

The most efficient method however, is the dye-sensitised photochemical excitation of ground state molecular oxygen. Commonly used dyes are aromatic compounds, Rose Bengal, methylene blue and tetraphenylporphine (TTP) (Figure 1.12).

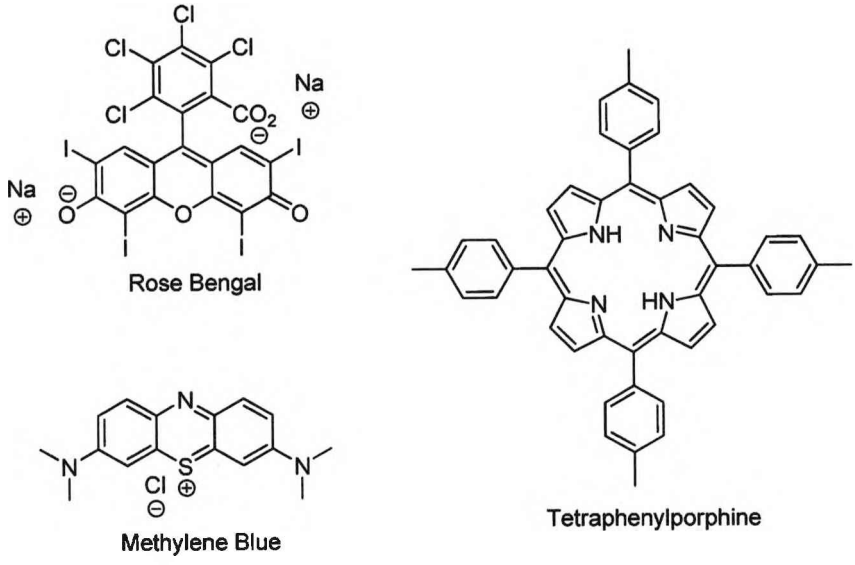

Figure 1.12 *Commonly used sensitiser dyes.*

Dye-sensitised photooxygenation is initiated by the excitation of a triplet ground state dye-molecule, by visible light, to the excited singlet state. Once the sensitiser is excited, three reaction paths are in fact available and are classified into 3 types: of note are Types I and II (Figure 1.13). Type I refers to an interaction between the excited dye-stuff and the substrate (H-atom extraction or electron transfer) to form radical species which react with ground state triplet oxygen to form the photooxygenation product. This pathway is often unfavourable as it facilitates degradation of the sensitiser dye.

Type II involves energy-transfer oxygenation where singlet oxygen is the reagent. Rapid intersystem crossing of the singlet state sensitiser molecule results in the formation of the excited triplet state of the dye, which can then undergo triplet-triplet energy transfer to molecular oxygen (triplet ground state). This energy transfer forms excited singlet oxygen and returns the sensitiser to its ground state. Singlet oxygen can then go on to react with the substrates present.

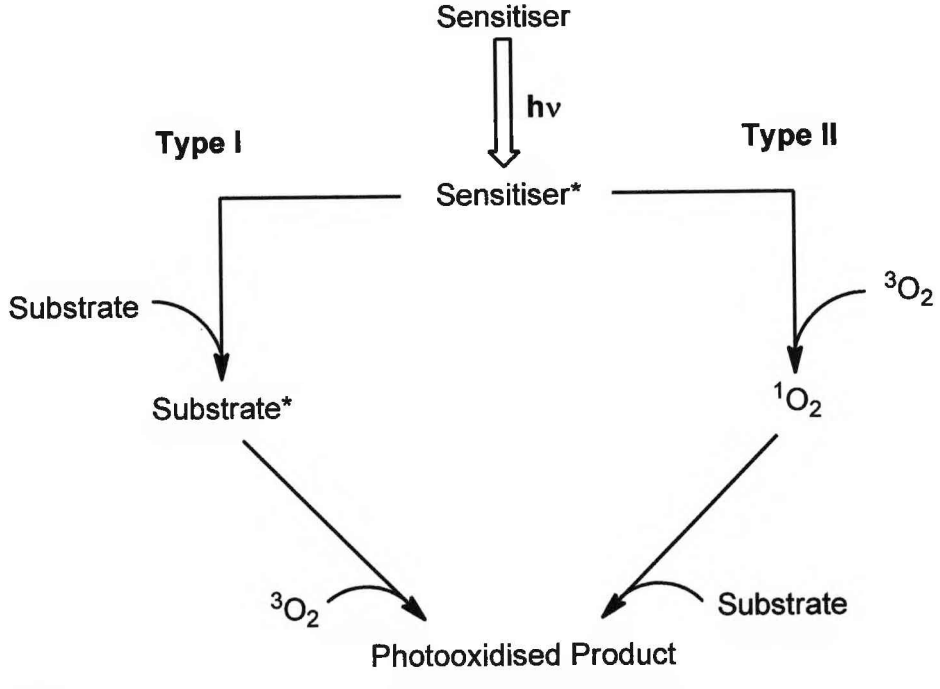

Figure 1.13 *Flow diagram to illustrate the pathways of photooxygenation.*

Prevalence of one of these pathways can be controlled by manipulation of the experimental conditions. The concentration of oxygen and substrate, temperature, lifetime of singlet oxygen in the chosen solvent and the selected dye, can all affect which process is followed.[67] Type II photooxygenation, in particular, has been used for numerous synthetic applications as singlet oxygen is highly reactive and at the

same time a selective reagent showing remarkable chemo-, regio- and stereoselectivity patterns.

1.2.4 Mechanistic Pathways of Singlet Oxygen

The most important examples of reactions that are facilitated by Type II photooxygenation are a) the ene-reaction with an olefin resulting in allylic hydroperoxides **18**, b) [4+2]-cycloaddition with a 1,3-diene yielding 1,4-endoperoxides **19** and c) [2+2]-cycloaddition with an electron rich olefin, or olefin lacking β-hydrogen atoms, to give 1,2-dioxetanes **20** (Figure 1.14). The oxidation of heteroatoms (e.g. sulphide to sulfoxide) is also a prominent side reaction.

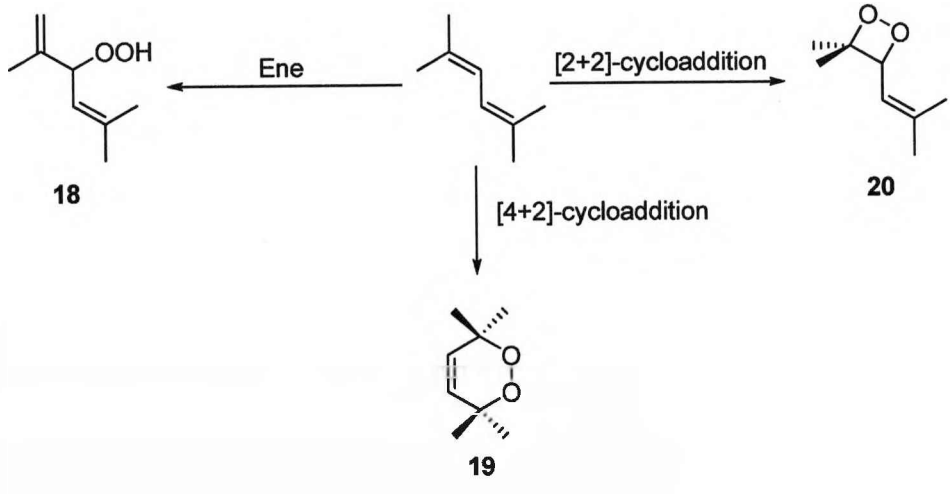

Figure 1.14 *Mechanistic pathways available to singlet oxygen.*

The exact mechanistic intermediates formed during these reactions have been a subject of debate since their discovery. Proposed mechanisms include concerted cycloadditions as well as stepwise processes *via* zwitterionic **21**, biradical **22** or perepoxide **23** intermediates or *via* an exciplex complex **24** (Figure 1.15).

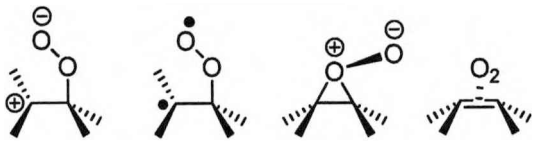

21 **22** **23** **24**

Figure 1.15 *Proposed intermediates of olefin photooxygenation.*

The precise pathways of the formally termed [4+2]- and [2+2]-cycloaddition reactions have been extensively discussed in reviews by Frimer[68] and Clennan[67] and shall be summarised shortly. For our purposes, we will then proceed to discuss in depth the mechanistic features and stereoselectivity of the Schenk-ene reaction.

1.2.4.1 Proposed Mechanisms of the $^1O_2$ [4+2]-Cycloaddition Reaction

The [4+2]-cycloaddition pathway is very versatile, occurring readily with acyclic, cyclic and aromatic 1,3-dienes, and can accommodate various substituents, latent functional groups and heteroatoms. A concerted pathway has often been favoured due to the structural similarity of the reactants, to those involved in the Diels Alder reaction. The often observed *cis*-stereoselectivity[69] of this reaction and its apparent insensitivity to solvent also indicated a concerted process.[70,71] Evidence contrary to a Diels Alder type mechanism is the fact that singlet oxygen [4+2]-cycloadditions have an activation barrier very close to zero.[72] Aubrey also later highlighted the sensitivity of reaction rate to solvent conditions through performing the [4+2]-cycloadition in 28 different solvents.[73] This has prompted support for a reversible exiplex complex (characterised by low activation barriers) with subsequent collapse to the 1,4-endoperoxide.[74,75]

1.2.4.2 Proposed Mechanisms of the $^1O_2$ [2+2]-Cycloaddition Reaction

The reaction path to 1,2-dioxetanes has been shown to have a higher activation energy to that of the formation of endoperoxides and hydroperoxides and appears only to occur when other paths are unavailable. An exception to this is the reaction of electron rich olefins which undergo [2+2]-cycloaddition even when allylic hydrogens are accessible, though the ene-product is formed competitively. Again, the stereochemical properties demonstrated by this pathway suggest a concerted mechanism. However, arguments for a polar intermediate, either an open zwitterionic or a closed perepoxide intermediate, have gathered weight in the form of observed solvent effects.[71] An example is the yield of dioxetane **27** from treatment of **25** with singlet oxygen, which was found to increase from 3 to 50% as the polarity of the solvent was increased (Figure 1.16).[76]

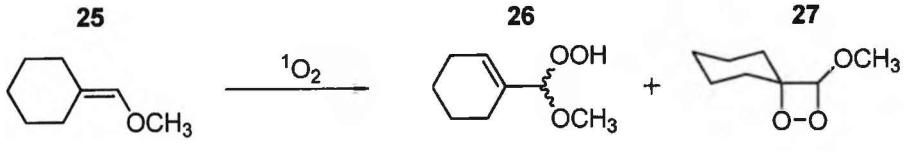

C_6H_6	97	3
CH_2Cl_2	73	27
CH_3OH	32	48

Figure 1.16 *Effect of solvent polarity on product distribution. Numbers refer to percentage yield.*

Wilson proposes a zwitterionic perepoxide intermediate having observed that the rate of reaction of enol ester **28** was insensitive to solvent change while the products formed are dramatically affected. **28** was found to undergo acyl shift to **29** in acetone, whereas conditions in methanol facilitated formation of 1,2-dioxetane **30**

(Figure 1.17). This supports the hypothesis that an intermediate to the formation of 1,2-dioxetanes requires intermolecular H-bonding (satisfied by MeOH) *i.e.* a dipolar intermediate.[77]

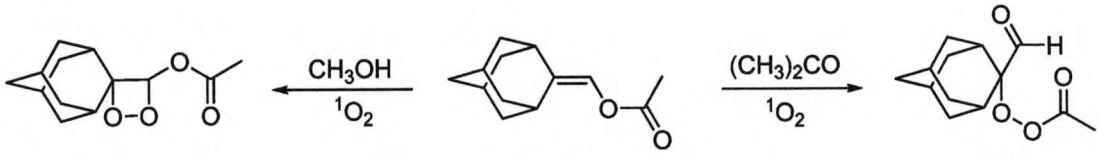

30 **28** **29**

Figure 1.17 *Use of a H-bonding solvent, such as MeOH, favours 1,2-dioxetane formation.*

1.2.4.3 Proposed Mechanisms of the $^1O_2$ Schenk-Ene Reaction

Early observations indicated a concerted mechanism analogous with that of a reactive enophile which undergoes the formal "ene" reaction with an olefin. These observations included: a) a *cis*-relationship between the newly formed C-O bond and the breaking allylic C-H bond[78], b) the inability of *cis*- and *trans*-olefins to isomerise during the reaction indicating no free rotation around an intermediary single bond[79] and c) examples of the powerful stereoselectivity indicated that the mechanism could not proceed *via* an initial H-abstraction leading to an allylic free radical.[58] However, elucidation of the *cis*-effect (discussed in more detail below) demonstrated that the ene-reaction was not in fact subject to steric constraints that would be observed if a concerted process were involved.[80]

Ab initio calculations have modelled a biradical intermediate as a major reaction pathway[81], however, these suggestions contradict the high stereoselectivity demonstrated by the ene-reaction.[82] Early suggestions presented by Jefford[83] stated that the intermediate must be dipolar as the one-point attachment of the incoming singlet oxygen, before H-abstraction, causes an imbalance of charge. However, later

literature only discusses a zwitterionic intermediate in the context of 1,2-dioxetanes, where the zwitterionic intermediate en route to the 1,2-dioxetane is intercepted by the solvent (*e.g.* methanol) to give the hydroperoxide.[76,84,85]

The majority of evidence supports the perepoxide intermediate as the pathway to the hydroperoxide product. The perepoxide intermediate was tentatively proposed by Sharp[86] and Kearns.[87,88] in the late 1960s. Semi-empirical methods highlighted the perepoxide on the CNDO/2 potential energy surface, and termed it a "quasi-intermediate". Frontier orbital theory describes singlet oxygen as having a very low energy LUMO, making it a strong electron acceptor, and presenting the olefin as providing the HOMO.

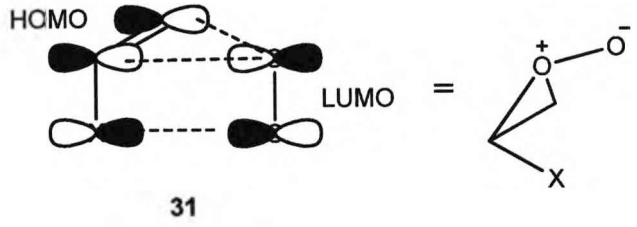

31

Figure 1.18 *Perepoxide interactions from the olefin HOMO to singlet oxygen LUMO.*

The HOMO/LUMO interaction is most effective when the reactive nuclei are arranged with the two nucleophilic centres of the e^--donor (olefin), and one electrophilic atom of the e^--acceptor ($^1O_2$), forming a triangle with the remaining atom of the acceptor tailing out of the trigonal plane giving perepoxide **31** (Figure 1.18).[89-91]

During the H-abstraction mechanistic step, singlet oxygen demonstrates preferences for certain allylic hydrogen atoms. These preferences have been studied by primary

isotope effects[82,92-95] demonstrated by tetramethylethylene-d_6 and show the following: a) substituents with a *cis*-relationship are in competition during H-abstraction which is consistent with a step-wise mechanism[94], b) singlet oxygen displays suprafacial selectivity which is most closely accommodated by the perepoxide intermediate model (the tailing O-atom can only interact with one face of the olefin to abstract a H-atom)[96] and c) in the case of trimethylethylene-d_6, singlet oxygen abstracts H-atoms from the most substituted face in what is termed the "*cis*-effect" (explained by the tailing O-atom of the perepoxide requiring stabilisation from adjacent methyl groups).[97-99] The *cis*-effect will be further discussed in Section 1.3 concerning the stereoselectivity of the ene-reaction.

Further support for perepoxides are the reaction of various trapping agents (*e.g.* sulfoxides, diphenyl sulphide, sulfenate/sulfinate esters and phosphites) with singlet oxygen to form the oxidised trapping agent and an epoxide of the olefin.[100,101]

It can be summarised that it is the differentiating of the intermediate that controls product distribution in these pathways: a) perepoxides giving hydroperoxides, b) exiplex complexes giving endoperoxides and c) polar intermediates giving 1,2,-dioxetanes. The factors driving the choice of intermediate are often substrate structure and solvent conditions. However, as often is the case, overlap of these pathways highlight exceptions that make definition of these highly transient species very difficult.

1.3 Regio- and Stereoselectivity of the Schenk-Ene Reaction

Thorough reviews of the factors influencing the selectivity of the Schenk-ene reaction with regard to a variety of substrates have been provided by Stratakis[102] and

Clennan[103]. For our purposes we shall focus on simple di- and trisubstituted alkenes including enol ethers and particularly allylic alcohols.

1.3.1 Methoxy Groups cis-Direct H-Abstraction

Early studies identified the polarity of the olefinic π-bond as driving regiocontrol and, in the case of enol ethers (Figure 1.19), the HOMO/LUMO interactions between attacking terminal oxygen atom and the methoxy group as exerting stereocontrol.[90] A classic experiment demonstrating the regio- and stereocontrol exerted by the presence of a methoxy group and the resulting *cis*-effect was performed by Rousseau in 1977.[97] The singlet oxygen was found to have such a strong preference for the position *cis* to the methoxy group that it overcomes the highly awkward formation of the α-cyclopropylidene (Figure 1.19).

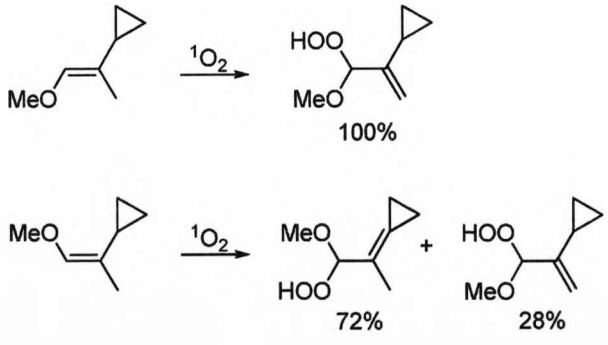

Figure 1.19 *Singlet oxygen displays a preference for H-abstraction cis to the methoxy group.*

Similarly, a methoxy group on a substituted styrene directs incoming $^1O_2$ attack *cis*, giving 1,4-addition, if the phenyl is *cis* to methoxy **32**, or the ene reaction if the methyl is *cis* to methoxy **33**. If no substituent was positioned *cis* to methoxy then 1,4-attack takes place but at a much slower rate **34** (Figure 1.20).[98]

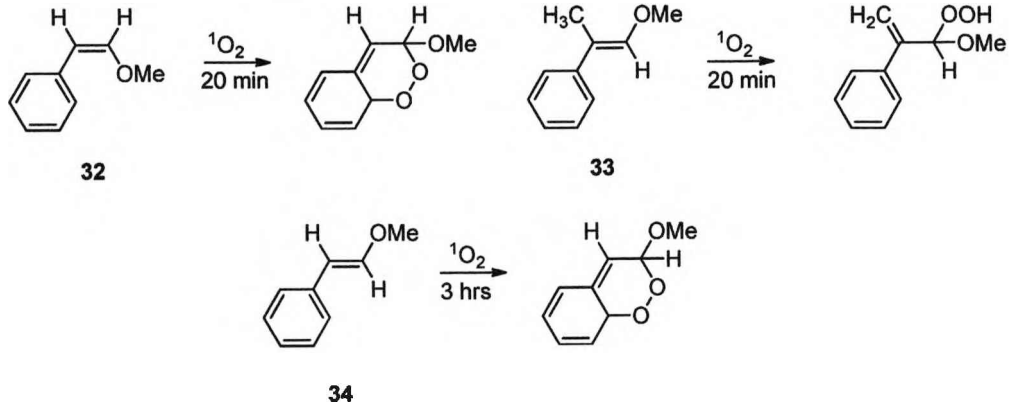

Figure 1.20 *Singlet oxygen displays a preference for H-abstraction cis to the methoxy group.*

As previously mentioned this preference for H-abstraction, suprafacial to a methoxy group, can be explained by the perepoxide model where the tailing oxygen atom is directed by interactions with the methoxy group to remove an allylic hydrogen from the *cis*-position.

1.3.2 H-Abstraction Occurs on the Most Congested Side of the Olefin

This observation of suprafacial H-abstraction was extended to the photooxygenation of trisubstituted alkenes as displayed by Orfanopoulos (Figure 1.21).[80]

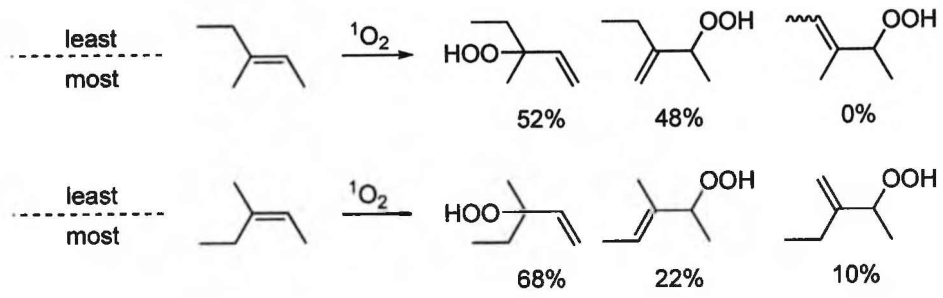

Figure 1.21 *Singlet oxygen displays preference for H-abstraction from the most congested side of the olefin.*

A preference for *syn*-ene addition to 1-methyl cycloalkenes was also demonstrated by singlet oxygen, which complies with a perepoxide intermediate where the trailing cationic O-atom is stabilised by allylic hydrogen atoms lying above the plane of the double bond (Figure 1.22).[104]

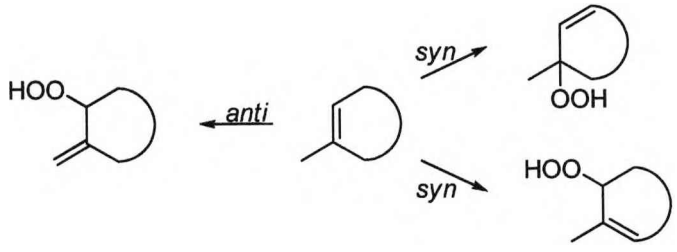

Figure 1.22 *Singlet oxygen demonstrates a preference to syn-addition to 1-methyl cycloalkenes.*

This stabilisation effect is supported by Stephenson[105] who postulates a secondary orbital interaction between the terminal oxygen LUMO and the allylic hydrogen contribution to the HOMO, stabilises the transition state leading to *syn*-addition.

An elegant hypothesis for the varied reactivity of, and preference for, specific allylic hydrogen atoms, was presented by Houk[106] with respect to acyclic alkenes. Houk agrees that allylic hydrogen atoms must be perpendicular to the olefin in order to facilitate *syn*-selectivity but postulates that rather than the stabilisation of a

perepoxide intermediate, the selectivity is derived from conformational barriers of alkyl substituents adopting the optimum perpendicular conformation. Houk also postulates that in a concerted transition state the bond to the allylic hydrogen which is being abstracted must also be perpendicular to the olefinic plane. It is therefore suggested that the differences in reactivity (% H-abstraction) of different substituents correlates to the differences in energy required to rotate to a perpendicular conformation.

1.3.3 An Anti cis-Effect has been Observed where t-Bu is Allylic

For trisubstituted alkenes, where an allylic position possesses a *t*-Bu substituent (Figure 1.23), an anti *cis*-effect has been observed.[102] For these substrates, the less substituted side of the double bond is more reactive.

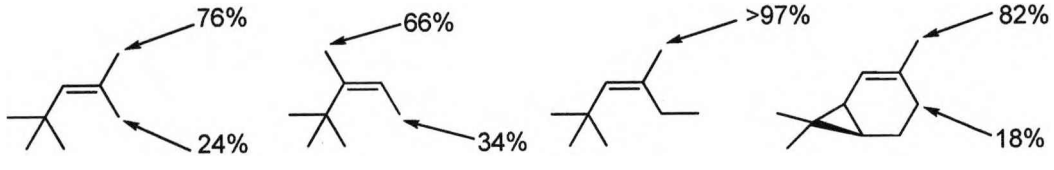

Figure 1.23 *Numbers indicate percentage allylic hydrogen abstraction. Substituents bearing a t-Bu group do not direct a cis-effect.*

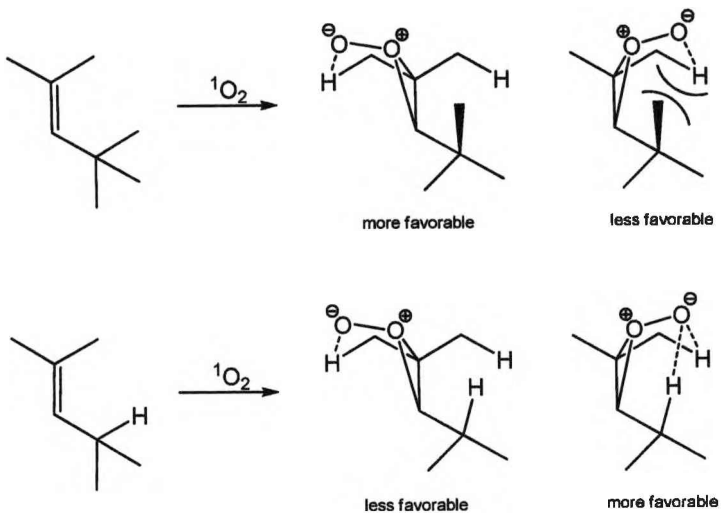

Figure 1.24 *The perepoxide model shows that H-abstraction from the most congested side of the olefin does not provide any additional stabilisation for the terminal O-atom.*

During the formation of the intermediate, the terminal oxygen finds no improved stabilisation on the more congested side as there is now equal distribution of allylic H-atoms on both sides of the olefin. Additionally, formation of a perepoxide intermediate on the more substituted side of the olefin is not favourable because of steric repulsion between the oxygen and the two alkyl groups (Figure 1.24).

1.3.4 Allylic Alcohols have a Directing Effect on Singlet Oxygen

In 1992, Adam and co-workers specifically looked at the directing effect of allylic alcohols and reported very high regio- and stereocontrol in one of the most diastereoselective examples of the ene reaction.[107,108] The reaction introduces a new stereogenic centre with a peroxy functionality adjacent to the hydroxyl group in a *threo* configured relationship (Figure 1.25). It was also observed that the substituents at R^1 and R^2 had a negligible effect on the excellent 97: 3 diastereomeric ratio.

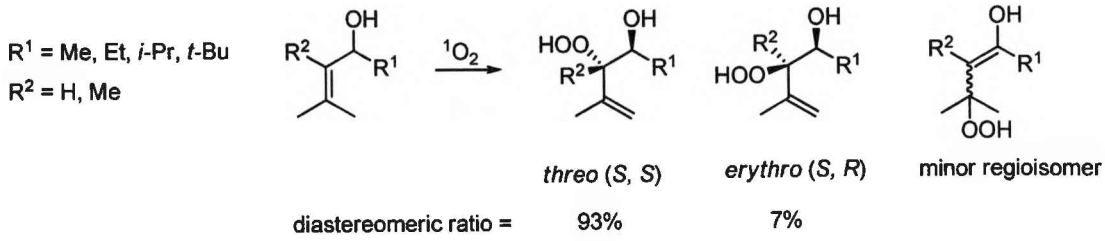

Figure 1.25 *Photooxygenation of allylic alcohols displays high diastereoselectivity in favour of the threo-conformation.*

Interestingly the diastereofacial selectivity of allylic alcohols behaves in an opposite respect to the "classical" *cis*-effect discussed above. The classical *cis*-effect dictates that the tailing oxygen atom is stabilised by *cis*-allylic hydrogen atoms positioned perpendicular to the plane of the olefin. If the classic *cis*-effect were operating one would not predict a *threo*-relationship (between hydroxyl and peroxy groups). The *threo*-conformation would not be viable as simultaneous positioning of the allylic hydrogen perpendicular to the olefinic bond would leave the remaining Me group orientated to maximise 1,3-allylic strain and a highly unstable intermediate **35** demonstrated in Figure 1.26. The classically predicted *erythro*-relationship (between hydroxyl and peroxy groups) would result in a conformation with minimised 1,3-allylic strain and a stable viable intermediate **36** (Figure 1.26).

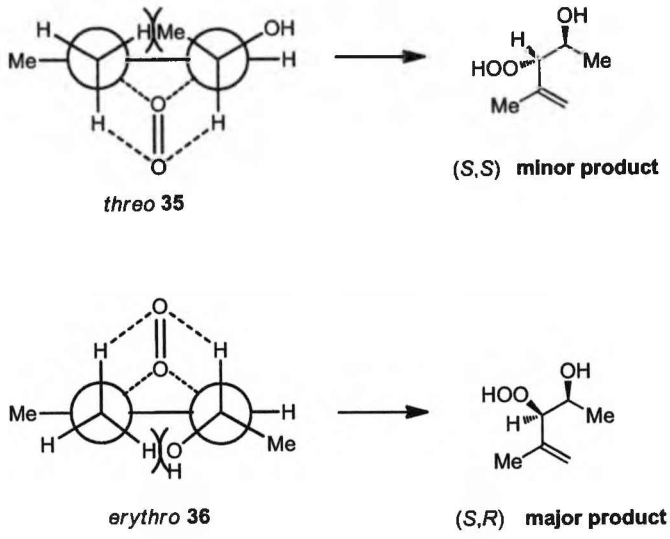

Figure 1.26 *Newman projection of the perepoxide intermediates if the classic cis-effect were operating.*

However, in the case of allylic alcohols the opposite *threo*-result is observed, thus indicating that it is not in fact an allylic hydrogen stabilising the tailing oxygen but the hydroxyl group. If we look at Figure 1.27, we see that a conformation where the hydroxyl group is positioned perpendicular, 1,3-allylic strain can also be minimised as the methyl group is directed away from the adjacent *cis*-alkyl group. It can be summarised that the selectivity is a combination of 1,3-allylic train disallowing the perpendicular positioning of a H-atom and the availability of a hydroxyl group to assume a perpendicular alignment to stabilise the tailing O-atom, producing a *threo*-relationship the between hydroxyl and peroxy groups.

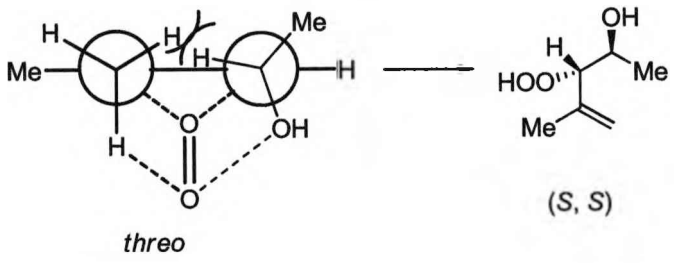

Figure 1.27 *Newman projection of a novel cis-effect where the tailing oxygen atom is stabilised by the -OH group.*

The hydroxyl group is essential for selectivity as demonstrated by solvent effects and functionalisation of the hydroxyl group. When the reaction was carried out in solvents that interact with the OH group *via* hydrogen bonding, *e.g.* MeOH and MeCN, a drop in diastereoselectivity was observed. Allylic ethers, **41** and **42**, still demonstrated significant stereoselectivity however an allylic acetate **40** inverted the selectivity to favour *erythro* following the classic *cis*-effect (Figure 1.28).

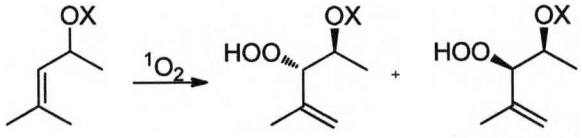

	X=		*threo*	*erythro*
(**37**)		CCl_4	93	7
(**38**)	H	MeOH	73	27
(**39**)		MeCN	76	24
(**40**)	Ac	CCl_4	39	61
(**41**)	$SiMe_3$	CCl_4	80	20
(**42**)	Me	CCl_4	72	28

Figure 1.28 *Solvent polarity and functionalisation of the hydroxyl group affect stereoselectivity.*

This trend is explained by the fact that the nucleophilic allylic oxygen functions are the initial interaction with incoming $^1O_2$ thereby directing the attack *threo* in examples **37** to **39**, **41** and **42**. The acetate group, being less nucleophilic, does not interact as strongly with $^1O_2$ thereby allowing the reaction to be governed by the *cis*-effect **40**.

In an analogous reaction, involving the photooxygenation of allylic amines, it was also observed that the free amine and its ammonium chloride proceeds with *threo*-selectivity. Similarly, for acylated amines *erythro*-selectivity was observed and the larger the nitrogen containing group, the higher the preference for an *erythro*-relationship.[109]

However, the position and direction of the hydroxyl group is ultimately decided by the orientation of the adjacent alkyl substituent, dictated by 1,3-allylic strain. The importance of 1,3-allylic strain in stereoselection was highlighted by comparison of *cis* and *trans* allylic alcohols **43**, **44** and **45** (Figure 1.29).

		Diastereomeric ratio	
	Substrate	*threo*	*erythro*
43	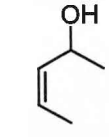	93	7
44	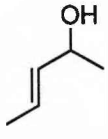	54	46
45	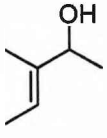	66	34

Figure 1.29 *Allylic alcohols, where 1,3-allylic strain can operate, demonstrate threo-selectivity.*

Absence of a methyl group *cis* to the hydroxyl bearing substituent, *i.e.* **44** and **45**, and therefore lacking 1,3-allylic government, demonstrate a loss stereoselectivity. Presence of a *gem*-methyl group, as in **45**, introducing 1,2-allylic strain, has only a small diastereoselective effect.

Adam supports these hypotheses by comparison with examples of m-CPBA and vanadium catalysed epoxidations. It is established that the selectivity demonstrated by these oxidations, mirroring that of the ene reaction, is a result of the combined effects of hydroxyl coordination and allylic strain.[107,108]

1.4 Synthesis of Antimalarial 1,2,4-Trioxanes

In 1983 Jefford reported on both the capture of 1,2-dioxetanes and 1,4-endoperoxides by acetaldehyde to form 1,2,4-trioxanes.[84,110] The formation and utility of these critical intermediates, as a route to 1,2,4-trioxanes, sparked a body of research committed to the synthesis of simplified artemisinin analogues. The two-fold purpose of these derivatives was firstly to provide novel, economically viable antimalarial agents, and secondly, as models in an effort to elucidate the mechanistic action of artemisinin. This work will be summarised in the following sections, divided into photooxygenation routes employing either [4+2]-cycloaddition, [2+2]-cycloaddition or the Schenk-ene reaction.

1.4.1 [4+2]-Cycloaddition as a Route to 1,2,4-Trioxanes

As mentioned above, the first reported use of photooxygenation (*via* [4+2]-cycloaddition pathways) to form a 1,4-endoperoxide, and its subsequent use in the

synthesis of 1,2,4-trioxanes, was by Jefford and co-workers (Figure 1.30).[110] Use of the 1,4-dimethoxynaphthalene starting material **46**, including the diene moiety, ensured that upon photooxygenation, the reaction would proceed *via* a [4+2]-cycloaddition pathway to provide the desired 1,4-endoperoxide **47**. To afford the 1,2,4-trioxane, an excess of acetaldehyde and catalytic amounts of the acidic amberlyst-15 resin were added to a solution of the 1,4-endoperoxide.

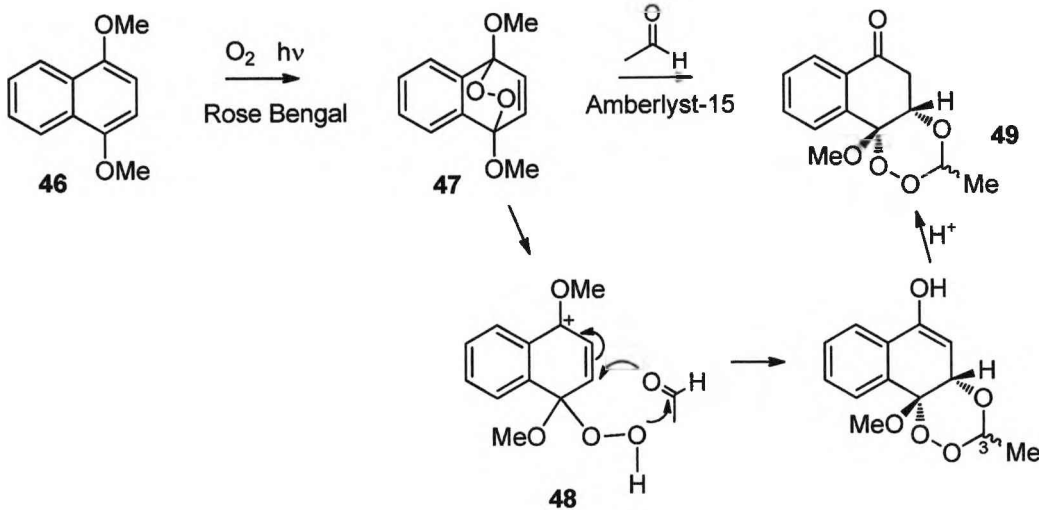

Figure 1.30 *Synthesis of a 1,2,4-trioxane via [4+2]-cycloaddition and a 1,4-endoperoxide intermediate.*

The condensation step was also shown to give similar results in the presence of trifluoroacetic acid and even aq. H_2SO_4. Acidic conditions allowed for the opening of the endoperoxide bridge, to give the hydroperoxide **48**, and its subsequent attack on the aldehyde to initiate cyclisation to the trioxane ring **49**. **49** was formed as a pair of epimers at the 3-position and with an exclusively *cis*-fused ring structure.[111]

[4+2]-Cycloaddition was used to synthesise a racemic mixture of *cis*-fused cyclopenteno-1,2,4-trioxanes which were then separated by chiral chromatography to afford enantiomerically pure trioxanes.[38] These enantiomers were then tested for

antimalarial activity to ascertain if the stereochemistry had any effect on activity. The synthetic 1,2,4-trioxanes displayed excellent activity, particularly the *p*-fluorinated derivative **50**. **50** showed oral activity better than that of the parent compound artemisinin and has been presented as a potentially clinically viable agent under the name of Fenozan B07.

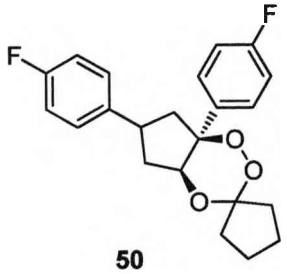

50

Figure 1.31 *Potent 1,2,4-trioxane antimalarial, Fenozan.*

However, there was no significant difference in activity of either the enantiopure or racemic compounds. This was linked to the hypothesis of activation by heme as it is also achiral. A proposed mechanism of action for these 1,2,4-trioxanes (Figure 1.32) is an initial coordination of the 1,2-peroxy group with the Fe(II) centre of heme **51** and subsequent cleavage of the peroxide bond *via* single electron transfer (SET) to form a spirocyclic acetal radical **52**. The newly formed negatively charged oxygen is now free to bond covalently to Fe(II) **53**. Radical mediated opening of the cyclopentyl ring forms an ester derivative with a primary carbon centred radical **54**, previously implicated in heme alkylation.[28-31] Opening of the cyclopentyl ring and the resulting ester formation is given credence by molecular modelling studies in which it is demonstrated to be a strongly exothermic process.[38]

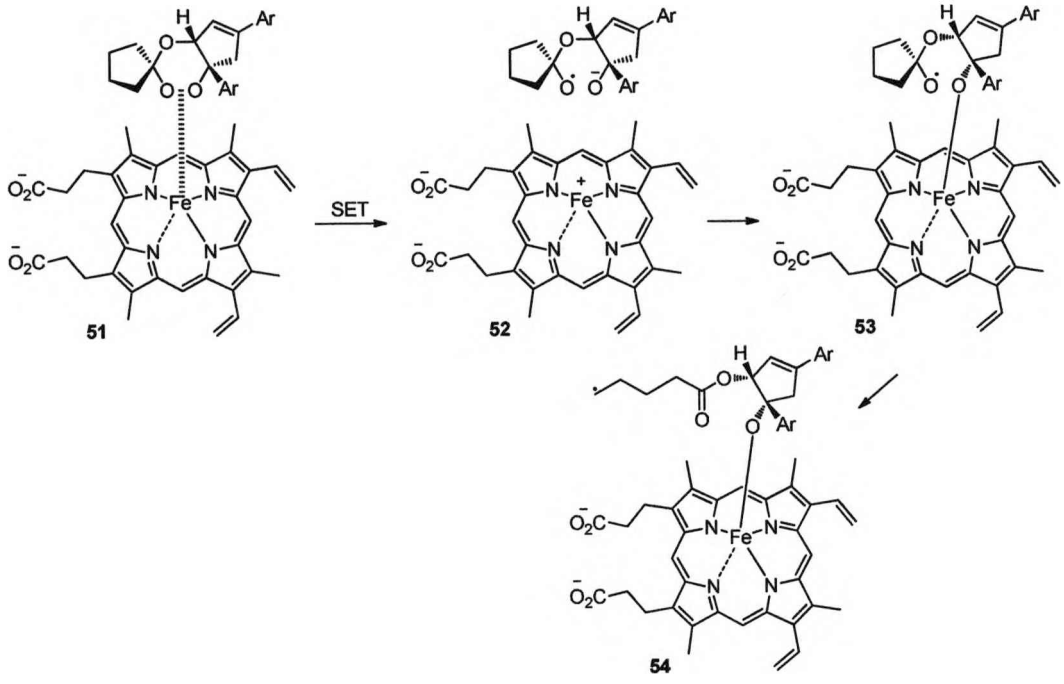

Figure 1.32 *A proposed mechanism of action of synthetic spirocyclic 1,2,4-trioxanes.*[38]

1.4.2 [2+2]-Cycloaddition as a Route to 1,2,4-Trioxanes

Jefford *et al.* ensured a [2+2]-cycloaddition reaction path by dye-sensitised photooxygenation of the vinyl ether, 2-norborneol methyl ether **55**.[84]

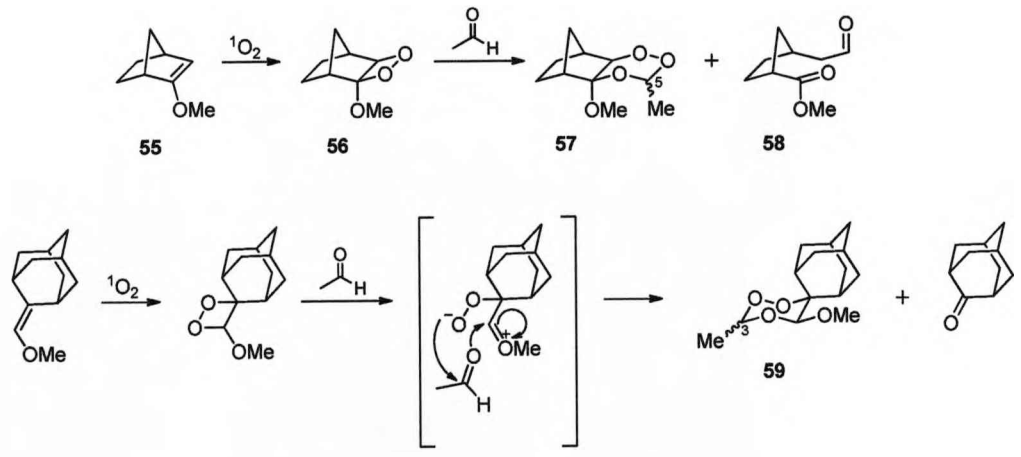

Figure 1.33 *Synthesis of a 1,2,4-trioxane via [2+2]-cycloaddition and a 1,2-dioxetane intermediate.*

Photooxygenation of **55** in acetaldehyde as the solvent, gave the *exo*-1,2,4-trioxane product as a mixture of two isomers at the 5-position **57** as well as the dioxetane cleavage product **58** (Figure 1.33). 2-(Methoxymethylene)adamantane was also treated under the same conditions to give isomer **59**, and 2-adamantanone.

This chemistry was extended to the synthesis of a series of artemisinin derivatives designed to lack one of the four ring functionalities found on the parent compound **60** (Figure 1.34).[41]

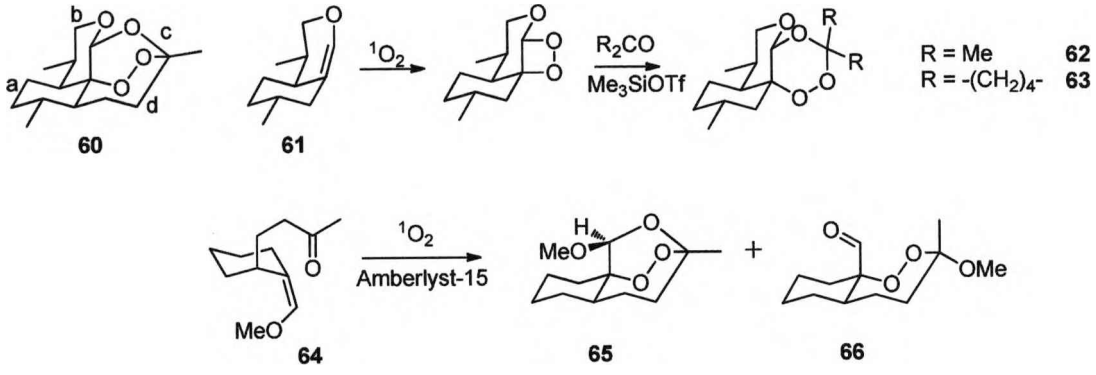

Figure 1.34 *Inter- and Intramolecular [2+2]-cycloaddition is employed in the synthesis of a variety of artemisinin **60** derivatives.*

The ring systems essential for antimalarial potency were elucidated by comparison of the antimalarial activity of analogues **62**, **63**, **65** and **66**. The derivative designed to lack the 1,2-dioxepane ring **d**, was synthesised from a dihydropyran derivative **61**. Photooxygenation to give the *exo*-1,2-dioxetane was followed by enlargement of the ring by acetone or cyclopentanone to afford **62** and **63** respectively. Products **62** and **63** had the precise chirality of artemisinin; however the trioxane **62** adopted a chair conformation unlike the boat conformation found on the parent compound. The

spirocyclic derivative **63** was proposed to have a conformational bias towards the boat structure.

An intramolecular variant of the condensation step was used to produce the second derivative lacking the δ-lactone ring **b**. Photooxygenation of vinyl ether **64** and subsequent intramolecular condensation gave the desired product **65** and by-product **66**. The spirocyclic compound **63** demonstrated the best antimalarial activity, attributed to the 1,2,4-trioxane being in a boat form, brought about by conformational compression of the spirocyclic group. **66** was also tested but displayed poor activity confirming that the trioxane is vital: a cyclic peroxide being insufficient for activity.

Posner used 1,2-dioxetanes to access the exact 1,2-dioxepane, 1,2,4-trioxane fused ring system found on artemisinin, in the synthesis of analogues **67a**, **67b** and **67c** (Figure 1.35), which showed antimalarial activity comparable to artemisinin.[112-114]

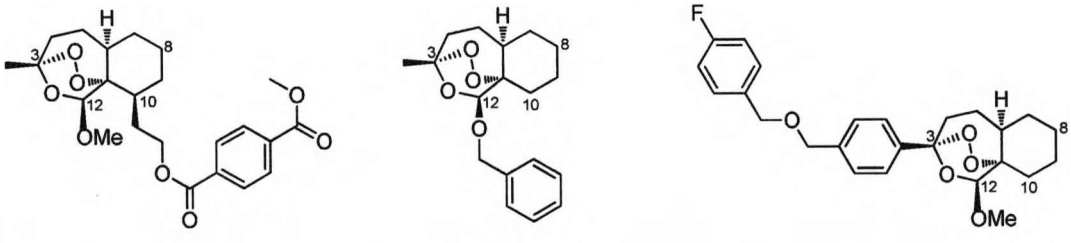

67a **67b** **67c**

Figure 1.35 *Artemisinin analogues **67a**[112], **67b**[113], and **67c**[114] with antimalarial activity comparable to that of the parent compound.*

This synthetic route, starting from cyclohexanone and pyrrolidine, was modified to facilitate an enantioselective synthesis.[39,42] The key step was the synthesis of the nitrile **70**, where an enamine reacting with a Michael acceptor in the presence of $MgCl_2$ proceeds with excellent enantiomeric excess. (*S*)-(-)-Pyrrolidine methanol **68**

provides the chiral starting material. The nitrile group of **71** allows for functionalisation of the C-3 position on the target **74**. Introduction of a *Z*-configured enol ether **71** allows for [2+2]-cycloaddition and subsequent intramolecular cyclisation to give **74**.

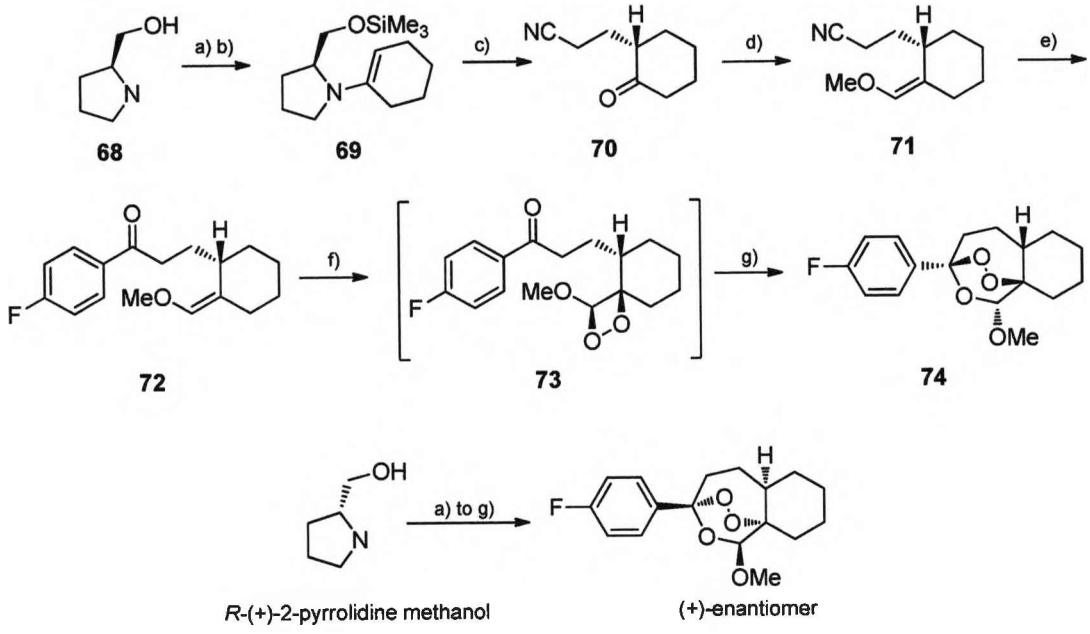

a) cyclohexanone, TsOH; b) TMSCl, DIPEA; c) acrylonitrile, $MgCl_2$; d) $Ph_3P^+CH_2OMeBr^-$, LDA; e) 4-F-PhLi; f) Methylene Blue, -78°C, O_2, hv; g) TBDMSOTf, Et_3N.

Figure 1.36 *Asymmetric synthesis of an antimalarial 1,2,4-trioxane via [2+2]-cycloaddition.*

The stereochemistry of the vinyl ether and the diastereospecific nature of the [2+2]-cycloaddition results in *si*-facial attack by singlet oxygen. Lewis acid catalysed dioxane opening and condensation to the trioxane is also stereoselective. The opposing enantiomer was easily synthesised using readily available (*R*)-(+)-pyrrolidine methanol as the starting material. Both enantiomers were obtained with 85% ee.

The eventual purpose of these enantiomerically pure artemisinin derivatives was to investigate the antimalarial activity of the opposing enantiomers. A difference in activity would have implications for the mechanism of action of artemisinin, *i.e.* a detrimental interaction with a specific protein target (*e.g. Pf*ATP6) rather than randomised attack of parasite macromolecules. However, the trioxane enantiomers showed the same level of *in vitro* antiparasitic activity arguing against specific interactions with a chiral protein or enzyme and supporting the achiral heme-activation hypothesis.

1.4.3 The Schenk-ene Reaction as a Route to 1,2,4-Trioxanes

In 1990, Singh and co-workers were first to use the synthesis of hydroperoxy alcohols in the context of 1,2,4-trioxanes as antimalarial agents.[115] The hydroperoxy alcohol intermediate **76** was stable enough to be handled at room temperature, and underwent condensation with cyclohexanone to afford the spirocyclic 1,2,4-trioxane **77** (Figure 1.37).

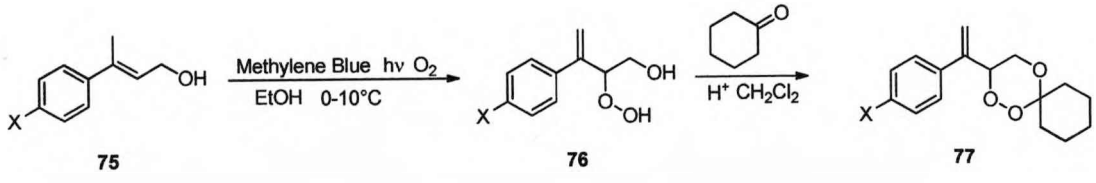

75 **76** **77**

Figure 1.37 *Synthesis of 1,2,4-trioxanes via hydroperoxy alcohols.*

1,2,4-Trioxane analogues have since been synthesised with aryl[115] and naphthyl[116,117] groups at the γ-position and withstood reductive amination conditions to furnish amino functionalised derivatives.[118]

Griesbeck and co-workers discussed in more depth the diastereoselectivity of the Schenk-ene reaction and its implications as a route to 1,2,4-trioxanes.[119] In order to characterise the major and minor isomers, the chiral allylic alcohol **78** underwent photooxygenation in methanol to give a 73:27 mixture of the *threo-* and *erythro-* hydroperoxy alcohol, **79** and **80** respectively (Figure 1.38).

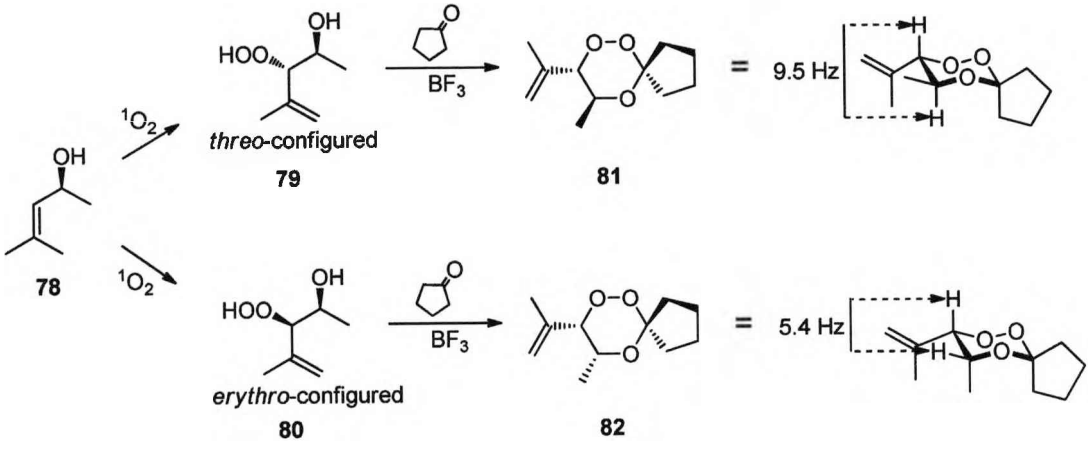

Figure 1.38 *NMR study of the coupling constants for cis- and trans-1,2,4-trioxanes.*

Condensation with cyclopentanone gave a *trans/cis* mixture of the 1,2,4-trioxane, **81/82** respectively. Measurement of the coupling constants unambiguously showed that the major diastereoisomer **81** has *trans*-configuration (J = 9.5 Hz) residual from the *threo*-hydroperoxyalcohol. Correspondingly, the minor diastereoisomer **82** displayed *cis*-configuration (J = 5.4 Hz) due to the *erythro*-starting material.

Griesbeck later reported on a number of spiroanellated 1,2,4-trioxanes, synthesised by the same route, with excellent antimalarial activities.[120] The spirocyclic products were derived from cyclic ketones and from antimalarial evaluation a clear structure activity relationship emerged:

monocyclic<spirocyclopentyl<spirocyclohexyl<spirocycloadamantyl.

The spirocycloadamantyl derivative **83** (Figure 1.39) demonstrated activity against *P. falciparum* in the range of artemisinin.

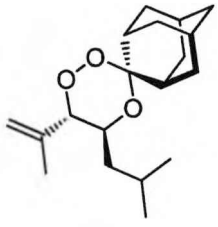

83

Figure 1.39 *Most potent antimalarial spirocyclic 1,2,4-trioxane in the series.*

83 was characterised by X-ray crystallography studies, which showed that the central trioxane adopts a near perfect cyclohexane chair conformation with substituents at C-5 and C-6 in an equatorial position.

1.5 Summary

1) Artemisinin has emerged as a mainstay in the treatment of advanced cases of malaria, its mechanism of action initiated by the cleavage of the endoperoxide bridge. Proposed parasite targets include: a) causing oxidative stress at lipid targets, b) alkylation of heme, c) inhibition of parasitic enzymes (*e.g.* cysteine proteases, NADH dehydrogenase, ATPase).

2) Synthetic 1,2,4-trioxanes incorporate the endoperoxide pharmacophore and have exhibited excellent antimalarial activity.

3) A popular route to 1,2,4-trioxanes is the use of singlet oxygen to generate the peroxide functionality and subsequent condensation with an aldehyde or ketone.

4) Excited state singlet oxygen is most commonly generated from ground state triplet oxygen *via* dye-sensitised photooxygenation. The sensitiser is excited by a photon of light and intersystem crossing allows for energy transfer to molecular oxygen and excitation to the singlet state.

5) Singlet oxygen reacts through 3 major pathways: a) [4+2]-cycloaddition to give 1,4-endoperoxides, b) [2+2]-cycloaddition to give 1,2-dioxetanes, c) ene-reaction to give hydroperoxides.

6) Singlet oxygen reacts in a highly regio- and stereospecific manner. One of the most diastereoselective examples is the photooxygenation of allylic alcohols demonstrating high *threo*-selectivity in non-protic solvents.

7) Acid catalysed treatment of 1,4-endoperoxides, 1,2-dioxetanes and hydroperoxy alcohols with cyclic ketones furnishes *cis*-fused and spirocyclic 1,2,4-trioxanes, where diastereoselectivity is conferred to the 1,2,4-trioxane target.

1.6 References

(1) Klayman, D. L., Lin, A. J., Acton, N., Scovill, J. P., Hoch, J. M., Milhous, W. K., Theoharides, A. D., Dobek, A. S., *J. Nat. Prod.* **1984**, *47*, 715-717.

(2) van Agtmael, M. A., Eggelte, T. A., van Boxtel, C. J., *Trends Phar.* **1999**, *20*, 199-205.

(3) China Cooperative Research Group *J. Trad. Chinese Med.* **1982**, *2*, 45.

(4) Brossi, A., Venugopalan, B., Dominguez Gerpe, L., Yeh, H. J. C., Flippen-Anderson, J. L., Buchs, P., Luo, X. D., Milhous, W., Peters, W., *J. Med. Chem.* **1988**, *31*, 645-650.

(5) O'Neill, P. M., Scheinmann, F., Stachulski, A. V., Maggs, J. L., Park, B. K., *J. Med. Chem.* **2001**, *44*, 1467-1470.

(6) Golenser, J., Waknine, J. H., Krugliak, M., Hunt, N. H., Grau, G. E., *Int. J. Parasit.* **2006**, *36*, 1427-1441.

(7) www.who.int/malaria/docs/TreatmentGuidelines2006.pdf.

(8) Vyas, N., Avery, B. A., Avery, M. A., Wyandt, C. M., *Antimicrob. Agents Chemother.* **2002**, *46*, 105-109.

(9) Klayman, D. L. *Science* **1985**, *228*, 1049-1055.

(10) Jefford, C. W., Vicente, M. G. H., Jacquier, Y., Favarger, F., Mareda, J., Millasson-Schmidt, P., Brunner, G., Burger, U., *Helv. Chim. Acta* **1996**, *79*, 1475-1487.

(11) Posner, G. H., Oh, C. H., *J. Am. Chem. Soc.* **1992**, *114*, 8328-8329.

(12) Jefford, C. W., Favarger, F., Vicente, M. H., Jacquier, Y., *Helv. Chim. Acta* **1995**, *78*, 452-458.

(13) Posner, G. H., Oh, C. H., Wang, D., Gerena, L., Milhous, W. K., Meshnick, S. R., Asawamahasadka, W., *J. Med. Chem.* **1994**, *37*, 1256-1258.

(14) Wu, W., Wu, Y., Wu, Y., Yao, Z., Zhou, C., Li, Y., Shan, F., *J. Am. Chem. Soc.* **1998**, *120*, 3316-3325.

(15) Butler, A. R., Gilbert, B. C., Hulme, P., Irvine, L. R., Renton, L., Whitwood, A. C., *Free Rad. Res.* **1998**, *28*, 471-476.

(16) Alberti, A., Macciantelli, D., Marconi, G., *Res. Chem. Intermed.* **2004**, *30*, 615-625.

(17) O'Neill, P. M., Miller, A., Bishop, L. P. D., Hindley, S., Maggs, J. L., Ward, S. A., Roberts, S. M., Scheinmann, F., Stachulski, A. V., Posner, G. H., Park, B. K., *J. Med. Chem.* **2001**, *44*, 58-68.

(18) Wu, Y. *Acc. Chem. Res.* **2002**, *35*, 255-259.

(19) Wu, Y., Yue, Z., Liu, H., *Helv. Chim. Acta* **2001**, *84*, 928-932.

(20) Haynes, R. K., Vonwiller, S. C., *Tet. Lett.* **1996**, *37*, 253-256.

(21) Haynes, R., K., Vonwiller, S. C., *Tet. Lett.* **1996**, *37*, 257-260.

(22) Krungkrai, S. R., Yuthavong, Y., *Trans. Roy. Soc. Trop. Med. Hyg.* **1987**, *81*, 710-714.

(23) Berman, P. A., Adams, P. A., *Free Rad. Biol. Med.* **1997**, *22*, 1283-1288.

(24) Fitch, C. D., Cai, G. Z., Chen, Y. F., Shoemaker, J. D., *Biochim. Biophys. Acta* **1999**, *1454*, 31-37.

(25) Hartwig, C. L., Rosenthal, A. S., D'Angelo, J., Griffin, C. E., Posner, G. H., Cooper, R. A., *Biochem. Pharmacol.* **2009**, *77*, 322-336.

(26) Meshnick, S. R., Thomas, A., Ranz, A., Xu, C., Pan, H., *Mol. Biochem. Parasit.* **1991**, *49*, 181-189.

(27) Hong, Y., Yang, Y., Meshnick, S. R., *Mol. Biochem. Parasit.* **1994**, *63*, 121-128.

(28) Robert, A., Meunier, R., *Chem. Soc. Rev.* **1998**, *27*, 273-279.

(29) Robert, A., Bonduelle, C., Laurent, S. A. L., Meunier, B., *J. Phys. Org. Chem.* **2006**, *19*, 562-569.

(30) Robert, A., Cazelles, J., Meunier, B., *Angew. Chem. Int. Ed.* **2001**, *40*, 1954-1957.

(31) Cazelles, J., Robert, A., Meunier, B., *Comptes Rendus Acad. Sci. Ser. IIC* **2001**, *4*, 85-89.

(32) Cazelles, J., Robert, A., Meunier, B., *J. Org. Chem.* **2002**, *67*, 609-619.

(33) Creek, D. J., Charman, W. N., Chiu, F. C. K., Prankerd, R. J., Dong, Y., Vennerstrom, J. L., Charman, S. A., *Antimicrob. Agents Chemother.* **2008**, *52*, 1291-1296.

(34) Pandey, A. V., Tekwani, B. L., Singh, R. L., Chauhan, V. S., *J. Biol. Chem.* **1999**, *274*, 19383-19388.

(35) Haynes, R. K., Krishna, S., *Microb. Infect.* **2004**, *6*, 1339-1346.

(36) Eckstein-Ludwig, U., Webb, R. J., van Goethem, I. D. A., East, J. M., Lee, A. G., Kimura, M., O'Neill, P. M., Bray, P. G., Ward, S. A., Krishna, S., *Nature* **2003**, *424*, 957-961.

(37) Jung, M., Kim, H., Nam, K. Y., No, K. T., *Bioorg. Med. Chem. Lett.* **2005**, *15*, 2994-2997.

(38) Jefford, C. W., Kohmoto, S., Jaggi, D., Timári, G., Rossier, J., Rudaz, M., Barbuzzi, O., Gérard, D., Burger, U., Kamalaprija, P., Mareda, J., Bernardinelli, G., Manzanares, I., Canfield, C. J., Feck, S. L., Robinson, B. L., Peters. W., *Helv. Chim. Acta* **1995**, *78*, 647-662.

(39) O'Neill, P. M., Rawe, S. L., Borstnik, K., Miller, A., Ward, S. A., Bray, P. G., Davies, J., Oh, C. H., Posner, G. H., *ChemBioChem* **2005**, *6*, 2048-2054.

(40) Li, W., Mo, W., Shen, D., Sun, L., Wang, J., Lu, S., Gitschier, J. M., Zhou, B., *PLoS Genet* **2005**, *1*, e36.

(41) Jefford, C. W., Velarde, J. A., Bernardinelli, G., Bray, D. H., Warhurst, D. C., Milhous, W. K., *Helv. Chim. Acta* **1993**, *76*, 2775-2788.

(42) O'Neill, P. M., Miller, A., Bickley, J. F., Scheinmann, F., Oh, C. H., Posner, G. H., *Tet. Lett.* **1999**, *40*, 9133-9136.

(43) Singh, C., Misra, D., Saxena, G., Chandra, S., *Bioorg. Med. Chem. Lett.* **1992**, 2, 497-500.

(44) Greer, A. *Acc. Chem. Res.* **2006**, *39*, 797-804.

(45) Mulliken, R. S. *Nature* **1928**, *122*, 505-505.

(46) Mulliken, R. S. *Rev. Mod. Phys.* **1932**, *4*, 1.

(47) Kautsky, H., de Bruijn, H., *Naturwissenschaften* **1931**, *19*, 1043-1043.

(48) Blum, H. F. *Physiol. Rev.* **1945**, *25*, 483-530.

(49) Kautsky, H. *Biochem. Zeitschrifte* **1937**, *291*, 271-284.

(50) Khan, A. U., Kasha, M., *J. Chem. Phys.* **1963**, *39*, 2105-2106.

(51) Khan, A. U., Kasha, M., *Nature* **1964**, *204*, 241-243.

(52) Khan, A. U., Kasha, M., *J. Am. Chem. Soc.* **1970**, *92*, 3293-3300.

(53) Wasserman, E., Murray, R. W., Kaplan, M. L., Yager, W. A., *J. Am. Chem. Soc.* **1968**, *90*, 4160-4161.

(54) Wasserman, E., Kuck, V. J., Delavan, W. M., Yager, W. A., *J. Am. Chem. Soc.* **1969**, *91*, 1040-1041.

(55) Kearns, D. R., Khan, A. U., Duncan, C. K., Maki, A. H., *J. Am. Chem. Soc.* **1969**, *91*, 1039-1040.

(56) Foote, C. S. *Acc. Chem. Res.* **1968**, *1*, 104-110.

(57) Kopecky, K. R., Reich, H. J., *Can. J. Chem.* **1965**, *43*, 2265-2270.

(58) Foote, C. S., Wexler, S., Ando, W., *Tet. Lett.* **1965**, *6*, 4111-4118.

(59) Kearns, D. R. *Chem. Rev.* **1971**, *71*, 395-427.

(60) Foote, C. S., Wexler, S., Ando, W., Higgins, R., *J. Am. Chem. Soc.* **1968**, *90*, 975-981.

(61) Aubry, J. M. *J. Am. Chem. Soc.* **1985**, *107*, 5844-5849.

(62) Pierlot, C., Nardello, V., Schrive, J., Mabille, C., Barbillat, J., Sombret, B., Aubry, J., *J. Org. Chem.* **2002**, *67*, 2418-2423.

(63) Murray, R. W., Kaplan, M. L., *J. Am. Chem. Soc.* **1969**, *91*, 5358-5364.

(64) Evans, D., Upton, M., *J. Chem. Soc., Dalton Trans.* **1985**, 1141-1145.

(65) Turro, N. J., Chow, M. F., *J. Am. Chem. Soc.* **1981**, *103*, 7218-7224.

(66) Wasserman, H. H., Scheffer, J. R., *J. Am. Chem. Soc.* **1967**, *89*, 3073-3075.

(67) Clennan, E. L. *Tetrahedron* **1991**, *47*, 1343-1382.

(68) Frimer, A. A. *Chem. Rev.* **1979**, *79*, 359-387.

(69) Rigaudy, J., Capdevielle, P., Combrisson, S., Maumy, M., *Tet. Lett.* **1974**, *15*, 2757-2760.

(70) Gollnick, K., Griesbeck, A., *Tetrahedron* **1984**, *40*, 3235-3250.

(71) Gollnick, K., Griesbeck, A., *Tet. Lett.* **1984**, *25*, 725-728.

(72) Koch, E. *Tetrahedron* **1968**, *24*, 6295-6318.

(73) Aubry, J., Mandard-Cazin, B., Rougee, M., Bensasson, R. V., *J. Am. Chem. Soc.* **1995**, *117*, 9159-9164.

(74) Gorman, A. A., Hamblett, I., Lambert, C., Spencer, B., Standen, M. C., *J. Am. Chem. Soc.* **1988**, *110*, 8053-8059.

(75) Gorman, A. A., Gould, I. R., Hamblett, I., *J. Am. Chem. Soc.* **1982**, *104*, 7098-7104.

(76) Asveld, E. W. H., Kellogg, R. M., *J. Am. Chem. Soc.* **1980**, *102*, 3644-3646.

(77) Wilson, S. L., Schuster, G. B., *J. Am. Chem. Soc.* **1983**, *105*, 679-681.

(78) Nickon, A., Bagli, J. F., *J. Am. Chem. Soc.* **1961**, *83*, 1498-1508.

(79) Gollnick, K., Schenk, G. O., *Pur. App. Chem.* **1964**, *83*, 507-525.

(80) Orfanopoulos, M., Grdina, Sr. M. B., Stephenson, L. M., *J. Am. Chem. Soc.* **1979**, *101*, 275-276.

(81) Harding, L. B., Goddard, W. A., *J. Am. Chem. Soc.* **1980**, *102*, 439-449.

(82) Orfanopoulos, M., Smonou, I., Foote, C. S., *J. Am. Chem. Soc.* **1990**, *112*, 3607-3614.

(83) Jefford, C. W. *Tet. Lett.* **1979**, *20*, 985-988.

(84) Jefford, C. W., Kohmoto, S., Boukouvalas, J., Burger, U., *J. Am. Chem. Soc.* **1983**, *105*, 6498-6499.

(85) Jefford, C. W. *Chem. Soc. Rev.* **1993**, 59-66.

(86) Sharp, D. B. In *139th Meeting of the American Chemical Society*; American Chemical Society: New York, 1960, p 79.

(87) Kearns, D. R. *J. Am. Chem. Soc.* **1969**, *91*, 6554-6563.

(88) Fenical, W. H., Kearns, D. R., Radlick, P., *J. Am. Chem. Soc.* **1969**, *91*, 3396-3398.

(89) Inagaki, S., Fukui, K., *J. Am. Chem. Soc.* **1975**, *97*, 7480-7484.

(90) Inagaki, S., Fujimoto, H., Fukui, K., *Chem. Lett.* **1976**, 749-752.

(91) Dewar, M., J. S., Thiel, W., *J. Am. Chem. Soc.* **1975**, *97*, 3978-3986.

(92) Stephenson, L. M., Grdina, M. J., Orfanopoulos, M., *Acc. Chem. Res.* **1980**, *13*, 419-425.

(93) Stratakis, M., Orfanopoulos, M., Chen, J. S., Foote, C. S., *Tet. Lett.* **1996**, *37*, 4105-4108.

(94) Grdina, M. B., Orfanopoulos, M., Stephenson, L. M., *J. Am. Chem. Soc.* **1979**, *101*, 3111-3112.

(95) Orfanopoulos, M., Foote, C. S., *J. Am. Chem. Soc.* **1988**, *110*, 6583-6584.

(96) Orfanopoulos, M., Stephenson, L. M., *J. Am. Chem. Soc.* **1980**, *102*, 1417-1418.

(97) Rousseau, G., Le Perchec, P., Conia, J. M., *Tet. Lett.* **1977**, *18*, 2517-2520.

(98) Lerdal, D., Foote, C. S., *Tet. Lett.* **1978**, *19*, 3227-3230.

(99) Adam, W., Catalani, L. H., Griesbeck, A., *J. Org. Chem.* **1986**, *51*, 5494-5496.

(100) Stratakis, M., Orfanopoulos, M., Foote, C. S., *Tet. Lett.* **1991**, *32*, 863-866.

(101) Clennan, E. L., Chen, M., Xu, G., *Tet. Lett.* **1996**, *37*, 2911-2914.

(102) Stratakis, M., Orfanopoulos, M., *Tetrahedron* **2000**, *56*, 1595-1615.

(103) Clennan, E. L. *Tetrahedron* **2000**, *56*, 9151-9179.

(104) Schulte-Elte, K. H., Rautenstrauch, V., *J. Am. Chem. Soc.* **1980**, *102*, 1738-1740.

(105) Stephenson, L. M. *Tet. Lett.* **1980**, *21*, 1005-1008.

(106) Houk, K. N., Williams, J. C., Mitchell, P. A., Yamaguchi, K., *J. Am. Chem. Soc.* **1981**, *103*, 949-951.

(107) Adam, W., Nestler, B., *J. Am. Chem. Soc.* **1992**, *114*, 6549-6550.

(108) Adam, W., Nestler, B., *J. Am. Chem. Soc.* **1993**, *115*, 5041-5049.

(109) Bruenker, H., Adam, W., *J. Am. Chem. Soc.* **1995**, *117*, 3976-3982.

(110) Jefford, C. W., Jaggi, D., Boukouvalas, J., Kohmoto, S., *J. Am. Chem. Soc.* **1983**, *105*, 6497-6498.

(111) Jefford, C. W., Jin, S., Bernardinelli, G., *Helv. Chim. Acta* **1997**, *80*, 2440-2455.

(112) Posner, G. H., Oh, C. H., Gerena, L., Milhous, W. K., *J. Med. Chem.* **1992**, *35*, 2459-2467.

(113) Posner, G. H., Oh, C. H., *Heteroat. Chem.* **1995**, *6*, 105-116.

(114) Posner, G. H., Cumming, J. N., Woo, S., Ploypradith, P., Xie, S., Shapiro, T. A., *J. Med. Chem.* **1998**, *41*, 940-951.

(115) Singh, C. *Tet. Lett.* **1990**, *31*, 6901-6902.

(116) Singh, C., Kanchan, R., Srivastava, D., Puri, S. K., *Bioorg. Med. Chem. Lett.* **2006**, *16*, 584-586.

(117) Griesbeck, A. G., El-Idreesy, T. T., Lex, J., *Tetrahedron* **2006**, *62*, 10615-10622.

(118) Singh, C., Malik, H., Puri, S. K., *Bioorg. Med. Chem. Lett.* **2004**, *14*, 459-462.

(119) Griesbeck, A. G., El-Idreesy, T. T., Fiege, M., Brun, R., *Org. Lett.* **2002**, *4*, 4193-4195.

(120) Griesbeck, A. G., El-Idreesy, T. T., Höinck, L., Lex, J., Brun, R., *Bioorg. Med. Chem. Lett.* **2005**, *15*, 595-597.

2.0 Results and Discussion - Endoperoxides as Antimalarials and the Application of Singlet Oxygen to the Synthesis of Key Synthetic Intermediates en Route to Synthetic 1,2,4-Trioxanes

Previously, Singh[1] and Griesbeck[2] have synthesised racemic trioxanes similar to trioxanes **89a-f** and reported excellent *in vitro* antimalarial activities against the K1 strain of *P.falciparum*. Given the promising profile of some of these endoperoxides we were interested in developing a general enantioselective route to 1,2,4-trioxanes in this class.

The hydroxy-directed regio- and diastereoselective photooxygenation of chiral allylic alcohols, to yield allylic hydroperoxides, was first discovered by Adam *et al.*[3] The synthesis of 1,2,4-trioxanes *via* dye-sensitised photooxygenation of achiral allylic alcohols to obtain hydroperoxy alcohols and the subsequent acid catalysed peroxyacetalisation with cyclic ketones has been used by Chandan Singh to access 1,2,4-trioxanes similar to **89a-f**.[1,4-7] The stereoselectivity of both reaction steps has been elucidated further by Griesbeck who has synthesised racemic *threo*-β-hydroperoxy alcohols that were in turn used to synthesise diastereomerically pure racemic chiral 1,2,4-trioxanes.[2,8] To our knowledge no one has ever reported the synthesis of enantiomerically enriched chiral 1,2,4-trioxanes. This chapter describes the development of a facile route to enantiomerically enriched 1,2,4-trioxanes *via* chiral allylic alcohols. We have also evaluated phosphite ozonide adducts, a chemical source of singlet oxygen, as an alternative to traditional dye-sensitised photochemical methods of oxygenation. Preliminary *in vitro* antimalarial activity of a series of individual conformers of enantiomerically enriched 1,2,4-trioxanes is also reported.

2.1 Threo-Selective Photooxygenation of Allylic Alcohols and the Synthesis of Racemic 1,2,4-Trioxanes

2.1.1 Threo-Selective Photooxygenation of Allylic Alcohols

2.1.1.1 Threo-Selective Photooxygenation of Mesityl Allylic Alcohol 78

To confirm the diastereomeric ratio and *threo*-selectivity reported by Griesbeck *et al.*[2], we performed photooxygenation of racemic allylic alcohol **78** which was obtained *via* $LiAlH_4$ reduction of mesityl oxide **84**.

Using tetraphenylporphine (TPP) as a sensitiser dye, photooxygenation of **78** was carried out in dichloromethane by irradiating with a single 400W tungsten lamp for 4 hours (Scheme 2.1).

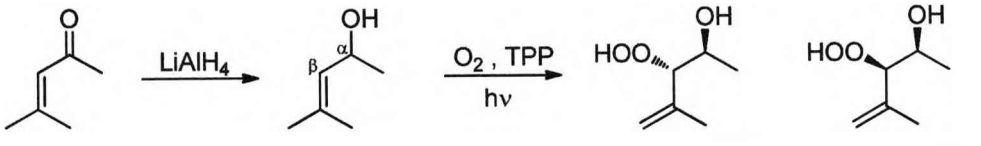

84 **78** 82% **79** (*threo*) 54% yield **80** (*erythro*)
d.r., *threo*:*erythro* = 90:10

Scheme 2.1 *Reagents and conditions:* i) $LiAlH_4$, EtO_2, 0 °C, 30 mins: ii) O_2, TTP, CH_2Cl_2, hν, 0 °C, 4 hr.

The reaction showed excellent diastereoselectivity (d.r., *threo*:*erythro* = 90:10), which was calculated using ^1H NMR spectroscopy on the crude reaction mixture. A doublet at δ 4.17 ($J_{H\alpha\text{-}H\beta}$ = 8.3 Hz) corresponds to the major *threo*-isomer **79** and the doublet at δ 4.31 ($J_{H\alpha\text{-}H\beta}$ = 4.6 Hz) indicates the presence of the *erythro*-configured isomer **80**. The crude reaction mixture was visualised on t.l.c. with *p*-anisaldehyde and showed the two diastereoisomers as two close spots staining purple, typical of

the peroxide moiety. The major *threo*-product was easily purified from the minor by column chromatography in 46% yield. Repeating the photooxygenation of **78** with an additional tungsten lamp resulted in the *threo*-isomer being isolated in 54% yield. After four hours of reaction time, there still remained some unreacted starting material. When the reaction time was increased to 16 hours, no increase in yield was observed. Monitoring by t.l.c. showed an impurity forming at the base of the plate after 4 hours of reaction and the intensity of this spot increased as the reaction progressed. Interestingly, the aeration of the solution with a stream of pure oxygen was not imperative, as it was observed that using a stream of compressed air in its place had no detrimental effect on the yield.

The volatility of the solvent and starting material also posed a problem, as the heat produced by the lamp and the air passing through the reaction caused it to evaporate, presumably before conversion occurred. To avoid the evaporation of the solvent a system to cool the flask was also needed. It was found that the most effective and easy to maintain, was to have a stream of water flowing around the outside of the flask.

2.1.1.2 Photooxygenation Conditions on Solid Support Media

Griesbeck[9] and co-workers also outlined a procedure for photooxygenation in a solvent-free system using a polystyrene solid support. In this set-up the sensitiser and substrate were pre-loaded onto the support media sequentially. The dry mixture was then irradiated for 4 hours. The product, and any remaining starting material, was then washed from the polystyrene support using methanol, leaving the sensitiser behind, still loaded onto the polystyrene. This was a great advantage as removal of

the TPP from the product by chromatography was a lengthy process. Moreover, solvent levels did not need to be constantly topped up. The desired *threo*-isomer was obtained in 47% yield.

However, ^{1}H NMR spectroscopy showed that the reaction performed on the solid support showed reduced diastereoselectivity (d.r., *threo*:*erythro* = 70:30) in contrast to the 90:10 selectivity obtained using the dichloromethane solvent system. Due to the reduced selectivity and a moderate yield of 47% under solid support conditions, all the succeeding photooxygenation reactions were carried out in dichloromethane.

The loading and removal of the substrate and TPP from the solid support media did allow us to readdress the problem of purification by column chromatography. Purification of the reaction mixture by column chromatography using a EtOAc/Hexane solvent system led to the contamination of the desired product with TPP. As TPP is soluble in CH_2Cl_2 whereas the oxygenated substrates are insoluble, all TPP was successfully removed from the column first by flushing with CH_2Cl_2. Thereafter the original EtOAc/Hexane eluent system could be applied to successfully purify the hydroperoxy alcohol.

2.1.1.3 Threo-Selective Photooxygenation of Benzylic Allylic Alcohol **87**

In an effort to make the photooxygenation step more efficient, we used a less volatile substrate with a higher molecular weight. A Grignard reaction was chosen as a suitable route to the racemic allylic alcohol **87**. The addition reaction of commercially available 2-methyl-1-propenyl magnesium bromide **86** to phenacetaldehyde **85**, afforded 4-methyl-1-phenyl-3-penten-2-ol **87** in 48% yield (Scheme 2.2).

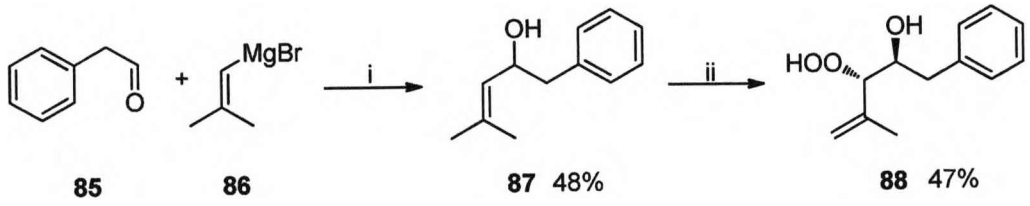

Scheme 2.2 *Reagents and conditions:* i) THF, -78 °C→r.t., 2 hr: ii) O_2, TTP, CH_2Cl_2, hv, 0 °C, 4 hr.

Photooxygenation of the benzyl substituted substrate **87**, gave the expected product, 3-hydroperoxy-4-methyl-1-phenyl-4-penten-2-ol **88**. However, no significant increase in yield was observed.

2.1.2 Synthesis of Racemic 1,2,4-Trioxanes

Jefford[10,11] previously demonstrated that acid-catalysed cyclisation of hydroperoxy alcohols with aldehydes and ketones afforded monocyclic and spirocyclic 1,2,4-trioxanes respectively. Previously employed Lewis acid catalysts include Amberlyst-15,[10] TMSOTf[12] and $BF_3.Et_2O$.[8] With two hydroperoxy alcohol intermediates in hand, **79** and **88**, we attempted the final peroxyacetalisation to give the desired 1,2,4-trioxanes **89a-f** (Scheme 2.3).

The allylic hydroperoxy alcohols **79** and **88** were treated with cyclic ketones: cyclopentanone, cyclohexanone and 2-adamantanone to obtain the six racemic 1,2,4-trioxanes **89a-f** in moderate yield. Initially, $BF_3.Et_2O$ was used to catalyse the reaction, but *p*-TsOH was found to be more convenient and afforded up to a 20% increase in yield in some cases.

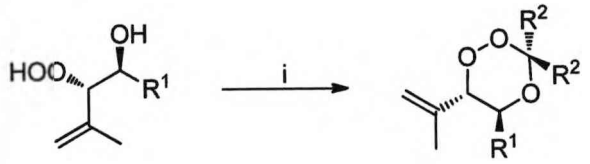

R^1 = Me **79**	R^1 = Me	R^2 = cyclopentyl	**89a**	26%
R^1 = Bn **88**	R^1 = Me	R^2 = cyclohexyl	**89b**	40%
	R^1 = Me	R^2 = adamantyl	**89c**	42%
	R^1 = Bn	R^2 = cyclopentyl	**89d**	42%
	R^1 = Bn	R^2 = cyclohexyl	**89e**	20%
	R^1 = Bn	R^2 = adamantyl	**89f**	12%

Scheme 2.3 *Reagents and conditions:* i) TsOH, R^2C =O, CH_2Cl_2, -10 °C, 30 min. *Hashed and bold wedged bonds differentiate between diastereoisomers.*

2.2 Enantioselective Synthesis of 1,2,4-Trioxanes via Diastereoselective Ene Reaction of Chiral cis-Allylic Alcohols

We then wanted to apply the highly efficient, stereoselective ene reaction to a chiral substrate in order to synthesise enantiomerically enriched 1,2,4-trioxanes. A *cis*-allylic alcohol was identified as a suitable substrate as it would only allow allylic H-abstraction from its single methyl substituent ensuring consistent regiochemistry between the desired products. Although the ene reaction is reported as demonstrating proficient regioselectivity, favouring H-abstraction from the most congested side of the olefin, we chose to make certain of H-abstraction from only one position.

2.2.1 Synthesis of the Chiral cis-Allylic Alcohol via Enantioselective Reduction of a Propargyl Ketone

We initially intended to synthesise propargyl alcohol ***R*-93a** by following a procedure outlined by Midland[13] and co-workers (Scheme 2.4).

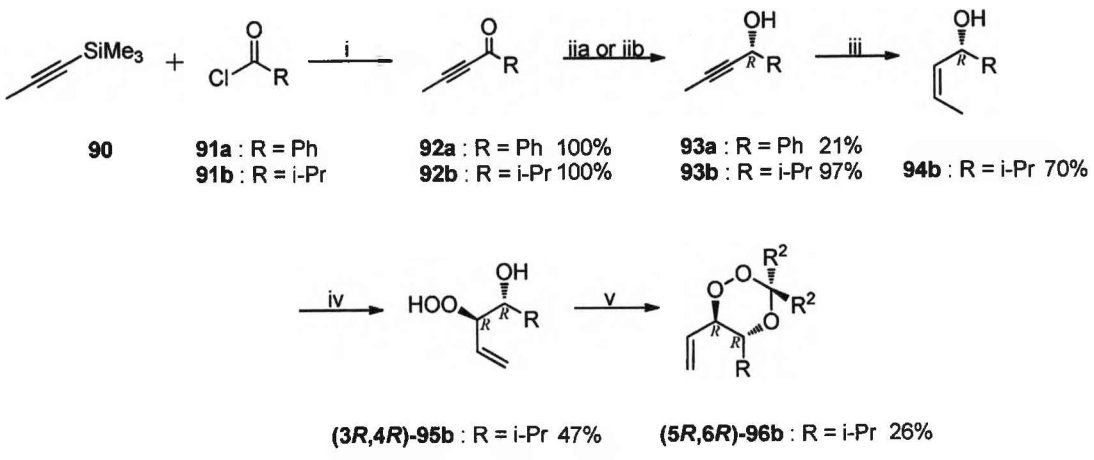

Scheme 2.4 *Reagents and conditions:* i) $AlCl_3$, CH_2Cl_2, 0 °C, 30 min: iia) (*R*)-Alpine-borane, propanal, H_2O_2, r.t., 16 hr: iib) $[Cp^*RhCl_2]_2$, (*R,R*)-TsDPEN, H_2O, NaOOCH, r.t., 2 hr: iii) Lindlar catalyst, 2,6-lutidine, H_2, n-Hex: iv) O_2, TTP, CH_2Cl_2, hν, 0 °C, 4 hr: v) *p*-TsOH, $R^2C{=}O$, CH_2Cl_2, -10 °C, 30 min.

The synthesis started with the treatment of trimethylsilylpropyne **90** with benzoyl chloride **91a** and $AlCl_3$ in dichloromethane at 0 °C for 30 minutes. This afforded 1-phenyl-2-butyn-1-one **92a** in quantitative yield.

It is well documented that during the asymmetric reduction of ketones by Alpine-borane, isopropyl groups impart additional selectivity. Therefore, isobutyryl chloride **91b** was selected for treatment with 1-trimethylsilylpropyne **90**. Similar reaction conditions and purification by Kugelrohr distillation furnished 2-methyl-hex-4-yn-3-one **92b** in quantitative yield.

At this point a sample of racemic alcohol was also synthesised, again using $LiAlH_4$ reduction conditions. Use of this expendable substrate in further reaction steps was informative in determining their efficiency without wasting valuable chiral material.

The racemic alcohol was also useful as a control for analysis of the enantiomeric purity of our chiral substrates by GC and NMR.

1-Phenyl-2-butyn-1-one **92a** was treated with concentrated (*R*)-Alpine-borane and allowed to react overnight at room temperature. Propionaldehyde was then added to destroy the Alpine-borane adduct, and the liberated (+)-α-pinene was removed *in vacuo*. The reaction was then quenched and purified by an oxidative work-up, column chromatography and Kugelrohr distillation at 100°C. This afforded 1-phenyl-2-butyn-1-ol ***R*-93a** in 21% yield.

The reduction of 2-methyl-4-hexyn-3-one **92b** by (*R*)-Alpine borane was also attempted; however, we had limited success. The desired product was observed on t.l.c. but could not be isolated and characterised.

As a result of the poor yields and the problematic workup, involving an inert nitrogen atmosphere throughout, we decided to explore alternative methods of asymmetric acetylenic ketone reduction. A Sharpless kinetic resolution of the secondary allylic alcohol was discounted as *Z*-disubstituted allylic alcohols were reported to be poor substrates and loss of half of our material was not ideal.[14]

An alternative synthetic route was chosen which involved Rh catalysed asymmetric transfer hydrogenation (ATH). Noyori and co-workers[15] first reported the ATH of acetylenic ketones using a chiral Ru(II)/diamine catalyst complex and 2-propanol as the hydrogen donor. For our purposes, we followed a procedure outlined by Wu *et al.*[16] It was reported that the ATH of aromatic ketones, catalysed by the Ru(II), Rh(III) and Ir(III) complexes of β-amino alcohols, can be carried out smoothly in water using NaOOCH as a hydrogen donor.

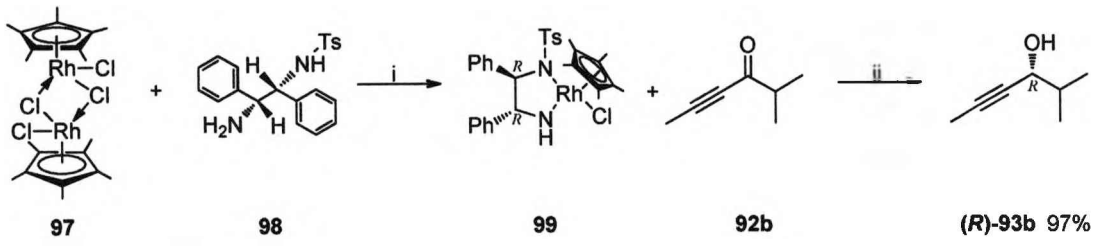

97 **98** **99** **92b** **(*R*)-93b** 97%

Scheme 2.5 *Reagents and conditions:* i) H_2O, 40 °C, 1 hr: ii) NaOOCH, r.t., 2 hr.

The pre-catalyst **99** was formed by stirring $[Cp^*RhCl_2]_2$ **97** and the ligand, (*R,R*)-TsDPEN **98** in water at 40 °C for an hour until a clear orange solution was formed (Scheme 2.5). Sodium formate, the hydrogen source, and 2-methyl-4-hexyn-3-one **92b** were finally added and the mixture was allowed to react for 2 hours with fast stirring. The product was extracted with ether and then purified by Kugelrohr distillation at 100 °C to give **(*R*)-93b** as a clear oil. Facile synthesis of the opposing enantiomer **(*S*)-93b** was performed using the (*S,S*)-TsDPEN/$[Cp^*RhCl_2]_2$ catalyst complex.

Analysis by chiral gc showed a conversion of >97% and showed the formation of one single enantiomer. This was confirmed by NMR analysis of the corresponding Mosher's ester (Scheme 2.6).[17]

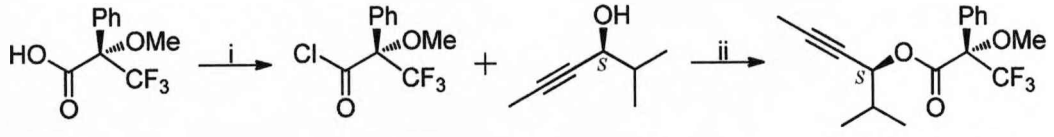

100 **101** **(*S*)-93b** **(*S*)-102** 6%

Scheme 2.6 *Reagents and conditions:* i) $SOCl_2$, NaCl, reflux, 16 hr: ii) pyridine, CH_2Cl_2, r.t., 12 hr.

Firstly the acid chloride was prepared by refluxing MTPA **100** with thionyl chloride and NaCl overnight. The thionyl chloride was removed *in vacuo* and the acid chloride **101** was used immediately to synthesise Mosher's esters ((***S***)-**102** and ***rac***-**102**) of both the *S*-configured substrate (***S***)-**93b** and an analogous racemic sample ***rac***-**93b**.

^{19}F NMR analysis of (***S***)-**102** showed a single peak at δ -71.56 ppm. In contrast, the racemic product ***rac***-**102** shows peaks at δ -71.56 ppm and δ -71.58 ppm confirming the enantiomeric purity of (***S***)-**93b**.

Lindlar catalyst, $Pd/CaCO_3$, is well known for the reduction of alkynes to alkenes in 100% *cis*-geometry. The presence of the alkyne moiety in our substrate gave us the geometric control needed to introduce the *cis*-alkene (Scheme 2.4). The control of the catalyst to only reduce to the alkene level is brought about by poisoning of the Pd with Pb and the inclusion of small amounts of 2,6-lutidine in the reaction mixture.

A solution of (***R***)- or (***S***)-**93b**, Lindlar catalyst and 2,6-lutidine in hexane was stirred vigorously under a H_2 atmosphere. H_2 uptake was monitored throughout the reaction and the reaction stopped once the required volume of H_2 was consumed. The reaction could not be monitored by t.l.c. as both substrate and product had identical R_F values. Full consumption of the starting material was important as the similarity in boiling point and polarity between the substrate and the product made purification by distillation or chromatography impossible. The reaction mixture was filtered through Celite to remove the catalyst and the organic extracts were washed with dil. HCl to remove the 2,6-lutidine. Finally, Kugelröhr distillation ensured complete removal of any remaining catalyst and impurities giving (***R***)- or (***S***)-**94b** as a pale yellow oil in 70% yield.

It is worth noting that a major hindrance, up to this point of the synthesis, was the low molecular weight and volatility of the substrates. All solvents had to be removed by simple distillation and at no point could a vacuum be applied without risking evaporation of the products.

2.2.2 Photooxygenation of the Chiral cis-Allylic Alcohol and a Modified Reaction Set-up.

Photooxygenation (Scheme 2.4) of the *cis*-allylic alcohol ***rac*-94b** was initially carried out as described in Scheme 2.1. Under these conditions, compound ***rac*-94b** yielded only 9% of the hydroperoxy alcohol ***rac*-95b**. As a result of this poor yield, we revised the equipment used for the photooxygenation reaction.

Some of the implications of practical photochemistry have been discussed by Hook and Booker-Milburn.[18]

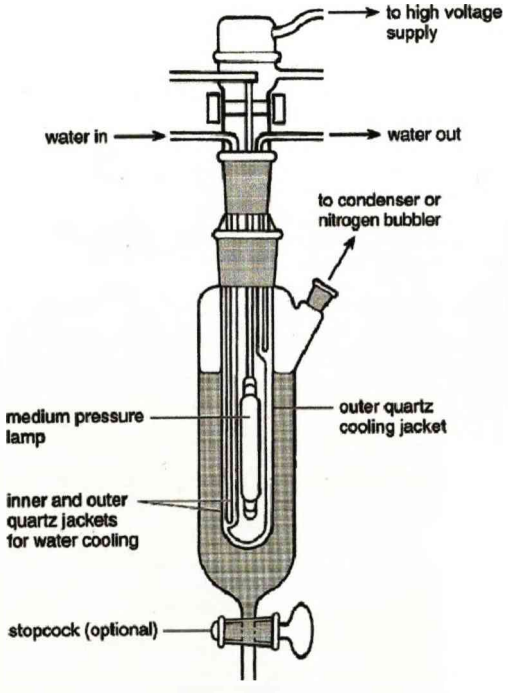

***Figure 2.1** Immersion well batch photochemical reactor.*[19]

They cite commonly used batch apparatus as the immersion well reactor (Figure 2.1). The light source is placed in a well, effectively "inside" the reaction mixture, with a water cooling jacket separating the lamp from the reaction medium.

As the majority of the photochemistry occurs within a short radius of the lamp, this setup allows for minimal distance between the light source and any part of the reaction solution and therefore an efficient reaction.

However, for our purposes we needed a setup that would also allow for aeration by O_2. With the apparatus available to us we constructed an elongated reaction vessel from a Liebig condenser which was sealed at the bottom (Figure 2.2).

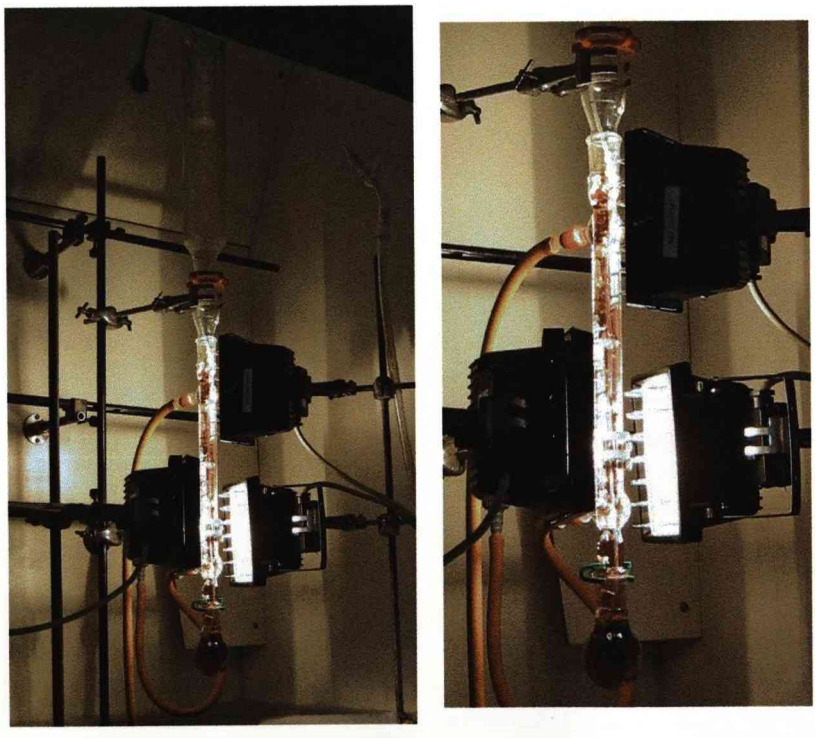

Figure 2.2 *Modified photooxygenation apparatus with an elongated, cooled reaction vessel.*

This was ideal as the volume of the reaction mixture was spread through a long narrow tube. The benefit of this was that more lamps could be fitted in close proximity around the vessel and no part of the reaction mixture was ever more than an inch away from a light source. Also, the use of the condenser supplied a ready-made sealed water jacket to cool the reaction. A cold finger condenser, cooled with acetone and dry ice, was also fitted onto the Liebig condenser to limit the evaporation of the solvent and starting material which worked very efficiently. Narrow bore PTFE tubing was passed through both condensers to the base of the reaction vessel where it delivered the O_2 gas which could then bubble up through the solvent, efficiently aerating the solution.

Four lamps were used in this set-up to furnish the *cis*-allylic hydroperoxy alcohol ***rac*-95b** in 43-47% yield. These conditions were then applied to the enantiomerically pure material (***R*)-** and (***S*)-94b** to furnish **(3*R*,4*R*)-95b** and **(3*S*,4*S*)-95b** in similar yields. This modified set up was also tried with the mesityl alcohol **78** but no net increase in yield was observed. The harsher conditions increased the rate of the reaction and led to the production of the polar by-product in a shorter time. However, this meant the reaction time could be reduced to 2.5-3 hours.

2.2.3 Synthesis of Enantioenriched cis-Substituted 1,2,4-Trioxanes

With samples of the *cis*-hydroperoxy alcohols, **(3*R*,4*R*)-95b**, **(3*S*,4*S*)-95b** and ***rac*-95b** in hand we continued to the final step, peroxyacetalisation with a cyclic ketone (Scheme 2.4; step v.). The hydroperoxy alcohols were treated with 2-adamantanone and *p*-TsOH to give the target, enantiomerically enriched, 1,2,4-trioxanes. The *R*-

configured, *S*-configured, and racemic substrates furnished **(5*R*,6*R*)-96b**, **(5*S*,6*S*)-96b** and ***rac*-96b** in 26%, 34% and 23% yield respectively (Figure 2.3).

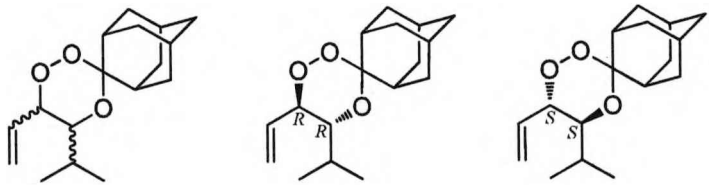

***rac*-96b** 30% **(5*R*,6*R*)-96b** 26% **(5*S*,6*S*)-96b** 34%

Figure 2.3 *Racemic and chiral cis-substituted 1,2,4-trioxanes.*

2.3 The Interaction of Phosphite Ozonide Adducts (POAs) with Allylic Alcohols

The use of dye-sensitised photooxygenation as method of generating singlet oxygen in order to introduce a hydroperoxide moiety has its limitations.[8,9,18] As previously mentioned, removal of dye stuffs can be problematic. More importantly, scale up of the process is impractical as photooxygenation is restricted to a batch process rarely used in an industrial setting. Chemical methods of generating singlet oxygen have been explored in the literature[20-25] but more specifically the use of phosphite ozonide adducts[26,27] piqued our interest. Previous work within our group demonstrated the use of phosphite ozonide adducts in the synthesis of endoperoxide anti-malarial agents and led to the successful synthesis of analogues of yingzhaosu A. However, its application in the synthesis of a Fenozan analogue proved problematic.[28]

To our knowledge there are no reports in the literature of the use of phosphite ozonides as a source of singlet oxygen in the targeted synthesis of biologically active 1,2,4-trioxanes. We initially wanted to establish if the diastereoselectivity witnessed *via* photooxygenation was maintained when using phosphite ozonides, and if so,

hoped to employ the technique in a novel enantioselective synthesis of 1,2,4-trioxanes. In the following sections we will firstly discuss the nature and reactivity of phosphite ozonides reported in the literature and then proceed to our investigations of the suitability of phosphite ozonide adducts in the synthesis of 1,2,4-trioxanes.

2.3.1 POAs as a Source of Singlet Oxygen

In 1961 Thompson[29] reported on the remarkable oxidising properties of a phosphite-ozone system. It was observed that some triaryl phosphites **103** formed stable 1:1 adducts with ozone **104** at low temperatures and that upon warming to room temperature, molecular oxygen was liberated and the phosphate ester **106** formed in quantitative yield. Addition of heteroatomic compounds, *e.g.* dimethyl sulphide and tributyl phosphine, to the low temperature adducts resulted in oxidation to dimethyl sulfone and tributyl phosphate respectively. ^{31}P NMR studies of the adduct indicated a pentavalent phosphorous centre and a cyclic structure **105** (Figure 2.4) was proposed.[30]

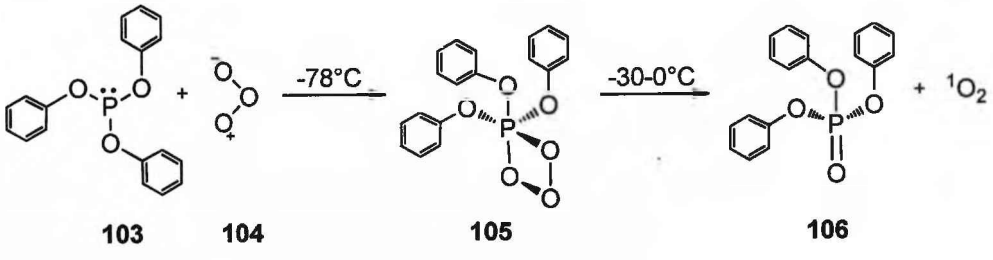

Figure 2.4 *Formation of the triaryl phosphite ozonide adduct with a pentavalent structure.*

It was later shown by Murray and Kaplan[26,27] that oxygen released from POAs has singlet multiplicity. Treatment of 1,3-dienes and tetrasubstituted ethylene with POA conditions gave products typical of singlet oxygen photooxidation.

Literature throughout the 1970s highlighted two reaction modes of POAs, the direct and free reaction. The synthesis was originally thought to proceed solely *via* a free reaction whereby warming of the adduct to room temperature would release free singlet oxygen, able to react with the substrate in very much the same manner as in the photochemical process. However, it was noted that tetramethylethylene underwent the typical transformation to the hydroperoxide when treated with POAs at a temperature of -60 °C.[31] However, extrusion of singlet oxygen from the adduct was known to only occur at temperatures >-15 °C, thus indicating a direct reaction between the adduct and substrate. This bimolecular reaction mode has implications for the mechanism, and correspondingly, the regio- and stereoselectivity of the oxygenation reaction due to the steric bulk of the phosphite ligands in close vicinity of the reaction centre.

A stark example of this is the oxygenation of *cis*- and *trans*-diethoxy ethylene, **107** and **108** (Figure 2.5).[32] It was observed that $^1O_2$ generated photochemically adds stereospecifically to these substrates providing the *cis*- and *trans*-dioxetanes respectively, **109** and **110**. *Via* the direct ozonide reaction the same products are given but as a mixture of isomers of the same ratio, irrespective of the starting material. As expected the less sterically hindered *trans*-product **110** is the major component.

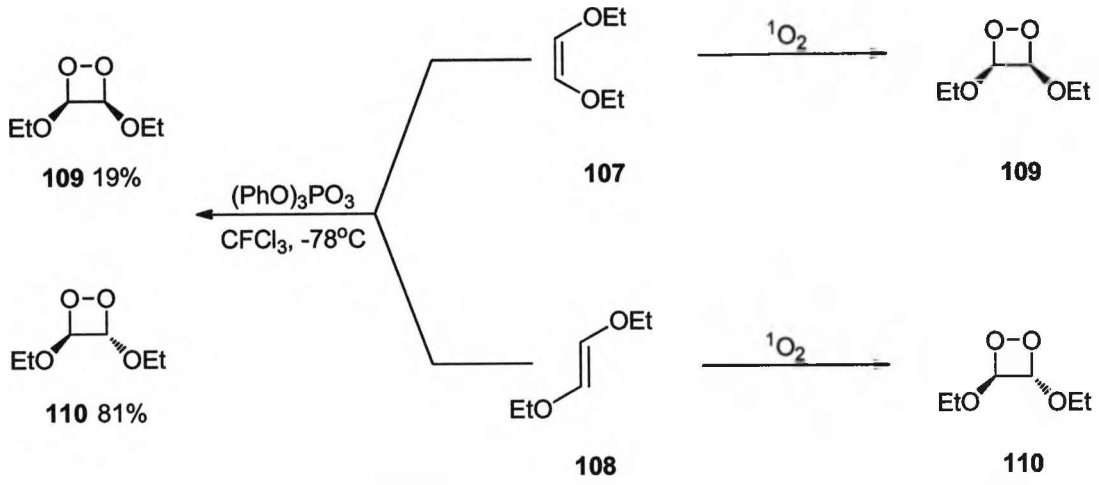

Figure 2.5 *Dioxetane product distribution from the treatment of diethoxy ethylene with photochemically generated singlet oxygen and a direct reaction with a POA.*

A proposed mechanism is stepwise *via* a zwitterionic intermediate in which rotation around the single bond results in a mixture of isomers, the major product being the most conformationally stable (Figure 2.6).

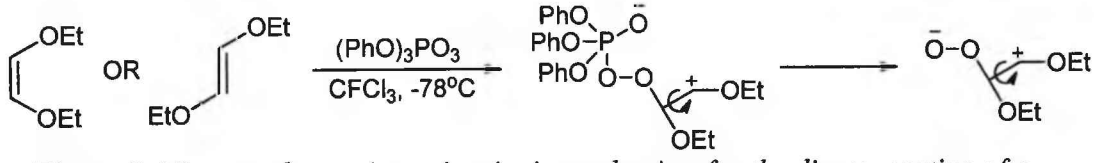

Figure 2.6 *Proposed stepwise zwitterionic mechanism for the direct reaction of a POA.*

Additional support for a zwitterionic/biradical intermediate was shown by Mori and co-workers[33] who have successfully isolated a peroxy phosphate **114** from the direct reaction of the triphenyl phosphite ozonide **112** with a silyl dienol ether **111** (Figure 2.7). The zwitterionic intermediate **113** is proposed, formed from nucleophilic attack on the central oxygen atom of the ozonide **112**. Theoretical electrostatic charge

calculations of **112** have also indicated the central oxygen atom as the most positively charged.

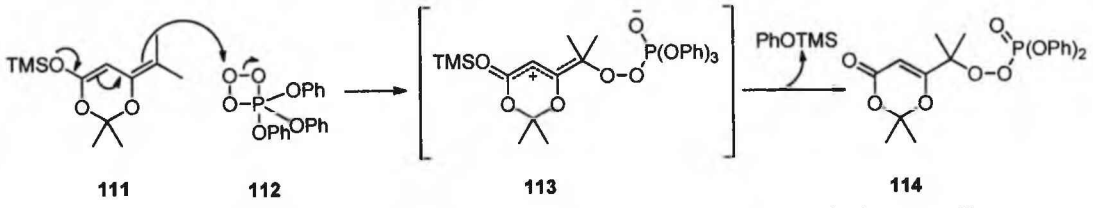

Figure 2.7 *Isolation of a peroxy phosphate supports a zwitterionic intermediate.*

Bartlett and Chu[34] have also reported that the polarity of the reaction media has no effect on product distribution of the direct reaction implying a biradical process: the substrate dihydropyran **115** formed the dioxetane **116** product over the ene-product **117** with a 10:1 preference in all cases (Figure 2.8). This is in conflict with the reaction of free singlet oxygen which favours the dioxetane product as solvent polarity increases.

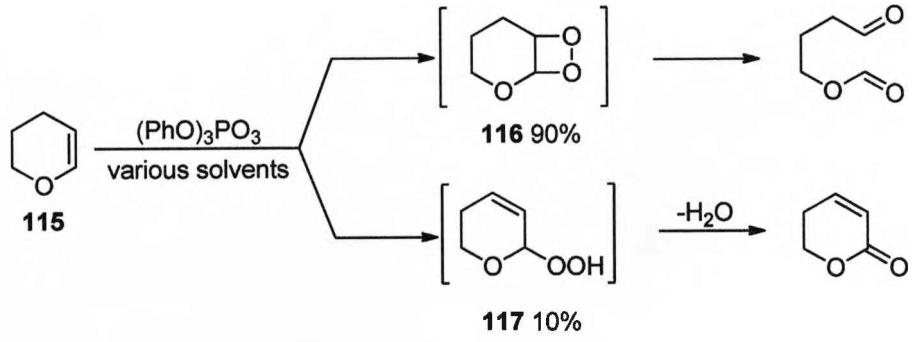

Figure 2.8 *Solvent polarity has no effect on the distribution of products formed via POAs.*

Some researchers have also found evidence for a perepoxide intermediate.[35] As previously discussed, isotope effect studies on tetramethyl ethylenes-d_6 have shown

that during photochemical singlet oxygen reactions, substituents positioned in a *cis*-relationship are in competition for H-abstraction by the nucleophilic tailing oxygen. This observed competition supports a mechanism involving a perepoxide intermediate, and has in fact similarly been observed for direct oxygenation reactions of POAs.

For the most part the predicted influence of the steric bulk of the phosphite portion has not been observed in practice and many examples show comparable regio- and stereoselectivity between both the free and direct reaction modes. The exceptions that have been reported are for substrates with considerable steric influence themselves.[34,36,37] For example, bulky bisadamantyl did not react under direct conditions, which was attributed to the hindrance of the large adamantyl groups to the phosphorous part of the ozonide.[34]

This trend was encouraging and we were optimistic that the selectivity displayed by the photooxygenation reaction for our substrates would be maintained through both the free and direct POA oxygenations.

2.3.2 Synthesis of Ascaridole via POA Conditions

In 1969 Murray and Kaplan[26] demonstrated that the treatment of α-terpinene **118** with triphenyl phosphite ozone adducts gave the classic photooxygenation [4+2]-cycloaddition product ascaridole **119** (Scheme 2.7). We chose to repeat this experiment as an initial study of the chemistry and conditions. Firstly, a solution of triphenyl phosphite in dichloromethane was cooled to -78 °C. The POA was then prepared by saturating the solution with O_3 indicated by the blue colour of the solution. Once completed the system was purged with N_2 to remove any excess O_3.

The α-terpinene **118** was then added dropwise and allowed to react with stirring at -78 °C generating direct reaction conditions.

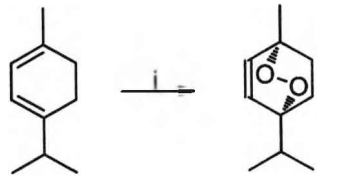

118 **119** 61%

Scheme 2.7 *Reagents and conditions:* i) $P(PhO)_3$, O_3, CH_2Cl_2, -78 °C, 30 min.

Consumption of the starting material was monitored by t.l.c and found to be complete after 30 minutes. Purification by column chromatography yielded ascaridole **119** in 61%.

2.3.3 Synthesis of Hydroperoxy Alcohols via POA Conditions

Mesityl alcohol **78** was subjected to this source of singlet oxygen to confirm that it would furnish the hydroperoxy alcohol **79** and to establish its diastereoselectivity (Scheme 2.8). The allylic alcohol was added dropwise to a prepared solution of the cooled phosphite ozonide adduct at -78 °C consistent with direct conditions. The reaction was monitored by t.l.c. and after 2.5 hours product formation was observed accompanied by some impurities. The reaction mixture was warmed to ambient temperature and purified by column chromatography to give **79** in 40% yield. We also explored the progression of the reaction under free POA conditions; however it proved less efficient than the direct reaction furnishing the hydroperoxy alcohol in only 23% yield. From here on, oxidation *via* POAs were performed under direct conditions unless otherwise stated.

The diastereoselectivity of this reaction was comparable to that of photooxygenation. Analysis by ^{1}H NMR showed a product consistent with that obtained by photooxygenation. A major doublet was observed at δ 4.17 (J = 8.3 Hz) indicating H_α coupling to H_β in the *threo*-configured product **79**. A smaller minor doublet at δ 4.30 (J = 5.1 Hz) indicates the presence of the minor *erythro*-configured product **80**. These peaks appear in a 90:10 ratio indicating diastereoselectivity comparable to the methodology using TPP and O_2.

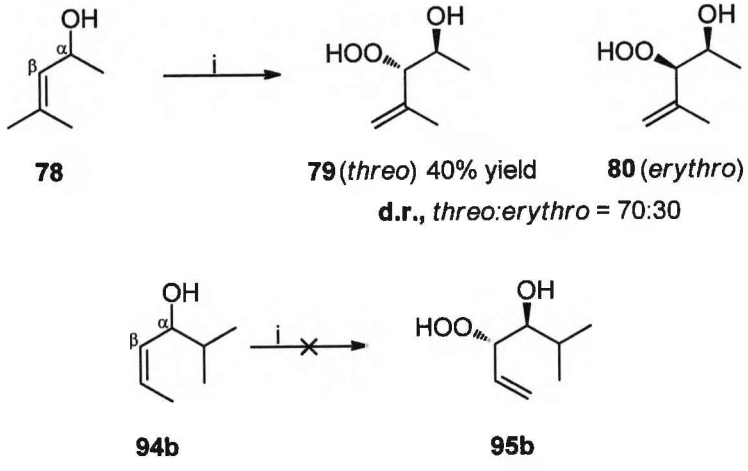

Scheme 2.8 *Reagents and conditions:* i) $P(PhO)_3$, O_3, CH_2Cl_2, -78°C, >2 hr.

Finally, conversion of the racemic *cis*-allylic alcohol **94b** to its corresponding hydroperoxy alcohol **95b** using the phosphite ozonide adduct conditions was attempted (Scheme 2.8). Aware that this substrate tended to need very harsh reaction conditions, a good yield was not expected for this reaction, however no reaction was observed which was disappointing in light of the excellent diastereoselectivity demonstrated by POA conditions.

2.3.4 Revaluation of the Synthetic Route

From these studies it became apparent that the *cis*-allylic alcohol was not a suitable singlet oxygen acceptor, whether *via* photooxygenation or treatment with phosphite ozonide adducts. This, coupled with the volatility of the substrates, meant we were obliged to return to the synthesis of disubstituted allylic alcohols, ideally *via* a more direct enantioselective synthesis. A route fulfilling these criteria was the enantioselective addition of various dialkyl zinc reagents to an appropriate aldehyde. This would furnish a variety of chiral allylic alcohols with methyl, ethyl, butyl, *i*-propyl and phenyl moieties, suitable for reaction with singlet oxygen (Figure 2.9).

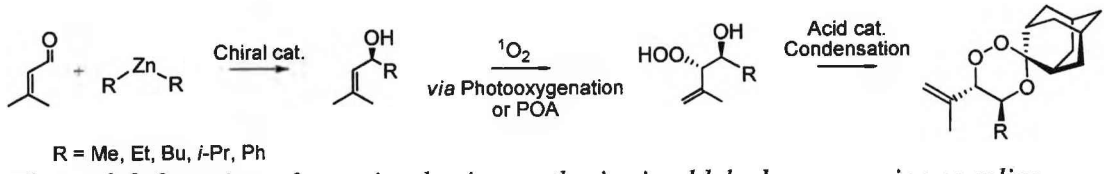

Figure 2.9 *Overview of enantioselective synthesis via aldehyde-organozinc coupling.*

2.3.5 Reactivity of Disubstituted Allylic Alcohols under POA Conditions

Initially, we wanted to compare the oxidation of the chiral disubstituted allylic alcohols by singlet oxygen, under photooxygenation and POA conditions, to establish whether POAs were a viable alternative. To avoid wasting valuable chiral material, analogous racemic allylic alcohols of **122a** and **122b** were synthesised *via* addition of the relevant Grignard reagent to 3-methylbut-2-en-al (Scheme 2.9).

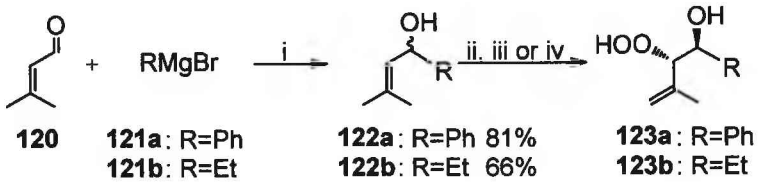

120 **121a**: R=Ph **121b**: R=Et **122a**: R=Ph 81% **122b**: R=Et 66% **123a**: R=Ph **123b**: R=Et

Scheme 2.9 *Reagents and conditions:* i) THF, 0 °C, 1 hr: ii) O_2, TTP, CH_2Cl_2, hν, 0 °C, 4 hr: iii) $P(PhO)_3$, O_3, CH_2Cl_2, -78 °C, >2 hr: iv) $P(PhO)_3$, O_3, CH_2Cl_2, -78 °C→ r.t..

The phenyl substituted allylic alcohol **122a** was synthesised by the addition of commercially sourced phenyl magnesium bromide **121a** to the aldehyde **120**. The completed reaction was initially quenched with dil. HCl, however these acidic conditions caused a rearrangement of the product to give compound **124** (Scheme 2.10). Quenching instead with milder NH_4Cl safely furnished the desired allylic alcohol **122a**. The ethyl magnesium bromide reagent **121b** was synthesised *in situ* and the aldehyde added directly. Again a mild acidic workup allowed allylic alcohol **122b**. The methyl substituted allylic alcohol **78**, was obtained through the reduction of mesityl oxide **84**.

The desired allylic alcohols were then oxygenated under photochemical, direct POA and free POA conditions. The results are shown in the Table 2.1.

	Schenk-ene product	Photooxygenation	POA	
			Direct	Free
123a	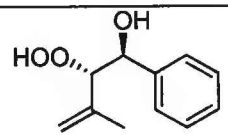	97%	7%	-
123b	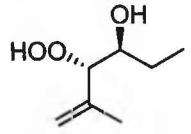	85%	25%	36%
123c	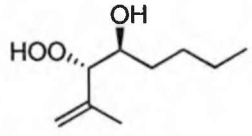	100%	28%	18%
123d	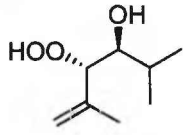	86%	-	-
79	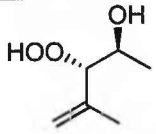	59%	40%	23%

Table 2.1 *Reactivity of disubstituted allylic alcohols under photochemical, direct POA and free POA conditions.*

All the substrates afforded the desired hydroperoxy-product in excellent yield *via* photooxygenation. However, when subject to phosphite ozonide adducts in both free and direct conditions, the yield was very poor and many byproducts were observed. When one compares the performance of the racemic mesityl hydroperoxy alcohol

compound **79** to the other four substrates, however, a trend appears. Compound **79** is given in a moderate yield of 59% under photooxygenation conditions. It also gives a slightly lower, yet still acceptable yield of 40% when treated with POA. This indicates that it is not as reactive when photooxygenated but also that its ene-product is stable enough to withstand POA conditions to give a moderate yield. The readily photooxygenated allylic alcohols, **122b** and **122c** give excellent yields *via* photooxygenation. Correspondingly their ene-products **123b** and **123c** are more reactive and consequently too unstable to give acceptable yields *via* POA conditions.

An interesting result was obtained from the POA reaction of the aromatic allylic alcohol **122a** (Scheme 2.10). After treatment of **122a** with the POA for 2.5-3 hours at -78 °C, it was observed by t.l.c. that some hydroperoxy alcohol product had been formed but that a lot of starting material remained. The reaction was stopped and the desired product **123a** was isolated in only 7% yield. What was believed to be starting material, from t.l.c., underwent analysis by ^{1}H NMR. This was in fact a by-product with structure **124**, obtained in 90% yield. Surprisingly, this was the same product observed through the harsh acidic workup of the previous Grignard reaction (Scheme 2.9).

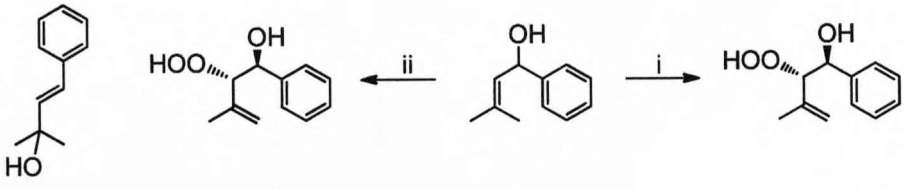

90% **124** 7% **123a** **122a** 97% **123a**

Scheme 2.10 *Reagents and conditions:* i) O_2, TTP, CH_2Cl_2, hv, 2 hr: ii) $P(PhO)_3$, O_3, CH_2Cl_2, -78 °C, >2 hr.

The ^{1}H NMR spectrum of **124** showed the presence of aromatic protons, two roofed doublets at δ 6.65 and δ 6.40 typical of olefinic hydrogens, and a singlet integrating for six equivalent protons. The compound determined as **124** was therefore proposed to be the result of an acid catalysed rearrangement of the starting material facilitated by the presence of an aromatic ring. Conversely, the photooxygenation of **122a** proceeded in 97% yield to give the desired product **123a**.

It can be postulated, that the conditions of the phosphite ozonide adduct are strongly acidic causing rearrangement of the starting material in this case. This was disappointing as the phenyl substituted 1,2,4-trioxane is a valuable candidate for SAR studies. However, despite these results we still planned to synthesise an optically pure sample of **123a** *via* photooxygenation, and to continue to the desired aromatic 1,2,4-trioxane.

As a result of these preliminary studies it was concluded that phosphite ozonide adducts were not a viable alternative to dye-sensitised oxygenation as a source of singlet oxygen. Although the observed diastereoselectivity of the Schenk-ene reaction[2] was also maintained through POA oxygenations, the yields were on the whole poor and in the case of the *cis*-substituted allylic alcohols no reaction was observed whatsoever.

2.4 An Enantioselective Route to Disubstituted 1,2,4-Trioxanes: Synthesis of Disubstituted Allylic Alcohols via Aldehyde-Organozinc Coupling using a Chiral MIB Catalyst

As discussed in Section 2.3.4., we planned to synthesise a series of enantiomerically enriched allylic alcohols ((***R***)- and (***S***)-**122**) through the coupling of the aldehyde **120** with a range of dialkyl zinc reagents **125**. We then intended to subject this enantio-enriched series to the highly diastereoselective ene-reaction to furnish the respective hydroperoxy alcohols ((**3*R*,4*R***)- and (**3*S*,4*S*)-123**). The hydroperoxy alcohols would then undergo acid catalysed cyclisation with cyclic ketones to yield the desired enantio-enriched, spirocyclic 1,2,4-trioxanes ((**3*R*,4*R***)- and (**3*S*,4*S*)-126**) (Scheme 2.11).

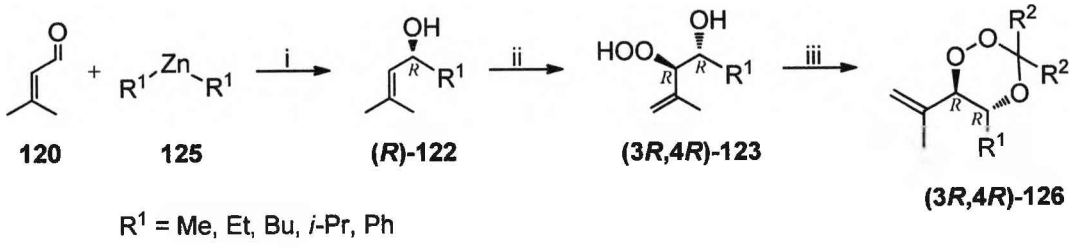

Scheme 2.11 *Reagents and conditions:* i) (+)-MIB, ZnR_2, 0 °C, Hexane or Toluene: ii) O_2, TTP, CH_2Cl_2, hv, 2 hr: iii) TsOH, $R^2C{=}O$, CH_2Cl_2, -10 °C, 30 min. *Synthesis of (R)-configured alcohol is shown using (+)-MIB.*

2.4.1 The Chiral MIB Catalyst

The first example of a highly enantioselective addition of dialkylzincs to aldehydes was reported by Noyori in 1986 with the advent of the chiral ligand (-)-3-

exodimethylaminoisoborneol (DAIB) derived from (*R*)-camphor.[38] DAIB continues to be a popular chiral catalyst particularly for the enantioselective promotion of addition to aromatic aldehydes. However more recently a novel camphor derivative, (2*R*)-(+)-exo-(morpholino)isoborneol ((+)-MIB), has been presented as a more stable alternative, more suited to α-branched aliphatic aldehydes.[39]

(-)-MIB, derived from (*R*)-camphor, is commercially available. The (*S*)-derived (+)-MIB **(+)-131** was synthesised as outlined by Chen and Nugent in three steps (Scheme 2.12).[40]

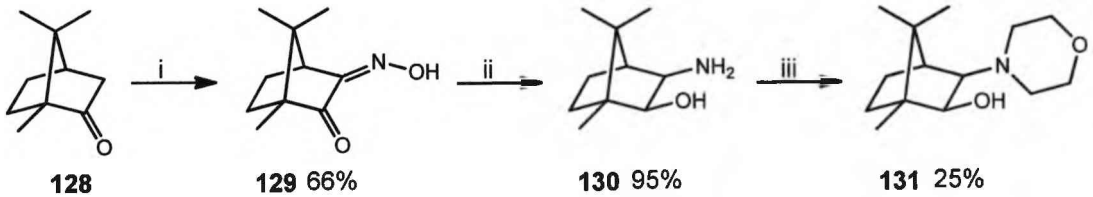

128 **129** 66% **130** 95% **131** 25%

Scheme 2.12 *Reagents and conditions:* i) KOtBu, *i*-amyl nitrite, Et_2O, -30 °C, 16 hr: ii) $LiAlH_4$, THF, reflux, 30 min: iii) bis(2-bromoethyl) ether, NEt_3, DMSO, r.t., 72 hr.

(*S*)-Camphor **128** was treated with potassium *t*-butoxide and isoamylnitrite successively and stirred overnight. The solution was then extracted with water and the aqueous mixture was acidified to give camphorquinone oxime **129** as an off-white solid in 66% yield. The camphorquinone oxime was then reduced with $LiAlH_4$ to give **130** in 95% yield. Compound **130** was finally treated with triethylamine and bis(2-bromoethyl) ether and stirred for 72 hours to give the desired product **(+)-131** in 25% yield.

2.4.2 Synthesis of Chiral Disubstituted Allylic Alcohols

A solution of dialkyl zinc (1M in hexane or toluene) was added to a solution of (-)-MIB at 0 °C, followed by the addition of 3-methylbut-2-en-al **120**. The mixture was stirred at 0 °C until complete consumption of the starting material was observed by t.l.c. The reaction was quenched with sat. NH_4Cl followed by a standard work-up and purification by column chromatography to give compounds **(*S*)-122a-d** and **(*S*)-78** (Scheme 2.13). The opposing (*R*)-enantiomers **(*R*)-122a-d** and **(*R*)-78** were provided by catalysis with (+)-MIB and excepting **(*R*)-122d** were kindly synthesised by Dr. S Sabbani of the University of Liverpool. The subsequent (*R*)-configured derivatives **(3*R*,4*R*)-123b-d**, **(3*R*,4*R*)-126b-d** and **(3*R*,4*R*)-132b-c** were also synthesised by Dr. S. Sabbani.

The yield and enantiomeric excess (ee) for each reaction is summarised in the table below (Table 2.2).

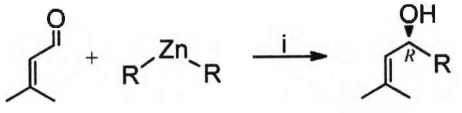

120 **125a**: R=Ph **(*R*)-122a**: R=Ph
125b: R=Et **(*R*)-122b**: R=Et
125c: R=Bu **(*R*)-122c**: R=Bu
125d: R=*i*-Pr **(*R*)-122d**: R=*i*-Pr
125e: R=Me **(*R*)-78**: R=Me

Scheme 2.13 *Reagents and conditions:* i) (+)-MIB, ZnR_2, 0 °C, Hexane or Toluene. *Synthesis of (R)-configured alcohol is shown using (+)-MIB.*

	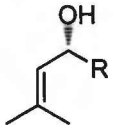	Reaction Time	Yield	(+)-ee	(-)-ee
78	R = Me	144 hrs	14%	79%	77%
122a	R = Ph	3 hrs	34%	_	79%
122b	R = Et	8 hrs	30%	94%	93%
122c	R = Bu	3 hrs	72%	90%	90%
122d	R = *i*-Pr	3 hrs	67%	98%	98%

***Table 2.2** Yield and ee of chiral disubstituted allylic alcohols.*

The ee of the ethyl, butyl and *i*-propyl products, **122b**, **122c** and **122d** were all above 90% with the *i*-propyl allylic alcohol displaying an excellent ee of 98%. We therefore chose ethyl, butyl and *i*-propyl allylic alcohols to undergo the Schenk-ene reaction.

The methyl and phenyl alcohols (**78** and **122a**) displayed poor ee and yield and so were discounted for further study. According to the literature, a highly enantioselective diphenylzinc addition reaction has always been notoriously difficult.[38] Dialkylzinc addition to aldehydes is known to proceed very slowly in the absence a catalyst, whereas diphenylzinc additions can continue smoothly even without a catalyst. This "background" reaction can therefore circumvent coordination with the chiral catalyst and addition to the aldehyde can continue without any chiral control resulting in a diminished ee.

The very long reaction time of the dimethylzinc addition to aldehyde **120** was consistent with similar reactions reported in the lierature.[38] This could probably be attributed to the lower nucleophilicity of the methyl substituent in comparison to the larger electron donating groups such as ethyl, butyl, *i*-propyl *etc*. However this does not explain the poor enantioselectivity of this reaction.

2.4.3 Synthesis of Enantioenriched Disubstituted 1,2,4-Trioxanes

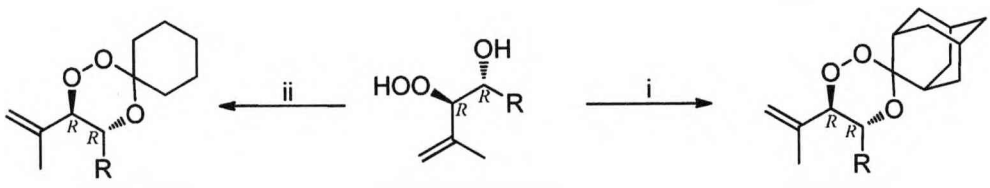

(5*R*,6*R*)-126b : R^1=Et
(5*R*,6*R*)-126c : R^1=Bu
(5*R*,6*R*)-126d : R^1=*i*-Pr

(5*R*,6*R*)-123b : R^1=Et
(5*R*,6*R*)-123c : R^1=Bu
(5*R*,6*R*)-123d : R^1=*i*-Pr

(5*R*,6*R*)-127b : R^1=Et
(5*R*,6*R*)-127c : R^1=Bu
(5*R*,6*R*)-127d : R^1=*i*-Pr

Scheme 2.14 *Reagents and conditions:* i) *p*-TsOH, 2-adamantanone, CH_2Cl_2, -10 °C, 30 min: ii) *p*-TsOH, cyclohexanone, CH_2Cl_2, -10 °C, 30 min. *Synthesis of* (5*R*,6*R*)-*configured 1,2,4-trioxanes shown.*

The chiral allylic alcohols, **(*R*)-** and **(*S*)-122b-d** underwent photooxygenation, as discussed in Section 2.3.5, to give the hydroperoxyalcohols **(3*R*,4*R*)-** and **(3*S*,4*S*)-123b-d** in excellent yield. The concluding step of this synthesis, the condensation of the hydroperoxy substrates with a cyclic ketone, was then carried out with cyclohexanone and 2-adamantanone. The reactions with cyclohexanone and 2-adamantanone progressed in moderate yield to afford the desired enantiomerically enriched 1,2,4,-trioxanes, **(5*R*,6*R*)-** and **(5*S*,6*S*)-126b-d**, **(5*R*,6*R*)-** and **(5*S*,6*S*)-127c**

and **d** as pale yellow oils. The ethyl substituted spiroadamantyl trioxane **(5*R*,6*R*)-** and **(5*S*,6*S*)-127b** was isolated as a white solid (Scheme 2.14). My co-worker Dr. S. Sabbani also carried out the successful condensation of the hydroperoxy alcohols, **(3*R*,4*R*)-123b-c**, with *N*-Boc-4-piperidone to give trioxanes **(5*R*,6*R*)-132b** and **(5*R*,6*R*)-132c** respectively. Yields and optical rotations are summarised in Table 2.3.

		Yield	Optical Rotation (c 1.0, $CHCl_3$)
(5*R*,6*R*)-126b	R^1 = Et spirocyclohexyl	76%	-123.1
(5*S*,6*S*)-126b		66%	+102.9
(5*R*,6*R*)-127b	R^1 = Et spiroadamantyl	74%	-86.4
(5*S*,6*S*)-127b		55%	+59.3
(5*R*,6*R*)-126c	R^1 = *n*-Bu spirocyclohexyl	78%	-102.6
(5*S*,6*S*)-126c		73%	+73.1
(5*R*,6*R*)-127c	R^1 = *n*-Bu spiroadamantyl	78%	-57.4
(5*S*,6*S*)-127c		65%	+89.5
(5*R*,6*R*)-126d	R^1 = *i*-Pr spirocyclohexyl	44%	-95.7
(5*S*,6*S*)-126d		61%	+102.0
(5*R*,6*R*)-127d	R^1 = *i*-Pr spiroadamantyl	64%	-100.3
(5*S*,6*S*)-127d		57%	+100.1
		Yield	Optical Rotation
(5*R*,6*R*)-132b	R^1 = Et *N*-Boc-4-piperidyl	16%	-85.0 (c 1.0, $CHCl_3$)
(5*R*,6*R*)-132c	R^1 = *n*-Bu *N*-Boc-4-piperidyl	18%	-64.0 (c 0.3, $CHCl_3$)

Table 2.3 *Yields and optical rotations of the target chiral 1,2,4-trioxanes.*

The crystallisation of **(5*R*,6*R*)-127b** allowed for X-ray crystallographic data to be obtained of the 1,2,4-trioxane structure (Figure 2.10).

The X-ray crystal structure shows the central trioxane ring in a chair conformation in accordance with that reported by Griesbeck[8] and confirms the *trans*-relationship between H3 and H4. The structure also demonstrates the *syn*-relationship across the C3-C16 bond between the peroxy (O2) and olefinic (C17) groups, thereby corroborating with the reported suprafacial nature of the ene-reaction and showing the maintenance of its stereospecificity through the peroxyacetalisation step.

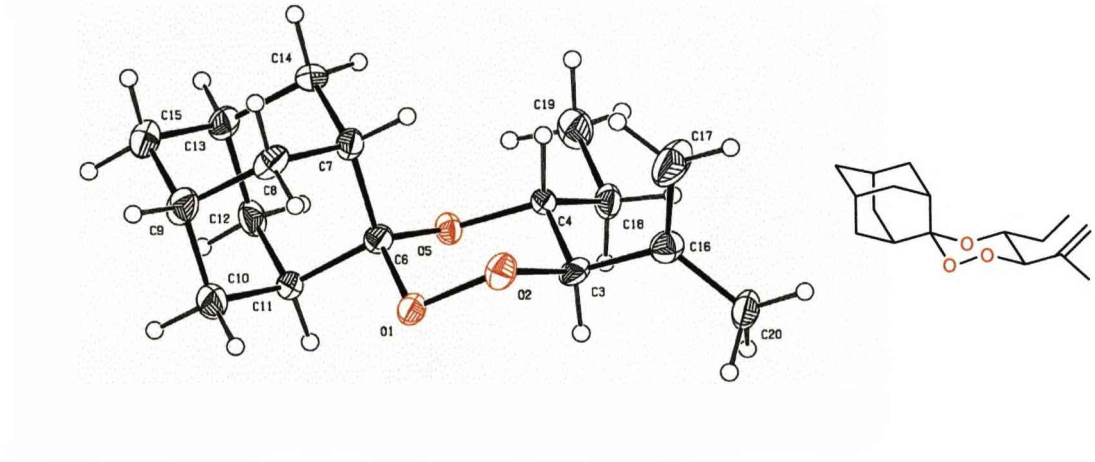

Figure 2.10 *X-ray crystal structure of chiral 1,2,4-trioxane* ***(5R,6R)-127b.***

2.5 Antimalarial Activity

The antimalarial activity of individual conformers of enantioenriched 1,2,4-trioxanes ((**5*R*,6*R*)-** and **(5*S*,6*S*)-126b-d**, **(5*R*,6*R*)-** and **(5*S*,6*S*)-127b-d** and **(5*R*,6*R*)-132b-c**) was evaluated *in vitro* against chloroquine-sensitive 3D7 strains of *P. falciparum* using artemisinin as a positive control (Table 2.4). The spiroadamantyl analogues, **(5*R*,6*R*)-** and **(5*S*,6*S*)-127b-d**, consistently showed potent activity in comparison to the spirocyclohexyl analogues, consistent with data trends reported in the literature. The *N*-Boc-4-piperidone analogues, **(5*R*,6*R*)-132b-c**, proved to be the most potent compounds of this series.

When comparing the antimalarial activity of the enantiomeric pairs of the 1,2,4-trioxanes there are small differences in the IC_{50} values. Of the straight chain analogues, with *n*-Bu or Et substituents, the (5*R*,6*R*)-configured structures show slightly better activity than those with the (5*S*,6*S*)-configuration. The branched, *i*-Pr substituted analogues, show improved activity of the (5*S*,6*S*)-configured trioxanes compared to the (5*R*,6*R*)-configured structures.

However, replication of this *in vitro* testing is ongoing from which we will be able to draw some more conclusions.

		IC_{50} (nM)			IC_{50} (nM)
(5*R*,6*R*)-127b	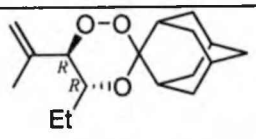	156	**(5*R*,6*R*)-126b**	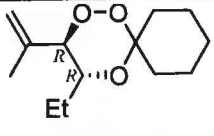	252
(5*S*,6*S*)-127b	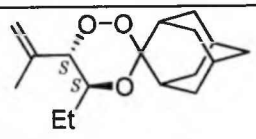	173	**(5*S*,6*S*)-126b**	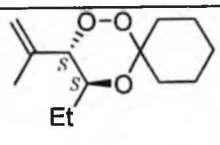	-
(5*R*,6*R*)-127c	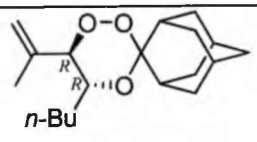	121	**(5*R*,6*R*)-126c**	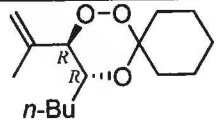	378
(5*S*,6*S*)-127c	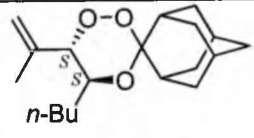	219	**(5*S*,6*S*)-126c**	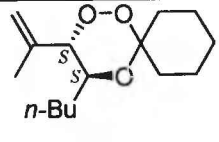	536
(5*R*,6*R*)-127d	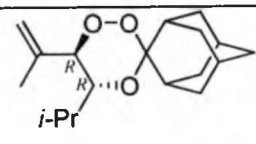	222	**(5*R*,6*R*)-126d**	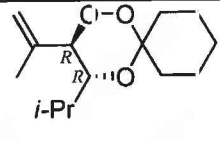	>1000
(5*S*,6*S*)-127d	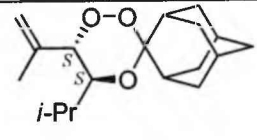	176	**(5*S*,6*S*)-126d**	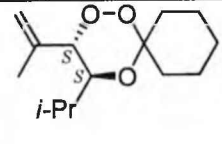	185
-	**Artemisinin**	9			
(5*R*,6*R*)-132b	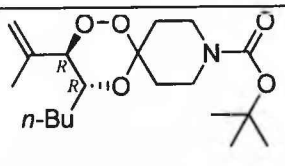	114	**(5*R*,6*R*)-132c**	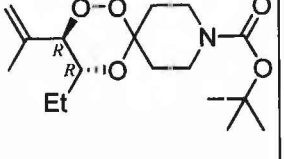	119

Table 2.4 *In vitro antimalarial activities of enantiomerically enriched spirocyclic 1,2,4-trioxanes against 3D7 strains of P. falciparum.*

2.6 Conclusion

Herein we have explored two enantioselective routes to the synthesis of 1,2,4-trioxanes implementing the diastereoselective ene-reaction of chiral allylic alcohols and thereafter peroxyacetalisation with cyclic ketones to furnish the enantioenriched trioxanes.

In the former we demonstrated the successful synthesis of *cis*-substituted 1,2,4-trioxanes with high enantioselectivity, however, the route proved problematic due to the volatility of many of the intermediates and the poor reactivity of the *cis*-allylic alcohol under photooxygenation conditions. The synthesis was thus deemed impractical for the synthesis of a series of opposing enantiomers of 1,2,4-trioxanes.

The latter, and ultimately more facile route, was carried out using (+)- and (-)-MIB catalysed addition of dialkylzincs to an α,β-unstaurated aldehyde to furnish disubstituted enantioenriched allylic alcohols in excellent yields. The allylic alcohols performed well under photooxygenation conditions to afford the desired hydroperoxy alcohols in excellent yield and subsequently a series of enantioenriched pairs of chiral 1,2,4-trioxanes. Currently we are investigating the potential differences in the antimalarial activities of mirror image pairs of enantiomers of trioxanes.

Phosphite ozonide adducts were examined with the intention that they would prove to be a potent alternative to photooxygenation methods. Promisingly, the reaction under phosphite ozonide conditions maintained the excellent diastereoselectivity observed in the ene-reaction. However, we were disappointed when the phosphite ozonide conditions furnished the hydroperoxy alcohols in poor yield in contrast to the excellent yields of dye-sensitised photooxygenation. For these reasons

oxygenation using phosphite ozonide adducts was ruled out as a viable source of hydroperoxy alcohols.

The concluding synthetic approach, by means of allylic alcohols derived from enantioselective addition of organozinc reagents to aldehydes, has proved to be highly efficient and may lend itself to a cost effective synthesis of chiral 1,2,4-trioxanes with high enantiomeric purity.

2.7 Acknowledgements

Compounds **(*R*)-122a-c**, **(*R*)-78**, **(5*R*,6*R*)-126b-c**, **(5*R*,6*R*)-127b-c**, **(5*R*,6*R*)-132b** and **(5*R*,6*R*)-132c** were prepared by Dr. S. Sabbani of the Department of Chemistry, University of Liverpool. *In vitro* antimalarial testing was performed by Dr. P. Stocks of the Liverpool School of Tropical Medicine.

2.8 References

(1) Singh, C. *Tet. Lett.* **1990**, *31*, 6901-6902.

(2) Griesbeck, A. G., El-Idreesy, T. T., Fiege, M., Brun, R., *Org. Lett.* **2002**, *4*, 4193-4195.

(3) Adam, W., Nestler, B., *J. Am. Chem. Soc.* **1993**, *115*, 5041-5049.

(4) Singh, C., Malik, H., Puri, S. K., *Bioorg. Med. Chem. Lett.* **2004**, *14*, 459-462.

(5) Singh, C., Kanchan, R., Srivastava, D., Puri, S. K., *Bioorg. Med. Chem. Lett.* **2006**, *16*, 584-586.

(6) Singh, C., Gupta, N., Puri, S. K., *Bioorg. Med. Chem. Lett.* **2003**, *13*, 3447-3450.

(7) Singh, C., Kanchan, R., Sharma, U., Puri, S. K., *J. Med. Chem.* **2007**, *50*, 521-527.

(8) Griesbeck, A. G., El-Idreesy, T. T., Höinck, L., Lex, J., Brun, R., *Bioorg. Med. Chem. Lett.* **2005**, *15*, 595-597.

(9) Griesbeck, A. G., Bartoschek, A., El-Idreesy, T. T., Höinck, O., Miara, C., *J. Mol.*

Cat. A: Chem. **2006**, *251*, 41-48.

(10) Jefford, C. W., Jaggi, D., Boukouvalas, J., Kohmoto, S., *J. Am. Chem. Soc.* **1983**, *105*, 6497-6498.

(11) Jefford, C. W., Kohmoto, S., Boukouvalas, J., Burger, U., *J. Am. Chem. Soc.* **1983**, *105*, 6498-6499.

(12) Jefford, C. W., Jin, S., Bernardinelli, G., *Helv. Chim. Acta* **1997**, *80*, 2440-2455.

(13) Midland, M., Tramontano, A., Kazubski, A., Graham, R. S., Tsai, D. J. S., Cardin, D. B., *Tetrahedron* **1984**, *40*, 1371-1380.

(14) Keith, J. M., Larrow, J. F., Jacobsen, E. N., *Adv. Synth. Catal.* **2001**, *343*, 5-26.

(15) Matsumura, K., Hashiguchi, S., Ikariya, T., Noyori, R., *J. Am. Chem. Soc.* **1997**, *119*, 8738-8739.

(16) Wu, X., Li, X., McConville, M., Saidi, O., Xiao, J., *J. Mol. Cat. A: Chem.* **2006**, *247*, 153-158.

(17) Dale, J. A., Mosher, H. S., *J. Am. Chem. Soc.* **1973**, *95*, 512-519.

(18) Hook, B. D. A., Dohle, W., Hirst, P. R., Pickworth, M., Berry, M. B., Booker-Milburn, K. I., *J. Org. Chem.* **2005**, *70*, 7558-7564.

(19) Harwood, L. M., Moody, C. J., Percy, J. M., *Experimental Organic Chemistry, Standard and Microscale*; 2nd ed.; Blackwell Science Ltd.: Cambridge, MA., 1999.

(20) Foote, C. S., Wexler, S., Ando, W., Higgins, R., *J. Am. Chem. Soc.* **1968**, *90*, 975-981.

(21) Aubry, J. M. *J. Am. Chem. Soc.* **1985**, *107*, 5844-5849.

(22) Pierlot, C., Nardello, V., Schrive, J., Mabille, C., Barbillat, J., Sombret, B., Aubry, J., *J.Org. Chem.* **2002**, *67*, 2418-2423.

(23) Evans, D., Upton, M., *J. Chem. Soc., Dalton Trans.* **1985**, 1141-1145.

(24) Turro, N. J., Chow, M. F., *J. Am. Chem. Soc.* **1981**, *103*, 7218-7224.

(25) Wasserman, H. H., Scheffer, J. R., *J. Am. Chem. Soc.* **1967**, *89*, 3073-3075.

(26) Murray, R. W., Kaplan, M. L., *J. Am. Chem. Soc.* **1969**, *91*, 5358-5364.

(27) Wasserman, E., Murray, R. W., Kaplan, M. L., Yager, W. A., *J. Am. Chem. Soc.* **1968**, *90*, 4160-4161.

(28) Rawe, S. L. PhD Thesis, University of Liverpool, 2003.

(29) Thompson, Q. E. *J. Am. Chem. Soc.* **1961**, *83*, 845-851.

(30) Dimitrov, A., Seppelt, K., *Eur. J. Inorg. Chem.* **2001**, *2001*, 1929-1932.

(31) Bartlett, P. D., Mendenhall, G. D., *J. Am. Chem. Soc.* **1970**, *92*, 210-211.

(32) Schaap, A. P., Bartlett, P. D., *J. Am. Chem. Soc.* **1970**, *92*, 6055-6057.

(33) Mori, A., Abe, M., Nojima, M., *J. Org. Chem.* **2001**, *66*, 3548.

(34) Bartlett, P. D., Chu, H-K., *J. Org. Chem.* **1980**, *45*, 3000-3004.

(35) Stephenson, L. M., Zielinski, M. B., *J. Am. Chem. Soc.* **2002**, *104*, 5819.

(36) Sam, T. W., Sutherland, J. K., *Chem. Comm.* **1972**, 424-425.

(37) Sam, T. W., Sutherland, J. K., *J. Chem. Soc. Perkin Trans. 1* **1975**, 2336-2340.

(38) Pu, L., Yu, H. B., *Chem. Rev.* **2001**, *101*, 757-824.

(39) Nugent, W. A. *Chem. Comm.* **1999**, 1369-1370.

(40) Chen, Y. K., Jeon, S. J., Walsh, P. J., Nugent, W. A., *Org. Syn.* **2005**, *82*, 87-90.

3.0 Experimental Procedure - Endoperoxides as Antimalarials and the Application of Singlet Oxygen to the Synthesis of Key Synthetic Intermediates en Route to Synthetic 1,2,4-Trioxanes

3.1 Chemical Procedures

Reaction procedure: Air- and moisture-sensitive reactions were carried out in oven-dried glassware sealed with rubber septa under a positive pressure of dry nitrogen from a balloon, unless otherwise indicated. Similarly, sensitive liquids and solutions were transferred via syringe or stainless steel cannula. Reactions were stirred using Teflon coated magnetic stir bars. Organic solutions were concentrated using a Buchi rotary evaporator with a diaphragm vacuum pump.

Purification of reagents and solvents: Anhydrous solvents were either obtained from commercial sources or dried and distilled immediately prior to use under a constant flow of dry nitrogen. THF, diethyl ether were distilled from Na/Ph_2CO, dichloromethane from CaH_2. All other reagents were used as received from commercial sources unless otherwise indicated.

Purification of products: Analytical thin layer chromatography was performed with 0.25 mm silica gel plates (Merck 60 F_{254}). Plates were visualised by ultraviolet light or by treatment with iodine, *p*-anisaldehyde, ninhydrin or potassium permanganate followed by gentle heating. Chromatographic purification of products was accomplished by flash chromatography performed on silica gel (BDH 60 230-400 mesh).

Analysis: NMR spectra were measured on a Bruker AMX 400 (^1H, 400 MHz and ^{13}C, 100 MHz) nuclear magnetic resonance spectrometer. Solvents are indicated in the text. Solids and liquids were used directly without any further treatment to record IR spectra using a JASCO FT/IR-4100 spectrometer. Mass spectra (MS) and high

resolution mass spectra (HRMS) were recorded on a VG analytical 7070E machine and a Fisons Trio 1000 quadrupole GC mass spectrometer using electron ionisation (EI) or chemical ionisation (CI) respectively. Reported mass values are within error limits of ±5 ppm. Microanalyses were determined by the University of Liverpool Microanalysis Laboratory.

Enantiomeric excesses of compounds **(*S*)-78**, **(*S*)-122b-d** and **(*R*)-122b-d** were determined using GC Varian 3800GC (Supelco β-Dex-120 column, 30 m × 0.25mm; He, 5 bar; air, 4 bar); GC Varian CP-3380 (Chromapack Chirasil Dex CB column, 25 m × 0.25mm; He, 5 bar) and Shimadzu GC-14B (Supelco α-Dex-120 column, 30 m × 0.25 × 0.25 μm; He, 50 KPa). Optical rotations were determined using a Perkin-Elmer polarimeter 343 plus instrument. Absolute configurations of enantiomerically enriched allylic alcohols **(*S*)-78**, **(*S*)-122b-d** and **(*R*)-122b-d** were determined by comparison of the optical rotations with the published optical rotations. X-ray analyses were carried out at the University of Liverpool.

4-Methyl-3-penten-2-ol 78

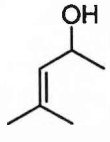

Mesityl oxide **84** (1.17 g, 10.18 mmol) was stirred in diethyl ether (25 mL) at 0 °C. $LiAlH_4$ (0.43 g, 11.21 mmol) was added over 15 minutes and the mixture was allowed to react for a further 15 minutes at room temperature.

The reaction was quenched sequentially with water (0.5 mL), NaOH 15% w/v (0.5 mL) and again water (1.5 mL). After stirring for another 30 minutes, the mixture was

filtered through a layer of celite, removing the Lithium precipitate. The solvent was removed *in vacuo* in a cold water bath to give **78** (0.82 g, 82%) as a yellow oil.

78: IR ν_{max} 3386 (ν_{O-H}), 2977, 2932 (ν_{C-H}) cm^{-1}; ^1H NMR (400 MHz, $CDCl_3$) δ 5.21 (1H, dsept, *J*=8.4, 1.3 Hz, -C<u>H</u>=C(CH_3)$_2$), 4.60 (1H, dq, *J*=8.4, 6.2 Hz, -<u>H</u>C(OH)CH_3), 2.70 (1H, brs, -O<u>H</u>), 1.71 (3H, d, *J*=1.4 Hz, -CH=C(C<u>H</u>$_3$)$_2$) 1.69 (3H, d, *J*=1.3 Hz, -CH=C(C<u>H</u>$_3$)$_2$), 1.23 (3H, d, *J*=6.4 Hz, -HC(OH)C<u>H</u>$_3$) ppm; ^{13}C NMR (100 MHz, $CDCl_3$) δ 134.5, 129.8, 65.2, 26.0, 24.0 and 18.4 ppm; *m/z* (CI) 100.11289 ($[M + NH_4]^+$); requires 100.11263.

4-Methyl-1-phenyl-3-penten-2-ol 87

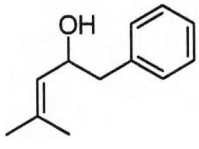

Phenacetaldehyde **85** (2.50 g, 20.80 mmol) was stirred in THF (50 mL) at -78 °C. 2-Methyl-1-propenyl magnesium bromide **86** (41.6 ml, 0.25 mmol) was added. The mixture was stirred for 30 minutes then allowed to warm to room temperature over 1.5 hours. The mixture was quenched with sat. NH_4Cl solution until effervescence ceased. Water (50 mL) was then added, the product extracted with ethyl acetate (3 × 50 mL) and the combined organic extracts then washed with brine (50 mL) and dried over $MgSO_4$. The solvent was removed *in vacuo* and the residue purified by column chromatography (90:10 Hexane: EtOAc) to give **87** (1.76 g, 48%) as yellow oil.

87: IR ν_{max} 3375 (ν_{O-H}), 3062, 3027 ($\nu_{C-H, Ar}$), 2970, 2916 (ν_{C-H}), 1602, 1495 ($\nu_{C=C, Ar}$) cm^{-1}; ^1H NMR (400 MHz, $CDCl_3$) δ 7.22 (5H, m, Ar-H), 5.21 (1H, dsept, *J*=8.5, 1.1 Hz, -C<u>H</u>=C(CH_3)$_2$), 4.54 (1H, dt, *J*=8.8, 6.6 Hz, -<u>H</u>C(OH)CH_2-), 2.77 (2H, d, *J*=7.0

Hz, -C<u>H</u>$_2$Ar), 1.71 (3H, d, *J*=1.4 Hz, -CH=C(C<u>H</u>$_3$)$_2$), 1.57 (3H, d, *J*=1.1 Hz, -CH=C(C<u>H</u>$_3$)$_2$) ppm; ^{13}C NMR (100 MHz, $CDCl_3$) δ 138.6, 135.7, 129.8, 128.8, 126.5, 121.0, 70.4, 43.1, 25.7 and 20.1 ppm; *m/z* (CI) 194.15471 ($[M + NH_4]^+$); requires 194.15448.

3-Methyl-1-phenyl-2-buten-1-ol 122a

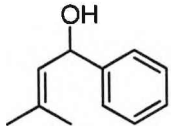

A solution of phenyl magnesiumbromide (1 M, 3.57 mL, 3.57 mmol) in THF was cooled in an ice-bath. A solution of 3-methylbut-2-en-al **120** (0.34 mL, 3.41 mmol) in THF (20 mL) was then added dropwise with stirring. The mixture was allowed to react for an hour, until complete consumption of the starting material was observed. The mixture was then poured into sat. NH_4Cl, and the aqueous mixture extracted with diethyl ether. The combined organic layers were washed with water and brine, dried over $MgSO_4$ and the solvents removed *in vacuo*. The crude product was purified by column chromatography (90:10 Hexane: EtOAc) to give **122a** (0.45 g, 81%) as a colourless oil.

122a: IR ν_{max} 3413 (ν_{O-H}), 3060, 3027 ($\nu_{C-H, Ar}$), 2970, 2916 (ν_{C-H}), 1602, 1495 ($\nu_{C=C, Ar}$) cm^{-1}; ^{1}H NMR (400 MHz, $CDCl_3$) δ 7.38-7.18 (5H, m, Ar-H), 5.46 (1H, d, *J*=8.7 Hz, -<u>H</u>C(OH)Ar), 5.42 (1H, dsept, *J*=8.7, 1.1 Hz, -C<u>H</u>=C(CH$_3$)$_2$), 1.79 (3H, d, *J*=1.1 Hz, -CH=C(C<u>H</u>$_3$)$_2$), 1.74 (3H, d, *J*=1.1 Hz, -CH=C(C<u>H</u>$_3$)$_2$) ppm; ^{13}C NMR (100 MHz, $CDCl_3$) δ 144.7, 135.6, 128.9, 128.2, 127.7, 126.3, 71.2, 26.2 and 14.6 ppm.

General Procedure 1

Photooxygenation of Allylic Alcohols in Solution

The allylic alcohol (ca. 5.0 mmol) and TPP (ca. 2 mg) was stirred in dichloromethane (80 mL). The reaction vessel was kept at 0 °C to reduce evaporation of the solvent. A stream of O_2 was then passed through the reaction mixture and the vessel irradiated with two tungsten lamps for 4 hours. The solvent was then removed *in vacuo* and the residue purified by column chromatography eluting with mixtures of hexane and ethyl acetate.

General Procedure 2

Photooxygenation of Allylic Alcohols on Solid Support

To load the sensitiser onto the solid support, TPP (ca. 2 mg) in dichloromethane was added to the polystyrene-divinylbenzene beads (60 ± 15 μm diameter unswelled) (ca. 1.5 g). The slurry like mixture was transferred to a watch glass once the polystyrene had fully expanded, and the solvent allowed to evaporate. The loaded support media was then placed in a glass Petri dish (10 cm) and a solution of the allylic alcohol (1.0 - 5.0 mmol) in diethyl ether (10 mL) was applied to the loaded polystyrene. Once again the solvent was allowed to evaporate. The lid of the Petri dish was replaced loosely and irradiated with a tungsten lamp for 4 hours. In order to protect the volatile substrate from the heat produced by the lamp, a glass plate was placed between the lamp and the dish and the set-up cooled by a fan. The support media was then washed with methanol (3 × 20 mL) to remove the product while leaving the TPP absorbed to the polystyrene. The solvent was removed *in vacuo* and

the residue was purified by column chromatography eluting with hexane and ethyl acetate.

General Procedure 3

Preparation of Phosphite Ozonides (POA)

A flask fitted with a Drechsel head was charged with a solution (0.2 M) of triphenyl phosphite in DCM. The vessel was cooled to -78 °C while a stream of O_3 was bubbled through the mixture. Once the mixture turned blue, thus indicating the solution was saturated with O_3, the flask was flushed with N_2 for at least 20 minutes. The singlet oxygen acceptor was then added in a solution of DCM, and stirring was continued at -78 °C.

3-Hydroperoxy-4-methyl-4-penten-2-ol 79

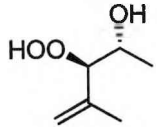

***via Photooxygenation*[1]**

Using the method outlined in General Procedure 1, photooxygenation of 4-methyl-3-penten-2-ol **78** (0.50 g, 4.90 mmol) for 4 hrs, and after chromatography (80:20 Hexane: EtOAc), gave a yellow oil **79** (0.36 g, 54%, d.r. 90:10 {*threo*:*erythro*}).

79: IR ν_{max} 3360 (ν_{O-H}), 2980 (ν_{C-H}), 1648($\nu_{C=C}$), 873, 830 ($\nu_{peroxide}$) cm^{-1}; ^1H NMR (400 MHz, $CDCl_3$) δ 5.09 (1H, m, -C=C$\underline{H}_2$), 5.08 (1H, m, -C=C$\underline{H}_2$), 4.15 (1H, d, *J*=8.3 Hz, -$\underline{H}$COOH), 3.87 (1H, dq, *J*=8.1, 6.3 Hz, -$\underline{H}$C(OH)CH_3), 1.75 (3H, m, =CC$\underline{H}_3$), 1.14 (3H, d, *J*=6.4 Hz, -HC(OH)C$\underline{H}_3$) ppm;

^{13}C NMR (100 MHz, $CDCl_3$) δ 144.7, 116.9, 96.6, 67.4, 19.2 and 18.3 ppm; *m/z* (CI) 150.11307 ($[M + NH_4]^+$); requires 150.11301.

***via Irradiation on Solid Support*[2]**

Using the method outlined in General Procedure 2, photooxygenation of 4-methyl-3-penten-2-ol **78** (0.38 g, 3.70 mmol) on solid support media for 4 hrs, and after chromatography (80:20 Hexane: EtOAc), afforded a yellow oil **79** (0.25 g, 47%, d.r. 70:30 {*threo*:*erythro*}).

Spectral data as above.

via Phosphite Ozonide Conditions: Direct Reaction

A solution of POA (triphenyl phosphite (1.57 mL, 6.00 mmol) in dichloromethane (30 mL)) was prepared as outlined in General Procedure 6. 4-Methyl-3-penten-2-ol **78** (0.20 g, 2.00 mmol) was then added dropwise and allowed to react for 4 hours at -78 °C. The solvents were removed *in vacuo* and the crude mixture purified by column chromatography (90:10 Hexane: EtOAc) to afford **79** (*Direct reaction*: 0.10 g, 40%, d.r. 90:10 {*threo*:*erythro*}) as a clear oil.

Spectral data as above.

via Phosphite Ozonide Conditions: Free Reaction

A solution of POA (triphenyl phosphite (1.11 mL, 4.22 mmol) in dichloromethane (20 mL)) was prepared as outlined in General Procedure 3. 4-Methyl-3-penten-2-ol **78** (0.14 g, 1.41 mmol) was added dropwise and the vessel allowed to warm to room temperature over 20 minutes. The solvents were removed *in vacuo* and the crude mixture purified by column chromatography (90:10 Hexane: EtOAc) to afford **79** (*Free reaction*: 0.04 g, 23%, dr 90:10 {*threo*:*erythro*}) as a clear oil.

Spectral data as above.

3-Hydroperoxy-1-phenyl-4-methyl-4-penten-2-ol 88

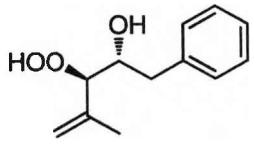

Using the method outlined in General Procedure 2, photooxygenation of 4-methyl-1-phenyl-3-penten-2-ol **87** (0.30 g, 1.70 mmol) on solid support media for 4 hrs, and after chromatography (80:20 Hexane: EtOAc), afforded a yellow oil **88** (0.17 g, 47%, d.r. 70:30 {*threo*:*erythro*}).

88: IR ν_{max} 3410 (ν_{O-H}), 3063, 3028 ($\nu_{C-H, Ar}$), 2926 (ν_{C-H}), 1603, 1584, 1496 ($\nu_{C=C, Ar}$) 864 ($\nu_{peroxide}$) cm^{-1}; ^1H NMR (200 MHz, $CDCl_3$) δ 7.26 (5H, m, Ar-H), 5.17 (1H, m, -C=C$\underline{H}_2$), 5.09 (1H, m, -C=C$\underline{H}_2$), 4.38 (1H, d, *J*=7.4 Hz, -$\underline{H}$COOH), 3.97 (1H, m, -$\underline{H}$C(OH)CH_3), 3.01 (1H, dd, *J*=13.8, 3.0 Hz, -C$\underline{H}_2$Ar), 2.75 (1H, dd, *J*=13.8 9.1, -C$\underline{H}_2$Ar), 1.85 (3H, m, =CC$\underline{H}_3$) ppm; ^{13}C NMR (100 MHz, $CDCl_3$) δ 141.7, 138.4, 129.9, 128.9, 127.0, 116.7, 91.7, 71.6, 39.5 and 19.3 ppm.

2-Hydroperoxy-1-phenyl-3-methyl-3-buten-1-ol 123a

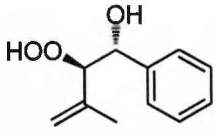

via Photooxygenation

Using the method outlined in General Procedure 6, photooxygenation of 3-methyl-1-phenyl-2-buten-1-ol **122a** (0.16 g, 0.99 mmol) for 1.5 hours, and thereafter purification by flash column chromatography (95:5 DCM: MeOH), gave a yellow oil **123a** (0.19 g, 97%, d.r. 90:10 {*threo*:*erythro*}).

123a: ^{1}H NMR (400 MHz, $CDCl_3$) δ 7.38-7.25 (5H, m, Ar-H), 4.92 (1H, m, -C=C$\underline{H}_2$), 4.88 (1H, m, -C=C$\underline{H}_2$), 4.71 (1H, d, *J*=8.4 Hz, -$\underline{H}$COOH), 4.51 (1H, d, *J*=8.5 Hz, -$\underline{H}$C(OH)Ar), 1.52 (3H, m, -CC$\underline{H}_3$) ppm; ^{13}C NMR (100 MHz, $CDCl_3$) δ 140.9, 136.8, 130.2, 128.6, 127.7, 116.6, 93.8, 75.8 and 19.8 ppm.

via Phosphite Ozonide Conditions: Direct Reaction

A solution of POA (triphenyl phosphite (0.96 mL, 3.69mmol) in dichloromethane (20 mL) was prepared as outlined in General Procedure 3. 3-Methyl-1-phenylbut-2-en-1-ol **122a** (0.168 g, 1.04 mmol) was then added dropwise and allowed to react with stirring. The reaction was monitored by t.l.c. and stopped after 2.5 hours. The solvents were then removed *in vacuo* and the crude mixture purified by column chromatography (90:10 Hexane: EtOAc) to afford **123a** (0.014 g, 7%, d.r. 90:10 {*threo*:*erythro*}) as a clear oil.

Spectral data as above.

(*E*)-3-Methyl-1-phenyl-1-buten-3-ol 124

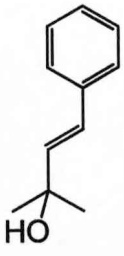

via Phosphite Ozonide Conditions: Direct Reaction

A solution of POA (triphenyl phosphite (0.96 mL, 3.69 mmol) in dichloromethane (20 mL) was prepared as outlined in General Procedure 3. 3-Methyl-1-phenyl-2-buten-1-ol **122a** (0.168 g, 1.04 mmol) was then added dropwise and allowed to react with stirring. The reaction was monitored by t.l.c. and stopped after 2.5 hours. The

solvents were then removed *in vacuo* and the crude mixture purified by column chromatography (95:5 Hexane: EtOAc) to afford **124** (0.15 g, 90%) as a clear oil.

124: ^{1}H NMR (400 MHz, $CDCl_3$) δ 7.25-7.14 (5H, m, Ar-H), 6.65 (1H, d, *J*=16.1 Hz, Ar-C<u>H</u>=CH-), 6.40 (1H, d, *J*=16.1 Hz, Ar-CH=C<u>H</u>-), 3.20 (1H, s, OH), 1.41 (6H, s, $-CH_3$) ppm; ^{13}C NMR (100 MHz, $CDCl_3$) δ 137.9, 137.3, 129.0, 127.9, 126.8, 126.8, 71.5 and 30.3 ppm; *m/z* (CI) 145.1021 ($[(M - H_2O) + H]^+$); requires 145.1017.

General Procedure 4

Preparation of 1,2,4-Trioxanes *via* Peroxyacetalization

The hydroperoxyalcohol (0.80 – 2.3 mmol) and the cyclic ketone (1.1 eq.) were stirred in dichloromethane (25 mL) at -10 °C. This was treated with catalytic amounts of *p*-TsOH (ca. 2 mg). This was allowed to react for 30 minutes at -10 °C then warmed to room temperature to react overnight. The solvent was removed *in vacuo* and the crude product purified by column chromatography eluting with hexane and ethyl acetate.

5-Methyl-6-(prop-1-en-2-yl)spiro-[1,2,4-trioxacyclohexane-3,2'-cyclohexane][3]

89b

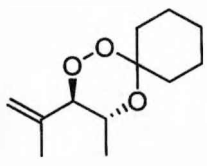

Condensation of 3-hydroperoxy-4-methyl-4-penten-2-ol **79** (0.16 g, 1.20 mmol) with cyclohexanone (0.14 ml, 1.32 mmol) for 30 minutes and purification by chromatography (90:10 Hexane: EtOAc), yielded **89b** (0.10 g, 40%) as a yellow oil.

89b: IR ν_{max} 3083 ($\nu_{C=C}$), 2926, 2854 (ν_{C-H}), 844 ($\nu_{peroxide}$) cm^{-1}; ^1H NMR (400 MHz, $CDCl_3$) δ 5.08 (2H, m, -C=C$\underline{H}_2$), 4.20 (1H, d, *J*=9.7 Hz, -$\underline{H}$COOC-), 4.11 (1H, dq, *J*=9.5, 6.1 Hz, -$\underline{H}$COC-), 2.24 (2H, m), 1.97 (2H, m), 1.76 (3H, m, =CC$\underline{H}_3$), 1.59 (6H, m), 1.11 (3H, d, *J*=6.3 Hz, -HC(O)C$\underline{H}_3$) ppm; ^{13}C NMR (100 MHz, $CDCl_3$) δ 142.2, 114.2, 103.3, 89.2, 75.0, 35.6, 30.0, 22.7 and 17.4 ppm; *m/z* (CI) 213.14887 ($[M + NH_4]^+$); requires 213.14906. Anal. $C_{12}H_{20}O_3$ requires C 67.89%, H 9.50%, found C 67.81%, H 9.53%.

5-Methyl-6-(prop-1-en-2-yl)spiro-[1,2,4-trioxacyclohexane-3,2'-cyclopentane] 89a

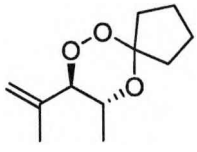

Condensation of 3-hydroperoxy-4-methyl-4-penten-2-ol **79** (0.30 g, 2.28 mmol) with cyclopentanone (0.20 ml, 2.51 mmol) for 30 minutes, and purification by chromatography (90:10 Hexane: EtOAc), afforded **89a** (0.09 g, 19%) as a yellow oil. **89a**: IR ν_{max} 3084 ($\nu_{C=C}$), 2976, 2875 (ν_{C-H}), 860 ($\nu_{peroxide}$) cm^{-1}; ^1H NMR (400 MHz, $CDCl_3$) δ 5.07 (2H, m, -C=C$\underline{H}_2$), 4.27 (1H, d, *J*=9.5 Hz, -$\underline{H}$COOC-), 3.95 (1H, dq, *J*=9.5, 6.3 Hz, -$\underline{H}$COC-), 2.53 (2H, m), 1.76 (3H, m, =CC$\underline{H}_3$), 1.62 (6H, m), 1.10 (3H, d, *J*=6.3 Hz, -HC(O)C$\underline{H}_3$) ppm; ^{13}C NMR (100 MHz, $CDCl_3$) δ 139.6, 118.0, 115.1, 89.1, 68.8, 37.8, 33.4, 25.1, 23.5, 19.9 and 17.2 ppm; *m/z* (CI) 199.13371 ($[M + NH_4]^+$); requires 199.13342.

5-Methyl-6-(prop-1-en-2-yl)spiro-[1,2,4-trioxacyclohexane-3,2'-adamantane][3]

86c

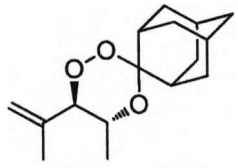

Condensation of 3-hydroperoxy-4-methyl-4-penten-2-ol **79** (0.30 g, 2.28 mmol) with 2-adamantanone (0.38 g, 2.51 mmol) for 30 minutes, and after purification by chromatography (90:10 Hexane: EtOAc), gave **89c** (0.25 g, 42%) as a pale yellow oil which crystallised upon drying.

89c: m.p. 42-44 °C; IR ν_{max} 3082 ($\nu_{C=C}$), 2916, 2857 (ν_{C-H}), 869, 803 ($\nu_{peroxide}$) cm^{-1}; ^1H NMR (400 MHz, $CDCl_3$) δ 5.07 (2H, m, -C=C$\underline{H}_2$), 4.20 (1H, d, *J*=9.5 Hz, -$\underline{H}$COOC-), 4.09 (1H, dq, *J*=9.5, 6.3 Hz, -$\underline{H}$COC-), 2.93 (2H, m), 2.41–1.55 (12H, m), 1.76 (3H, m, =CC$\underline{H}_3$), 1.10 (3H, d, *J*=6.2 Hz, -HC(O)C$\underline{H}_3$) ppm; ^{13}C NMR (100 MHz, $CDCl_3$) δ 139.8, 113.8, 105.3, 86.8, 75.0, 65.5, 38.8, 37.7, 30.3, 27.4 and 18.1 ppm; *m/z* (CI) 265.18012 ($[M + NH_4]^+$); requires 265.18039. Anal. $C_{16}H_{24}O_3$ requires C 72.69%, H 9.15%, found C 72.17%, H 9.41%.

5-Benzyl-6-(prop-1-en-2-yl)spiro-[1,2,4-trioxacyclohexane-3,2'-cyclohexane] 89e

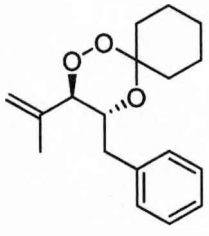

Condensation of 3-hydroperoxy-1-phenyl-4-methyl-4-penten-2-ol **88** (0.27 g, 1.30 mmol) with cyclohexanone (0.15 mL, 1.43 mmol) for 30 minutes and after

purification by chromatography (90:10 Hexane: EtOAc), gave a pale yellow oil **89e** (0.07 g, 20%) which later crystallised upon drying.

89e: m.p. 43-45 °C; IR ν_{max} 3081 ($\nu_{C=C}$), 3064, 3028 ($\nu_{C-H,\ Ar}$), 2937, 2858 (ν_{C-H}), 1603, 1496, 1454 ($\nu_{C=C,\ Ar}$), 874, 823 ($\nu_{peroxide}$) cm^{-1}; ^1H NMR (400 MHz, $CDCl_3$) δ 7.26 (5H, m, Ar-H), 5.17 (2H, m, -C=C$\underline{H}_2$), 4.38 (1H, d, *J*=9.6 Hz, -$\underline{H}$COOC-), 4.17 (1H, td, *J*=9.6, 3.1 Hz, -$\underline{H}$COC-), 2.79 (1H, dd, *J*=14.4, 3.1 Hz, -C$\underline{H}_2$Ar), 2.70 (1H, dd, *J*=14.4, 8.2 Hz, -C$\underline{H}_2$Ar), 2.23–1.17 (10H, m), 1.80 (3H, m, =CC$\underline{H}_3$) ppm; ^{13}C NMR (100 MHz, $CDCl_3$) δ 142.2, 138.4, 129.4, 128.4, 126.6, 119.0, 103.5, 87.6, 70.6, 37.8, 35.4, 29.8, 26.0, 22.6 and 20.1 ppm; *m/z* (CI) 306.20762 ($[M + NH_4]^+$); requires 306.20694.

5-Benzyl-6-(prop-1-en-2-yl)spiro-[1,2,4-trioxacyclohexane-3,2'-cyclopentane] 89d

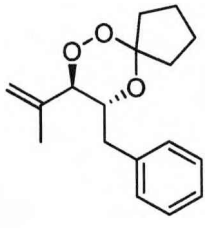

Condensation of 3-hydroperoxy-1-phenyl-4-methyl-4-penten-2-ol **88** (0.30 g, 1.44 mmol) with cyclopentanone (0.20 mL, 1.58 mmol) for 30 minutes, and after purification by chromatography (90:10 Hexane: EtOAc), gave a pale yellow oil **89d** (0.24 g, 60%).

89d: IR ν_{max} 3080, 3070 ($\nu_{C=C}$), 3026 ($\nu_{C-H,\ Ar}$), 2954 (ν_{C-H}), 1496, 1454 ($\nu_{C=C,\ Ar}$), 912 ($\nu_{peroxide}$) cm^{-1}; ^1H NMR (400 MHz, $CDCl_3$) δ 7.28-7.19 (5H, m, Ar-H), 5.14 (1H, s, -C=C$\underline{H}_2$), 5.12 (1H, m, -C=C$\underline{H}_2$), 4.43 (1H, d, *J*=9.5 Hz, -$\underline{H}$COOC-), 4.10 (1H, td,

J=9.7, 3.0 Hz, -HCOC-), 2.79 (1H, dd, *J*=14.6, 2.8 Hz, -CH_2Ar), 2.70 (1H, dd, *J*=14.6, 8.4 Hz, -CH_2Ar), 1.87–1.58 (8H, m), 1.76 (3H, m, =CCH_3) ppm; ^{13}C NMR (100 MHz, $CDCl_3$) δ 139.4, 138.4, 129.8, 128.5, 126.7, 119.2, 115.3, 87.6, 73.1, 37.7, 37.5, 33.3, 25.1, 23.5 and 19.9 ppm; *m/z* (ES) 297.1481 ([M + Na]$^+$) requires 297.1467. Anal. $C_{17}H_{22}O_3$ requires C 74.42%, H 8.08%, found C 75.12%, H 8.22%.

5-Benzyl-6-(prop-1-en-2-yl)spiro-[1,2,4-trioxacyclohexane-3,2'-adamantane] 89f

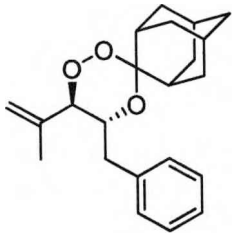

Condensation of 3-hydroperoxy-1-phenyl-4-methyl-4-penten-2-ol **88** (0.17 g, 0.81 mmol) with 2-adamantanone (0.19 g, 0.90 mmol) for 30 minutes, and after purification by chromatography (90:10 Hexane: EtOAc), afforded a pale yellow oil **89f** (0.03 g, 12%).

89f: IR ν_{max} 3081 ($\nu_{C=C}$), 3064, 3028 ($\nu_{C-H, Ar}$), 2937, 2858 (ν_{C-H}), 1603, 1496, 1454 ($\nu_{C=C, Ar}$), 874, 823 ($\nu_{peroxide}$) cm^{-1}; ^{1}H NMR (400 MHz, $CDCl_3$) δ 7.31 (5H, m, Ar-H), 5.02 (1H, m, -C=CH_2), 4.93 (1H, m, -C=CH_2), 4.09 (1H, d, *J*=8.4 Hz, -HCOOC-), 3.99 (1H, m, -HCOC-), 2.87 (2H, m, -CH_2Ar), 1.99 (4H, m), 1.83 (3H, m), 1.74 (3H, s, =CCH_3), 1.69 (7H, m) ppm; ^{13}C NMR (100 MHz, $CDCl_3$) δ 142.6, 138.7, 130.0, 128.5, 126.7, 114.8, 112.1, 84.5, 79.1, 39.1, 38.7, 38.1, 37.7, 35.4, 35.1, 34.8, 30.1, 27.3 and 17.7 ppm. *m/z* (ES) 363.1940 ([M + Na]$^+$) requires 363.1936.

General Procedure 4

Preparation of the Propargyl Ketone

Trimethylsilylpropyne **90** (1.33 mL, 8.91 mmol) was stirred in DCM at 0 °C. The acid chloride (1.1 eq.) was added, followed by anhyd. $AlCl_3$ (1.1 eq.). The reaction was stirred for a further 30 minutes at 0 °C. This was quenched with a mixture of 10% aq. HCl and ice (10 mL, 50:50). The aqueous phase was extracted with dichloromethane (3 × 10 mL) and the organic extracts combined and washed with sat. $NaHCO_3$ solution (10 mL) and dried over $MgSO_4$. The solvent was removed *in vacuo* in a cold water bath to leave an oil residue.

1-Phenyl-2-butyn-1-one 92a

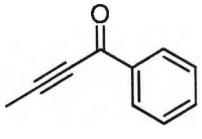

Trimethylsilylpropyne **90** (1.33 mL, 8.91 mmol) was stirred with benzoyl chloride **91a** (1.14 mL, 9.80 mmol) for 30 minutes at 0 °C. This afforded 1-phenyl-2-butyn-1-one, **92a** (1.16 g, 90%), as a green oil.

92a: IR ν_{max} 3091, 3065 ($\nu_{C\text{-}H,\ Ar}$), 2925, 2862 ($\nu_{C\text{-}H}$), 1714 ($\nu_{C=O}$), 2249, 2212 ($\nu_{C\equiv C}$), 1655, 1570, 1496 ($\nu_{C=C,\ Ar}$) cm^{-1}; ^1H NMR (400 MHz, $CDCl_3$) δ 7.47 (5H, m, Ar-H), 2.15 (3H, s, ≡CC<u>H</u>$_3$) ppm; ^{13}C NMR (100 MHz, $CDCl_3$) δ 178.8, 137.5, 134.5, 130.2, 129.0, 93.0, 79.6 and 4.9 ppm. *m/z* (CI) 145.06510 ($[M + NH_4]^+$); requires 145.06534.

2-Methyl-4-hexyn-3-one 92b

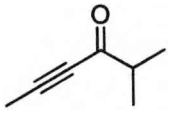

Trimethylsilylpropyne **90** (1.33 mL, 8.91 mmol) was stirred with isobutyryl chloride **91b** (1.03 mL, 9.80 mmol) for 30 minutes at 0 °C. This afforded 2-methyl-4-hexyn-3-one, **92b** (0.92 g, 92%), as an orange oil.

For **92b**: IR ν_{max} 2974 (ν_{C-H}), 2218 ($\nu_{C\equiv C}$), 1674 ($\nu_{C=O}$) cm^{-1}; ^1H NMR (400 MHz, $CDCl_3$) δ 2.54 (1H, sept, *J*=7.0 Hz, -C<u>H</u>$(CH_3)_2$), 1.97 (3H, s, ≡CC<u>H</u>$_3$), 1.10 (6H, d, *J*=7.0 Hz, -CH(C<u>H</u>$_3)_2$) ppm; ^{13}C NMR (100 MHz, $CDCl_3$) 190.4, 88.7, 77.3, 41.0, 29.0, 16.0 and 2.1 ppm. *m/z* (CI) 128.10787 ($[M + NH_4]^+$); requires 128.10753.

2-Methyl-4-hexyn-3-ol[4] *rac*-93b

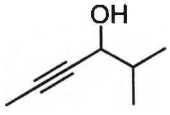

2-Methyl-4-hexyn-3-one **92b** (0.50 g, 4.45 mmol) was stirred in diethyl ether (10 mL) at 0 °C. $LiAlH_4$ (0.19 g, 4.95 mmol) was added over 15 minutes and the mixture was allowed to react for a further 15 minutes at room temperature.

The reaction was quenched sequentially with water (0.5 mL), NaOH 15% w/v (0.5 mL) and again water (1.5 mL). This was stirred for 30 minutes. The mixture was filtered through a layer of celite, removing the Li precipitate. The solvent was removed *in vacuo* in a cold water bath to give ***rac*-93b** (0.48 g, 96%) as a yellow oil.

***rac*-93b**: IR ν_{max} 3374 (ν_{O-H}), 2962 (ν_{C-H}), 2223 ($\nu_{C\equiv C}$) cm^{-1}; ^1H NMR (400 MHz, $CDCl_3$) δ 4.13 (1H, m, -C<u>H</u>(OH)-), 1.85 (3H, d, *J*=2.3 Hz, ≡CC<u>H</u>$_3$), 1.90-1.70 (1H, m, -C<u>H</u>$(CH_3)_2$), 0.99 (6H, t, *J*=3.7 Hz, -CH(C<u>H</u>$_3)_2$), ppm; ^{13}C NMR (100 MHz, $CDCl_3$) δ 81.9, 79.5, 74.5, 34.7, 18.5, 17.8 and 3.8 ppm; *m/z* (CI) 130.12349 ([M + NH_4]$^+$); requires 130.12318.

1-Phenyl-2-butyn-1-ol (*R*)-93a

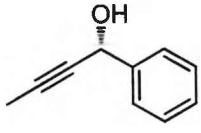

A 3-necked round bottom flask was charged with (*R*)-Alpine Borane (0.5 M in THF, 15 mL, 7.58 mmol). Under nitrogen, the vessel was transferred to a rotary evaporator where the THF was removed under vacuum at 40 °C. The flask was then released from the vacuum under nitrogen and cooled to 0 °C. 1-Phenyl-2-butyn-1-one **92a** (0.69 g, 4.77 mmol) was added and the vessel was allowed to warm to room temperature and left to react overnight.

Freshly distilled propionaldehyde (0.36 mL, 5.01 mmol) was added and the mixture allowed to stir for an hour at room temperature. The flask was again transferred to the rotary evaporator under nitrogen and the liberated (+)-α-pinene was removed *in vacuo* at 40 °C. Once removed from the rotary evaporator, THF (4.00 mL) was added, NaOH (3 M, 2.50 mL) and finally H_2O_2 (30%, 2.50 mL). The latter was added dropwise at 0 °C as the reaction is exothermic. This was allowed to warm to room temperature, then heated to 40 °C and stirred for 3 hours. At this point the vessel was removed from the nitrogen atmosphere, the product was extracted with

diethyl ether (3 × 10 mL) and the extracts combined and dried over $MgSO_4$. The solvent was removed *in vacuo* in a cold water bath and the residue was purified by column chromatography (70:30 DCM: Pet. Ether) to give a yellow oil. This was further distilled from a Kügelrohr oven (100 °C) to give ***R*-93a** (0.15 g, 21%) as a colourless liquid. The absolute configuration was determined by comparison with the report that *R*-Alpine borane derived from (+)-α-pinene gives exclusively the *R*-enantiomer.[4]

***R*-93a**: IR ν_{max} 3418 (ν_{O-H}), 3063, 3031 ($\nu_{C-H,\ Ar}$), 2919, 2856 (ν_{C-H}), 2243, 2206 ($\nu_{C\equiv C}$), 1643, 1580, 1494 ($\nu_{C=C,\ Ar}$) cm^{-1}; ^1H NMR (400 MHz, $CDCl_3$) δ 7.36 (5H, m, Ar-H), 5.38 (1H, q, *J*=2.1 Hz, -C<u>H</u>(OH)-), 1.87 (3H, d, *J*=2.3 Hz, ≡CC<u>H</u>$_3$) ppm; ^{13}C NMR (100 MHz, $CDCl_3$) δ 141.8, 129.0, 128.5, 127.0, 83.3, 79.8, 65.0 and 4.0 ppm; *m/z* (CI) 146.09644 ($[M + NH_4]^+$); requires 146.09697.

(*S*)-2-Methyl-4-hexyn-3-ol (*S*)-93b

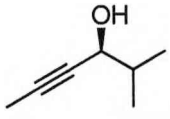

The precatalyst was formed *in situ* by stirring (*S,S*)-TsDPEN **(*S,S*)-98** (13 mg, 0.04 mmol), with $[Cp^*RhCl_2]_2$ **97** (18 mg, 0.03 mmol) in H_2O (10 mL) at 40 °C for 1 hr. Sodium formate (0.99 g, 14.54 mmol) and 2-methyl-4-hexyn-3-one **92b** (0.40 g, 3.63 mmol) were added sequentially. The mixture was stirred vigorously at room temperature overnight. Finally, additional sodium formate was added to increase conversion and stirred for a further 2 hrs. The organic phase was then extracted with diethyl ether (3 × 10 mL) and filtered through celite. The solvent was

removed by simple distillation to give **(*S*)-93b** as a pale yellow oil (97% conversion, 93% ee). The absolute configuration was determined by comparing the optical rotations of a series of similar alcohols and it is reported that the handedness of diphenylethylene diamine ligand is transferred to the alcohol product.[5,6]

(*S*)-93b: NMR and other analytical data were similar to that of ***rac*-93b**.

(*R*)-2-Methyl-4-hexyn-3-ol (*R*)-93b

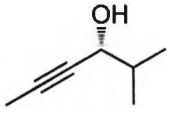

The precatalyst was formed *in situ* by stirring (*R,R*)-CsDPEN **(*R,R*)-98** (13 mg, 0.04 mmol), with $[Cp^*RhCl_2]_2$ **97** (18 mg, 0.03 mmol) in H_2O (10 mL) at 40 °C for 1hr. Sodium formate (0.99 g, 14.54 mmol) and 2-methyl-4-hexyn-3-one **92b** (0.40 g, 3.63 mmol) were added sequentially. The mixture was stirred vigorously at room temperature overnight. Finally, additional sodium formate was added to increase conversion and stirred for a further 2 hrs. The organic phase was then extracted with diethyl ether (3 × 10 mL) and filtered through celite. The solvent was removed by simple distillation to give **(*R*)-93b** as a pale yellow oil (97% conversion, 93% ee).

(*R*)-93b: NMR and other analytical data were similar to that of ***rac*-93b**.

α-Methoxy-α-trifluoromethylphenylacetyl chloride 101

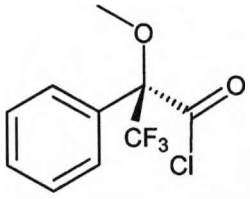

A mixture of MTPA **100** (0.09 g, 0.34 mmol), $SOCl_2$ (ca. 1.5 mL) and NaCl (ca. 1 mg) was allowed to reflux overnight. The $SOCl_2$ was then removed *in vacuo* in preparation for the acid chloride **101** to be used immediately.

2-Methyl-4-hexyn MTPA ester *rac*-102

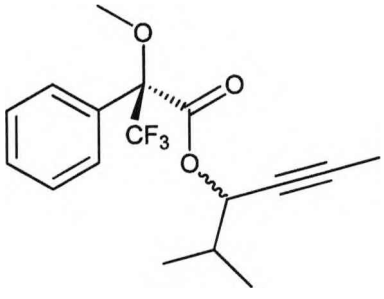

A mixture of 2-methyl-4-hexyn-3-ol ***rac*-93b** (0.10 g, 0.89 mmol), anhyd. pyridine (0.5 mL) and DCM (0.5 mL) was added to the acid choride **101** (0.34 mmol) and allowed to stir for 12 hours. The reaction was quenched by adding water (1 mL) and the mixture was extracted with diethyl ether (20 mL). The organic extracts were then washed with dil. HCl (20 mL), $NaHCO_3$ (20 mL) and water (20 mL) and dried over $MgSO_4$. The Mosher's ester was then isolated by column chromatography (80:20 Hexane: EtOAc) to furnish clear oil ***rac*-102** (0.030 g, 10%).

***rac*-102**: ^{1}H NMR (400 MHz, $CDCl_3$) δ 7.59 (1H, m, Ar-H), 7.42-7.36 (4H, m, Ar-H), 5.36 (1H, m, -C<u>H</u>(O)-), 3.59 (3H, s, -OC<u>H</u>$_3$)$_S$, 3.55 (3H, s, -OC<u>H</u>$_3$)$_R$, 2.02-1.94 (1H, m, -C<u>H</u>(CH$_3$)$_2$), 1.87 (3H, d, *J*=2.3 Hz, ≡CC<u>H</u>$_3$)$_S$, 1.83 (3H, d, *J*=2.1 Hz,

≡CC$\underline{H}_3)_R$, 1.02 (3H, d, *J*=6.6, -CH(C$\underline{H}_3)_2)_R$, 1.01 (3H, d, *J*=6.6, -CH(C$\underline{H}_3)_2)_R$, 0.95 (3H, d, *J*=6.6 Hz, -CH(C$\underline{H}_3)_2)_S$, 0.93 (3H, d, *J*=6.6 Hz, -CH(C$\underline{H}_3)_2)_S$; ^{13}C NMR (100 MHz, $CDCl_3$) δ 166.2, 133.0, 129.9, 128.7, 127.8, 124.1, 83.7, 74.8, 72.1, 55.8, 33.0, 30.1, 18.2, 18.0 and 3.8 ppm; ^{19}F (376 MHz, $CDCl_3$) δ -71.56, -71.58 ppm; *m/z* (ES) 351.1183 ($[M + Na]^+$); requires 351.1184.

2-Methyl-4-hexyn MTPA ester (*S*)-102

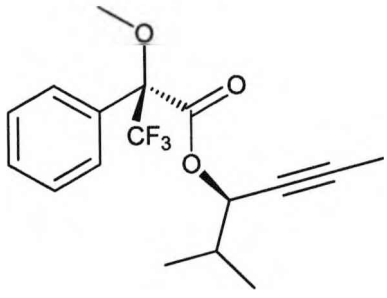

A mixture of 2-methyl-4-hexyn-3-ol **(*S*)-93b** (0.10 g, 0.89 mmol), anhyd. pyridine (0.5 mL) and DCM (0.5 mL) was added to the acid choride **101** (0.34 mmol) and allowed to stir for 12 hours. The reaction was quenched by adding water (1 mL) and the mixture was extracted with diethyl ether (20 mL). The organic extracts were then washed with dil. HCl (20 mL), $NaHCO_3$ (20 mL) and water (20 mL) and dried over $MgSO_4$. The Mosher's ester was then isolated by column chromatography (80:20 Hexane: EtOAc) to furnish clear oil **(*S*)-102** (0.02 g, 6%).

(*S*)-102: ^{1}H NMR (400 MHz, $CDCl_3$) δ 7.59 (1H, m, Ar-H), 7.42-7.36 (4H, m, Ar-H), 5.36 (1H, dq, *J*=5.7, 2.3 Hz, -C$\underline{H}$(O)-), 3.59 (3H, s, -OC$\underline{H}_3$), 2.02-1.94 (1H, m, -C$\underline{H}$(CH$_3$)$_2$), 1.87 (3H, d, *J*=2.1 Hz, ≡CC$\underline{H}_3$), 0.95 (3H, d, *J*=6.6 Hz, -CH(C$\underline{H}_3)_2$), 0.93 (3H, d, *J*=6.6 Hz, -CH(C$\underline{H}_3)_2$) ppm; ^{13}C NMR (100 MHz, $CDCl_3$) δ 166.2, 133.0, 129.9, 128.7, 127.8, 124.1, 83.7, 74.8, 72.1, 55.8, 33.0, 30.1, 18.2, 18.0 and 3.8 ppm;

^{19}F (376 MHz, $CDCl_3$) δ -71.56 ppm; *m/z* (CI) 346.16195 ($[M + NH_4]^+$); requires 346.16302.

General Procedure 5

(Z)-Selective Reduction of an Alkyne

A solution of 2-methyl-4-hexyn-3-ol **93b** (approx. 9 mmol), Lindlar catalyst (100 mg) and 2,6-lutidine (50 µl) in hexane was stirred vigorously while exposed to H_2 atmosphere. More catalyst was periodically added for up to 3 hours, until H_2 uptake ceased, monitored by Hg-bubbler column. The catalyst was then removed by filtration through celite and the mixture washed with dil. HCl to remove the 2,6-lutidine. The organic layer was dried over $MgSO_4$ and the solvent removed *in vacuo* in a cold water bath to give a yellow oil. Due to similar R_F values of the starting material and product, the resulting (*Z*)-2-methyl-4-hexen-3-ol could not be purified so full analysis was carried out on the crude product and this was taken on to the next step.

(Z)-2-Methyl-4-hexen-3-ol[4] *rac*-94b

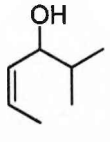

A solution of 2-methyl-4-hexyn-3-ol ***rac*-93b** (1.00 g, 8.92 mmol) was treated with Lindlar catalyst (100 mg) and 2,6-lutidine (50 µl) following General Procedure 5 to give (*Z*)-2-methyl-4-hexen-3-ol ***rac*-94b** as a yellow oil.

***rac*-94b**: IR ν_{max} 3443 (ν_{O-H}), 2968 (ν_{C-H}); ^{1}H NMR (400 MHz, $CDCl_3$) δ 5.63 (1H, dqd, *J*=11.0, 6.8, 0.9 Hz, -C<u>H</u>=CHCH$_3$), 5.42 (1H, ddq, *J*=11.0, 8.9, 1.7 Hz, -CH=C<u>H</u>CH$_3$), 4.18 (1H, dd, *J*=8.9, 6.6 Hz, -C<u>H</u>(OH)-), 1.76-1.68 (1H, m, -C<u>H</u>(CH$_3$)$_2$), 1.69 (3H, dd, *J*=6.8, 1.7 Hz, -CH=CHC<u>H</u>$_3$), 1.35 (1H, br, OH), 0.96 (3H, d, *J*=6.8 Hz, -CH(C<u>H</u>$_3$)$_2$), 0.88 (3H, d, *J*=6.8 Hz, -CH(C<u>H</u>$_3$)$_2$) ppm; ^{13}C NMR (100 MHz, $CDCl_3$) δ 131.8, 127.1, 72.3, 34.2, 18.5, 18.3 and 13.5 ppm.

^{1}H NMR confirmed the product to have 100% (*Z*)-double bond geometry.

(*S*,*Z*)-2-Methyl-4-hexen-3-ol[4] (*S*,*Z*)-94b

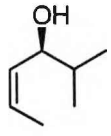

A solution of (*S*)-2-methyl-4-hexyn-3-ol **(*S*)-93b** (1.00 g, 8.92 mmol) was treated with Lindlar catalyst (100 mg) and 2,6-lutidine (50 µl) following General Procedure 5 to give (*S*,*Z*)-2-methyl-4-hexen-3-ol **(*S*,*Z*)-94b** as a yellow oil.

(*S*,*Z*)-94b: NMR and other analytical data were similar to that of ***rac*-94b**.

(*R*,*Z*)-2-Methyl-4-hexen-3-ol[4] (*R*,*Z*)-94b

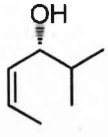

A solution of (*S*)-2-methyl-4-hexyn-3-ol **(*R*)-93b** (1.00 g, 8.92 mmol) was treated with Lindlar catalyst (100 mg) and 2,6-lutidine (50 µl) following General Procedure 5 to give (*R*,*Z*)-2-methyl-4-hexen-3-ol **(*R*,*Z*)-94b** as a yellow oil.

(*R*,*Z*)-94b: NMR and other analytical data were similar to that of ***rac*-94b**.

General Procedure 6

Modified General Procedure for the Photooxygenation of Allylic Alcohols

A standard B24 Liebig condenser was sealed off at the lower end and fitted with a cold-finger trap condenser containing dry ice and acetone. PTFE tubing was fed through the equipment in order to deliver O_2 from the bottom of the Liebig condenser. The reaction mixture consisting of the allylic alcohol (ca. 0.9 mmol) and TPP (ca. 2 mg) in dichloromethane (50 mL), filled the condenser and was cooled externally by the water jacket. This was then aerated with O_2 and irradiated with 4 tungsten lamps (2-4 hours). The solvent was removed *in vacuo* and the crude product purified by column chromatography eluting with dichloromethane and methanol.

4-Hydroperoxy-2-methyl-5-hexen-3-ol[1] ***rac*-95b**

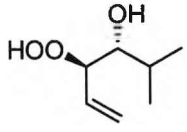

The allylic alcohol (*Z*)-2-methyl-4-hexen-3-ol ***rac*-94b** (0.5 g, 4.38 mmol) underwent photooxygenation for 4 hours as outlined in General Procedure 1. This was then purified by column chromatography (99:1 DCM: MeOH) to give ***rac*-95b** (0.06 g, 9%, d.r. 90:10 {*threo*:*erythro*}) as a clear oil.

***rac*-95b**: ^{1}H NMR (400 MHz, $CDCl_3$) δ 5.89 (1H, ddd, *J*=17.4, 10.4, 8.0 Hz, -HC=CH_2), 5.47 (1H, d, J_{trans} =17.2 Hz, -C=CH_2), 5.42 (1H, d, J_{cis} =10.4 Hz, -C=CH_2), 4.35 (1H, t, *J*=8.0 Hz, -HCOOH), 3.51 (1H, dd, *J*=7.8, 3.8 Hz, -CH(OH)-), 2.54 (1H, br, OH), 1.80 (1H, m, -CH$(CH_3)_2$), 1.02 (3H, d, *J*=6.8 Hz, -CH(CH_3)$_2$), 0.92 (3H, d, *J*=6.8 Hz, -CH(CH_3)$_2$) ppm;

^{13}C NMR (100 MHz, $CDCl_3$) δ 133.9, 121.2, 89.4, 76.8, 29.9, 19.1 and 15.7 ppm.

(3*S*,4*S*)-4-Hydroperoxy-2-methyl-5-hexen-3-ol (3*S*,4*S*)-95b

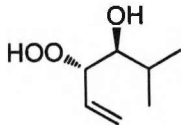

The allylic alcohol (*S*,*Z*)-2-methyl-4-hexen-3-ol **(*S*,Z)-94b** (0.10 g, 0.88 mmol) underwent photooxygenation for 4 hours as outlined in General Procedure 6. This was then purified by column chromatography (99:1 DCM: MeOH) to give **(3*S*,4*S*)-95b** (0.06 g, 43%, d.r. 90:10 {*threo*:*erythro*}) as a clear oil.

(3*S*,4*S*)-95b: NMR and other analytical data were similar to that of ***rac*-95b**.

(3*R*,4*R*)-4-Hydroperoxy-2-methyl-5-hexen-3-ol (3*R*,4*R*)-95b

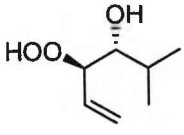

The allylic alcohol (*R*,*Z*)-2-methyl-4-hexen-3-ol **(*R*,Z)-94b** (0.25 g, 2.19 mmol) underwent photooxygenation for 4 hours as outlined in General Procedure 6. This was then purified by column chromatography (99:1 DCM: MeOH) to give **(3*R*,4*R*)-95b** (0.15 g, 47%, d.r. 90:10 {*threo*:*erythro*}) as a clear oil.

(3*R*,4*R*)-95b: NMR and other analytical data were similar to that of ***rac*-95b**.

5-Isopropyl-6-(vinyl)spiro-[1,2,4-trioaxcyclohexane-3,2'-adamantane] *rac*-96b

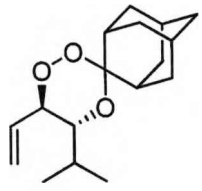

Condensation of 4-hydroperoxy-2-methyl-5-hexen-3-ol ***rac*-95b** (0.06 g, 0.41 mmol) with 2-adamantanone (0.07 g, 0.45 mmol) overnight and after purification by chromatography (90:10 Hexane: EtOAc), yielded ***rac*-96b** as a pale yellow oil (0.03 g, 30%).

***rac*-96b**: IR ν_{max} 2906, 2856 ($\nu_{C\text{-}H}$), 925 ($\nu_{peroxide}$); ^{1}H NMR (400 MHz, $CDCl_3$) δ 5.67 (1H, ddd, J=17.4, 10.4, 7.8 Hz, -HC=CH_2), 5.49 (1H,d, J_{trans}=17.5 Hz, -C=CH_2), 5.39 (1H, d, J_{cis}=9.9 Hz, -C=CH_2), 4.53 (1H, dd, J=9.6, 7.6 Hz, -HCOOC-), 3.67 (1H, dd, J=9.6, 2.8 Hz, -CHOC-), 2.14-1.23 (14H, m), 1.78 (1H, m, -CH(CH_3)$_2$), 1.02 (3H, d, J=7.0 Hz, -CH(CH_3)$_2$), 0.93 (3H, d, J=6.8 Hz, -CH(CH_3)$_2$) ppm; ^{13}C NMR (100 MHz, $CDCl_3$) δ 131.6, 123.1, 105.0, 83.4, 73.9, 37.7, 37.01, 34.0, 33.7, 33.4, 32.0, 29.9, 28.6, 27.7, 20.5 and 15.6 ppm; *m/z* (CI) 279.19510 ([M + NH_4]$^+$); requires 279.19600. Anal. $C_{17}H_{26}O_3$ requires C 73.34%, H 9.41%, found C 74.47%, H 9.69%.

(5*S*,6*S*)-(-)-5-Isopropyl-6-(vinyl)spiro-[1,2,4-trioaxcyclohexane-3,2'-adamantane] (5*S*,6*S*)-96b

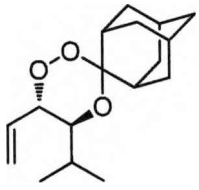

Condensation of 4-hydroperoxy-2-methyl-5-hexen-3-ol **(3*S*,4*S*)-95b** (0.08 g, 0.55 mmol) with 2-adamantanone (0.09 g, 0.60 mmol) overnight and after purification by chromatography (90:10 Hexane: EtOAc), yielded **(5*S*,6*S*)-96b** as a pale yellow oil (0.05 g, 34%).

(5*S*,6*S*)-96b: $[\alpha]^{20}_{D}$ -163.0 (c 1.4, $CHCl_3$). NMR and other analytical data were similar to that of ***rac*-96b**.

(5*R*,6*R*)-(+)-5-Isopropyl-6-(vinyl)spiro-[1,2,4-trioaxcyclohexane-3,2'-adamantane] (5*R*,6*R*)-96b

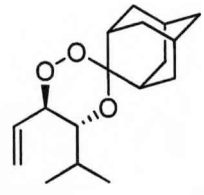

Condensation of 4-hydroperoxy-2-methyl-5-hexen-3-ol **(3*R*,4*R*)-95b** (0.15 g, 1.03 mmol) with 2-adamantanone (0.17 g, 1.13 mmol) overnight, and after purification by chromatography (90:10 Hexane: EtOAc), yielded **(5*R*,6*R*)-96b** as a pale yellow oil (0.08 g, 26%).

(5*R*,6*R*)-96b: $[\alpha]^{20}_{D}$ +115.0 (c 1.5, $CHCl_3$); NMR and other analytical data were similar to that of ***rac*-96b**.

1-Isopropyl-4-methyl-2,3-dioxabicyclo[2.2.2]oct-5-ene[7] 119

A solution of the POA (triphenyl phosphite (0.68 mL, 2.59 mmol) in DCM (10 mL)) was prepared as outlined in General Procedure 3. α-Terpinene **118** (0.24 mL, 1.28 mmol) was then added dropwise and allowed to react with stirring. The reaction was monitored by t.l.c. and reached completion after 30 minutes. The solvents were then removed *in vacuo* and the crude mixture purified by column chromatography (90:10 Hexane: EtOAc) to afford **119** (0.13 g, 61%) as a colourless oil.

119: ^{1}H NMR (400 MHz, $CDCl_3$) δ 6.51 (1H, d, *J*=8.5 Hz, C<u>H</u>=CH), 6.42 (1H, d, *J*=8.5 Hz C<u>H</u>=CH), 2.07-1.98 (4H, m, -C<u>H</u>$_2$-C<u>H</u>$_2$-), 1.97 (1H, sept, *J*=7.0 Hz, -C<u>H</u>$(CH_3)_2$), 1.37 (3H, s, -CC<u>H</u>$_3$), 1.00 (6H, d, *J*=6.5 Hz, -CH$(C$<u>H</u>$_3)_2$) ppm; ^{13}C NMR (100 MHz, $CDCl_3$) δ 136.8, 133.5, 79.8, 74.3, 32.5, 29.9, 26.0, 21.8, 17.6 and 17.5 ppm.

Camphorquinone Oxime[8] 129

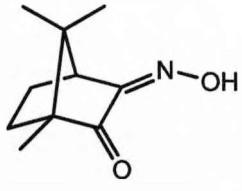

A solution of potassium *t*-butoxide (2.21 g, 19.71 mmol) in diethyl ether (20 mL) was purged with N_2 and cooled to –30 °C. To this was added a solution of *S*-camphor **128** (2.00 g, 13.13 mmol) in diethyl ether (10 mL), the reaction mixture was

then allowed to warm to room temperature and stirred for 30 minutes. The reaction vessel was again cooled to -30 °C and *i*-amyl nitrite (2.31 g, 19.71 mmol) added. The mixture was warmed to room temperature and allowed to stir overnight. The solution was then extracted with water (3 × 10 mL), and the combined aqueous layers were cooled in an ice bath with stirring. The aqueous mixture was acidified to pH 4 by drop-wise addition of conc. HCl. As the pH approached 4, an off-white solid precipitated out. The mixture was extracted with dichloromethane (3 × 20 mL) and the combined organic extracts were washed with sat. $NaHCO_3$ (20 mL), water (20 mL) and brine (20 mL). The organic layers were then dried over $MgSO_4$ and the solvent removed *in vacuo* to give camphorquinone oxime **129** (1.58 g, 66%) as an off-white solid. The crude product was carried through to the next step of the synthesis without further purification.

129: mp 114-116 °C; IR ν_{max} 3423 (ν_{O-H}), 2958 (ν_{C-H}), 1738 ($\nu_{C=O}$), 1641 ($\nu_{C=N}$) cm^{-1}; ^1H NMR (400 MHz, $CDCl_3$) *Anti*: δ 8.50 (1H, brs, =NOH), 3.26 (1H, d, *J*=4.4 Hz, -HCC=NOH), 2.08 (1H, m, $-CH_2-$), 1.80 (1H, m, $-CH_2-$), 1.60 (2H, m, $-CH_2-$), 1.03 (3H, s, $-C(CH_3)_2$), 1.01 (3H, s, $-C(CH_3)_2$), 0.89 (3H, s, $-CCH_3$) ppm; ^{13}C NMR (100 MHz, $CDCl_3$) δ 204.6, 160.4, 58.9, 47.0, 45.3, 31.1, 24.2, 21.1, 18.0 and 9.4 ppm.

Syn: ^1H NMR (400 MHz, $CDCl_3$) δ 8.50 (1H, br, =NOH), 2.72 (1H, d, *J*=4.2 Hz, -HCC=NOH), 2.16 (1H, m, $-CH_2-$), 1.87 (1H, m, $-CH_2-$), 1.68 (2H, m, $-CH_2-$), 1.02 (3H, s, $-C(CH_3)_2$), 1.01 (3H, s, $-C(CH_3)_2$), 0.93 (3H, s, $-CCH_3$) ppm; ^{13}C NMR (100 MHz, $CDCl_3$) δ 205.3, 156.6, 60.0, 50.0, 47.4, 30.3, 25.4, 21.0, 18.4 and 8.8 ppm; *m/z* (CI) 199.14517 ($[M + NH_4]^+$); requires 199.14465.

(2*R*)-(+)-3-exo-Aminoisoborneol[8] 130

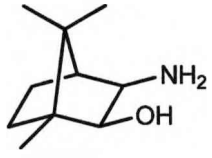

A flask charged with camphorquinone oxime **129** was fitted with a liebig condenser and the system purged with N_2. THF (10 mL) was added *via* syringe and the solution cooled to 0 °C. A solution of $LiAlH_4$ in THF (3.5 M, 3.70 mL, 13.25 mmol) was added drop-wise, and once H_2 evolution had ceased the reaction vessel was allowed to warm to room temperature and then heated to reflux for 30 minutes. The solution was again cooled to 0 °C, diluted with diethyl ether and the $LiAlH_4$ quenched with successive addition of water (0.5 mL), NaOH 10% w/v (0.5 mL) and finally water (1.0 mL). The reaction mixture was filtered through a pad of celite and the filter cake was washed with THF (3 × 10 mL). The filtrate was combined and the solvents removed *in vacuo* to afford (2*R*)-(+)-3-exo-aminoisoborneol **130** (1.43 g, 95%) as a pale yellow wax. The compound was used in the next step without further purification.

130: m.p. 123-125 °C; IR ν_{max} 3289 (ν_{O-H}), 2954 (ν_{C-H}), 1612 (ν_{N-H}) cm^{-1}; ^1H NMR (400 MHz, $CDCl_3$) δ 3.41 (1H, d, *J*=7.4 Hz, -HCOH), 3.06 (1H, d, *J*=7.4 Hz, -HCNH$_2$), 1.92 (1H, m, -HCHCNH$_2$), 1.74 (2H, m, -CH$_2$-), 1.43 (2H, m, -CH$_2$-), 1.08 (3H, s, -C(CH$_3$)$_2$), 0.95 (3H, s, -C(CH$_3$)$_2$), 0.79 (3H, s, -CCH$_3$) ppm; ^{13}C NMR (100 MHz, $CDCl_3$) δ 79.5, 58.0, 54.0, 49.2, 47.0, 33.6, 27.3, 22.4, 21.6 and 11.8 ppm;

(2*R*)-(+)-exo-(Morpholino)isoborneol[8] 131

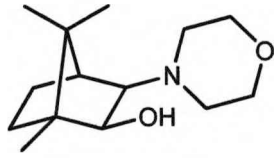

To a flask charged with (2*R*)-(+)-3-exo-aminoisoborneol **130**, was added reagent grade DMSO (10 mL) and triethylamine (3.52 mL, 25.34 mmol). Bis(2-bromoethyl) ether (1.27 mL, 10.14 mmol) in DMSO (10 mL) was then added drop-wise and the reaction mixture stirred at ambient temperature, under N_2, for 72 hours. The solution was poured into water (100 mL), the aqueous mixture was extracted with diethyl ether (3 × 20 mL) and the combined organic extracts washed with water (20 mL), brine (20 mL) and dried over $MgSO_4$. The solvent was then removed *in vacuo* and the crude mixture purified by column chromatography (80:20 Hexane: EtOAc) to give (2*R*)-(+)-exo-(morpholino)isoborneol **131** (0.42 g, 25%) as a pale yellow crystalline solid.

131: m.p. 58-60 °C; IR ν_{max} 3356 (ν_{O-H}), 2951 (ν_{C-H}), 2883 (ν_{N-CH-}) cm^{-1}; ^1H NMR (400 MHz, $CDCl_3$) δ 4.26 (1H, brs, -OH), 3.68 (4H, brs, -CH_2OCH_2), 3.47 (1H, d, *J*=7.1 Hz, -HCOH), 2.61 (4H, brs, -CH_2NCH_2-), 2.42 (1H, d, *J*=7.0 Hz, -HCN-), 2.02 (1H, d, *J*=4.8 Hz, -HCHCN-), 1.78 (2H, m, -CH_2-), 1.46 (2H, m, -CH_2-), 1.03 (3H, s, -CCH_3), 0.96 (3H, s, -CCH_3), 0.77 (3H, s, -CCH_3) ppm; ^{13}C NMR (100 MHz, $CDCl_3$) δ 79.0, 73.3, 67.4, 49.5, 46.9, 45.5, 32.6, 28.1, 22.4, 21.3 and 11.8 ppm; *m/z* (CI) 240.19668 ($[M + H]^+$); requires 240.19635.

General Procedure 7

Asymmetric Addition of Dialkylzincs to 3-Methylbut-2-en-al

A 100mL flask containing (+)- or (-)-exo-(morpholino)isoborneol ((+)- or (-)-MIB) **131** (ca. 1.00 mmol) and anhydrous toluene (20 mL) was flushed with N_2 then cooled to 0 °C. A solution of the desired dialkylzinc reagent **125** in toluene (1.0 M, ca. 35.00 mmol) was then added, followed by addition of freshly distilled 3-methylbut-2-en-al **120** (ca. 18.00 mmol). The reaction was stirred at 0 °C until complete consumption of the starting material was observed. The reaction mixture was quenched with sat NH_4Cl (10 mL) and extracted with diethyl ether (3 × 20 mL). The combined organic extracts were washed successively with brine (20 mL), water (20 mL) and dried over $MgSO_4$. The solvents were removed *in vacuo* and the crude mixture purified by column chromatography.

(*S*)-4-Methyl-3-penten-2-ol (*S*)-78

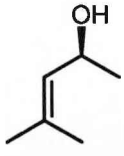

3-Methylbut-2-en-al **120** (1.71 mL, 17.83 mmol) was treated with $ZnMe_2$ in toluene (1.2 M, 29.70 mL, 35.66 mmol) and (-)-MIB (0.17 g, 0.71 mmol) as outlined in General Procedure 7, with complete consumption of the starting material taking 6 days. Purification of the crude mixture was performed by column chromatography (85:15 Hexane: EtOAc) to give (-)-4-methyl-3-penten-2-ol **(*S*)-78** (0.25 g, 14% yield, 77% ee) as a colourless oil. The absolute configuration was determined by comparing the optical rotations for a series of similar alcohols and the fact that

(+)-MIB has demonstrated selectivity to give (*R*)-configured alcohols.[9,10]

(*S*)-78: IR ν_{max} 3435 (ν_{O-H}), 2949, 2879 (ν_{C-H}), 1679 ($\nu_{C=C}$) cm^{-1}; ^1H NMR (400 MHz, $CDCl_3$) δ 5.23 (1H, dsept, *J*=8.5, 1.5 Hz, -C<u>H</u>=C(CH_3)$_2$), 4.60 (1H, dq, *J*=8.5, 6.3 Hz, -<u>H</u>C(OH)CH_3), 2.70 (1H, brs, -O<u>H</u>), 1.71 (3H, d, *J*=1.1 Hz, -CH=C(C<u>H</u>$_3$)$_2$), 1.69 (3H, d, *J*=1.1 Hz, -CH=C(C<u>H</u>$_3$)$_2$), 1.24 (3H, d, *J*=6.3 Hz, -HC(OH)C<u>H</u>$_3$) ppm; ^{13}C NMR (100 MHz, $CDCl_3$) δ 134.7, 129.7, 65.2, 26.1, 24.0 and 18.4 ppm; *m/z* (CI) 100.11253 ($[(M-H_2O) + NH_4]^+$); requires 100.11262.

(*S*)-(-)-5-Methyl-4-hexen-3-ol[9] (*S*)-122b

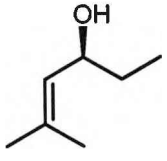

3-Methylbut-2-en-al **120** (1.71 mL, 17.83 mmol) was treated with $ZnEt_2$ in toluene (1.0 M, 35.66 mL, 35.66 mmol) and (-)-MIB (0.17 g, 0.71 mmol) as outlined in General Procedure 7, with complete consumption of the starting material taking 8 hours. Purification of the crude mixture was performed by column chromatography (88:12 Hexane: EtOAc) to give (*S*)-(-)-5-methyl-4-hexen-3-ol **(*S*)-122b** (0.56 g, 30% yield, 93% ee) as a colourless oil. The absolute configuration was determined by comparing the optical rotation of **(*S*)-122b** with the published optical rotation of the same enantiomer.[9]

(*S*)-122b: $[\alpha]^{20}_D$ -1.7 (c 1.0, $CHCl_3$); Lit.[9] $[\alpha]^{20}_D$ -10.5 (c. 0.002, $CHCl_3$, 95% ee); IR ν_{max} 3338 (ν_{O-H}), 2962, 2925 (ν_{C-H}), 1678 ($\nu_{C=C}$) cm^{-1}; ^1H NMR (400 MHz, $CDCl_3$) δ 5.17 (1H, dsept, *J*=8.7, 1.3 Hz, -C<u>H</u>=C(CH_3)$_2$), 4.30 (1H, dt, *J*=8.7, 6.7 Hz, -<u>H</u>C(OH)Et), 1.74 (3H, d, *J*=1.3 Hz, -CH=C(C<u>H</u>$_3$)$_2$), 1.69 (3H, d, *J*=1.3 Hz, -

$CH=C(C\underline{H}_3)_2$), 1.65-1.40 (2H, m, $-HC(OH)C\underline{H}_2CH_3$), 0.91 (3H, t, J=7.4 Hz, $-HC(OH)CH_2C\underline{H}_3$) ppm; ^{13}C NMR (100 MHz, $CDCl_3$) δ 135.7, 128.3, 70.5, 31.0, 26.2, 18.7 and 10.1 ppm; *m/z* (CI) 114.1281 ($[M + NH_4]^+$); requires 114.1283.

(*R*)-(+)-5-Methyl-4-hexen-3-ol (*R*)-122b

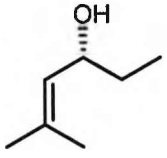

3-Methylbut-2-en-al **120** (3.00 mL, 31.20 mmol) was treated with $ZnEt_2$ in toluene (1.0 M, 62.40 mL, 62.40 mmol) and (+)-MIB (0.30 g, 1.25 mmol) as outlined in General Procedure 7, with complete consumption of the starting material taking 4 hours. Purification by column chromatography (88:12 Hexane: EtOAc) to give (+)-5-methyl-4-hexen-3-ol **(*R*)-122b** (2.97 g, 83% yield, 94% ee) as a colourless oil.

(*R*)-122b: $[\alpha]^{20}_D$ +1.3 (c 1.0, $CHCl_3$). NMR and other analytical data were similar to that of **(*S*)-122b**.

(*S*)-(-)-2-Methyl-2-octen-4-ol (*S*)-122c

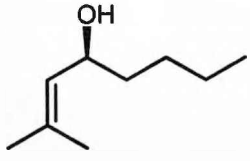

3-Methylbut-2-en-al **120** (1.71 mL, 17.83 mmol) was treated with $ZnBu_2$ in heptane (1.0 M, 35.66 mL, 35.66 mmol) and (-)-MIB (0.17 g, 0.71 mmol) as outlined in General Procedure 7, with complete consumption of the starting material taking 3 hours. Purification of the crude mixture was done by column chromatography

(88:12 Hexane: EtOAc) to give (*S*)-(-)-2-methyl-2-octen-4-ol **(*S*)-122c** (1.83 g, 72% yield, 90% ee) as a colourless oil. The absolute configuration was determined by comparing the optical rotations for a series of similar alcohols and the fact that (+)-MIB has demonstrated selectivity to give (*R*)-configured alcohols.[9,10]

(*S*)-122c: $[\alpha]^{20}_{D}$ -15.8 (c 1.0, $CHCl_3$); IR ν_{max} 3309 (ν_{O-H}), 2927, 2862 (ν_{C-H}), 1678 ($\nu_{C=C}$) cm^{-1}; ^1H NMR (400 MHz, $CDCl_3$) δ 5.18 (1H, dsept, *J*=8.7, 1.3 Hz, -C<u>H</u>=C(CH_3)$_2$), 4.36 (1H, dt, *J*=8.7, 6.6 Hz, -<u>H</u>C(OH)*n*-Bu), 1.73 (3H, d, *J*=1.3 Hz, -CH=C(C<u>H</u>$_3$)$_2$), 1.69 (3H, d, *J*=1.3 Hz, -CH=C(C<u>H</u>$_3$)$_2$), 1.63 (2H, m, -HC(OH)C<u>H</u>$_2$-), 1.46-1.21 (4H, m, -C<u>H</u>$_2$C<u>H</u>$_2$CH$_3$), 0.92 (3H, t, *J*=7.0 Hz, -CH$_2$CH$_2$C<u>H</u>$_3$) ppm; ^{13}C NMR (100 MHz, $CDCl_3$) δ 135.3, 128.7, 69.1, 37.8, 28.0, 26.2, 23.1, 18.6 and 14.5 ppm; *m/z* (CI) 142.1596 ([M + NH_4]-H_2O]$^+$); requires 142.1596.

(*R*)-(+)-2-Methyl-2-octen-4-ol (*R*)-122c

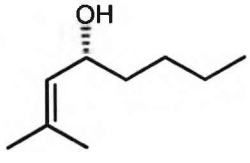

3-Methylbut-2-en-al **120** (2.00 mL, 20.80 mmol) was treated with $ZnBu_2$ in heptane (1.0 M, 41.60 mL, 41.60 mmol) and (+)-MIB (0.20 g, 0.83 mmol) as outlined in General Procedure 7, with complete consumption of the starting material taking 3 hours. Purification of the crude mixture was done by column chromatography (88:12 Hexane: EtOAc) to give (+)-(*R*)-2-methyl-2-octen-4-ol **(*R*)-122c** (2.80 g, 95% yield, 90% ee) as a colourless oil.

(*R*)-122c: $[\alpha]^{20}_{D}$ +15.4 (c 1.0, $CHCl_3$). NMR and other analytical data were similar to that of **(*S*)-122c**.

(*S*)-(+)-2,5-Dimethyl-4-hexen-3-ol (*S*)-122d

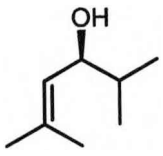

3-Methylbut-2-en-al **120** (0.57 mL, 5.94 mmol) was treated with Zn*i*-Pr_2 in toluene (1.0 M, 11.88 mL, 11.88 mmol) and (-)-MIB (0.06 g, 0.24 mmol) as outlined in General Procedure 7, with complete consumption of the starting material taking 3 hours. Purification by column chromatography (85:15 Hexane: EtOAc) gave (*S*)-(+)-2,5-dimethyl-4-hexen-3-ol **(*S*)-122d** (0.51 g, 67% yield, 98% ee) as a colourless oil.

(*S*)-122d: $[\alpha]^{20}_{D}$ +17.0 (c 1.0, $CHCl_3$); IR ν_{max} 3325 (ν_{O-H}), 2958, 2914 (ν_{C-H}), 1676 ($\nu_{C=C}$) cm^{-1}; ^1H NMR (400 MHz, $CDCl_3$) δ 5.21 (1H, dsept, *J*=8.9, 1.3 Hz, -C<u>H</u>=C(CH_3)$_2$), 4.06 (1H, dd, *J*=8.9, 6.8 Hz, -<u>H</u>C(OH)*i*-Pr), 1.74 (3H, d, *J*=1.3 Hz, -CH=C(C<u>H</u>$_3$)$_2$), 1.72-1.63 (1H, sept, *J*=6.8 Hz, -HC(OH)C<u>H</u>(CH_3)$_2$), 1.69 (3H, d, *J*=1.5 Hz, -CH=C(C<u>H</u>$_3$)$_2$), 1.35 (1H, s, -O<u>H</u>), 0.96 (3H, d, *J*=6.8 Hz, -HC(OH)CH(C<u>H</u>$_3$)$_2$), 0.87 (3H, d, *J*=6.8 Hz, -HC(OH)CH(C<u>H</u>$_3$)$_2$) ppm; ^{13}C NMR (100 MHz, $CDCl_3$) δ 136.0, 126.9, 74.1, 34.8, 26.2, 18.7 and 18.5 ppm; *m/z* (CI) 128.14358 ([M + NH_4]-H_2O]$^+$); requires 128.14392.

(*R*)-(-)-2,5-Dimethyl-4-hexen-3-ol (*R*)-122d

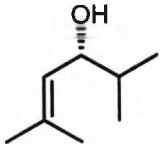

3-Methylbut-2-en-al **120** (0.77 mL, 8.00 mmol) was treated with Zn*i*-Pr_2 in toluene (1.0 M, 16.00 mL, 16.00 mmol) and (+)-MIB (0.08 g, 0.32 mmol) as outlined in

General Procedure 7, with complete consumption of the starting material taking 3 hours. Purification of the crude mixture was done by column chromatography (85:15 Hexane: EtOAc) to give (*R*)-(-)-2,5-dimethyl-4-hexen-3-ol **(*R*)-122d** (0.87 g, 85% yield, 98% ee) as a colourless oil.

(*R*)-122d: $[\alpha]^{20}_{D}$ -13.8 (c 1.0, $CHCl_3$). NMR and other analytical data were similar to that of **(*S*)-122d**.

(3*S*,4*S*)-4-Hydroperoxy-5-methyl-5-hexen-3-ol (3*S*,4*S*)-123b

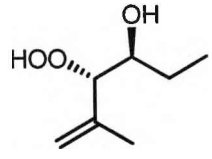

via Photooxygenation

(*S*)-(-)-5-Methyl-4-hexen-3-ol **(*S*)-122b** (0.20 g, 1.75 mmol) underwent photooxygenation as outlined in General Procedure 6. Complete consumption of the starting material was observed after 1.5 hours. The solvent was removed *in vacuo* and the crude mixture purified by column chromatography (99:1 DCM: MeOH) to give (3*S*,4*S*)-4-hydroperoxy-5-methyl-5-hexen-3-ol as a pale yellow oil **(3*S*,4*S*)-123b** (0.22 g, 85% yield, d.r. 90:10 {*threo*:*erythro*}).

(3*S*,4*S*)-123b: IR ν_{max} 3323 (ν_{O-H}), 2968, 2877 (ν_{C-H}), 1668 ($\nu_{C=C}$), 816 ($\nu_{peroxide}$) cm^{-1}; ^1H NMR (400 MHz, $CDCl_3$) δ 5.11 (1H, m, -C=C$\underline{H}_2$), 5.09 (1H, s, -C=C$\underline{H}_2$), 4.24 (1H, d, *J*=8.4 Hz, -$\underline{H}$COOH), 3.66 (1H, dt, *J*=8.5, 3.4 Hz, -$\underline{H}$C(OH)Et), 1.75 (3H, s, =CC$\underline{H}_3$), 1.59-1.32 (2H, m, -HC(OH)C$\underline{H}_2$CH$_3$), 1.00 (3H, t, *J*=7.4 Hz, -HC(OH)CH$_2$C$\underline{H}_3$) ppm; ^{13}C NMR (100 MHz, $CDCl_3$) δ 141.7, 117.0, 93.8, 72.4, 26.0, 18.6 and 10.1 ppm; *m/z* (CI) 164.12917 ($[M + NH_4]^+$); requires 164.12867.

(3*R*,4*R*)-4-Hydroperoxy-5-methyl-5-hexen-3-ol (3*R*,4*R*)-123b

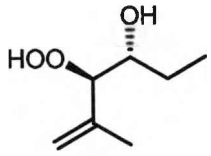

via Photooxygenation

(*R*)-(+)-5-Methyl-4-hexen-3-ol **(*R*)-122b** (1.53 g, 13.42 mmol) underwent photooxygenation as outlined in General Procedure 6. Complete consumption of the starting material was observed after 1.5 hours. The solvent was removed *in vacuo* and the crude mixture purified by column chromatography (99:1 DCM: MeOH) to give (3*R*,4*R*)-4-hydroperoxy-5-methyl-5-hexen-3-ol as a pale yellow oil **(3*R*,4*R*)-123b** (1.28 g, 66% yield, d.r. 90:10 {*threo*:*erythro*}).

(3*R*,4*R*)-123b: NMR and other analytical data were similar to that of **(3*S*,4*S*)-123b**.

via Phosphite Ozonide Conditions

A solution of POA (triphenyl phosphite (1.11 mL, 4.22 mmol) in dichloromethane (20 mL)) was prepared as outlined in General Procedure 3. 5-Methyl-4-hexen-3-ol ***rac*-122b** (0.16 g, 1.41 mmol) was added dropwise and allowed to react with stirring. The solvents were then removed *in vacuo* and the crude mixture purified by column chromatography (90:10 Hexane: EtOAc) to afford ***rac*-123b** as a clear oil (*Free reaction*: 0.08 g, 36% yield, d.r. 90:10 {*threo*:*erythro*}; *Direct reaction*: 0.05 g, 25% yield, d.r. 90:10 {*threo*:*erythro*}).

Spectral data as above.

(3*S*,4*S*)-3-Hydroperoxy-2-methyl-1-octen-4-ol (3*S*,4*S*)-123c

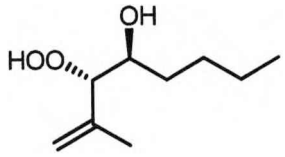

via Photooxygenation

Using the method summarised in General Procedure 6, (*S*)-(-)-2-methyl-2-octen-4-ol **(*S*)-122c** (0.20 g, 1.40mmol) underwent photooxygenation for 1.5 hours. Purification by column chromatography (99:1 DCM: MeOH) afforded (3*S*,4*S*)-3-hydroperoxy-2-methyl-1-octen-4-ol **(3*S*,4*S*)-123c** (0.24 g, 100% yield, d.r. 90:10 {*threo*:*erythro*}) as a pale yellow oil in quantitative yield.

(3*S*,4*S*)-123c: IR ν_{max} 3357 (ν_{O-H}), 2952, 2864 (ν_{C-H}), 1712 ($\nu_{C=C}$), 901 ($\nu_{peroxide}$) cm^{-1}; ^1H NMR (400 MHz, $CDCl_3$) δ 5.11 (1H, m, -C=C$\underline{H}_2$), 5.07 (1H, s, -C=C$\underline{H}_2$), 4.21 (1H, d, *J*=8.4 Hz, -$\underline{H}$COOH), 3.71 (1H, dt, *J*=8.4, 3.0 Hz, -$\underline{H}$C(OH)*n*-Bu), 2.15 (1H, br, -O$\underline{H}$), 1.75 (3H, s, =CC$\underline{H}_3$), 1.52-1.25 (6H, m, -C$\underline{H}_2$C$\underline{H}_2$C$\underline{H}_2$CH$_3$), 0.91 (3H, t, *J*=7.2 Hz, -CH$_2$CH$_2$C$\underline{H}_3$) ppm; ^{13}C NMR (100 MHz, $CDCl_3$) δ 141.7, 117.1, 94.1, 71.1, 32.7, 27.8, 23.0, 18.6 and 14.4 ppm; *m/z* (CI) 192.16053 ($[M + NH_4]^+$); requires 192.15997.

via Phosphite Ozonide Conditions

A solution of POA (triphenyl phosphite (1.11 mL, 4.22 mmol) in dichloromethane (20 mL)) was prepared as outlined in General Procedure 3. (*S*)-(-)-2-Methyl-2-octen-4-ol **(*S*)-122c** (0.20 g, 1.41 mmol) was added dropwise and allowed to react with stirring. The solvents were then removed *in vacuo* and the crude mixture purified by column chromatography (90:10 Hexane: EtOAc) to afford **(3*S*,4*S*)-123c** as a clear oil

(*Free reaction*: 0.04 g, 18% yield, d.r. 90:10 {*threo*:*erythro*}; *Direct reaction*: 0.07 g, 28% yield, d.r. 90:10 {*threo*:*erythro*}).

Spectral data as above.

(3*R*,4*R*)-3-Hydroperoxy-2-methyl-1-octene-4-ol (3*R*,4*R*)-123c

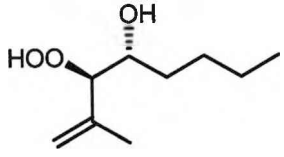

Using the method summarized in General Procedure 6, (*R*)-(+)-2-methyl-2-octen-4-ol **(*R*)-122c** (1.91 g, 13.42 mmol) underwent photooxygenation for 1.5 hours. Purification by column chromatography (99:1 DCM: MeOH) afforded (3*R*,4*R*)-3-hydroperoxy-2-methyl-1-octene-4-ol **(3*R*,4*R*)-123c** (1.67 g, 72% yield, d.r. 92:8 {*threo*:*erythro*}) as a pale yellow oil in quantitative yield.

(3*R*,4*R*)-123c: NMR and other analytical data were similar to that of **(3*S*,4*S*)-123c**.

(3*S*,4*S*)-4-Hydroperoxy-2,5-dimethyl-5-hexen-3-ol (3*S*,4*S*)-123d

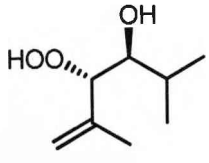

The reaction was conducted as in General Procedure 6, with (*S*)-(+)-2,5-dimethyl-4-hexen-3-ol **(*S*)-122d** (0.20 g, 1.56 mmol) undergoing photooxygenation for 1.5 hours. The solvents were removed *in vacuo* and the crude mixture was then purified by column chromatography (99:1 DCM: MeOH) to yield (3*S*,4*S*)-4-hydroperoxy-2,5-dimethyl-5-hexen-3-ol **(3*S*,4*S*)-123d** (0.22 g, 86% yield, d.r. 91:9 {*threo*:*erythro*}) as

a pale yellow oil.

(3*S*,4*S*)-123d: ^{1}H NMR (400 MHz, $CDCl_3$) δ 5.06 (2H, m, -C=C$\underline{H}_2$), 4.29 (1H, d, *J*=8.2 Hz, -$\underline{H}$COOH), 3.48 (1H, dd, *J*=8.2, 3.2 Hz, -$\underline{H}$C(OH)*i*-Pr), 2.40 (1H, br, -O$\underline{H}$), 1.70 (3H, t, *J*=1.6 Hz, =CC$\underline{H}_3$), 1.71-1.63 (1H, septd, *J*=6.8, 3.2 Hz, -HC(OH)C$\underline{H}$(CH$_3$)$_2$), 0.96 (3H, d, *J*=6.9 Hz, -HC(OH)CH(C$\underline{H}_3$)$_2$), 0.86 (3H, d, *J*=6.8 Hz, -HC(OH)CH(C$\underline{H}_3$)$_2$) ppm; ^{13}C NMR (100 MHz, $CDCl_3$) δ 141.5, 117.0, 92.2, 75.2, 29.7, 20.7, 18.6 and 15.5 ppm; *m/z* (CI) 160.13412 ([M + NH_4]-H_2O]$^+$); requires 160.13375.

(3*R*,4*R*)-4-Hydroperoxy-2,5-dimethyl-5-hexen-3-ol (3*R*,4*R*)-123d

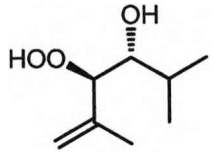

The reaction was conducted as in General Procedure 6, with (*R*)-(-)-2,5-dimethyl-4-hexen-3-ol **(*R*)-122d** (0.64 g, 4.99 mmol) undergoing photooxygenation for 1.5 hours. The solvents were removed *in vacuo* and the crude mixture was then purified by column chromatography (99:1 DCM: MeOH) to yield (3*R*,4*R*)-4-hydroperoxy-2,5-dimethyl-5-hexen-3-ol **(3*R*,4*R*)-123d** (0.80 g, 97% yield, d.r. 92:8 {*threo*:*erythro*}) as a pale yellow oil.

(3*R*,4*R*)-123d: NMR and other analytical data were similar to that of **(3*S*,4*S*)-123d**.

(5*S*,6*S*)-(+)-5-Ethyl-6-(prop-1-en-2-yl)spiro-[1,2,4-trioxacyclohexane-3,2'-cyclohexane] (5*S*,6*S*)-126b

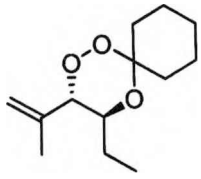

Using the method described in General Procedure 4, (3*S*,4*S*)-4-hydroperoxy-5-methyl-5-hexen-3-ol **(3*S*,4*S*)-123b** (0.10 g, 0.68 mmol) underwent condensation with cyclohexanone (0.07 g, 0.75 mmol) catalysed by *p*-TsOH (ca. 2 mg). Purification by column chromatography (98:2 Hexane: EtOAc), afforded (5*S*,6*S*)-(+)-5-ethyl-6-(prop-1-en-2-yl)spiro-[1,2,4-trioxacyclohexane-3,2'-cyclohexane] **(5*S*,6*S*)-126b** (0.10 g, 66%) as a clear oil.

(5*S*,6*S*)-126b: $[\alpha]^{20}_{D}$ +102.9 (c 1.0, $CHCl_3$); IR ν_{max} 2933 (ν_{C-H}), 1649 ($\nu_{C=C}$) 850 ($\nu_{peroxide}$) cm^{-1}; ^1H NMR (400 MHz, $CDCl_3$) δ 5.08 (2H, m, -C=C$\underline{H}_2$), 4.29 (1H, d, *J*=9.7 Hz, -$\underline{H}$COOC-), 3.86 (1H, dt, *J*=9.1, 3.0 Hz, -$\underline{H}$COC-), 2.20 (1H, m), 2.07 (1H, m), 1.77 (3H, t, *J*=1.3 Hz, =CC$\underline{H}_3$), 1.66-1.43 (8H, m), 1.51-1.26 (2H, m, -HC(O)C$\underline{H}_2$CH$_3$), 1.00 (3H, t, *J*=7.4 Hz, -HC(O)CH$_2$C$\underline{H}_3$) ppm; ^{13}C NMR (100 MHz, $CDCl_3$) δ 139.8, 118.2, 103.3, 87.9, 70.9, 35.5, 29.9, 26.1, 24.3, 22.9, 22.8, 20.2 and 10.5 ppm; *m/z* (CI) 244.19142 ([M + NH_4]$^+$); requires 244.19127. Anal. $C_{13}H_{22}O_3$ requires C 68.99%, H 9.80%, found C 68.82%, H 9.84%.

(5*R*,6*R*)-(-)-5-Ethyl-6-(prop-1-en-2-yl)spiro-[1,2,4-trioxacyclohexane-3,2'-cyclohexane] (5*R*,6*R*)-126b

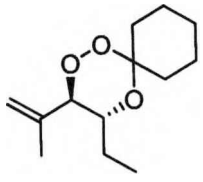

Using the method described in General Procedure 4, (3*R*,4*R*)-4-hydroperoxy-5-methyl-5-hexen-3-ol **(3*R*,4*R*)-123b** (0.25 g, 1.72 mmol) underwent condensation with cyclohexanone (0.27 g, 2.72 mmol) catalysed by *p*-TsOH (ca. 2 mg). Purification by column chromatography (98:2 Hexane: EtOAc), afforded (5*R*,6*R*)-(-)-5-ethyl-6-(prop-1-en-2-yl)spiro-[1,2,4-trioxacyclohexane-3,2'-cyclohexane] **(5*R*,6*R*)-126b** (0.30 g, 76%) as a clear oil.

(5*R*,6*R*)-126b: $[\alpha]^{20}_{D}$ -123.1 (c 1.0, $CHCl_3$). NMR and other analytical data were similar to that of **(5*S*,6*S*)-126b**.

(5*S*,6*S*)-(+)-5-Ethyl-6-(prop-1-en-2-yl)spiro-[1,2,4-trioxacyclohexane-3,2'-adamantane] (5*S*,6*S*)-127b

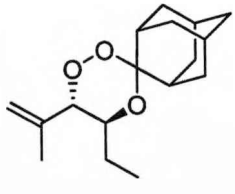

Condensation of (3*S*,4*S*)-4-hydroperoxy-5-methyl-5-hexen-3-ol **(3*S*,4*S*)-123b** (0.10 g, 0.68 mmol) with 2-adamantanone (0.09 g, 0.75 mmol) overnight, and after purification by chromatography (98:2 Hexane: EtOAc), yielded (5*S*,6*S*)-(+)-5-ethyl-

6-(prop-1-en-2-yl)spiro-[1,2,4-trioxacyclohexane-3,2'-adamantane] **(5*S*,6*S*)-127b** (0.11 g, 57%) as a pale yellow oil.

(5*S*,6*S*)-127b: $[\alpha]^{20}_{D}$ +59.3 (c 1.0, $CHCl_3$); IR ν_{max} 2913, 2856 (ν_{C-H}), 1643 ($\nu_{C=C}$) 741 ($\nu_{peroxide}$) cm^{-1}; ^1H NMR (400 MHz, $CDCl_3$) δ 5.08 (2H, m, -C=C$\underline{H}_2$), 4.28 (1H, d, *J*=9.5 Hz, -$\underline{H}$COOC-), 3.86 (1H, dt, *J*=9.5, 2.7 Hz, -$\underline{H}$COC-), 2.93 (1H, m), 2.15-1.55 (13H, m), 1.76 (3H, t, *J*=1.3 Hz, =CC$\underline{H}_3$), 1.51-1.30 (2H, m, -HC(O)C$\underline{H}_2$CH$_3$), 1.02 (3H, t, *J*=7.4 Hz, -HC(O)CH$_2$C$\underline{H}_3$) ppm. ^{13}C NMR (100 MHz, $CDCl_3$) δ 139.9, 118.2, 105.2, 88.0, 70.4, 37.6, 37.1, 34.0, 33.8, 33.7, 33.4, 30.2, 27.6, 27.4, 24.4, 20.3 and 10.2 ppm; *m/z* (CI) 279.19580 ($[M + NH_4]^+$); requires 279.19602. Anal. $C_{17}H_{26}O_3$ requires C 73.34%, H 9.41%, found C 74.10%, H 9.92%.

(5*R*,6*R*)-(-)-5-Ethyl-6-(prop-1-en-2-yl)spiro-[1,2,4-trioxacyclohexane-3,2'-adamantane] (5*R*,6*R*)-127b

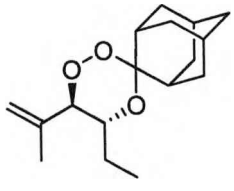

Condensation of (3*R*,4*R*)-4-hydroperoxy-5-methyl-5-hexen-3-ol **(3*R*,4*R*)-123b** (0.25 g, 1.71 mmol) with 2-adamantanone (0.41 g, 2.70 mmol) overnight, and after purification by chromatography (98:2 Hexane: EtOAc), yielded (5*R*,6*R*)-(-)-5-ethyl-6-(prop-1-en-2-yl)spiro-[1,2,4-trioxacyclohexane-3,2'-adamantane] **(5*R*,6*R*)-127b** (0.35 g, 74%) as a pale yellow oil.

(5*R*,6*R*)-127b: $[\alpha]^{20}_D$ -86.4 (c 1.0, $CHCl_3$). NMR and other analytical data were similar to that of **(5*S*,6*S*)-127b**.

(5*S*,6*S*)-(+)-5-Butyl-6-(prop-1-en-2-yl)spiro-[1,2,4-trioxacyclohexane-3,2'-cyclohexane] (5*S*,6*S*)-126c

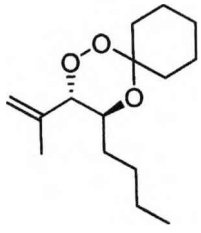

(3*S*,4*S*)-3-Hydroperoxy-2-methyl-1-octene-4-ol **(3*S*,4*S*)-123c** (0.10 g, 0.57 mmol) was condensed with cyclohexanone (0.07 g, 0.63 mmol) overnight as outlined in General Procedure 4. The solvents were then removed *in vacuo* and the crude mixture purified by column chromatography (98:2 Hexane: EtOAc) to afford (5*S*,6*S*)-(+)-5-butyl-6-(prop-1-en-2-yl)spiro-[1,2,4-trioxacyclohexane-3,2'-cyclohexane] **(5*S*,6*S*)-126c** (0.10 g, 68%) as a colourless oil.

(5*S*,6*S*)-126c: $[\alpha]^{20}_D$ +73.1 (c 1.0, $CHCl_3$); IR ν_{max} 2932, 2854 (ν_{C-H}), 1646 ($\nu_{C=C}$) 848 ($\nu_{peroxide}$) cm^{-1}; ^1H NMR (400 MHz, $CDCl_3$) δ 5.08 (2H, m, -C=C$\underline{H}_2$), 4.26 (1H, d, *J*=9.7 Hz, -$\underline{H}$COOC-), 3.94 (1H, td, *J*=9.5, 3.2 Hz, -$\underline{H}$COC-), 2.20 (1H, m), 2.06 (1H, m), 1.77 (3H, m, =CC$\underline{H}_3$), 1.63-1.30 (14H, m), 0.92 (3H, t, *J*=7.0 Hz, -HC(O)$(CH_2)_3C\underline{H}_3$) ppm; ^{13}C NMR (100 MHz, $CDCl_3$) δ 138.2, 116.7, 101.7, 86.6, 68.0, 33.9, 30.6, 28.9, 26.9, 22.9, 24.0, 21.3, 21.2, 21.1, 18.6 and 12.7 ppm; *m/z* (CI) 272.22180 ($[M + NH_4]^+$); requires 272.22257. Anal. $C_{15}H_{26}O_3$ requires C 70.83%, H 10.30%, found C 70.93%, H 10.33%.

(5*R*,6*R*)-(+)-5-Butyl-6-(prop-1-en-2-yl)spiro-[1,2,4-trioxacyclohexane-3,2'-cyclohexane] (5*R*,6*R*)-126c

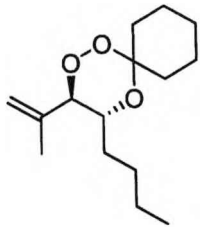

(3*R*,4*R*)-3-hydroperoxy-2-methyl-1-octen-4-ol **(3*R*,4*R*)-123c** (0.30 g, 1.71 mmol) was condensed with cyclohexanone (0.27 g, 2.70 mmol) overnight as outlined in General Procedure 4. The solvents were then removed *in vacuo* and the crude mixture purified by column chromatography (98:2 Hexane: EtOAc) to afford (5*R*,6*R*)-(+)-5-butyl-6-(prop-1-en-2-yl)spiro-[1,2,4-trioxacyclohexane-3,2'-cyclohexane] **(5*R*,6*R*)-126c** (0.34 g, 78%) as a colourless oil.

(5*R*,6*R*)-126c: $[\alpha]^{20}_{D}$ -102.6 (c 1.0, $CHCl_3$). NMR and other analytical data were similar to that of **(5*S*,6*S*)-126c**.

(5*S*,6*S*)-(+)-5-Butyl-6-(prop-1-en-2-yl)spiro-[1,2,4-trioxacyclohexane-3,2'-adamantane] (5*S*,6*S*)-127c

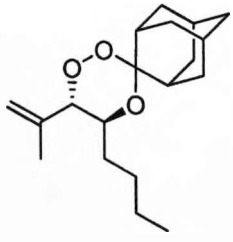

Condensation of (3*S*,4*S*)-3-hydroperoxy-2-methyl-1-octen-4-ol **(3*S*,4*S*)-123c** (0.10 g, 0.57 mmol) with adamantanone (0.10 g, 0.63 mmol) overnight, and after purification

by chromatography (98:2 Hexane: EtOAc), yielded (5*S*,6*S*)-(+)-5-butyl-6-(prop-1-en-2-yl)spiro-[1,2,4-trioxacyclohexane-3,2'-adamantane] **(5*S*,6*S*)-127c** (0.10 g, 56%) as a pale yellow oil.

(5*S*,6*S*)-127c: $[\alpha]^{20}_{D}$ +89.5 (c 1.0, $CHCl_3$); IR ν_{max} 2908, 2856 (ν_{C-H}), 1649 ($\nu_{C=C}$), 732 ($\nu_{peroxide}$) cm^{-1}; ^1H NMR (400 MHz, $CDCl_3$) δ 5.08 (2H, m, -C=C$\underline{H}_2$), 4.27 (1H, d, *J*=9.7 Hz, -$\underline{H}$COOC-), 3.94 (1H, dt, *J*=8.7, 2.9 Hz, -$\underline{H}$COC-), 2.14-1.55 (14H, m), 1.76 (3H, t, *J*=1.1 Hz, =CC$\underline{H}_3$), 1.40-1.25 (6H, m), 0.92 (3H, t, *J*=5.1 Hz, -HC(O)$(CH_2)_3C\underline{H}_3$) ppm; ^{13}C NMR (100 MHz, $CDCl_3$) δ 139.8, 118.3, 105.2, 88.1, 69.1, 37.6, 37.1, 34.0, 33.8, 33.7, 33.4, 30.2, 27.8, 27.7, 23.0, 20.3 and 14.5 ppm; *m/z* (CI) 307.22736 ($[M + H]^+$); requires 307.22732. Anal. $C_{19}H_{30}O_3$ requires C 74.47%, H 9.87%, found C 74.24%, H 10.03%.

(5*R*,6*R*)-(+)-5-Butyl-6-(prop-1-en-2-yl)spiro-[1,2,4-trioxacyclohexane-3,2'-adamantane] (5*R*,6*R*)-127c

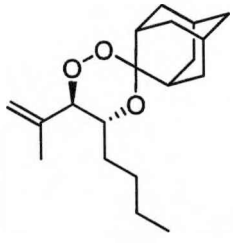

Condensation of (3*R*,4*R*)-3-hydroperoxy-2-methyl-1-octen-4-ol **(3*R*,4*R*)-123c** (0.30 g, 1.71 mmol) with 2-adamantanone (0.41 g, 2.70 mmol) overnight, and after purification by chromatography (98:2 Hexane: EtOAc), yielded (5*R*,6*R*)-(+)-5-butyl-6-(prop-1-en-2-yl)spiro-[1,2,4-trioxacyclohexane-3,2'-adamantane] **(5*R*,6*R*)-127c** (0.41 g, 78%) as a pale yellow oil.

(5*R*,6*R*)-127c: $[\alpha]^{20}_{D}$ -57.4 (c 1.0, $CHCl_3$). NMR and other analytical data were

similar to that of **(5*S*,6*S*)-127c**.

(5*S*,6*S*)-(+)-5-Isopropyl-6-(prop-1-en-2-yl)spiro-[1,2,4-trioxacyclohexane-3,2'-cyclohexane] (5*S*,6*S*)-126d

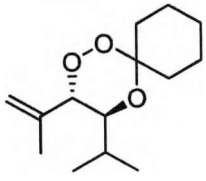

Using the method described in General Procedure 4, (3*S*,4*S*)-4-hydroperoxy-2,5-dimethyl-5-hexen-3-ol **(3*S*,4*S*)-123d** (0.10 g, 0.62 mmol) underwent condensation with cyclohexanone (0.07 g, 0.69 mmol) catalysed by *p*-TsOH (ca. 2 mg). Purification by column chromatography (98:2 Hexane: EtOAc) gave (5*S*,6*S*)-(+)-5-isopropyl-6-(prop-1-en-2-yl)spiro-[1,2,4-trioxacyclohexane-3,2'-cyclohexane] **(5*S*,6*S*)-126d** (0.11 g, 73%) as a clear oil.

(5*S*,6*S*)-126d: $[\alpha]^{20}_{D}$ +102.0 (c 1.0, $CHCl_3$); IR ν_{max} 2935 (ν_{C-H}), 1647 ($\nu_{C=C}$), 849 ($\nu_{peroxide}$) cm^{-1}; ^1H NMR (400 MHz, $CDCl_3$) δ 5.10 (2H, m, -C=C$\underline{H}_2$), 4.47 (1H, d, *J*=9.8 Hz, -$\underline{H}$COOC-), 3.84 (1H, dd, *J*=9.8, 2.5 Hz, -$\underline{H}$COC-), 2.25 (1H, m), 1.98 (1H, m), 1.65-1.35 (8H, m) 1.78 (1H, septd, *J*=6.9, 2.6 Hz, -HC(O)C$\underline{H}_2$CH$_3$), 1.77 (3H, t, *J*=1.1 Hz, =CC$\underline{H}_3$), 1.00 (3H, d, *J*=7.0 Hz, -HC(OH)CH(C$\underline{H}_3$)$_2$), 0.93 (3H, d, *J*=6.8 Hz, -HC(OH)CH(C$\underline{H}_3$)$_2$) ppm; ^{13}C NMR (100 MHz, $CDCl_3$) δ 140.0, 118.2, 103.1, 86.1, 73.1, 37.1, 29.8, 28.5, 26.1, 22.8, 22.7, 20.5, 20.1 and 15.4 ppm; *m/z* (CI) 258.20660 ([M + NH_4]$^+$); requires 258.20692. Anal. $C_{14}H_{24}O_3$ requires C 69.96%, H 10.07%, found C 70.13%, H 10.11%.

(5*R*,6*R*)-(-)-5-Isopropyl-6-(prop-1-en-2-yl)spiro-[1,2,4-trioxacyclohexane-3,2'-cyclohexane] (5*R*,6*R*)-126d

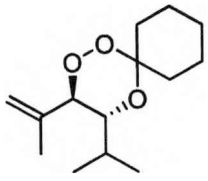

Using the method described in General Procedure 4, (3*R*,4*R*)-4-hydroperoxy-2,5-dimethyl-5-hexen-3-ol **(3*R*,4*R*)-123d** (0.06 g, 0.62 mmol) underwent condensation with cyclohexanone (0.07 g, 0.69 mmol) catalysed by *p*-TsOH (ca. 2 mg). Purification by column chromatography (98:2 Hexane: EtOAc) afforded (5*R*,6*R*)-(-)-5-isopropyl-6-(prop-1-en-2-yl)spiro-[1,2,4-trioxacyclohexane-3,2'-cyclohexane] **(5*R*,6*R*)-126d** (0.07 g, 45%) as a clear oil.

(5*R*,6*R*)-126d: $[\alpha]^{20}_{D}$ -95.7 (c 1.0, $CHCl_3$). NMR and other analytical data were similar to that of **(5*S*,6*S*)-126d**.

(5*S*,6*S*)-(+)-5-Isopropyl-6-(prop-1-en-2-yl)spiro-[1,2,4-trioxacyclohexane-3,2'-adamantane] (5*S*,6*S*)-127d

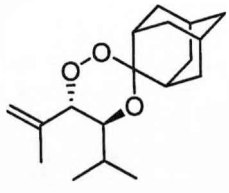

Condensation of (3*S*,4*S*)-4-hydroperoxy-2,5-dimethyl-5-hexen-3-ol **(3*S*,4*S*)-123d** (0.10 g, 0.62 mmol) with 2-adamantanone (0.10 g, 0.69 mmol) overnight, and after purification by flash column chromatography (98:2 Hexane: EtOAc), yielded

(5*S*,6*S*)-(+)-5-isopropyl-6-(prop-1-en-2-yl)spiro-[1,2,4-trioxacyclohexane-3,2'-adamantane] **(5*S*,6*S*)-127d** (0.12 g, 64%) as a pale yellow oil.

(5*S*,6*S*)-127d: $[\alpha]^{20}_{D}$ +100.1 (c 1.0, $CHCl_3$); IR ν_{max} 2904, 2856 (ν_{C-H}), 1649 ($\nu_{C=C}$), 742 ($\nu_{peroxide}$) cm^{-1}; ^1H NMR (400 MHz, $CDCl_3$) δ 5.02 (2H, m, -C=C$\underline{H}_2$), 4.40 (1H, d, *J*=9.9 Hz, -$\underline{H}$COOC-), 3.78 (1H, dd, *J*=9.8, 2.6 Hz, -$\underline{H}$COC-), 2.85-1.47 (15H, m), 1.70 (3H, t, *J*=1.1 Hz, =CC$\underline{H}_3$), 0.95 (3H, d, *J*=6.9 Hz, -HC(OH)CH(C$\underline{H}_3$)$_2$), 0.87 (3H, d, *J*=6.8 Hz, -HC(OH)CH(C$\underline{H}_3$)$_2$) ppm; ^{13}C NMR (100 MHz, $CDCl_3$) δ 140.0, 118.2, 104.9, 85.9, 72.5, 37.6, 37.0, 34.0, 33.7, 33.4, 30.2, 28.6, 27.7, 20.7, 20.2 and 15.2 ppm; *m/z* (CI) 293.21077 ($[M + NH_4]^+$); requires 293.21167. Anal. $C_{18}H_{28}O_3$ requires C 73.93%, H 9.65%, found C 74.83%, H 9.90%.

(5*R*,6*R*)-(-)-5-Isopropyl-6-(prop-1-en-2-yl)spiro-[1,2,4-trioxacyclohexane-3,2'-adamantane] (5*R*,6*R*)-127d

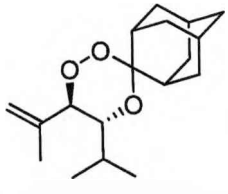

Condensation of (3*R*,4*R*)-4-hydroperoxy-2,5-dimethyl-5-hexen-3-ol **(3*R*,4*R*)-123d** (0.10 g, 0.62 mmol) with 2-adamantanone (0.10 g, 0.69 mmol) overnight, and after purification by flash column chromatography (98:2 Hexane: EtOAc) yielded (5*R*,6*R*)- (-)-5-isopropyl-6-(prop-1-en-2-yl)spiro-[1,2,4-trioxacyclohexane-3,2'-adamantane] **(5*R*,6*R*)-127d** (0.12 g, 64%) as a pale yellow oil.

(5*R*,6*R*)-127d: $[\alpha]^{20}_{D}$ -100.3 (c 1.0, $CHCl_3$). NMR and other analytical data were similar to that of **(5*S*,6*S*)-127d**.

3.2 Biological Testing

Plasmodium falciparum in vitro culture and parasite growth inhibition assays

All parasite clones, isolates and strains were acquired from MR4 (Malaria Research and Reference Reagent Resource Center, Manassas, Virginia, USA). Strains/isolates used in this study were: the drug sensitive 3D7 clone of the NF54 isolate (unknown origin). *In vitro* culture of *P. falciparum* was carried out following standard methods.[11] *In vitro* parasite growth inhibition was assessed by the incorporation of [^{3}H] hypoxanthine based on the method used by Desjardins.[12] Briefly, stock drug solutions were dissolved in 100% dimethylsulfoxide (Sigma, Dorset, UK) and 50 µl of a 3-fold dilution series (10.0, 3.33, 0.111, 0.0370, 0.0123, and 0.0041 µg/mL) of the drugs prepared in assay medium (RPMI 1640 supplemented with 0.5% Albumax II (Invitrogen), 0.2% w/v glucose, 0.03% L-glutamine, and 5 µM hypoxanthine) added to each well of 96-well plates in triplicate. Fifty microlitres of asynchronous (65–75% ring stage) *P. falciparum* culture (0.5% parasitemia) or uninfected erythrocytes (blank) were added to each well reaching a final volume of 100 µL per well, a final hematocrit of 2.5% and final dimethylsulfoxide concentrations ≤0.01%. Plates were incubated at 37 °C in 5% CO_2, and 95% air mixture for 24 h, at which point 10 µL (0.2 µCi/well) of [^{3}H]hypoxanthine (Perkin-Elmer, Hounslow, UK), was added to each well. After an additional 24 h incubation period, the experiment was terminated by placing the plates in a -80 °C freezer. Plates were thawed and harvested onto glass fibre filter mats using a 96-well cell harvester (Harvester 96, Tomtec, Oxon, UK) and left to dry. After the addition of MeltiLex solid scintillant

(Perkin–Elmer, Hounslow, UK) the incorporated radioactivity was counted using a Wallac 1450 Betalux scintillation counter (Wallac).

Data acquired by the Wallac BetaLux scintillation counter were exported into a MICROSOFT EXCEL spreadsheet (Microsoft), and the IC_{50} values of each drug were calculated by using XLFit line fitting software (ID Business Solutions, UK). DHA, as a standard drug, and control wells with untreated infected and uninfected erythrocytes were included in all assays.

3.3 References

(1) Adam, W., Nestler, B., *J. Am. Chem. Soc.* **1993**, *115*, 5041-5049.

(2) Bartoschek, A., El-Idreesy, T. T., Griesbeck, A. G., Hoinck, L., Miara, C., Neudorfl, J. M., *Synthesis* **2005**, 2433-2444.

(3) Griesbeck, A. G., El-Idreesy, T. T., Höinck, L., Lex, J., Brun, R., *Bioorg. Med. Chem. Lett.* **2005**, *15*, 595-597.

(4) Midland, M., Tramontano, A., Kazubski, A., Graham, R. S., Tsai, D. J. S., Cardin, D. B., *Tetrahedron* **1984**, *40*, 1371-1380.

(5) Noyori, R., Tomino, I., Yamada, M., Nishizawa, M., *J. Am. Chem. Soc.* **1984**, *106*, 6717-6725.

(6) Matsumura, K., Hashiguchi, S., Ikariya, T., Noyori, R., *J. Am. Chem. Soc.* **1997**, *119*, 8738-8739.

(7) Murray, R. W., Kaplan, M. L., *J. Am. Chem. Soc.* **1969**, *91*, 5358-5364.

(8) Chen, Y. K., Jeon, S. J., Walsh, P. J., Nugent, W. A., *Org. Syn.* **2005**, *82*, 87-90.

(9) Lurain, A. E., Maestri, A., Rowley-Kelly, A., Carroll, P. J., Walsh, P. J., *J. Am. Chem. Soc.* **2004**, *126*, 13608-13609.

(10) Nugent, W. A. *Chem. Comm.* **1999**, 1369-1370.

(11) Trager, W., Jensen, J. B., *Science* **1976**, *193*, 673-675.

(12) Desjardins, R. E., Caufield, C. J., Haynes, J. D., Chulay, J. D., *Antimicrob. Agents Chemother.* **1979**, *16*, 710-718.

4.0 Introduction - Synthesis and Biological Activity of Minor Groove Binding Artemisinin Conjugates

4.1 Artemisinin as an Anti-Cancer Agent

4.1.1 Artemisinin and Derivatives with Cytotoxic Activity

Woerdenbag and co-workers were the first to report the cytotoxic activity exhibited by artemisinin and its first generation derivatives.[1] Their original aim was to use cytotoxicity towards Ehrlich Ascite tumour cells as a model for human cells to study the therapeutic index of these clinical antimalarial agents. Artemisinin and dihydroartemisinin (DHA) showed some cytotoxic effect (IC_{50} = 29.8 and 83.4 μM respectively). However, artemether, arteether, sodium artesunate, artelinic acid and sodium artelinate were more potent, with IC_{50} values from 12.2 to 19.9 μM. The most active compound was an artemisinin ether dimer **133** (IC_{50} = 1.4 μM), which was more potent than *cis*-platin in this assay. The remarkable potency of these derivatives was in part attributed to their increased lipophilicty, compared to the parent compound. Artemistene **135**, incorporating an exocyclic methylene group at the C-9 position, also performed well (IC_{50} = 6.8 μM). The endoperoxide bridge of artemisinin was shown to be crucial as desoxyartemisinin **10** exerted no effect up to concentrations of 1mM.[2] Artemisinin and its ether dimer **133** were shown to induce growth inhibition rather than cell death, whereas artemistene **135** exerted toxicity *via* cell death. The methylene group of artemistene could potentially alkylate cellular macromolecules through a Michael Addition which may account for its cell killing effect.

Further examination of the artemisinin ether dimers showed that stereochemistry had an effect on cytotoxicity.[3] Symmetrical dimers **134** were less active than non-symmetrical **133** (IC_{50} = 2.00 and 0.11 μM respectively). Stereoisomers of the

epoxide of artemistene were also tested with the *R*-epoxide **136** (IC_{50} = 12.7 μM) being markedly more potent than the *S*-epoxide **137** (IC_{50} = > 100 μM).

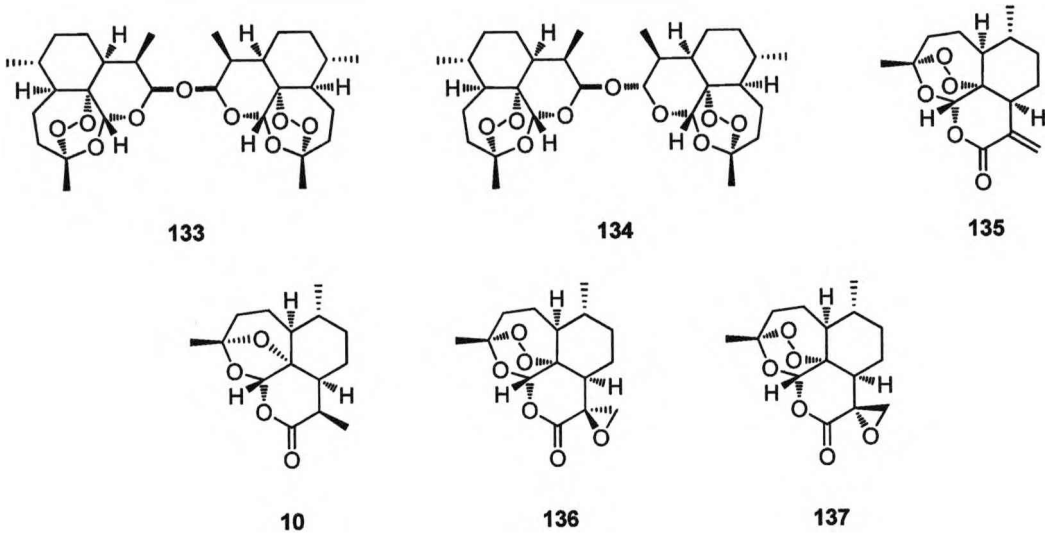

Figure 4.1 *Artemisinin and derivatives tested for cytotoxic activity by Woerdenbag and co-workers.*

Subsequent work by Posner has shown that this class of artemisinin dimer demonstrates particular cytotoxic specificity towards leukaemia cell lines and some types of colon cancer, over the other 60 cell lines tested by the National Cancer Institute's (NCIs) Developmental and Therapeutics Program.[4-6] Hydrolytically labile C-10 acetal-linked dimers were synthesised and testing showed promising results *in vitro* as well as no acute toxicity to mice *in vivo*, even at a maximum tolerated dose of 400 mg/kg.[4] It is worth noting that two acetal linked dimers that had significant cytotoxic activity, both had 3-carbon linkers, namely glutarate diester and *m*-phthalate diester linkers.[4] These structures also reflected the high activity of a glutarate diester of DHA.

Facile synthesis of chemically robust C-10 carba dimers became of interest. Dimer **138** (Figure 4.2) was prepared and substantially reduced cancer cell mass in mice,

suggesting greater stability *in vivo*.[5,7-9] A new series of acetal linked dimers have been recently reported with *in vivo* activity: a stereochemically symmetrical cyclohexane linked dimer having antitumour activity comparable with paclitaxel.[10]

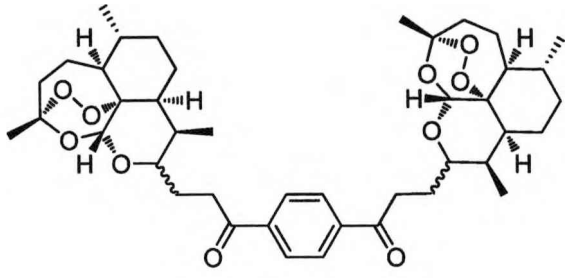

138

Figure 4.2 *A chemically robust C-10 carba linked dimer.*

In a series of C-10 carba phosphate- and C-10 carba phosphonate-linked dimers, synthesised by the O'Neill group, the influence of linker-length on activity was studied. Methyl, ethyl and propyl ester links were employed from phosphorus to artemisinin. As a general trend, an increase of linker length led to an increase in potency against HL-60 cancer cell lines. An amide-linked dimer also showed significant antiproliferative activity.[11]

An artemisinin trimer **139** with a non-acetal C-10 linker was also successfully synthesised and tested (Figure 4.3).[12] A carboxyethyl artemisinin intermediate was coupled with an L-glutamic diethylester linker using EDC/HOBt amide coupling reagents. The two ester groups were hydrolysed to give the diacid which then underwent double coupling (EDC/HOBt) with 2 equivalents of aminoethyl artemisinin. The *in vitro* cytotoxicity of the trimer **139** (IC_{50} = 0.09 μg/mL) was comparable to that of adriamycin (IC_{50} = 0.10 μg/mL), mitomycin (IC_{50} = 0.02

μg/mL) and taxol (IC_{50} = 0.01 μg/mL) againt HT-29 human colorectal adenocarcinoma.

A corresponding C-10 carba dimer of deoxyartemisinin was also synthesised and tested to reiterate the importance of the endoperoxide bridge in cytotoxic potency. As expected, the deoxy-dimer showed no activity even at concentrations of 1 μM.[6]

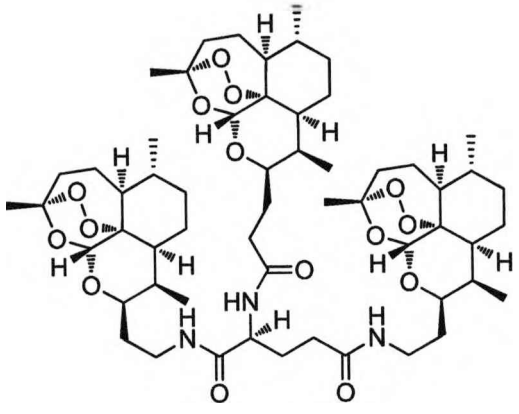

139

Figure 4.3 *Artemisinin trimer.*

4.1.2 Specificity and Cytotoxic Potency of Artemisinin

As previously discussed in Chapter 1.0, the artemisinin class of antimalarials agents exert their effect by iron mediated cleavage of the endoperoxide bridge and subsequent formation of free radicals. This is supported by a body of work showing that removal of the peroxide bridge from artemisinin type compounds results in a loss of antimalarial and cytotoxic acivity.[13] The iron content of tumour cells is generally higher than that of normal cells.[14] Accordingly, bioactivation of artemisinin by iron, and differentiation between healthy and cancerous cells by iron concentration, provides a strategy for selective cytotoxicity by artemisinin and its derivatives.

The elevated iron concentration of cancerous cells is a result of over-expression of transferrin receptors (TfR) on the cell surface. These trans-membrane proteins mediate iron transport into cells resulting in high intracellular iron concentrations in cancer cells. Rapidly proliferating cancer cells lines, such as leukemic, lung, breast and colon cancers, have a high metabolic requirement for iron and show a particularly high distribution of TfR, elevating iron influx.[14] Correspondingly, and supporting the iron activation hypothesis, artemisinin demonstrates a heightened cytotoxic affect upon these iron rich cell lines.

The specificity and activity of artemisinin were highlighted in studies carried out by Lai and co-workers. Co-administration of artemisinin derivatives and ferrous compounds to tumour cells greatly augmented cytotoxic activity: whereas administration of artemisinin alone and administration of the combination to healthy cells resulted in significantly less cell death.[15-18] In a recent publication, holotransferrin was covalently tagged to artemisinin. This allowed artemisinin to be selectively picked up, endocytosed and concentrated by cancerous cells.[19] Futhermore, both artemisinin and iron would be transported into the cell in one package. Accordingly, artemisinin-tagged transferrin is highly selective and potent toward the human leukaemia cell line, Molt-4.[19]

4.1.3 Biological Targets and Cytotoxic Mechanism of Action

It has been established, like many other cytotoxic agents, that artemisinin causes apoptosis of tumour cells; however the precise biological target that artemisinin uses to exert its activity still remains elusive.[20,21] Efferth has attempted to shed light on the response of cancerous cells to artemisinin using genetic pathways. mRNA profiles

were monitored in order to evaluate the cellular response to artesunate, arteether and artemether. It was found that a common mechanism of action is implicated for all three *i.e.* the intervention of cellular proliferation.[22] Similar results have been reported by Hou.[23]

Efferth also looked at the correlation of mRNA expression of genes involved in oxidative stress response with the IC_{50} values of artemisinin derivatives. Expression of a group of these genes indicated that oxidative stress plays an important part in the mechanism of action of artemisinin.[24]

Using similar methods, anti-angiogenesis and anti-lymphangiogenesis has also been implicated as a cytotoxic mode of action for artemisinin derivatives. Angiogenesis, can be defined as the formation of new blood vessels or lymphatic vessels from pre-existing ones, and is essential for tumour growth. Consequently, anti-angiogenic therapy might be clinically useful for the treatment of tumours. Again a positive correlation was found between the activity of artemisinin derivatives and the expression of angiogenesis related genes.[25,26]

Evidence for DNA damage caused by artesunate, contributing to its therapeutic effect, has also been reported. A study by Li, measuring the level of γ-H2AX (an indication of double strand breaks) and single cell gel electrophoresis, indicated induction of DNA breakage in a dose dependent manner. In addition, mutant cells, deficient in certain polymerases responsible for repairing strand breaks, were more sensitive to artesunate than the wild-type which are able to repair DNA damage.[27]

4.2 Pyrrole-Amidine Antibiotics

4.2.1 Netropsin and Distamycin A: Discovery and Structural Motifs

Netropsin (Nt) and Distamycin A (Dst) are the most widely known members of the pyrrole-amidine class of naturally occurring oligopeptidic pyrrole chains. Netropsin, discovered in 1951 by Finlay, was isolated from the bacterium *Streptomyces netropsis* and initially showed an inhibitory effect on a number of microorganisms and toxicity in mice.[28] Without the benefit of NMR spectroscopy, Finlay correctly identified the presence of amide linkages and a guanidine moiety. The structure of Nt **140**, as shown in Figure 4.4, was confirmed in 1963.[29] Distamycin A **141**, isolated from *Streptomyces distallicus*, was reported seven years later[30,31] and exhibited activity against bacteria and DNA-viruses such as herpes simplex, the vaccinia virus and Rous sarcoma.[32] The chemical structure, as shown in Figure 4.4, was established by total synthesis[29] and chemical analysis of Dst by Arcamone.[33]

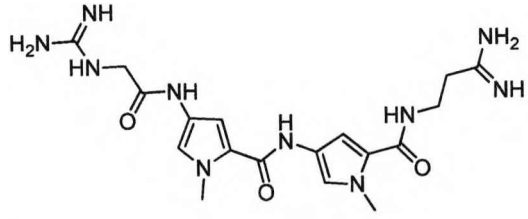

140

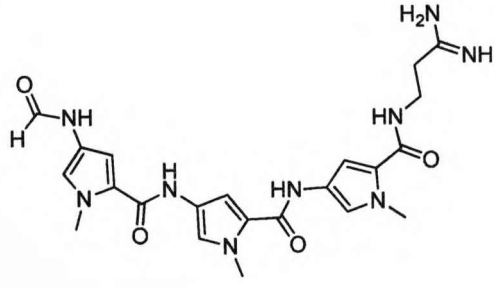

141

***Figure 4.4** Netropsin **140** and Distamycin A **141**.*

Single-crystal X-ray diffraction data of Nt sulphate indicated that its two pyrrole rings are not co-planar and have an angle of 20°.[34,35] The regiochemistry of Nt also suggests a "bowed" oilgopeptide backbone with the concave side, containing amide

linkages, forming hydrogen bonds to water, and a hydrophobic convex side consisting of carbonyl and methyl groups. It later became apparent that the hydrophilic concave shape of Nt and Dst made them a perfect fit for the floor of the minor groove of B-DNA.

4.2.2 Properties of Netropsin and Distamycin A

Early work indicated that biological damage caused by Nt and Dst was facilitated by interactions with DNA. Thus, extensive studies were carried out to confirm the interactions of oligopeptides with DNA *in vitro*, using the techniques of UV-absorption, thermal melting and circular dichroism experiments. A summary of this work is included as follows.

4.2.2.1 Netropsin and Distamycin A bind to cellular DNA and not RNA

Chandra, Zimmer and Thrum initially studied the effects of Dst.[36] It was firstly observed that the UV-absorbance of *E. Coli*-DNA decreased in the presence of Dst and the melting temperature of native DNA increased with an increase of Dst concentration. Analogously, Nt also showed a protective effect against temperature.[37] It was concluded that there is a strong binding between Dst/Nt and native DNA.

In order to link this strong interaction with the toxic effect of these antibiotics, the effect of Dst on the template activity of native DNA in the RNA-polymerase system was studied and showed an inhibitory effect. To prove that Dst was not causing enzyme inhibition by blocking the active site of RNA-polymerase, Dst was pre-incubated with DNA for increasing time periods, and correspondingly, inhibition of

template activity increased with incubation time. Therefore, inhibition of RNA-polymerase was attributed to DNA-Dst binding.[36]

Krey and Hahn similarly found that the presence of Dst shifted the absorption maximum of duplex calf thymus DNA (ctDNA) from 303 nm to 321 nm.[38] Dst was also shown to displace methyl green from its complex with DNA, as indicated by a decrease in absorbance at 642 nm and the loss of green colour. The displacement reaction was calculated to be second order with time, dependent on the concentration of the two species, showing the binding of Dst to DNA has an effect on the displacement of methyl green.

Nt and Dst are optically inactive and DNA itself does not absorb wavelengths past 310nm. However, the optical rotatory dispersion (ORD) spectrum produced from the complexation of Nt and Dst with DNA showed additional optical transitions (Cotton effects) at 340nm and 350nm respectively.[39] It was proposed, therefore, that upon complex formation there is perturbation of the chromophores of Nt and Dst and potentially a perturbation of the secondary structure of B-DNA.

Interestingly, Nt and Dst had no effect on the ORD of RNA indicating no binding affinity for RNA, and explaining the antiviral activity towards DNA-viruses and not RNA-viruses. Circular dichroism (CD) experiments by Luck and co-workers concurred with these results.[40] Again an additional Cotton effect was observed in the long wavelength region of DNA-oligopeptide complexes, indicating the induced chirality of the oligopeptides upon DNA-complexation. No such Cotton effect appeared in the case of RNA. RNA exists in the A-form, which is similar to the B-form DNA in that it is a right handed double helix and that it has minor and major grooves. However, it has a tighter rotational angle giving a deepened major groove

and a shallower minor groove. Nt and Dst lack of binding affinity to RNA signified some sort of hindrance to the A-conformation. This is supported by the fact that Nt binding to DNA is diminished when DNA is in ethanol, and is known to transit from the B- to A-form.

4.2.2.2 Netropsin and Distamycin A Show Specificity to A and T Rich DNA Tracts

During the above work, it had been noted that the distribution of the adenine/thymine and guanine/cytosine base pairs affected Nt binding. The intensity of ORD spectra of Nt- and Dst-DNA complexes increased with the adenine and thymine content of the DNA being used. For example ctDNA at 58 mole % AT produced a more intense spectrum than *E. Coli* DNA at 47 mole %. Viscosity tests were also used to compare Nt affinity and specificity for DNA as small additions of Nt to DNA lead to increased viscosity.[37] DNA with a high AT content (*e.g. S. maxima* DNA = 71 mole % AT) showed a pronounced and immediate increase in viscosity. DNA which predominantly consists of GC (*e.g. M. Lysodeikicus* DNA = 28 mole % AT) showed an initial reduction in viscosity.

Extensive thermal melting experiments, performed at varying ionic strengths, were also carried out by Luck *et al.*[40] Luck stated that in low ionic strength solutions, Nt and Dst will bind to both GC and AT tracts, but at moderate to high ionic strength (> 10^{-1} M Na^+) both oligopeptides show specific binding towards AT rich regions. At 0.1 and 0.5 M Na^+ solutions Nt and Dst bound tightly to synthetic alternating AT (poly(dA-T).(dA-T)) and IC (poly(dI-C).(dI-C)) tracts, and consecutive A-tracts complementary with T (poly(dA).(dT)). As expected, at the same ionic strengths, Nt and Dst did not show strong binding to the consecutive G-tract complementary with

C, (poly(dG).(dC)). More specifically, Nt showed the strongest binding affinity for the synthetic polynucleotide poly(dA).(dT). In 4M NaCl conditions the Nt-poly(dA).(dT) complex melted at ~95°C, whereas the Nt-poly(dA-T).(dA-T) complex melted at ~80°C (Figure 4.5).

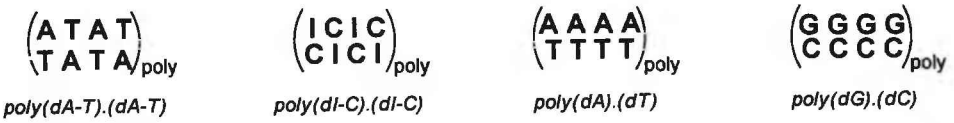

Figure 4.5 *Qualitative diagram of the synthetic polynucleotide tracts tested by Luck[40] and Wartell[41].*

This trend was further developed by Wartell *et al.*[41] Wartell studied the binding of Nt to synthetic DNA tracts of A-T, I-C and G-C. It was found that Nt bound strongly to A-T and I-C but not G-C. By process of elimination, the only feature missing from the two former, and present in the latter was the 2-amino group of guanine (Figure 4.6). It was correctly theorised that steric hindrance of the guanine 2-amino group, protruding into the minor groove of DNA, blocked Nt binding. This theory implicated the minor groove as the Nt and Dst binding site which will be discussed in Section 4.2.2.4.

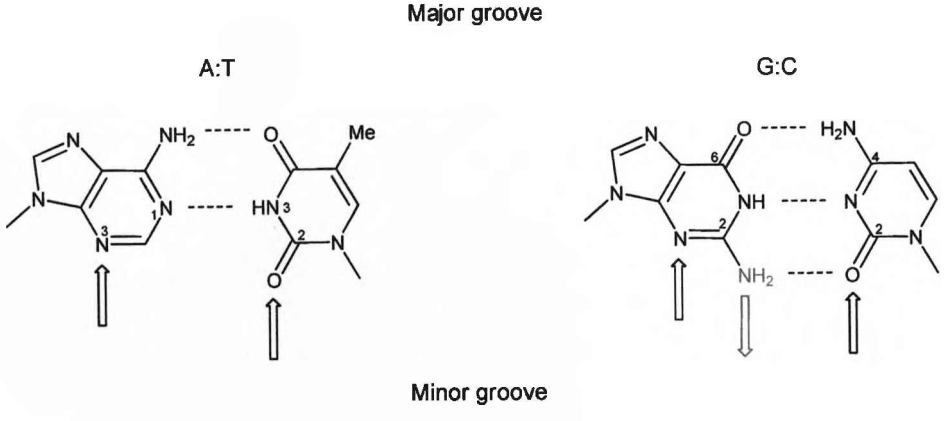

Figure 4.6 *Molecular structure of the AT and GC base pairs with the 2-amino group of guanine highlighted. Arrows indicate H-bond acceptors and donors.*

4.2.2.3 Netropsin and Distamycin A Bind to the DNA-Duplex via Hydrogen Bonding as well as Ionic Forces

Luck also hypothesised that two types of binding interaction were taking place between the oligopeptides and DNA.[40] Melting curves were taken at various molar ratios of the antibiotic to DNA up to 0.1 moles Nt/DNA. Complex formation (association) was observed at 260nm shown as a sharp increase in absorbance as temperature increases. Similarly dissociation of the antibiotic from DNA was observed at 320nm producing a sharp decrease in absorbance as temperature increases. Association at 0.01 moles Nt/DNA showed two steps in the curve at ~65°C and ~78°C. This suggested two types of binding interactions of differing strengths. This was supported by the dissociation curve which showed release of the antibiotic only at ~78°C *i.e.* the antibiotic is released when a more strongly stabilised fraction of the DNA melts.

As discussed previously (Section 4.2.2.2), Nt and Dst bind tightly to AT-rich regions in very concentrated salt solutions (up to 4 M NaCl). This implies that recognition of AT-rich portions by the oligopeptide molecules probably occurs through hydrogen bonding, in addition to long range electrostatic interactions. Additional evidence is that hydrogen and hydrophobic bond breaking agents have been shown to cause partial or complete dissociation of the DNA-antibiotic complex.

4.2.2.4 Netropsin and Distamycin Bind to the Minor Groove of DNA

Luck went on to link hydrogen bonding to specificity for the minor groove of DNA.[40] Charged Nt has eleven H-bond donor and three H-bond acceptor sites and it was recognised that the minor groove has suitable corresponding acceptor/donor sites

in the form of oxygen from the phosphate backbone, deoxyribose groups and the C-2 carbonyl groups of thymine. This theory was elucidated more clearly in later years with the availability of x-ray crystal structures and ^{1}H-NMR NOE experiments, which will be discussed in Section 4.2.2.5.

As discussed in Section 4.2.2.2, Wartell's theory also implicated the minor groove in Nt binding.[41] The preference for AT-rich rather than GC-rich tracts of DNA was explained by steric hindrance of the bulky 2-amino group of guanine protruding into the minor groove and blocking Nt binding. To prove further that Nt binds to the minor groove, DNA-Nt binding was studied for tracts of synthetic DNA where dT was substituted for dU or dBrU and dC was substituted for dBrC. It was found that this change produced no detrimental effects to DNA-Nt binding. This confirmed that interaction with the minor groove as the Br atoms, with large atomic radii, occupy the major groove. To further elucidate the mechanism of Nt binding, the interaction of Nt with supercoiled DNA (M13 RFI) was studied. Molecules which intercalate to DNA can unwind and rewind supercoiled DNA, which can be monitored by measuring the respective fall and rise of sedimentation velocity of the DNA as the amount of bound ligand is increased. Nt binding showed no change in sedimentation, therefore not initiating unwinding and proving it does not interact with DNA *via* intercalation. Similar results were found with supercoiled PM2 DNA.

Finally, this attraction for the minor groove is also consistent with the lack of affinity that Nt and Dst show for RNA and DNA in the A-conformation. As previously mentioned the structure of the A-conformation renders the major groove deeper and the minor groove shallower; too shallow to facilitate successful binding of Nt and Dst.

4.2.2.5 Visualising DNA-Oligopeptide Complexes via X-ray Crystallography and NMR Methods

To further elucidate the position Nt and Dst adopt with the minor grove of DNA, NMR, NOE and X-ray crystallographic experiments were performed throughout the 1980s. DNA tracts focused on were various natural DNAs, (dA-dT) polynucleotides and dodecamers such as d(CGCGAATTCGCG), d(CGCAAATTTGCG) and alternating sequences d(CGCGATATCGCG).

The 4 base pair AT tract contained within d(CGCGAATTCGCG), has been the minimum length AT tract studied due to the findings of Dervan, who noted that Nt and Dst having *n* amides characteristically bind to *n* + 1 successive base pairs.[42] Additionally, AT tracts in runs greater than four, display particular stabilising properties. One observes an increased propeller twist of the base pairs of 17°,[43] which is proposed to allow for deeper and narrower minor grooves, enhancing minor groove binding.[44]

NOE experiments of the Nt and Dst complexed with d(CGCGAATTCGCG) demonstrated a 1:1 binding mode and highlighted several points of contact between the inner, concave surface of the antibiotic and the minor groove of the d(AATT) segment of the dodecanucleotide.[45,46] This unambiguously positions the drug spanning the central AATT segment.

In 1985 Kopka *et al.* performed X-ray crystallographic studies on Nt bound to d(CGCGAATTCGCG).[42,47] It confirmed the Nt molecule sits tightly within the minor groove having displaced the spine of hydration. Its position is at the centre of the AATT tract. It was seen to widen the groove by 0.5-2.0 Å and bent the helix axis by 8°, however there was no evidence of unwinding or elongation of the helix in

agreement with the non-intercalative activity of Nt. Nt sits symmetrically in the centre of the groove with its pyrrole rings slightly non-co-planar, as also previously observed for free Nt, so that each ring is parallel with its region of groove wall. The amide NH forms bifurcated hydrogen bonds bridging the adenine N-3 and thymine O-2 atoms (Figure 4.7). In fact Nt forms exactly the same hydrogen bonding pattern as the spine of hydration.

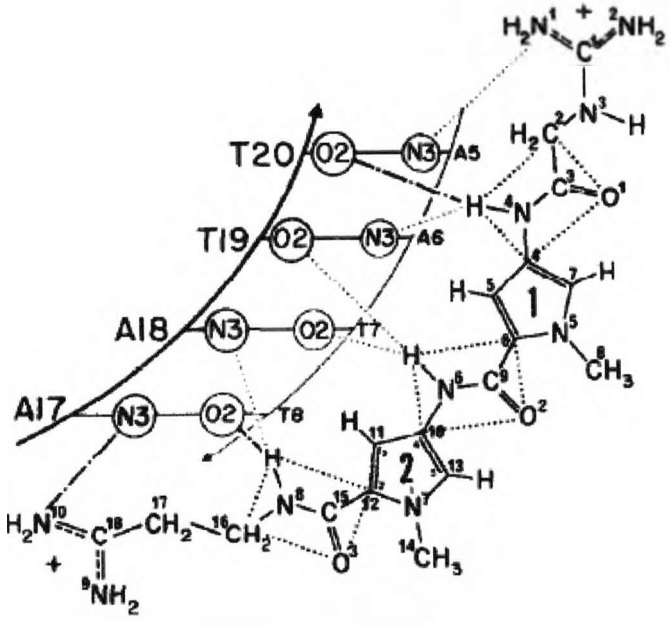

Figure 4.7 *Schematic diagram of the interactions between Nt* ***140****, adenine N-3 and thymine O-2. Dot-dash lines indicate normal H-bonds (2.5-2.8Å), Dotted lines indicate longer H-bonds (>3.0Å). Figure taken from reference 42.*

Electrostatic interactions are also formed from the amidinium and guanidinium termini of Nt with the phosphate backbone, although both these cationic groups sit in the centre of the minor groove and do not interact with a specific phosphate group. The amidinium also forms normal length hydrogen bonds with adenine N-3 and the more rigid guanidinium forms longer hydrogen bonds with its adjacent adenine N-3.

The synthetic dodecamer d(CGCAAATTTGCG), with a six base pair AT segment also shows a high propeller twist at adenine-6. From X-ray crystallography it was determined that Dst lies near the centre of the DNA fragment covering five of the six AT base pairs.[48] The shorter Nt could occupy several positions along the lengthened AT tract but no sign of positional disorder was observed. The drug chooses a central position which must be one of the possible structures with lower energy *i.e.* almost all possible drug-DNA H-bonds are satisfied.

A 2:1 binding mode of drug to AT-tract was also first observed through NOE experiments of Dst interacting with the d(CGCAAATTTGCG) dodecamer. At low drug-DNA ratios (0.5 equivalents), both one-drug and two-drug binding modes were observed. At higher ratios (2 equivalents), the two-drug complex was the primary species. The data was consistent with a model in which two drug molecules bind simultaneously, overlapping in the minor groove with each drug sliding between 5'-AATT-3' and 5'-ATTT-3', the minor groove expanded relative to the 1:1 complex.[49] It was also found that Nt occupies a more central position than Dst and the orientation of both drugs in the d(CGCAAATTTGCG) dodecamer is reversed when compared to that in the d(CGCGAATTCGCG) dodecamer.[50]

Alternating AT tracts were also examined, firstly in the form of dodecamer d(CGCGATATCGCG).[51] In general, Nt shows better binding affinity for a d(A).d(T) tract than a d(AT) tract, but X-ray diffraction analysis showed Nt binding in the minor groove of the central ATAT region as expected. However, unlike the last example, the drug binds in two different orientations equally well. Also individual to this case, is the finding that Nt binds by single hydrogen bonds rather than bifurcating bonds. This is believed to be caused by uneven spacing of H-bond

acceptors along the floor of the minor groove in the alternating tract. This results in a reduced binding affinity. Moreover, two of the four AT base pairs in the ATAT stretch have very low propeller twists, potentially leading to a wider minor groove. The longer alternating AT-tract, d(CGCATATATGCG), was indeed confirmed to have a wider minor groove in comparison to oligo(dA).d(T) tracts. This wider minor groove allowed Dst a preference for a 2:1 binding mode, with two drug molecules alongside each other in the groove. The 2:1 complex appears well below stoichiometric addition of the drug, indicating a positive cooperativity in binding. In fact this binding mode was observed at a lower stoichiometric amount then that needed to bind 2:1 at AAATTT tracts, suggesting especially facile binding in the 2:1 mode towards the alternating tract.[52]

4.2.3 Effect of Netropsin and Distamycin on Plasmodium Falciparum

Driven by the emerging resistance of malaria parasites to established antimalarial treatments, novel agents to combat the disease are of great interest. Recently, Dst was found to possess antiprotozoal activity, particularly against both chloroquine sensitive and resistant strains of *Plasmodium falciparum*. The DNA of the malaria parasite is significantly richer in A and T bases than that of mammalian cells, being over 80% in most malaria species compared to only 59% in man. Also the proliferation of the malaria parasite during blood stage of its life-cycle, is reminiscent of malignant rather than healthy mammalian cells. Therefore this cytotoxic agent could potentially have a detrimental effect on the reproductive cycle of the malaria parasite.

4.2.3.1 Minor Groove Binders Exhibit Antiprotozoal Activity

Ginsburg *et al.* initially studied the effect of a variety of minor groove binding antibiotics, with a preference for AT-rich DNA tracts, on *Plasmodium falciparum* malaria.[53] Dst, Nt, 4'-6-diamidino-2-phenylindole (DAPI) and bis-benzimide (Hoechst 33258) were found to inhibit the growth and propagation of *P. falciparum*. The toxicity of these AT-specific antibiotics towards parasites and mammalian cells was also compared to two GC-specific antibiotics chromomycin A_3 and mithramycin A. It was found that the AT-targeting compounds were considerably more toxic to parasites than to mammalian cells and the compounds which bind preferentially to GC–rich sequences, were either equally toxic or more harmful to mammalian cells. This data exhibits the selective power of these AT-specific agents and their potential as specific anti-malarial agents, but also highlights an important difference in parasite and mammalian physiology that could be exploited.

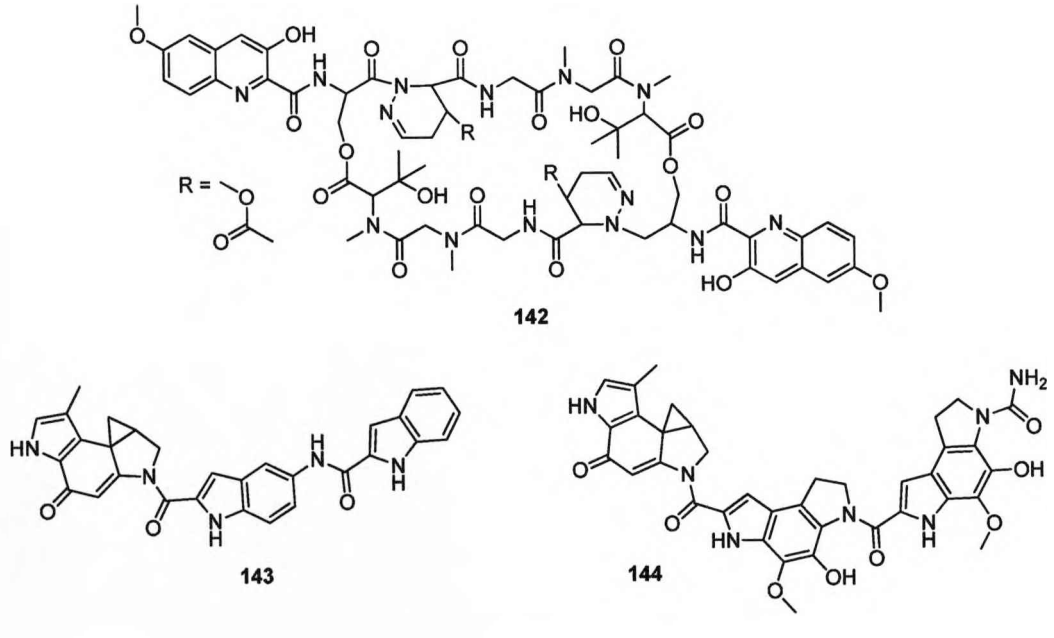

Figure 4.8 *The cytotoxic agents luzopeptin* ***142****, U71184* ***143*** *and CC1065* ***144*** *demonstrate potent in vitro activity against P. falciparum.*

In the same year Lee and Inselburg published the sensitivity of *P. falciparum* to 14 cytotoxic agents *in vitro*.[54] Dst exhibited an LD_{50} (lethal dose concentration for 50% of parasites) of 3.3×10^{-7} M, however compounds having the most profound effect were luzopeptin **142**, U71184 **143** and CC1065 **144** (Figure 4.8), all being active in the picomolar range.

Although Nt and Dst have shown a preference for parasitic cells over mammalian cells due to their AT-specificity, they still display very high toxicity in healthy human cells, thus prohibiting their development as drugs. Lombardi and Crisanti[32] hoped to maintain anti-malarial activity whilst reducing toxicity *via* a number of synthetic analogues of distamycin. This was achieved by replacement of the *N*-formyl group, situated at the terminus of Dst, with either an *N*-formimidoyl (**145-148**) or carbamoyl group (**149-151**), whilst varying the number of pyrrole units from 1 to 4 (Figure 4.9).

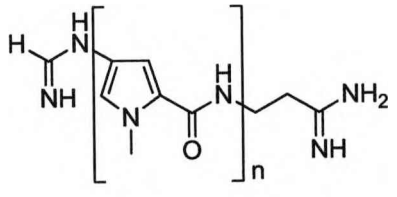

145-147 n = 1,3,4

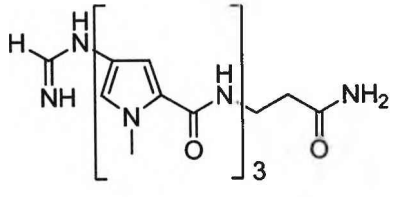

148

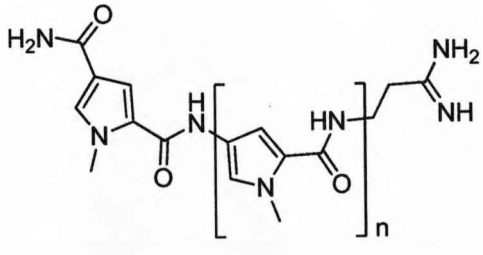

149-151 n = 2,3,4

Figure 4.9 *Dst analogues designed to maintain antimalarial activity while reducing cytotoxicity.*[32]

Dst and the synthetic analogues were tested against the chloroquine-sensitive ITO4 strain of *P. falciparum* and the ID_{50} estimated from dose-effect curves. DNA binding was studied using calf thymus DNA, as was cytotoxic effect by measuring cell proliferation in Hep-2 cell lines. The carbamoyl analogues showed a lower affinity for DNA than distamycin, suggesting that the formylamino group plays an important role in DNA–drug interactions. The carbamoyl analogues also showed very low cytotoxicity paired with excellent anti-parasitic activity ($n = 3$, $ID_{50} = 0.25\mu M$). Elegantly, an increase in anti-parasitic activity directly follows an increase in the number of pyrrole units, irrespective of the terminal substituent or the other parameters studied. This can be explained by the hypothesis that the increased numbers of amide bonds provide more H-bonding interactions with AT rich regions, inducing tighter binding to the duplex.

4.2.3.2 P. falciparum Helicase Enzymes as a Target for Antibiotic Agents

More recently and more specifically, Pradhan and Tuteja have studied the effect of DNA-interacting compounds on the activity of *P. falciparum* helicase enzymes.[55,56] Helicases are a class of ubiquitous enzymes that catalyse the unwinding of duplex DNA and RNA, thereby allowing transcription and replication, powered by nucleoside triphosphate. This class of enzymes have been recognized as a potential drug target. A differential gene expression study in the presence of chloroquine has indicated that RNA helicase proteins may be involved in the anti-malarial action of the drug and it has been shown that helicases are essential for viability of various bacteria and viruses. DNA-interacting ligands, particularly intercalators, have been shown to inhibit the action of helicases either by causing a physical block to the path

of the helicase along the DNA duplex or by causing structural changes to the duplex thereby preventing efficient enzyme activity.[57-59]

In 2006 Pradhan characterised *Plasmodium falciparum* DNA helicase 60 (*Pf*DH60) and tested various minor groove binders (including netropsin in this case), intercalators and non-intercalating topoisomerase inhibitors against *Pf*DH60.[55]

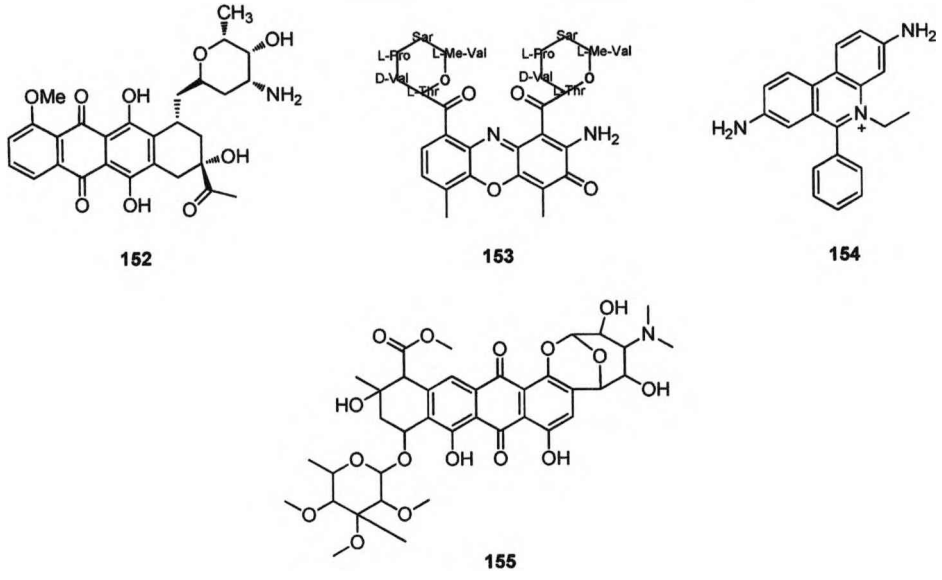

Figure 4.10 *Daunorubicin **152**, actinomycin **153**, ethidium bromide **154** and nogalamycin **155** demonstrate inhibition of PfDH60.*

These ligands were tested by including 50μM of each antibiotic in the standard helicase assay and daunorubicin **152**, actinomycin **153**, netropsin **140**, ethidium bromide **154** and nogalamycin **155** inhibited DNA-unwinding activity of *Pf*DH60 effectively (Figure 4.10). IC_{50} values of these ligands were calculated to be 0.3, 0.8, 1.2, 1.5 and 2 μM, respectively. These same five compounds also inhibited the ssDNA-dependent ATPase activity of *Pf*DH60 in the standard ATPase assay. Calculation of IC_{50} values showed nogalamycin as the most effective (IC_{50} = 0.5μM) and netropsin at fourth most active (IC_{50} = 3.0μM). These five ligands were then

tested for growth inhibition of *P. falciparum in vitro* and although netropsin showed the poorest activity, it still slowed growth to only ~30% after 72hrs.

In 2008 Pradhan also tested a similar library of DNA-interacting ligands on *Pf*H45 (*Plasmodium falciparum* helicase 45), also including Dst.[56] Again netropsin inhibited the DNA-unwinding and ssDNA dependent ATPase activity of *Pf*H45 effectively. Calculation of IC_{50} values showed netropsin was the most potent *Pf*H45 inhibitor (IC_{50} = 0.5 μM) and the second most potent ATPase inhibitor (IC_{50} = 1.5μM) after nogalamycin (IC_{50} = 0.8 μM). Dst however showed no inhibitory activity towards either mode of *Pf*H45.

4.3 Design and Biological Activity of Netropsin/Distamycin Analogues and Hybrids

Since the elucidation of the remarkable binding properties of Nt and Dst and their preference for AT rich regions of DNA, the modification of these structures has been explored on two fronts: firstly, their affinity for specific base pairs, adenine and thymine, raised the question of whether these molecules could be tailored to bind to specific DNA sequences, and secondly, their tethering to alkylating, intercalating and DNA cleaving agents in an attempt to "deliver" cytotoxic agents directly to the minor groove of DNA and enhance increase cytotoxicity. In this review we shall mainly concentrate on the latter category, with a brief summary of the former.

4.3.1 Monomers, Dimers and Lexitropsins

Agents such as Nt and Dst exert their limited toxicity by binding to the minor groove of B-helical DNA and therefore blocking the path of transcription factors and

enzymes, thus disrupting the DNA replication process. By increasing the binding affinity of these carboxamide chains to DNA, it was hoped to increase cytotoxicity. A design strategy for this was to increase the number of pyrrole units so extending the chain and extending the length of the binding site allowing for more binding interactions.[60]

Tris, tetra, penta and hexa *N*-methylpyrrolecarboxamide derivatives of Nt and Dst can bind to sequences containing five, six, seven and eight contiguous AT base pairs respectively.[61,62] The tetrapyrrole Dst homologue is almost 20 times more potent than the parent natural product and increasing the number of pyrrolic units of the oligopeptide frame increases the sequence specificity for longer tracts of DNA AT-rich sequences, as a result of the greater availability of hydrogen bonding and van der Waals surface.[63] However, hepta *N*-methylpyrrolecarboxamide derivatives were found not to fit with the natural twist of helix DNA, presumably because the molecule becomes out of phase with the base pairs along the minor groove floor of the double helix.[64]

An alternative strategy to circumvent the poor phasing between the DNA and ligand is to join two Nt or Dst molecules by a linker of a suitable length to allow bidentate binding to DNA. A considerable number of bis(netropsin) and bis(distamycin) compounds have been designed and synthesised including flexible polymethylene ($(CH_2)_{1\text{-}10}$) linkers and also more rigid tethers incorporating a cyclic or unsaturated portion, allowing for bidentate ligand interactions with DNA. An important biological application of these compounds has arisen with the synthesis of two bis(distamycin) derivatives containing a 3,5-*m*-pyridyl or a *trans*-vinyl linker **156**

(Figure 4.11). These compounds were found to be the most effective bis-linked lexitropsins at inhibiting transcription by HIV-1 reverse transcriptase.[65]

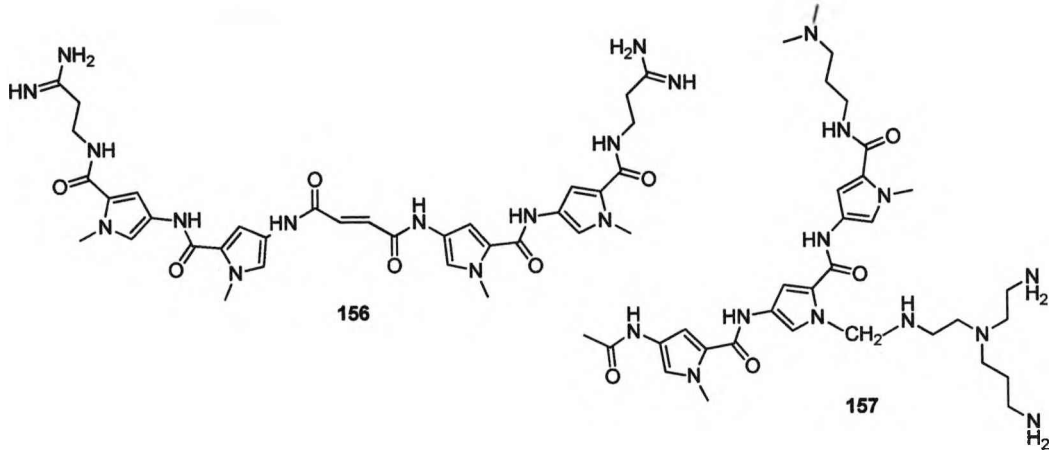

Figure 4.11 *Examples of a potent bis(distamycin)* ***156*** *and a tren-microgonotropen* ***157****.*

One of the most recent strategies for the synthesis of polyamide analogues with very high DNA binding affinity has involved linkage to polyamines to yield the "microgonotropens" *e.g.* **157**.[66,67] Replacement of the central pyrrole *N*-methyl moiety with branched polyamines allows for the projection of the substituent out of the minor groove. DNA binding affinity is enhanced by the polyamine acting as a "hook", forming bonding interactions with the phosphodiester backbone or the major grove of DNA. This class of compounds can efficiently compete with sequence specific binding of regulatory proteins to DNA.[68]

As previously discussed, the intrusion of the 2-amino H-bond donor group of guanidine into the minor groove is a major facilitator of the AT preference exhibited by Nt, Dst and analogous *N*-methylpyrrolecarboxamide chains. It was therefore proposed that the introduction of a H-bond acceptor heteroatom in the pyrrole rings

of Nt might permit the drug to bind to GC sequences. The so-called "lexitropsins" or "information reading oligopeptides" were born and it was hypothesised that by substituting imidazole, thiazole, triazole, pyrazole or oxazole heterocycles for the *N*-methyl pyrrole ring, one could design drugs capable of binding to sequences containing one or two GC pairs embedded in an AT sequence. Among the numerous lexitropsins synthesised so far, imidizole lexitropsins display the most pronounced capacity for binding to GC-containing sequences. However, the lexitropsin strategy based on a 1:1 binding complex has led to minor groove binders with enhanced tolerance to GC base pairs in the binding site, but did not yield a purely GC specific molecule. The lexitropsin hypothesis took on a new direction with the discovery that the minor groove of DNA can expand to accommodate two distamycin molecules associated side-by-side in an antiparallel head-to-tail orientation. This development inspired the design of homo- and heterodimeric ligands. An imidazole-containing peptide (Figure 4.12) was found to bind specifically to GCGC sequences, the first minor groove binding lexitropsin to be directed uniquely to GC sites.[69]

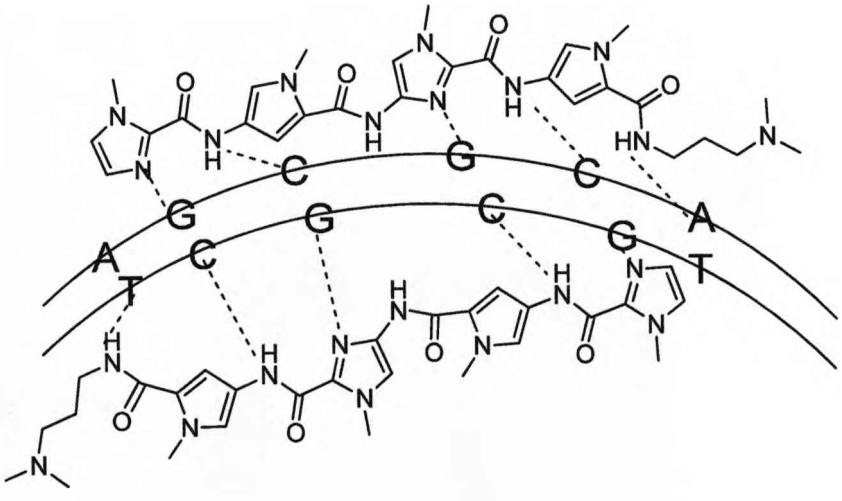

***Figure 4.12** A GC specific imidazole containing peptide.*

Members of a structural class known as the hairpin polyamides have demonstrated affinities and specificities for DNA comparable with transcription factors and other DNA binding regulatory proteins.[70] The hairpin polyamide has proved to be a very successful template in the synthesis of rationally designed ligands capable of tight and specific binding to a target sequence of double stranded DNA. Consisting of two covalently linked lexitropsins connected *via* an amino-butyric acid linker, anti-parallel pairing of imidazole opposite a pyrrole residue recognises a GC base pair, whereas the opposite combination recognises the CG pair.[71] Discrimination from TA and AT has been achieved by the use of a bulkier 3-hydroxypyrrole unit instead of the original pyrrole.

Discrimination apparently arises from destabilisation of interactions at the undesirable sequences *i.e.* position of the hydroxypyrrole opposite an adenine residue results in steric hinderance that destabilises polyamide binding.[72] The effect of a targeted polyamide on a biological system was first fully illustrated by an eight ring hairpin polyamide. The polyamide was shown to enter the nucleus of cultured frog fibroblast cells, target the binding site of transcription factor TFIIIA and specifically inhibit the transcription of the 5S RNA gene.[73]

4.3.2 Minor Groove Binders as a DNA Delivery System

4.3.2.1 Minor Groove Binding–Alkylating Conjugates

Alkylating agents have arisen as very effective clinical agents. Most alkylating drugs interact with DNA *via* formation of an electron deficient carbonium ion which then ungergoes electrophilic attack, thereby forming a covalent bond with the DNA target.

The nitrogen at position 7 (N7) on guanine, being strongly nucleophilic, is probably the main molecular target for alkylation in DNA. Bi-functionalised agents, having the ability to covalently bond at two points, can cause intra- or interstrand crosslinking, leading to disruption of transcription and replication.

However these compounds have also been shown to cause DNA damage in an unspecific manner, displaying toxicity to both neoplastic and normal tissues. In practise, unwanted effects are myelosuppression, nephrotoxicity, sterility and risk of non-lyphocytic leukaemia.[74]

With these incentives in mind, researchers have proposed that by tethering potent alkylating agents to a DNA delivery system, such as Nt and Dst, one can increase specificity for desired DNA targets, increase cytotoxicity and reduce adverse toxic effects. Early work focused on linkage of Dst and its tetrapyrrole homologue to different electrophilic moieties, where the formyl group was substituted for benzoyl nitrogen mustard, nitrogen mustard, halogenoacryloyl, and epoxycarbonyl functionalities. Many derivatives have proved substantially more cyctotoxic than the minor groove binders alone, often with a positive correlation between the number of pyrrole units and potency. This body of work has been comprehensively reviewed by Baraldi.[75]

A more specific SAR study was reported by both Baraldi[76,77] and Lown [78] where the number of pyrrole units tethered to the [2,1-*c*][1,4] benzodiazepine (PBD) moiety was compared with biological activity. Naturally occurring PBD-containing compounds, including anthramycin and DC-81, exert their alkylating activity *via* an N10-C11 carbinolamine/imine moiety, which covalently binds to the C-2 NH_2 of guanine residues in the minor groove (Figure 4.13).[79] X-ray crystallography and

DNA footprinting studies on covalent PBD-DNA adducts have shown a high specificity for G-C rich regions.

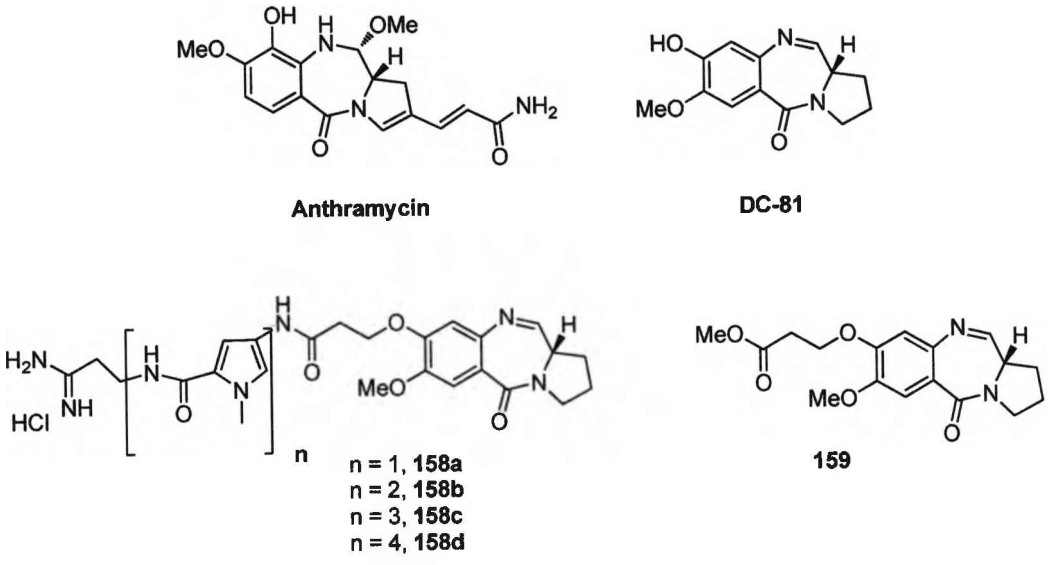

Figure 4.13 *PBD polypyrrole conjugates synthesised and tested by Baraldi.*

Novel hybrids consisting of one, two, three or four pyrrole units linked to PBD through a spacer arm were synthesised, and the structure activity relationship studied between the length of the carboxamide chain and antiproliferative activity. The antiproliferative activity of the hybrids **158a-d**, Dst and the PBD methyl ester **159** (Figure 4.13) was evaluated *in vitro* using both human chronic myeloid leukaemia K562 and T-lymphoblastoid Jurkat cell lines. A direct positive relationship was found between the number of pyrrole rings present in the hybrids and the antiproliferative effect of each hybrid. The hybrid consisting of the tetrapyrrole was found to be the most active hybrid both against K562 and Jurkat cell lines and displayed greater activity than PBD alone. The analogue incorporating the dipyrrole chain exhibited, to some extent, antiproliferative activity (but no improvement on

either parent compound) against the K562 cell line (IC_{50} = 6 μM), but was scarcely active on the Jurkat cell line (IC_{50} = 50 μM). Conclusions drawn were that an increased number of pyrrole rings increased the stability of the drug-DNA complex.

(+)-CC-1065 is a natural product of the class of cyclopropylindole (CPI) antitumour antibiotics and consists of a long chain, heterocyclic structural motif reminiscent of Dst. It imparts its biological activity through binding to B-DNA within the minor groove at AT rich sequences and selectively alkylates the N-3 position of 3'-adenine by its cyclopropylindole subunit.[80] Despite its high potency and broad spectrum of activity, (+)-CC-1065 was never developed clinically due to irreversible toxicity. Baraldi's group have previously developed two CPI analogues duplicating the left hand portion of (+)-CC-1065.[63] Conjugation with a pyrazole-polypyrrole unit **160a-f** (Figure 4.14) was proposed to increase the DNA specificity, affinity and water solubility of such an analogue.

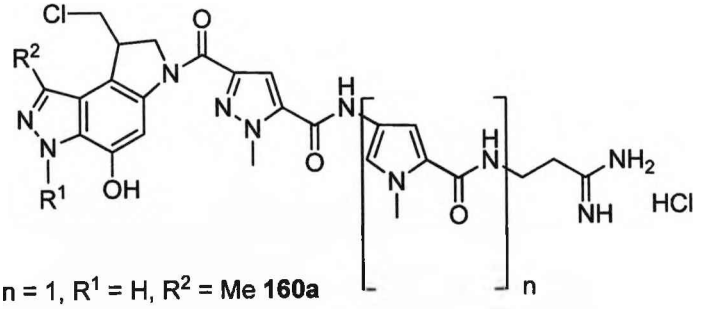

n = 1, R^1 = H, R^2 = Me **160a**
n = 2, R^1 = H, R^2 = Me **160b**
n = 3, R^1 = H, R^2 = Me **160c**
n = 1, R^1 = Bn, R^2 = H **160d**
n = 2, R^1 = Bn, R^2 = H **160e**
n = 3, R^1 = Bn, R^2 = H **160f**

Figure 4.14 *CPI pyrazole-polypyrrole conjugates synthesised and tested by Baraldi.*

Again the "longer" tripyrrole analogue **160c** proved to be the most active against five different cancer cell lines *in vitro* especially against T- and B-lymphoblast cells with IC_{50} values between 7.4 and 7.1 nM. Again for this series of hybrids, it is possible to correlate structure with biological activity, as increasing the number of pyrrole rings from one to three results in increased cyctotoxic activity.

Another aspect of the structure activity relationship was explored by Baraldi *et al* by varying linker length. Uramustine **162** (Figure 4.15), a clinically available alkylating agent, was tethered to the tripyrrole Dst, but in this case the linker length varied and the antiproliferative effect examined. A flexible polymethylene spacer was chosen, varying from one to six methylene units, allowing the nitrogen mustard of uramustine to interact more closely with the DNA target. All the hybrids showed enhanced activity compared to either parent compound when tested against the K562 human leukaemia cell line. Optimum activity was displayed when methylene units numbered six (IC_{50} = 0.07 μM).

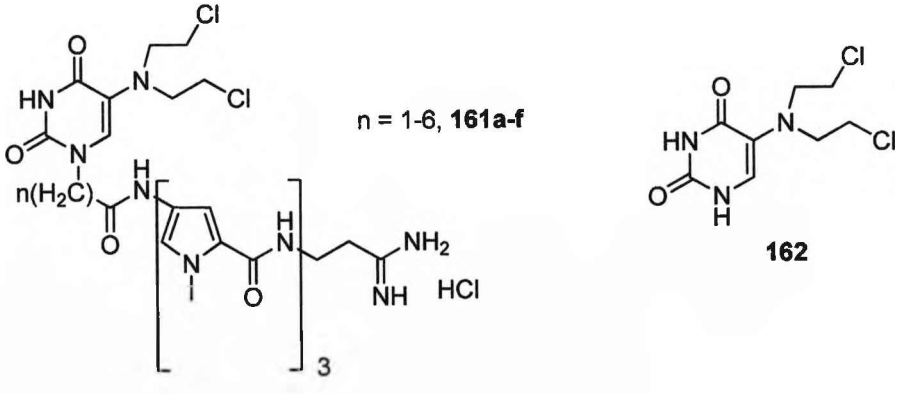

Figure 4.15 *Uramustine tripyrrole conjugates with varying linker length synthesised and tested by Baraldi.*

However, DNA footprinting studies on compounds **161a-f** (Figure 4.15) showed that progressive enhancement in cytotoxic potency with the length of polymethylene chain does not correspond to increased alkylation intensity and increased cytotoxicity may be attributed to increased cellular uptake.[81]

4.3.2.2 Linkage of Minor Grove Binders to Intercalating Agents: The Combilexins

Intercalating drugs are planar aromatic molecules that bind to DNA by insertion of the aromatic system between base pairs. This leads to extension of the DNA duplex and local unwinding and inhibition of enzymes involved in transcription. Many naturally occurring intercalators have been successfully developed into antitumour drugs and have been used clinically in cancer treatment.

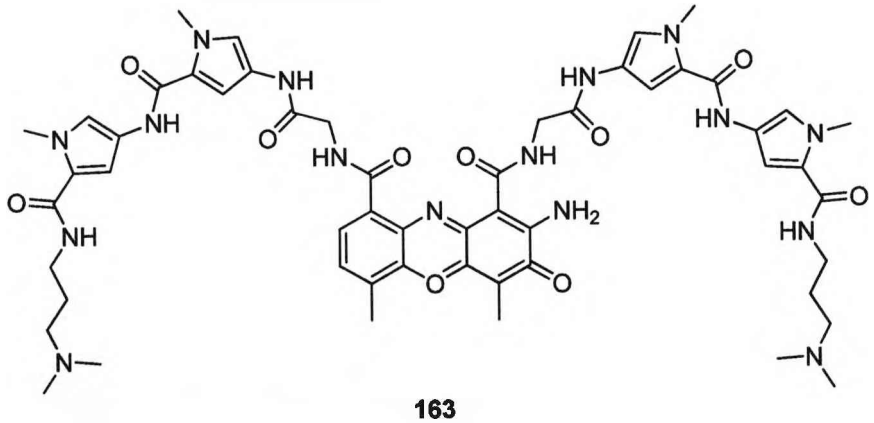

163

Figure 4.16 *An early combilexin. A phenoxazone chromophore fitted with polypyrrole units.*

In 1984 Krivtsora reported one of the earliest attempts to couple an intercalator with a minor groove binding portion in a series of "distactins".[60] Based on the structure and DNA binding mechanism of the natural product actinomycin D, a phenoxazone chromophore was fitted with mono-, di- or tripyrroles at positions 1 and 9 **163**

(Figure 4.16). A bidentate reaction with DNA was observed involving intercalation of the chromophore and successful minor groove interactions of the mono- and dipyrrole chains.

In 1988 Eliadis studied the effect of the variation of methylene spacers (2-, 3- and 4-carbon) of a series of 9-amino acridine-netropsin and -distamycin hybrids.[82] Lengthening of DNA was observed, consistent with the intercalative action of acridine. Dissociation of the ligand-DNA complex was 1000 times slower for the hybrid than for the acridine or minor groove binder alone, suggesting a cooperative binding to DNA. It was reported the optimum linker length in this case was a 3-carbon chain **164** (Figure 4.17).

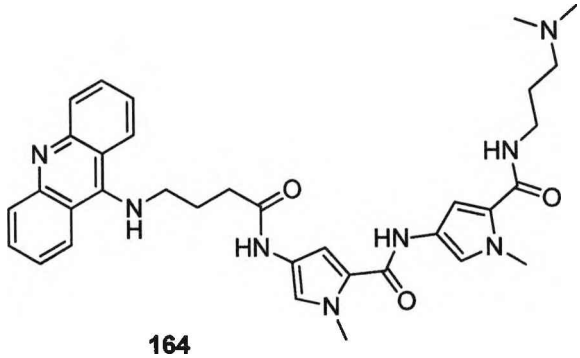

164

Figure 4.17 *Optimum spacer length in an SAR study of acridine-minor groove binder hybrids.*

An example of a combilexin with a rigid linker was the amscarine derivative **165** (Figure 4.18). Studies showed that the rigid linker did not permit optimal intercalation of the acridine and apparently slightly restricted the netropsin moiety from fitting deeply into the minor groove.[60] However despite this it is a potent topoisomerase II inhibitor and its interactions with DNA have been studied in depth

including its action as a threading intercalator when acridine is substituted at the 4-position.[83-86]

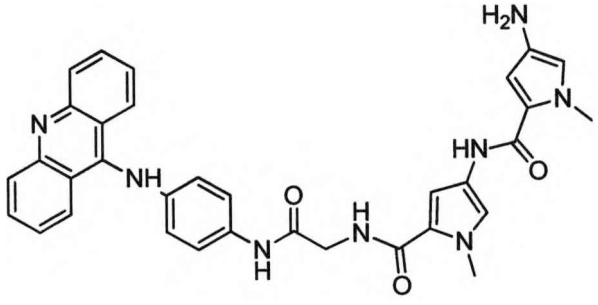

165

Figure 4.18 *An amsacrine-dipyrrole hybrid incorporating a rigid linker did not permit optimal DNA binding.*

More recently Hotzel reported on the synthesis of a series of intercalator-carboxamide hybrids, their cytotoxic activity, DNA binding affinity and topoisomerase inhibition profile.[87] In the initial study the intercalating portion (heterocycles and anthraquinone), the pyrrole terminus and the number of pyrrole units was varied. All the conjugates showed poor activity and DNA binding affinity. This highlighted the importance of the *N,N*-dimethylamine terminus of other powerful minor groove binding ligands which in this case had been substituted for methyl ester, carboxylic acid or propionitrile groups.

In a later study, the same intercalating agents were coupled to synthetic carboxamide chains where the *N,N*-dimethylamine terminal group was reinstated.[88] As expected the hybrids demonstrated good binding affinity confirming the importance of the electrostatic interactions formed between a positively charged terminal; an amidine group on Nt and Dst, and the *N, N*-dimethylamine group on the synthetic analogues.

In 2007 an in depth SAR study of a series of combilexins was carried out by David-Cordonnier and co-workers.[89] A flexible spacer at the *N*-terminal end of a pyrrole chain, varying in length, was linked to acridone, acridine and anthraquinone. The most active tended to be the acridone conjugates with the most active consisting only of the monopyrrole unit **166** (Figure 4.19). From DNA melting studies, the best DNA binding affinity was exhibited by those hybrids incorporating the dipyrrole chain. Interestingly in these studies there was not always a direct correlation between activity and binding affinity. In the case of the acridine combilexins, lengthening of the linker had a considerable effect on the binding affinity causing an increase in melt temperature; when the linker was 4-carbon, **167**, and 2-carbon atoms in length, T_m = 26 and 18 °C respectively (Figure 4.19).

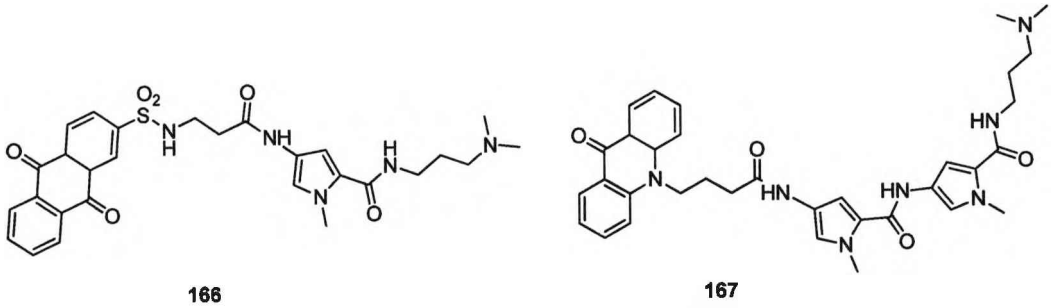

166 **167**

Figure 4.19 *An SAR study of combilexins show structure* ***166*** *with the most potent cytotoxic activity and structure* ***167*** *with strongest DNA binding affinity.*

4.3.2.3 Linkage of Minor Groove Binders to Free Radical-Generating Cytotoxic Agents

The AT specific, DNA delivery properties of Nt and Dst have also been exploited to enhance the activity of photosensitive and photoactivated DNA cleaving agents. The triggering of these agents by photons of light result in rearrangements that generate highly reactive radical species; oxy radicals, singlet oxygen, aryl radicals and Auger

electrons, reminiscent of the proposed DNA cleavage mechanism of artemisinin. Nt and its homologues have been previously conjugated to quinones, *p*-nitrobenzoyls, bromofurans, benzylsulphonamido groups and platinum to form photosensitive hybrids.[60]

Isoalloxazine is photoactivated in the presence of molecular oxygen, whereupon the flavin chromophore oxidises and generates oxy radicals capable of causing DNA breaks. Synthesis and biological testing on 5'-end-labeled DNA fragments, of an isoalloxazine-netropsin hybrid **168** (Figure 4.20), showed single-strand breaks at specific loci and a double-strand break at a specific locus in AT regions.[90] This showed an asymmetric binding mode in one orientation and properties similar to a restriction endonuclease.

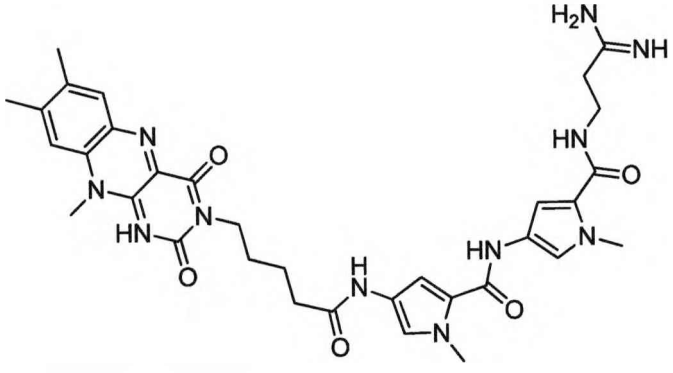

168

Figure 4.20 *Isoalloxazine-netropsin hybrid synthesised by Herfeld.*

Photoinduced DNA cleavage has been reported with oligo-*N*-methylpyrrolecarboxamide derivatives substituted with a benzylsulfonamido group such as the *p*-chlorobenzenesulfonamide-polypyrrole hybrid **169** (Figure 4.21). In this case, the efficiency of single-strand cleavage under UV-A irradiation clearly

depends on the length of the pyrrolecarboxamide chain. Tetrapyrrolesulfonamide conjugates are more efficient DNA cleavers than the corresponding analogues containing three or two pyrrole units, and conjugates with only one pyrrole are practically inactive.[91]

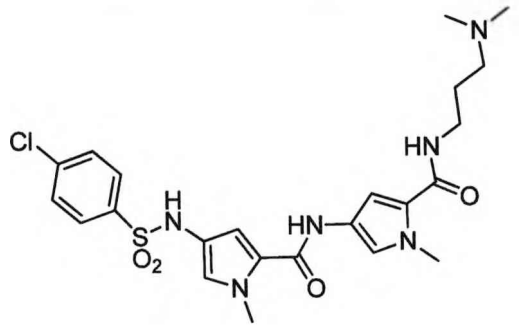

169

Figure 4.21 *p-Chlorobenzenesulphonamido-polypyrrole conjugate.*

Diazenes, based on DNA cleavage agents trimethylenemethane (TMM), can form diyl radicals upon activation either thermally or photochemically. Bregant *et al.* synthesised the diazine-dipyrrole hybrid **170** which upon irradiation forms diyl **171** (Figure 4.22).[92]

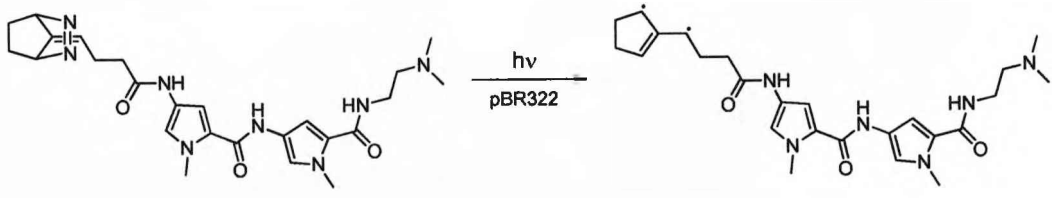

170 **171**

Figure 4.22 *Photochemical activation of diazene-netropsin hybrid to Diyl radical-netropsin hybrid.*

Activation in the presence of restriction fragments of pBR322 DNA showed that TMM diyls are capable of cutting DNA, with specificity for AT rich tracts facilitated by netropsin.

4-Bromoacetophenones, under photoinduced C-X bond cleavage, generate monophenyl radicals capable of H-atom abstraction and have therefore been presented as a photoactivated DNA cleavage agent (Figure 4.23). A series of 4-bromoacetophenone analogues incorporating carboxamide chains of various length (n = 1-3) **172a-c** were synthesised and tested for DNA cleavage potency using supercoiled DNA.[93]

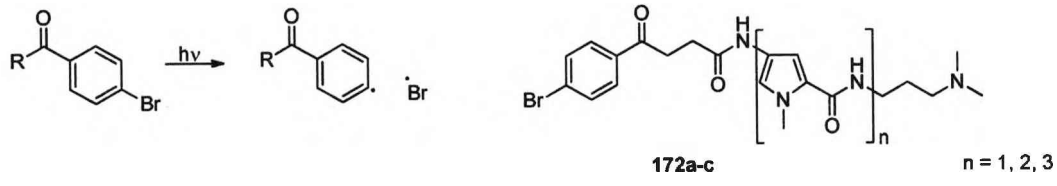

Figure 4.23 *Bromoacetophenone-carboxamide hybrids display DNA cleavage activity via photoinduced formation of monophenyl radicals.*

Again an increased number of pyrrole units resulted in an increase in DNA cleavage potency. The tripyrrole analogue demonstrated nicked and linear DNA at micromolar concentrations (3 and 20 μM respectively) compared to the millimolar concentrations of the parent compound needed for a comparable effect. DNA footprinting studies also showed a preference for cleavage at AT-rich tracts.

4.3.2.4 Linkage of Minor Groove Binders to Enediyne Free Radical Generating Agents

A large body of research has collected surrounding the development of enediyne-minor groove binding hybrids. The enediyne class of natural products were first defined in the 1980s with the discovery of calicheamicin **173**, isolated from *Micomonaspora echinospora* ssp.*calichensis* (Figure 4.24).[94]

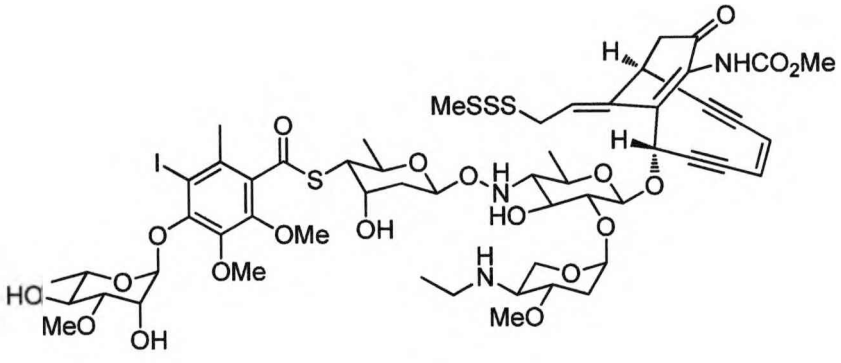

173

Figure 4.24 *Natural enediyne calicheamicin.*

These natural products have shown remarkable biological activity including high antibacterial activity and extreme potency against murine tumors such as P388 and L1210 leukemias and solid neoplasms such as colon 26 and B16 melanoma with optimal doses of 0.15-5 μg/kg. The enediyne antibiotics are believed to exert their biological activity by acting as highly potent DNA cleaving agents giving rise to sequence-selective double-strand cuts. This class of compound exert their cytotoxic activity by rearrangement of the enediyne moiety *via* Bergman cyclisation to form a reactive 1,4-benzeneoid diradical species (Figure 4.25).

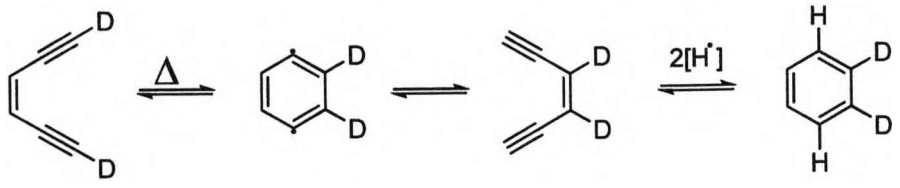

Figure 4.25 *The Bergman thermal cycloaromatisation reaction.*

In nature the cyclisation and subsequent radical formation is believed to be triggered by the trisulfide functionality situated in close proximity to the enediyne "warhead". A nucleophile (*e.g.*, glutathione or DNA) attacks the central sulfur atom of the trisulfide group, causing the formation of a thiolate or a thiol which adds intramolecularly to the adjacent α,β-unsaturated ketone. This change in structural geometry imposes strain on the 10-membered enediyne ring which is subsequently relieved by undergoing the Bergman reaction. The calicheamicin diradical abstracts hydrogen atoms from duplex DNA leading to double strand cleavage. Remarkably, naturally occurring calicheamicin is ready fitted with a minor groove binding element in the form of the aryloligosaccharide chain extending from the enediyne portion. This series of ring structures bind tightly to the minor groove of B-DNA and display high specificity for sequences such as 5'-TCCT-3' and 5'-TTTT-3'.

Inspired by this natural molecular architecture, giving potent and specific DNA cleavage properties, a number of research groups have designed and synthesised hybrids incorporating enediyne model systems and DNA delivery systems such as Nt and Dst.

Tokuda *et al.*[95] hoped to improve the DNA cleaving abilities of previously synthesised neocarzinostatin chromophore analogues **174** and **175**, by conjugation to a DNA-binding group (Figure 4.26). Synthesis of an enediyne-netropsin hybrid **176**

followed, *via* amide coupling of an activated ester intermediate with the netropsin amine previously synthesised by Shibuya's method.[96] Diradical production and subsequent aromatisation of the hybrid was triggered *in vitro* by addition of 3 equivalents of thioglycolate in methanol. DNA cleavage studies showed that the hybrid **176** cleaved the covalently closed supercoiled pBR322 DNA to the open circular DNA and the linear form more effectively than the neocarzinostatin chromophore alone. These results demonstrate the importance of the minor groove binder portion, delivering the radical source to the desired biological target.

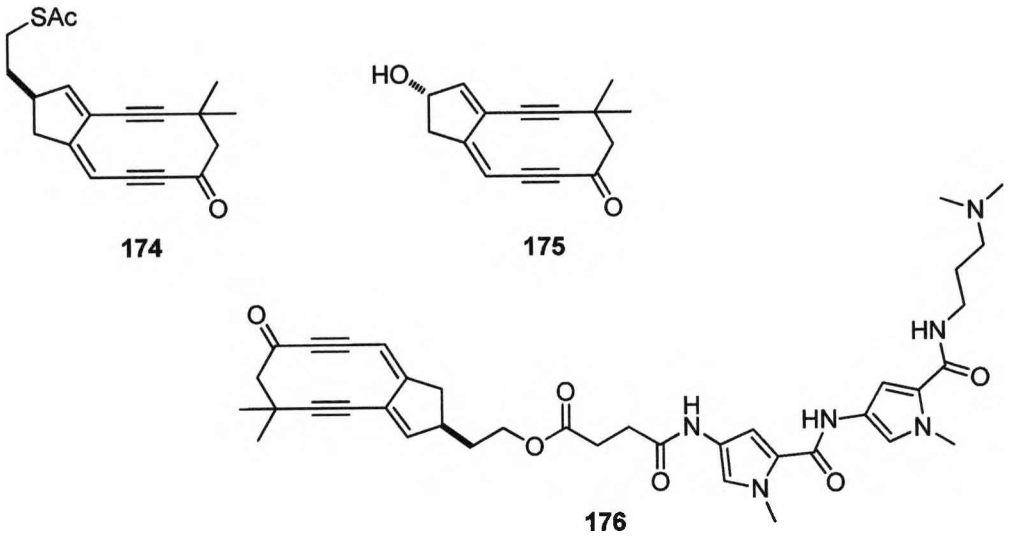

Figure 4.26 *Neocarzinostatin analogues **174**, **175** and enediyne-netropsin hybrid **176**.*

Similarly, Wittman *et al.* hoped to improve the cytotoxic activity of simplified, synthetic enediynes such as **177**, by incorporation of a carboxamide chain **178** (Figure 4.27).[97] Molecular modelling studies of calicheamicin **173** (Figure 4.24) suggested that the hydroxylamino saccharide, adjacent to the enediyne portion, acts as a scaffold-linker, directing the remaining saccharide chain to interact with the

minor groove. Based on these studies, Wittman hypothesised that insertion of a rigid spacer unit between the enediyne and carboxamide chain would perform a similar role. The minor groove binding element would be allowed to fit closely to the floor of the minor groove while still preserving an optimal position for the enediyne portion to facilitate strand cleavage. A benzylic imidate with a *p*-methyl ester was used for a rigid linker, enabling ether formation with the propargylic alcohol of the enediyne and amide coupling with the carboxamide amine respectively.

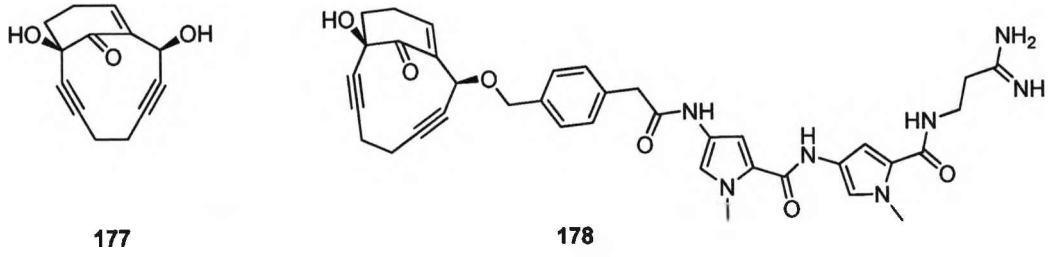

177 **178**

Figure 4.27 *Synthetic enediyne **177** and enediyne-netropsin hybrid **178** with benzylic linker.*

It was found that the addition of a binding domain improved the DNA cleavage potency 100 fold but an increase in cytotoxicity against HCT-116 human colon cancer cell lines was not observed. The hybrid was also inactive *in vivo* up to the tolerated dose. A possible explanation for the lack of correlation in the data was that enediyne **177** has been shown to damage cellular proteins. By directing the synthetic enediyne to the DNA site, it had in fact eliminated its activity towards its actual cellular targets. Despite the queries raised by this publication, the remarkable increase in DNA binding affinity provided by the carboxamide chain again confirms its function as a potent DNA delivery system.

Semmelhack *et al.* synthesised two enediyne-netropsin hybrids with acetate and crontonate linkers (Figure 4.28).[98] The synthetic enediyne **179** studied displayed

single strand DNA cleavage and was found to be 7×10^{-4} less potent than the natural product calicheamicin when the concentration needed to cause 50% DNA cleavage was compared. The acetate linked enediyne-netropsin hybrid **180** was synthesised *via* formation of the enediyne carboxylic acid and subsequent amide coupling with the dipyrrole amine using DMAP and DCC.

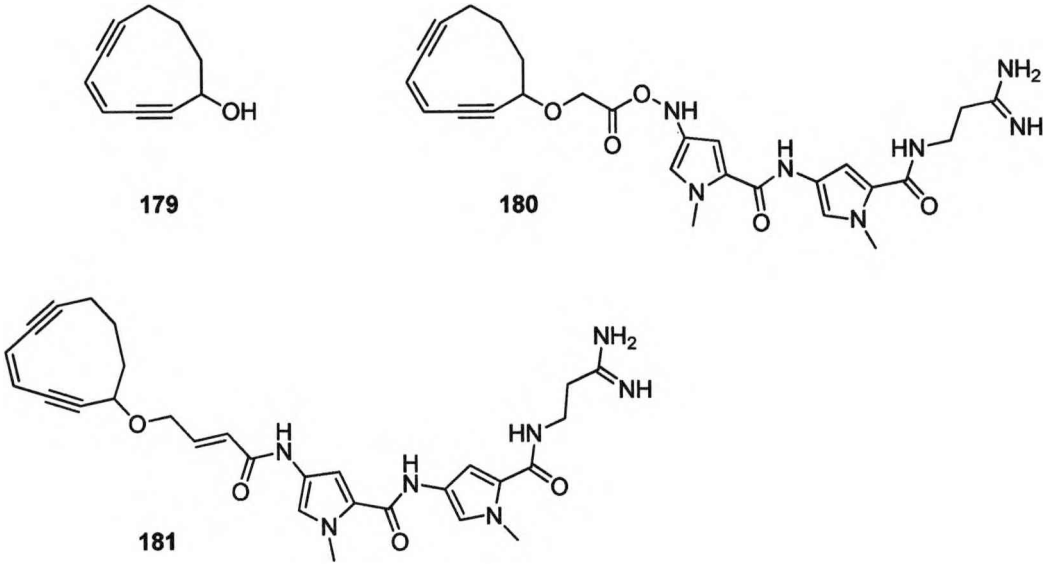

Figure 4.28 *Synthetic enediyne **179**, enediyne-Nt hybrid with acetate tether **180** and enediyne-Nt hybrid with crotonate tether **181**.*

However, CD (circular dichroism) spectroscopy showed that hybrid **180** binds weakly compared to netropsin and the dipyrrole amine intermediate. Again molecular modelling studies, carried out by Semmelhack, shed some light on this result.[98] The molecular modelling showed that with the short acetate tether, it is difficult for the dipyrrole to simultaneously form H-bonding and van der Waals interactions with the minor groove while orientating the enediyne into the minor groove. Steric interactions repulse the enediyne away from the minor groove so effectively "holding" back the pyrrole from interacting with the minor groove.

Correspondingly, it was also confirmed by molecular modelling, that having a longer tether would allow for the simultaneous placement of both parts of the hybrid.

To this end, a hybrid with a crotonate tether **181** was synthesised. The enediyne-alcohol was treated with the triflate of methyl 4-hydroxycrotonate ester. Subsequent hydrolysis of the ester and amide coupling with the dipyrrole chain afforded the desired hybrid. CD studies indicated that the hybrid **181** bound strongly to AT tracts. DNA cleavage studies showed that the hybrid was 2000-fold more potent than the enediyne alone and only 40-fold less potent than the natural enediyne calicheamicin. Compared to the cleavage efficiency of the acetate linked hybrid **180**, the crotonate analogue **181** is 150-fold more potent.

Propargyl sulfones are small synthetic molecules that mimic the chemical action of enediynes by cleaving DNA in a pH-dependent fashion. Xie *et al.* have synthesised and demonstrated the DNA cleavage ability of a series of propargyl sulfone-carboxamide hybrids **182a-c** (Figure 4.29).[99]

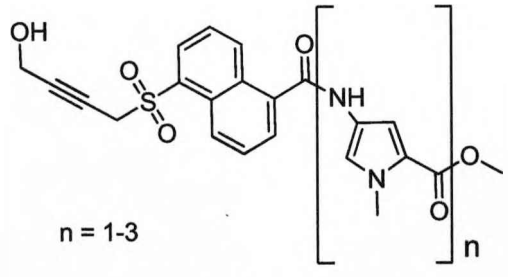

182a-c

Figure 4.29 *Propargyl sulphone-carboxamide hybrids.*

More recently, Banfi and co-workers have synthesised lactenediyne-carboxamide conjugates in an effort to achieve double-strand cutting efficiency comparable to that

of calicheamicin.[100] The Banfi group have previously designed and studied an enediyne prodrug class, the lactenediynes, which can be characterised by the fusion of a β-lactam with a cyclodeca-3-ene-1,5-diyne **183** (Figure 4.30).

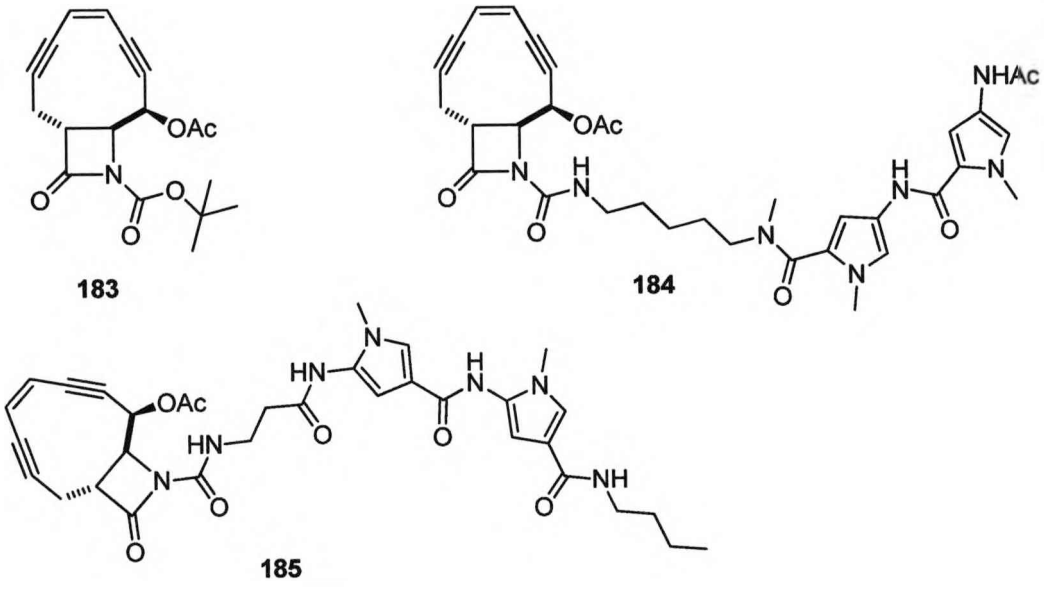

Figure 4.30 *Synthetic lactenediyne warhead **183**, 5-carbon tethered netropsin-hybrid **184** and 2-carbon tethered netropsin hybrid **185**.*

In this system the role of the lactam is as a "safety catch", completely suppressing cycloaromatisation of the enediyne. Opening of the β-lactam ring by hydrolysis, unfastens the warhead so leading to the typical diradical species. One of the main motivations of this research is the high potency of calicheamicin diplayed by its ability to cause double strand cleavage of plasmid DNA, preferring this cleavage mode to single strand breaks in a 2:1 ratio.[101] This ability, rarely observed in cyctotoxic agents (*e.g.* bleomicin has a ratio of 1:9), leads to apoptosis in cells. The warhead of calicheamicin, when isolated from its saccharide binding domain, has shown a single to double strand break ratio of 30:1, indicating the remarkable influence of the oligosaccharide. The studied lactenediynes, such as **183** displayed a

ratio of 1:15 single- to double-strand breaks, so it was hoped to improve this ratio by addition of either a carboxamide or naphthyl moiety.

The desired carboxamide chain was tethered to the lactenediyne *via* 2- and 5-carbon linkers, **185** and **184**, through the nitrogen of the β-lactam ring. Analogue **185** showed remarkable cleavage efficiency with a double to single strand cleavage ratio of 1:6 which, it is claimed, ranks them among the most effective simplified artificial enediynes synthesised so far.

However, the expected increase in potency of these hybrids when compared to the natural parent compound calicheamicin has not been satisfied. A possible reason for this is that the enediyne "warhead" requires a very precise docking position onto DNA in order to facilitate efficient cleavage.

In summary, the majority of SAR studies exploring novel Nt and Dst hybrids find that an increased number of pyrrole units leads to an increase in efficacy.[75] Linker length and flexiblility is another variable SAR subject. In the case of uramustine hybrids, the longer linker gave increased potency, but this could be attributed to increased lipophilicity.[81] Through CD experiments and molecular modelling, Semmelhack attributed a short acetate linker with poor cleavage and binding, and found a longer crotonate tether much more potent.[98] A rigid linker was also proposed as a key element such as that found in the potent natural product calicheamicin.[97]

4.4 Strategies for Artemisinin-Minor Groove Binding Conjugates

In the search for potent and selective antitumor agents, the development of an artemisinin-polypyrrole hybrid is an interesting route to examine. Artemisinin displays a remarkable selectivity for rapidly proliferating cancerous cells, and has

recently been shown to induce DNA damage. Coupling this selectivity with an agent that can deliver artemisinin to the DNA target could afford a compound with unique properties. These hybrids also have the potential for excellent antimalarial potency. The coincidence of the high affinity of the minor groove binders for AT rich regions, and high AT composition of *P. falciparum* renders these hybrids ideal for specific antimalarial activity.

4.5 Summary

1) As well as antimalarial activity, artemisinin also demonstrates potent activity and selectivity toward cancerous cells. Selectivity is conferred by the high iron content of cancer cells facilitating activation of the artemisinin peroxide bridge.
2) Netropsin and distamycin, isolated from bacteria, are naturally occurring oligopeptidic pyrrole chains that demonstrate: a) reversible binding (H-bonding and ionic interactions) at the minor groove of DNA, specifically at A and T rich tracts, and b) an inhibitory effect on microorganisms and DNA-viruses.
3) Netropsin and distamycin have a potent and specific antiprotazoal effect towards *P. falciparum*. Specificity is imparted by the AT rich DNA of the malaria parasite (80%) compared to man (59%). Proposed targets are the inhibition of DNA helicases.
4) Analogues of netropsin and distamycin, termed lexitropsins, have been "programmed" to bind to specific DNA sequences including G and C tracts.
5) Analogues of netropsin and distamycin have been exploited as DNA delivery units and through coupling to other cytotoxic agents (alkylating agents, intercalators, free radical generating agents) minor groove binding hybrids have been synthesised.
6) SAR studies of these hybrids identify: a) an increased number of pyrrole units lead to an increase in cytotoxic activity and DNA binding affinity and b) that the length and flexibility of the linker joining the hybrid units affects activity and DNA binding affinity.

4.6 References

(1) Woerdenbag, H. J., Moskal, T. A., Pras, N., Malingre, T. M., El-Feraly, F. S., Kampinga, H. H., Konings, A. W. T., *J. Nat. Prod.* **1993**, *56*, 849-856.

(2) Beekman, A. C., Woerdenbag, H. J., Kampinga, H. H., Konings, A. W. T., *Phytother. Res.* **1996**, *10*, 140-144.

(3) Beekman, A. C., Barentsen, A. R. W., Woerdenbag, H. J., Van Uden, W., Pras, N., Konings, A. W. T., El-Feraly, F. S., Galal, A. M., Wikstrom, H. V., *J. Nat. Prod.* **1997**, *60*, 325-330.

(4) Posner, G. H., Ploypradith, P., Hapangama, W., Wang, D., Cumming, J. N., Dolan, P., Kensler, T. W., Klinedinst, D., Shapiro, T. A., Qun Yi, Z., Murray, C. K., Pilkington, L. G., Jayasinghe, L. R., Bray, J. F., Daughenbaugh, R., *Bioorg. Med. Chem.* **1997**, *5*, 1257-1265.

(5) Posner, G. H., Ploypradith, P., Parker, M. H., O'Dowd, H., Woo, S., Northrop, J., Krasavin, M., Dolan, P., Kensler, T. W., Xie, S., Shapiro, T. A., *J. Med. Chem.* **1999**, *42*, 4275-4280.

(6) Posner, G. H., Northrop, J., Paik, I., Borstnik, K., Dolan, P., Kensler, T. W., Xie, S., Shapiro, T. A., *Bioorg. Med. Chem.* **2002**, *10*, 227-232.

(7) Posner, G. H., Paik, I., Sur, S., McRiner, A. J., Borstnik, K., Xie, S., Shapiro, T. A., *J. Med. Chem.* **2003**, *46*, 1060-1065.

(8) Posner, G. H., McRiner, A. J., Paik, I., Sur, S., Borstnik, K., Xie, S., Shapiro, T. A., Alagbala, A., Foster, B., *J. Med. Chem.* **2004**, *47*, 1299-1301.

(9) Jeyadevan, J. P., Bray, P. G., Chadwick, J., Mercer, A. E., Byrne, A., Ward, S. A., Park, B. K., Williams, D. P., Cosstick, R., Davies, J., Higson, A. P., Irving, E., Posner, G. H., O'Neill, P. M., *J. Med. Chem.* **2004**, *47*, 1290-1298.

(10) Galal, A. M., Gul, W., Slade, D., Ross, S. A., Feng, S., Hollingshead, M. G., Alley, M. C., Kaur, G., ElSohly, M. A., *Bioorg. Med. Chem.* **2009**, *17*, 741-751.

(11) Chadwick, J., Mercer, A. E., Park, B. K., Cosstick, R., O'Neill, P. M., *Bioorg. Med. Chem.* **2009**, *17*, 1325-1338.

(12) Jung, M., Lee, S., Ham, J., Lee, K., Kim, H., Kim, S. K., *J. Med. Chem.* **2003**, *46*, 987-994.

(13) Mercer, A. E., Maggs, J. L., Sun, X., Cohen, G. M., Chadwick, J., O'Neill, P. M., Park, B. K., *J. Biol. Chem.* **2007**, *282*, 9372-9382.

(14) May, W. S., Cuatrecasas, P., *J. Membrane Biol.* **1985**, *88*, 205-215.

(15) Lai, H., Singh, N. P., *Cancer Lett.* **1995**, *91*, 41-46.

(16) Moore, J. C., Lai, H., Li, J., Ren, R., McDougall, J. A., Singh, N. P., Chou, C., *Cancer Lett.* **1995**, *98*, 83-87.

(17) Singh, N. P., Lai, H., *Life Sciences* **2001**, *70*, 49-56.

(18) Sadava, D., Phillips, T., Lin, C., Kane, S. E., *Cancer Lett.* **2002**, *179*, 151-156.

(19) Lai, H., Sasaki, T., Singh, N. P., Messay, A., *Life Sciences* **2005**, *76*, 1267-1279.

(20) Wang, J., Guo, Y., Zhang, B., Chen, Z., Gao, J., *Pharmacology* **2007**, *80*, 207-208.

(21) Li, Y., Shan, F., Wu, J., Wu, G., Ding, J., Xiao, D., Yang, W., Atassi, G., Léonce, S., Caignard, D., Renard, P., *Bioorg. Med. Chem. Lett.* **2001**, *11*, 5-8.

(22) Efferth, T., Olbrich, A., Bauer, R., *Biochem. Pharma.* **2002**, *64*, 617-623.

(23) Hou, J., Wang, D., Zhang, R., Wang, H., *Clin. Cancer Res.* **2008**, *14*, 5519-5530.

(24) Efferth, T., Oesch, F., *Biochem. Pharma.* **2004**, *68*, 3-10.

(25) Anfosso, L., Efferth, T., Albini, A., Pfeffer, U., *Pharmacogenomics J.* **2006**, *6*, 269-278.

(26) Wang, J., Zhang, B., Guo, Y., Li, G., Xie, Q., Zhu, B., Gao, J., Chen, Z., *Pharmacology* **2008**, *82*, 148-155.

(27) Li, P. C. H., Lam, E,. Roos, W. P., Zdzienicka, M. Z., Kaina, B., Efferth, T., *Cancer Res.* **2008**, *68*, 4347-4351.

(28) Finlay, A. C., Hochstein, F. A., Sobin, B. A., Murphy, F. X., *J. Am. Chem. Soc.* **1951**, *73*, 341-343.

(29) Zimmer, C., Wähnert, U., *Prog. Biophys. Mol. Biol.* **1986**, *47*, 31-112.

(30) Arcamone, F., Bizioli, F., Canevazzi, G., Grein, A., In *German Patent* 1958; Vol. 1, p 667.

(31) Arcamone, F., Bizioli, F., Canevazzi, G., Grein, A., *Chem. Abs.* **1961**, *55*, 2012.

(32) Lombardi, P., Crisanti, A., *Pharmacol. Therapeutics* **1997**, *76*, 125-133.

(33) Arcamone, F., Penco, S., Orezzi, P., Nicolella, V., Pirelli, A., *Nature* **1964**, *203*, 1064-1065.

(34) Berman, H. M., Neidle, S., Zimmer, C., Thrum, H., *Biochim. Biophys. Acta.* **1979**, *561*, 124-131.

(35) Gurskaya, G. V., Grokhovsky, S. L., Zhuze, A. L., Gottikh, B. P., *Biochim. Biophys. Acta.* **1979**, *563*, 336-342.

(36) Chandra, P., Zimmer, C., Thrum, H., *FEBS Lett.* **1970**, *7*, 90-94.

(37) Zimmer, C., Reinert, K. E., Luck, G., Wähnert, U., Löber, G., Thrum, H., *J. Mol. Biol.* **1971**, *58*, 329-348.

(38) Krey, A. K., Hahn, F. E., *FEBS Lett.* **1970**, *10*, 175-178.

(39) Zimmer, C., Luck, G., *FEBS Lett.* **1970**, *10*, 339-342.

(40) Luck, G., Triebel, H., Waring, M., Zimmer, C., *Nucl. Acids Res.* **1974**, *1*, 503-530.

(41) Wartell, R. M., Larson, J. E., Wells, R. D., *J. Biol. Chem.* **1974**, *249*, 6719-6731.

(42) Kopka, M. L., Yoon, C., Goodsell, D., Pjura, P., Dickerson, R. E., *Proc. Natl. Acad. Sci. USA.* **1985**, *82*, 1376-1380.

(43) Drew, H. R., Wing, R. M., Takano, T., Broka, C., Tanaka, S., Itakura, K., Dickerson, R. E., *Proc. Natl. Acad. Sci. USA.* **1981**, *78*, 2179-2183.

(44) Wing, R., Drew, H., Takano, T., Broka, C., Tanaka, S., Itakura, K., Dickerson, R., *Nature* **1980**, *287*, 755-758.

(45) Patel, D. J. *Proc. Natl. Acad. Sci. USA.* **1982**, *79*, 6424-6428.

(46) Klevit, R. E., Wemmer, D. E., Reid, B. R., *Biochemistry* **1986**, *25*, 3296-3303.

(47) Kopka, M. L., Yoon, C., Goodsell, D., Pjura, P., Dickerson, R. E., *J. Biol. Chem.* **1985**, *183*, 553-563.

(48) Coll, M., Frederick, C. A., Wang, A. H. J., Rich, A., *Proc. Natl. Acad. Sci. USA.* **1987**, *84*.

(49) Pelton, J., Wemmer, D., *J. Am. Chem. Soc.* **1990**, *112*, 1393-1399.

(50) Taberno, L., Verdaguer, N., Coll, M., Fita, I., van der Marel, G. A., van Boom, J. H., Rich, A., Aymami, J., *Biochemistry* **1993**, *32*, 8403-8410.

(51) Coll, M., Aymami, J., Van der Marel, G. A., Van Boom, J. H., Rich, A., Wang, A. H. J., *Biochemistry* **1989**, *28*, 310-320.

(52) Fagan, P., Wemmer, D. E., *J. Am. Chem. Soc.* **1992**, *114*, 1080-1081.

(53) Ginsburg, H., Nissani, E., Krugliak, M., Williamson, D. H., *Mol. Biochem. Parasit.* **1993**, *58*, 7-15.

(54) Lee, S., Inselburg, J., *J. Parasitol.* **1993**, *79*, 780-782.

(55) Pradhan, A., Tuteja, R., *FEBS J.* **2006**, *273*, 3545-3556.

(56) Pradhan, A., Hussain, E. M., Tuteja, R., *Gene* **2008**, *420*, 66-75.

(57) George, J. W., Ghate, S., Matson, S. W., Besterman, J. M., *J. Biol. Chem.* **1992**, *267*, 10683-10689.

(58) Bachur, N. R., Yu, F., Johnson, R., Hickey, R., Wu, Y., Malkas, L., *Mol. Pharmacol.* **1992**, *41*, 993-998.

(59) Brosh, R. M., Karow, J. K., White, E. J., Shaw, N. D., Hickson, I. D., Bohr, V. A., *Nucl. Acids Res.* **2000**, *28*, 2420-2430.

(60) Bailly, C., Chaires, J. B., *Bioconjug. Chem.* **1998**, *9*, 513-538.

(61) Youngquist, R. S., Dervan, P. B., *Proc. Natl. Acad. Sci. USA.* **1985**, *82*, 2565-2569.

(62) Dervan, P. B. *Science* **1986**, *232*, 464-471.

(63) Baraldi, P. G., Preti, D., Fruttarolo, F., Tabrizi, M. A., Romagnoli, R., *Bioorg. Med. Chem.* **2007**, *15*, 17-35.

(64) Goodsell, D., Dickerson, R. E., *J. Med. Chem.* **1986**, *29*, 727-733.

(65) Filipowsky, M. E., Kopka, M. L., Brazil-Zison, M., Lown, J. W., Dickerson, R. E., *Biochemistry* **1996**, *35*, 15397-15410.

(66) Blaskó, A., Bruice, T. C., *Proc. Natl. Acad. Sci. USA.* **1993**, *90*, 10018-10022.

(67) Xue, T., Browne, K. A., Bruice, T. C., *Bioconjug. Chem.* **1995**, *6*, 82-87.

(68) Bruice, T. C., Sengupta, D., Blaskó, A., Chiang, S. Y., Beerman, T. A., *Bioorg. Med. Chem.* **1997**, *5*, 685-692.

(69) Geierstanger, B. H., Mrksich, M., Dervan, P. B., Wemmer, D. E., *Science* **1994**, *266*, 646-650.

(70) Geierstanger, B. H., Mrksich, M., Dervan, P. B., Wemmer, D. E., *Nat. Struct. Mol. Biol.* **1996**, *3*, 321-324.

(71) Kielkopf, C. L., Baird, E. E., Dervan, P. B., Rees, D. C., *Nat. Struct. Mol. Biol.* **1998**, *5*, 104-109.

(72) White, S., Szewczyk, J. W., Turner, J. M., Baird, E. E., Dervan, P. B., *Nature* **1998**, *391*, 468-471.

(73) Gottesfeld, J. M., Neely, L., Trauger, J. W., Baird, E. E., Dervan, P. B., *Nature* **1997**, *387*, 202-205.

(74) Rang, H. P., Dale, M. M., Ritter, J. M., Moore, P. K., *Pharmacology*; Fifth ed.; Churchill Livingstone, 2003.

(75) Baraldi, P. G., Bovero, A., Fruttarolo, F., Preti, D., Tabrizi, M. A., Pavani, M. G., Romagnoli, R., *Med. Res. Rev.* **2004**, *24*, 475-528.

(76) Baraldi, P. G., Cacciari, B., Guiotto, A., Leoni, A., Romagnoli, R., Spalluto, G., Mongelli, N., Howard, P. W., Thurston, D. E., Bianchi, N., Gambari, R., *Bioorg. Med. Chem. Lett.* **1998**, *8*, 3019-3024.

(77) Baraldi, P. G., Balboni, G., Cacciari, B., Guiotto, A., Manfredini, S., Romagnoli, R., Spalluto, G., Thurston, D. E., Howard, P. W., Bianchi, N., Rutigliano, C., Mischiati, C., Gambari, R., *J. Med. Chem.* **1999**, *42*, 5131-5141.

(78) Damayanthi, Y., Praveen Reddy, B. S., Lown, J. W., *J. Org. Chem.* **1999**, *64*, 290-292.

(79) Thurston, D. E., Bose, D. S., *Chem. Rev.* **1994**, *94*, 433-465.

(80) Reynolds, V. L., Molineux, I. J., Kaplan, D. J., Swenson, D. H., Hurley, L. H., *Biochemistry* **1985**, *24*, 6228-6237.

(81) Baraldi, P. G., Romagnoli, R., Guadix, A. E., Pineda de las Infantas, M. J., Gallo, M. A., Espinosa, A., Martinez, A., Bingham, J. P., Hartley, J. A., *J. Med. Chem.* **2002**, *45*, 3630-3638.

(82) Eliadis, A., Phillips, D. R., Reiss, J. A., Skorobogaty, A., *J. Chem. Soc., Chem. Commun.* **1988**, 1049-1052.

(83) Fosse, P., Rene, B., Saucier, J., Henichart, J., Waring, M. J., Colson, P., Houssier, C., Bailly, C., *Biochemistry* **2002**, *33*, 9865-9874.

(84) Bailly, C., Collyn-d'Hooghe, M., Lantoine, D., Fournier, C., Hecquet, B., Fosse, P., Saucier, J., Colson, P., Houssier, C., Hénichart, J., *Biochem. Pharm.* **1992**, *43*, 457-466.

(85) Rene, B., Fosse, P., Khelifa, T., Jacquemin-Sablon, A., Bailly, C., *Mol. Pharmacol.* **1996**, *49*, 343-350.

(86) Bourdouxhe-Housiaux, C., Colson, P., Houssier, C., Waring, M. J., Bailly, C., *Biochemistry* **1996**, *35*, 4251-4264.

(87) Hotzel, C., Marotto, A., Pindur, U., *Eur. J. Med. Chem.* **2002**, *37*, 367-378.

(88) Hotzel, C., Marotto, A., Pindur, U., *Eur. J. Med. Chem.* **2003**, *38*, 189-197.

(89) David-Cordonnier, M., Hildebrand, M., Baldeyrou, B., Lansiaux, A., Keuser, C., Benzschawel, K., Lemster, T., Pindur, U., *Eur. J. Med. Chem.* **2007**, *42*, 752-771.

(90) Bouziane, M., Ketterle, C., Helissey, P., Herfeld, P., Le Bret, M., Giorgi-Renault, S., Auclair, C., *Biochemistry* **1995**, *34*, 14051-14058.

(91) Matsumoto, T., Sakai, Y., Toyooka, K., Shibuya, M., *Heterocycles* **1992**, *33*.

(92) Bregant, T. M., Groppe, J., Little, R. D., *J. Am. Chem. Soc.* **1994**, *116*, 3635-3636.

(93) Jeon, R., Wender, P., *Arch. Pharmacol. Res.* **2001**, *24*, 39-43.

(94) Nicolaou, K. C., Smith, A. L., Yue, E. W., *Proc. Natl. Acad. Sci. USA.* **1993**, *90*, 5881-5888.

(95) Tokuda, M., Fujiwara, K., Gomibuchi, T., Hirama, M., Uesugi, M., Sugiura, Y., *Tet. Lett.* **1993**, *34*, 669-672.

(96) Nishiwaki, E., Tanaka, S., Lee, H., Shibuya, M., *Heterocycles* **1988**, *27*, 1945.

(97) Wittman, M. D., Kadow, J. F., Langley, D. R., Vyas, D. M., Rose, W. C., Solomon, W., Zein, N., *Bioorg. Med. Chem. Lett.* **1995**, *5*, 1049-1052.

(98) Semmelhack, M. F., Gallagher, J. J., Ding, W. D., Krishnamurthy, G., Babine, R., Ellestad, G. A., *J. Org. Chem.* **1994**, *59*, 4357-4359.

(99) Xie, G., Morgan, A. R., Lown, J. W., *Bioorg. Med. Chem. Lett.* **1993**, *3*, 1565-1570.

(100) Banfi, L., Basso, A., Bevilacqua, E., Gandolfo, V., Giannini, G., Guanti, G., Musso, L., Paravidino, M., Riva, R., *Bioorg. Med. Chem.* **2008**, *16*, 3501-3518.

(101) Drak, J., Iwasawa, N., Danishefsky, S., Crothers, D. M., *Proc. Natl. Acad. Sci. USA.* **1991**, *88*, 7464-7468.

5.0 Results and Discussion - Synthesis and Biological Activity of Minor Groove Binding-Artemisinin Conjugates

The specific and potent cytotoxicity of artemisinin towards cancerous cells has been documented thoroughly.[1-5] A literature report by Li and co-workers demonstrates the DNA cleavage profile of artemisinin and implicates DNA cleavage as one potential mode of cytotoxic action.[6] Hybrid compounds with cytotoxic (*e.g.* alkylators, intercalators and free radical generating agents) and DNA binding moieties have been synthesised widely.[7] Of particular interest are the conjugates of the minor groove binders, netropsin and distamycin.[8] Netropsin and distamycin are naturally occurring antibiotics, consisting of a chain of amide-linked *N*-methyl pyrrole units, demonstrating high affinity for the minor grove of DNA.[9] The hybrid strategy has often allowed for compounds with enhanced activity as a result of their efficient delivery to the DNA target.

With these developments in mind we decided to attempt the synthesis of conjugates of artemisinin with synthetic analogues of netropsin and distamycin. We then planned to assess these conjugates for DNA binding affinity: a vital parameter in the action of agents causing cleavage of the DNA duplex.[10-14] Literature reports on the SARs of these conjugates have highlighted the influence of the number of *N*-methyl pyrrole units in the minor groove binding portion, and the effect of the incorporation of a flexible or rigid linker between the conjugated portions.[8,12,13,15] With this in mind, we planned to synthesise a series of conjugates by varying the length of the pyrrole chain (*m*), the length of the flexible linker (*n*) and the carboxylic acid tether employed at the C-10 position of artemisinin (*Q*) (Figure 5.1).

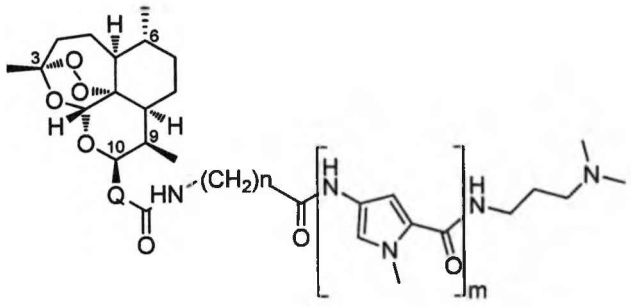

Figure 5.1 *Proposed points of diversification of minor grove binding-artemisinin conjugates.*

5.1 Modification of Artemisinin at the C-10 Position

The initial part of the synthesis was the modification of artemisinin at the C-10 position. Our synthetic route was focused on the amide coupling of the minor groove binding component to the artemisinin unit, making a carboxylic acid functionality on the artemisinin portion imperative.

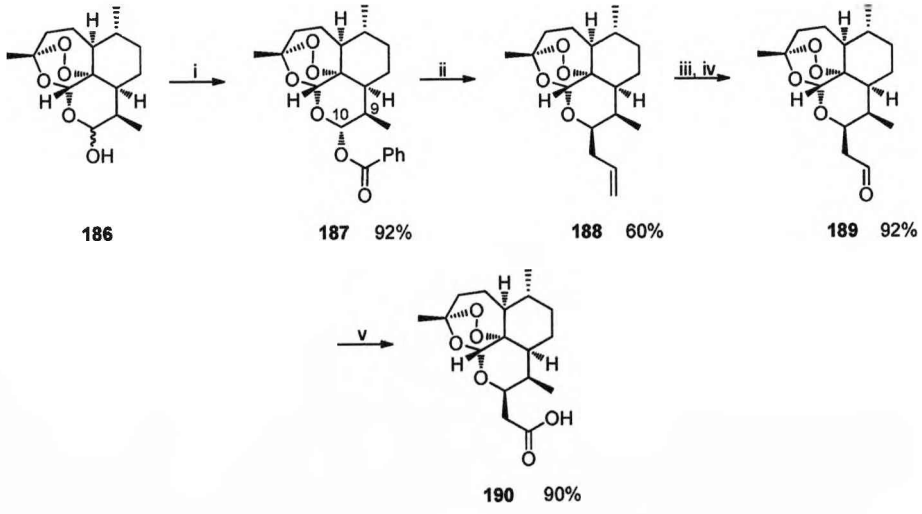

Scheme 5.1 *Reagents and conditions:* i) BzCl, py, CH_2Cl_2, 0 °C, 16 hr; ii) Allyl trimethylsilane, $ZnCl_2$, 4Å molecular sieves, DCE, 0 °C, 3 hr; iii) O_3, MeOH, -78 °C, 1 hr; iv) PPh_3, MeOH, -78 °C – rt; v) $NaClO_2$, 2-methyl-2-butene, NaH_2PO_4, *t*-BuOH/H_2O, r.t., 2 hr.

Two alternative carboxylic acid linkers were proposed as suitable intermediates, the metabolically stable C-10 carba-linker[16] **190** (Scheme 5.1) and C-10 phenoxy-linker[17] **199** (Scheme 5.2). These two intermediates should allow for structural diversity in the target conjugates. The route to the C-10 carba-carboxylic acid was previously developed within the O'Neill group and is shown in Scheme 5.1.[18]

Acylation of dihydroartemisinin **186** with benzoyl chloride provided the α-configured benzoate **187** in excellent yield. The stereoselectivity at the C-10 position was determined from ^{1}H NMR spectra. A doublet at 6.02 ppm with J = 9.8 Hz is a result of coupling of H-10 with H-9 and is typical of a *trans*-diaxial relationship between the adjacent protons.

The observed diastereoselectivity is due to the nucleophilic nature of the pyridine catalyst and its formation of a reactive acyl pyridinium intermediate **191** (Figure 5.2). The acyl pyridinium ion undergoes steric interactions with the methyl group at C-9 and ensures that only the artemisinin conformer with the α-directed hydroxyl group undergoes acylation.[18]

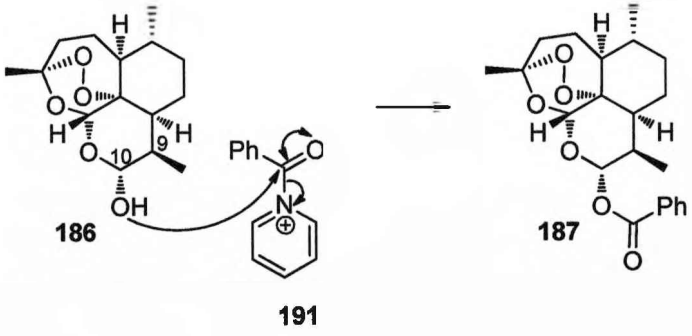

***Figure 5.2** Formation of an acyl pyridinium ion intermediate **191** ensures diastereoselectivity.*

The benzoate **187** was then treated with a solution of the mild Lewis acid $ZnCl_2$ and allyl trimethylsilane in optimised conditions outlined by O'Neill *et al.*.[16] This

furnished the versatile allyl intermediate **188** in moderate yield and with reversed β-diastereoselectivity. The Lewis acid catalyst facilitates the formation of an oxonium ion intermediate **192**, which in turn ensures axial attack of the allylic nucleophile providing β-selectivity.[16] Previous methods outlined in the literature, using $BF_3.Et_2O$, reported anhydroartemisinin (AHA) **193** as a major by-product formed by deprotonation of the oxonium intermediate (Figure 5.3).[19] We presumed some AHA was formed as t.l.c of the crude reaction mixture visualised a red spot when developed with *p*-anisaldehyde. However AHA formation was kept to a minimum by using reaction conditions that facilitated controlled generation of the oxonium intermediate. The good benzoyl leaving group, as shown in **187**, together with the use of a weaker Lewis acid and a large excess of allyl TMS, ensured that throughout the reaction there were large quantities of nucleophile available to react with the oxonium intermediate.

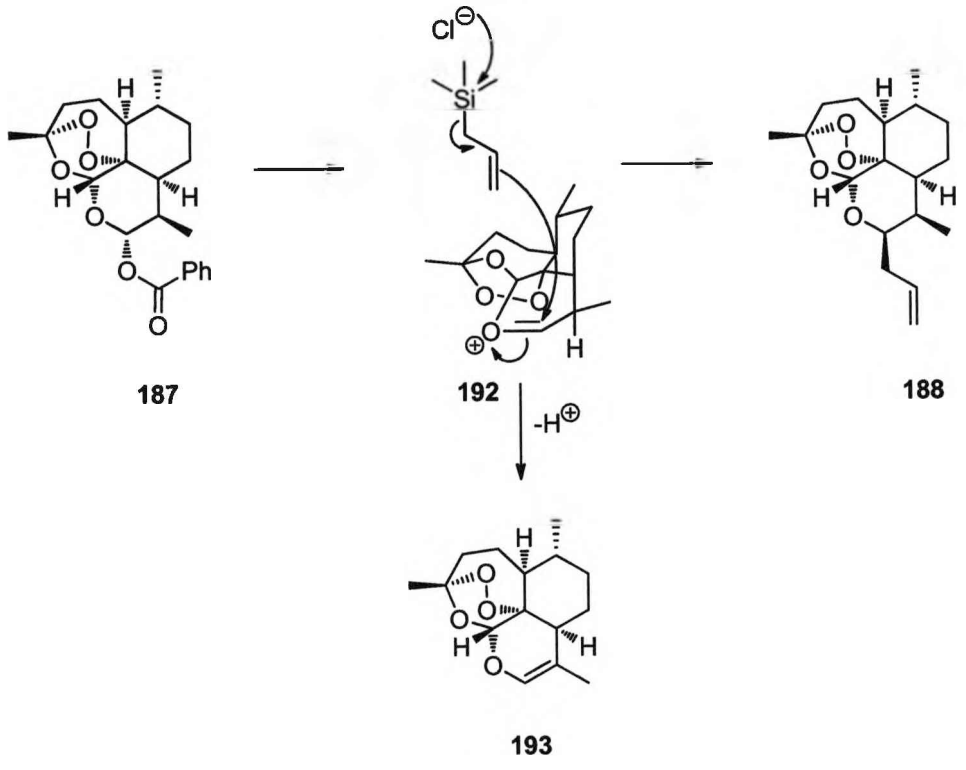

Figure 5.3 *The oxonium intermediate and potential formation of anhydroartemisinin (AHA)* ***193.***

A highly effective oxidation of the allyl intermediate to the carboxylic acid had been previously used by our group which we subsequently implemented. Firstly synthesis of the aldehyde **189** proceeded *via* the ozonolysis of **188** in methanol to give an α-hydroperoxy ether intermediate **197** (Figure 5.4). Subsequent addition of triphenyl phosphine to **197** facilitated reduction to the desired aldehyde **189**. The ozonolysis of the allyl functionality initially forms a molozonide **195** followed by reverse 1,3-dipolar addition to a dipolar carbonyl oxide **196**, which in alcoholic solvents is trapped out to the aforementioned ether **197**.

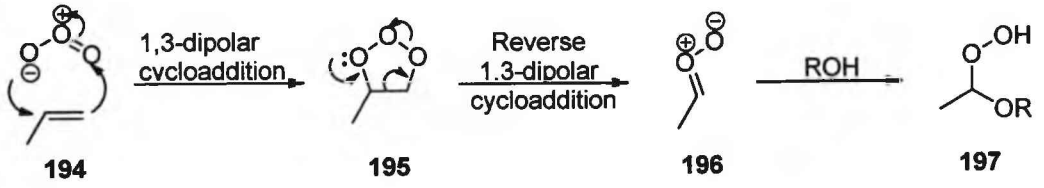

***Figure 5.4** Ozonolysis of the allyl group provides an α-hydroperoxy ether.*

Finally, oxidation of the aldehyde **189** with sodium chlorite gave the desired carboxylic acid **190** (Scheme 5.1) in excellent yield.

Facile synthesis of the C10-aryl ether linker was then carried out in two steps (Scheme 5.2). DHA **186** was treated with methyl-3-hydroxybenzoate and a TMSOTf/$AgClO_4$ catalyst system to furnish the β-epimer of the phenoxy ester **198**. Saponification of the ester subsequently provided the phenoxy carboxylic acid **199** in excellent yield.

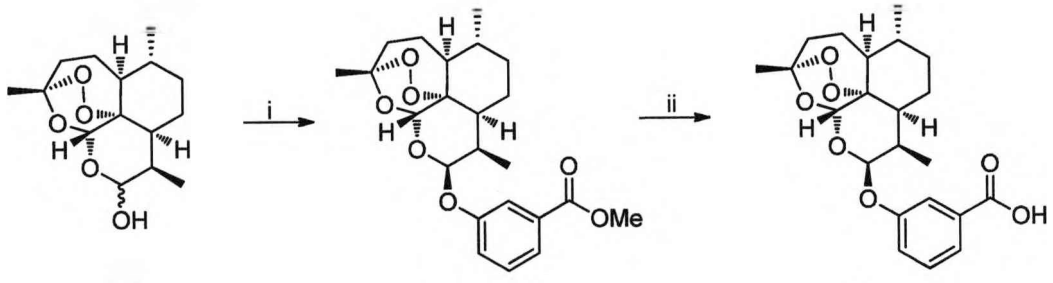

Scheme 5.2 *Reagents and conditions:* i) Methyl-3-hydroxybenzoate, TMSOTf, $AgClO_4$, NEt_3, CH_2Cl_2, -78 °C, 3 hrs; ii) 5% KOH/MeOH, r.t., 4 days.

Earlier approaches to the addition of phenols to DHA (Scheme 5.2, step (i)) mainly involved the use boron trifluoride etherate catalysis; however the major product formed from this route was the anhydro derivative AHA **193** (Figure 5.3) and the product was formed as a mixture of α- and β-anomers. In 2001 the O'Neill group

reported the use of a TMSOTf-$AgClO_4$ catalyst system whereby the desired ether was formed in excellent yield and diastereoselectivity, favouring the β-isomer.[17] These conditions were originally developed by Toshima[20] for the *C*-arylglycosylation of 1-*O*-methyl sugars where the phenoxy glycoside intermediate underwent an *O*- to *C*-aryl glycoside rearrangement as shown in Figure 5.5.

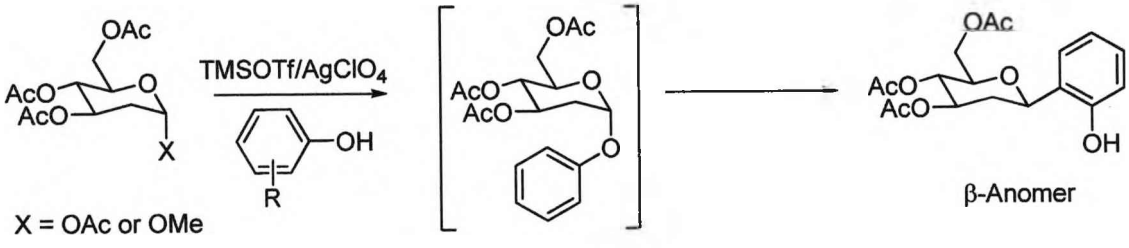

Figure 5.5 *C-aryl glycosidation of 1-O-methyl sugars using the TMSOTf-$AgClO_4$ catalyst system.*

The identification of dihydroartemisinin lactol as related to a pyranose sugar with a free anomeric hydroxyl group allowed for the application of the conditions outlined by Toshima *et al.* for the functionalisation of artemisinin. Only minor quantities of AHA **193** (Figure 5.3) were reported by O'Neill and no such *O*- to *C*-glycoside rearrangement was noted, possibly as a result of the low temperature reaction conditions (-78 °C).[17] The productivity and stereoselectivity of this system over other Lewis acid catalysts has no obvious explanation: it could be a result of either stabilisation of the oxonium ion or the catalysis of its slow formation thereby minimising AHA formation and optimising the yield. Correspondingly, we obtained **198** in excellent yield.

Previous methods of saponification of **198** to **199** (Scheme 5.2) involved the use of 2.5% KOH/MeOH solution and was reported to give complete transformation to the

acid in 21 days.[18] We improved this method by reducing the reaction time to 4 days by increasing the concentration of the base with no detriment to the delicate artemisinin peroxide bridge. Careful acidification to neutral pH allowed for safe workup of the peroxide product.

5.2 Synthesis of the Carboxamide Chain: Netropsin Analogue

With the artemisinin-carboxylic acid intermediates in hand, we progressed to the synthesis of the minor groove binding portion of the conjugates, the carboxamide chain. The first three steps were conditions reported by Zhao and Lown.[21]

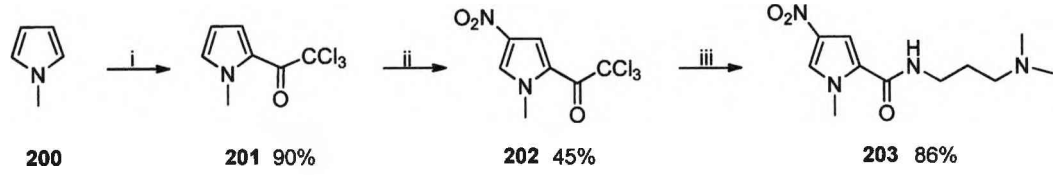

200 **201** 90% **202** 45% **203** 86%

Scheme 5.3 *Reagents and conditions* i) Cl_3CCOCl, CH_2Cl_2, r.t. 3 hr: ii) 70% HNO_3, Ac_2O, -40 °C 0.5 hr: iii) 3-Dimethylaminopropylamine, THF, 0 °C → r.t. 1hr.

The first step involved the substitution of trichloroacetyl chloride to the inexpensive *N*-methyl pyrrole starting material **200** (Scheme 5.3). This furnished the pyrrole ring with a versatile trichloroacetyl group at the 2-position in 90% yield **201**. The trichloroacetylated product **201** was then treated with nitric acid at -40 °C, which ensured regiospecific substitution at the 4-position.[22] Recrystallisation at -20°C with isopropyl alcohol gave **202** in 45% yield. In subsequent nitration reactions, recrystallisation greatly benefited from seeding with a sample of **202**.

Compound **202**, being the basic pyrrole unit of which the carboxamide chains are comprised, could then undergo a variety of transformations.

To synthesise the terminal unit of the carboxamide chain, **202** was treated with 3-dimethylaminopropyl amine to give **203** in 86% yield. This terminal group allows for a positive charge to be distributed across the dimethylamine group thereby forming electrostatic interactions with DNA tracts.

The pyrrole chain could then be built from the terminal unit **203** (Scheme 5.4). Reduction of the nitro group would give a reactive amine **203a** and subsequent addition of the pyrrole unit **202** to **203a** would give the dipyrrole **204**.

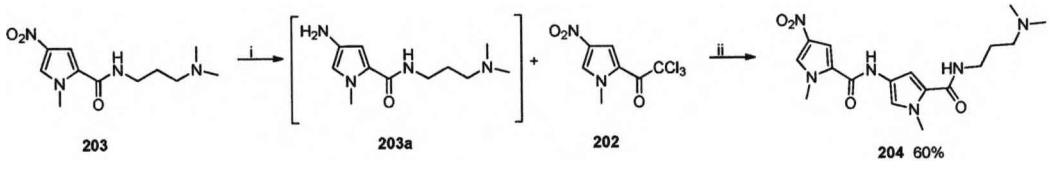

Scheme 5.4 *Reagents and conditions:* i) H_2, 1 atm, PtO_2, MeOH, 16 hr: ii) DMF, 0 °C → r.t, 1 hr.

The nitro group of **203** was hydrogenated at atmospheric pressure using catalytic platinum (IV) oxide in MeOH. However, upon removal of the solvents *in vacuo* decomposition of the product was observed and only very polar degradation products were recovered. This problem was overcome by using a technique proposed by Hotzel.[23] The hydrogenation was repeated in MeOH as before, however upon completion of reaction, MeOH was removed under vacuum, the vacuum released to an inert atmosphere of nitrogen, and the residue immediately dissolved in DMF. The DMF was removed under vacuum until half of the original volume had been

evaporated, ensuring complete removal of all MeOH. The vacuum was again released to an inert atmosphere and a solution of **202** in DMF was added to the solution of **203a** at 0 °C. The solution was allowed to warm to room temperature with stirring.

Subsequent removal of the solvent and purification by column chromatography gave the carboxamide dipyrrole **204**, in 60% yield (Scheme 5.4).

Literature methods reported purification of product **204** could be achieved by recrystalisation of the crude residue in isopropyl alcohol.[23] However, the residue we obtained assumed a gum-like appearance which did not crystallise. We therefore found column chromatography the most effective method of purification using a $MeOH/CH_2Cl_2$ eluent (1:10) containing 0.25% v/v NH_3 to aid elution of the polar product.

An area of structure activity relationship we wished to explore was the effect of the length of the pyrrole unit on the DNA binding affinity of the conjugates. We therefore also synthesised a tripyrrole carboxamide unit **205**. Reduction of **204** to give the reactive amine intermediate **204a** and subsequent addition of pyrrole unit **202** provided the tripyrrole carboxamide unit **205** in 44% yield (Scheme 5.5).

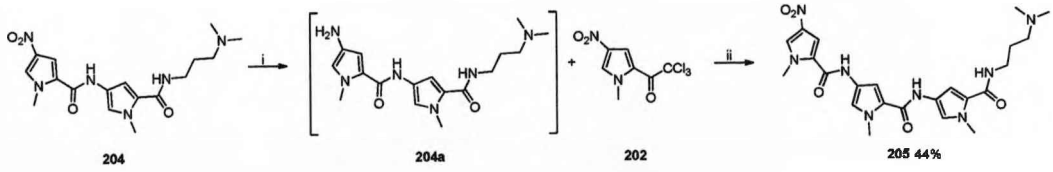

Scheme 5.5 *Reagents and conditions:* i) H_2, 1 atm, PtO_2, MeOH, 16 hr: ii) DMF, 0 °C → r.t, 1 hr.

5.3 Synthesis of the Target Conjugates via Amide Coupling

The final step, to synthesise our two most simplified conjugates, was the amide coupling of the synthetic carboxamide chain to the artemisinin carboxylic acid derivatives (Figure 5.6).

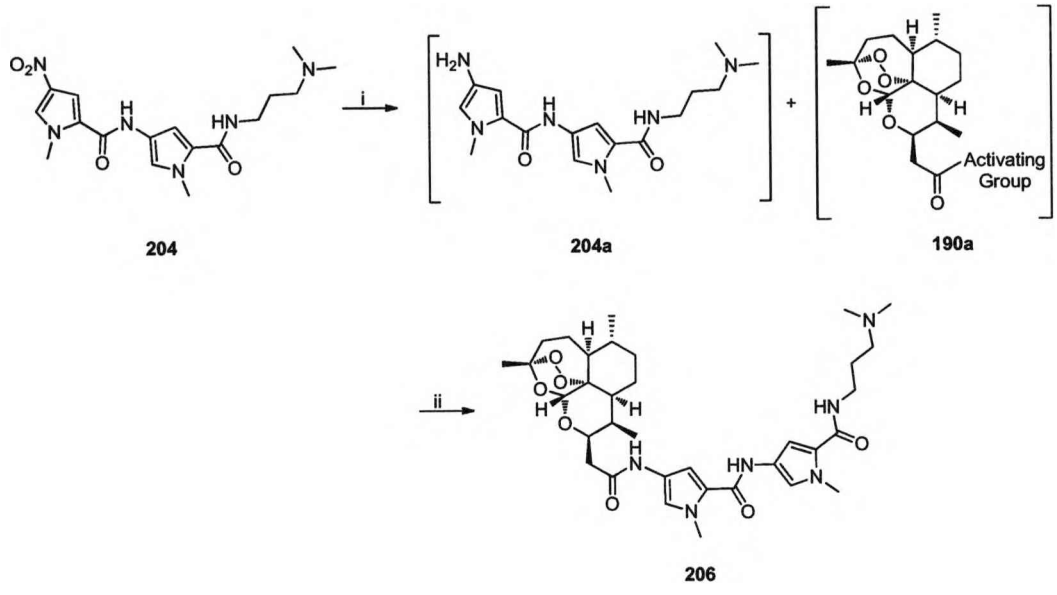

Figure 5.6 *Proposed amide coupling method to furnish the minor groove binding artemisinin conjugates.*

From our previous practical experience, it was realised that the reduction of the nitro group to the amine **204a** must be performed as described above (Section 5.2) and the activated artemisinin carboxylic acid **190a** would need to be added *in situ*. A number of methods and amide coupling reagents were tried. Formation of the acid chloride of artemisinin derivative **190** and subsequent addition to the amine was attempted initally. Analysis by t.l.c. showed a large amount of artemisinin starting material and no discernable spot relating to our proposed product **206**. Similarly, when the reaction was carried out using mixed anhydride conditions[24] and then later

carbodiimide coupling reagents (EDC)[25-27] no impact was made on the starting materials. We attributed these problems to the steric bulk of both portions we wished to couple. Disillusioned by these results, we attempted the coupling reaction using the artemisinin C-10 aryl ether derivative **199** (Scheme 5.2), hoping that the extended linker of **199** would readily facilitate a coupling reaction more removed from the steric bulk of artemisinin.

We carried out this coupling using the uronium salt coupling reagent *O*-(1*H*-benzotriazol-1-yl)-*N*,*N*,*N*',*N*'-tetramethyluronium hexafluorophosphate (HBTU) **207** (Figure 5.7).[28] Uronium coupling reagents consist of the aforementioned salt, an *O*-benzotriazole (OBt) portion and a counter ion that has been shown to have no practical influence on the reaction course.[29,30] Attack on HBTU **207** by the carboxylate anion forms an amidinium ion **208** which, driven by the loss of urea **210**, initiates attack by the OBt portion **209**. The active OBt ester **211** is subsequently formed, available for attack from an amine to furnish the amide product **212**.

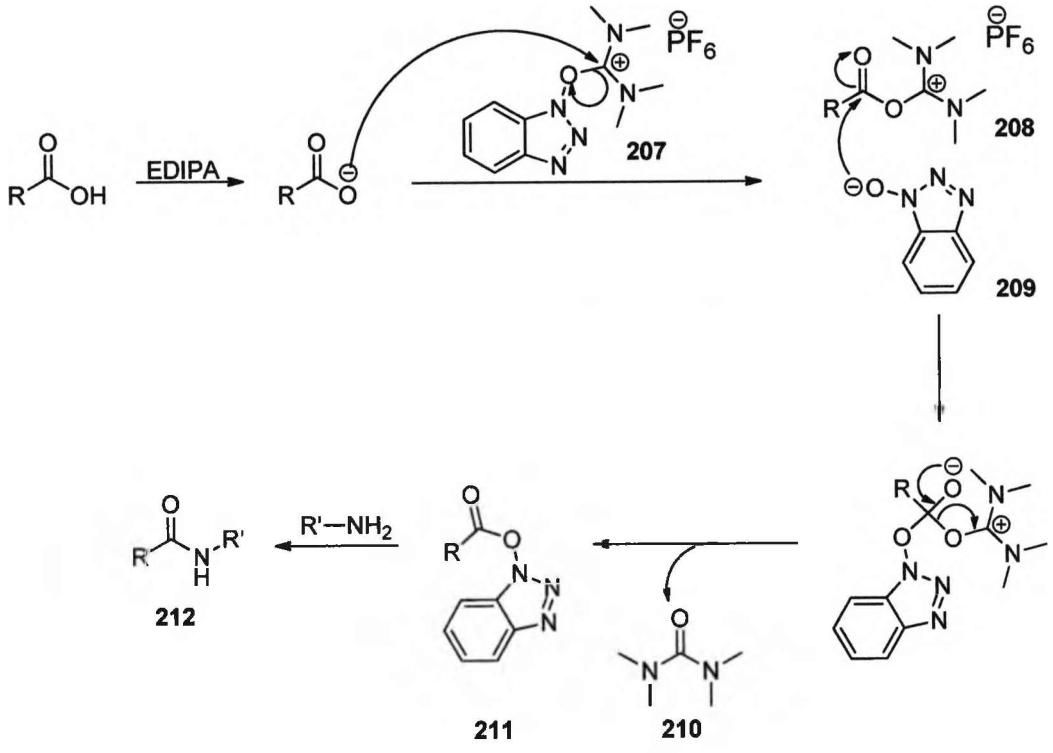

Figure 5.7 *Activation process using the HBTU coupling reagent.*[29]

The artemisinin C-10 aryl ether **199** was thus treated with EDIPA and HBTU, and the prepared amine **204a** was added in situ at 0 °C (Scheme 5.6).

Analysis by t.l.c. indicated the formation of a very polar product, showing a faint purple/brown tone when developed with *p*-anisaldehyde, typical of a peroxide containing compound. Purification by column chromatography furnished the desired hybrid **213** in 40% yield. However, ^{1}H NMR indicated strong contamination from the 1-hydroxy benzotriazole by-product **215** (Figure 5.8) which proved difficult to completely remove by conventional chromatography. Additional purification by HPLC furnished the pure product in low yields but sufficient amounts were isolated for biological testing.

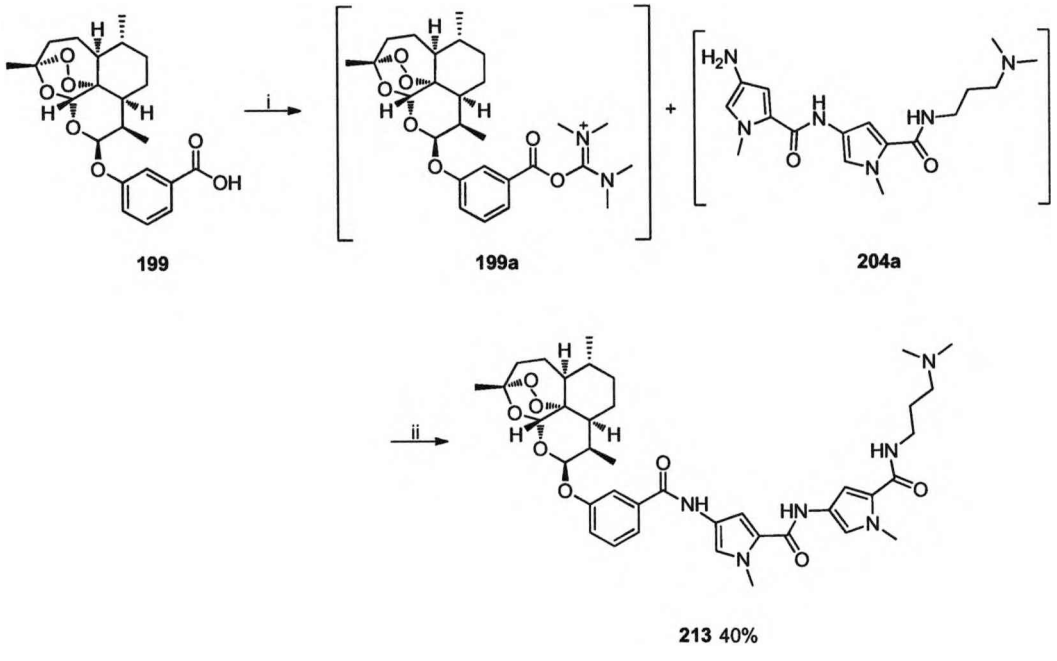

Scheme 5.6 *Reagents and conditions:* i) HBTU, EDIPA, DMF, 0 °C, 30 min: ii) DMF, 0 °C → r.t., 3 hr.

Similar conditions gave limited success in the coupling of the C10-carba linked artemisinin **190** to the dipyrrole **204a**, the proposed synthesis shown in Figure 5.6. The product **206** was found to be more difficult to visualise by t.l.c., with it appearing as a more intense area within a smudge of material moving up the plate. Purification by column chromatography only gave a very impure sample of the product. This material was confirmed to contain the product by high resolution mass spectrometry (HRMS). A poorly resolved ^{1}H NMR spectrum showed doublets typical of methyl groups 6-Me and 9-Me of artemisinin (δ 0.94 ppm, J = 6.1 Hz and δ 0.90 ppm, J = 7.7 Hz respectively), a singlet corresponding to H-12 of artemisinin (δ 5.50 ppm), dimethyl amine of the pyrrole terminus (δ 2.89 ppm), *N*-methyl groups of pyrroles (δ 3.85 ppm) and pyrrolic protons (approx. δ 7.16 and 6.78 ppm)

potentially confirming the correct structure (see appendix for full characterisation). However, subsequent efforts to purify the products *via* HPLC were unsuccessful. The inconclusive characterisation and questionable purity of this compound meant that it would not be suitable for biological testing.

A common side reaction when using uronium salts is the guanidylation of the free amine if unreacted HBTU is still present in the reaction mixture (Figure 5.8).[29,30]

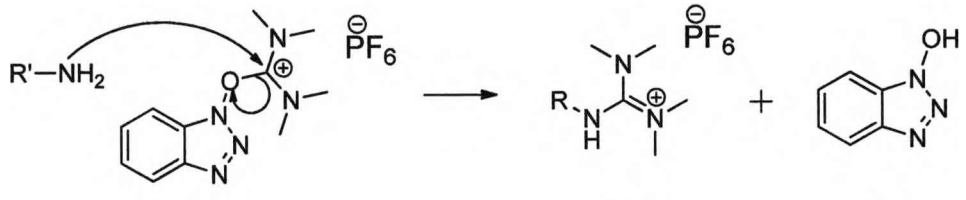

Figure 5.8 *Guanidinium formation with uronium type coupling reagents.*

This transformation could potentially be one side reaction leading to the observed mixture of products if the pathway to the attack of uronium was more favourable than that of the activated C-10 carba linked carboxylic acid.

This problem could be circumvented in the future by only using a 1:1 stoichiometry of the acid to coupling reagent. Inclusion of additional HOBt has also been reported to reduce the guanidylation side reaction. Furthermore, perhaps the use of HATU reagents, known to facilitate cleaner coupling reactions, would be more suited to this substrate.[30]

5.4 Synthesis of Structurally Modified Conjugates

After some success with the synthesis of the more simplified conjugates, we continued with the synthesis of analogues incorporating tethers of various lengths. A search of commercially available amino esters with varying chain lengths highlighted reagents **216** and **217** (Scheme 5.7). The linkers were Boc protected and subsequently hydrolysed to allow efficient amide coupling with the dipyrrole unit **204a** (Scheme 5.7, step iii and iv) using the HBTU coupling conditions outlined in Figure 5.7.

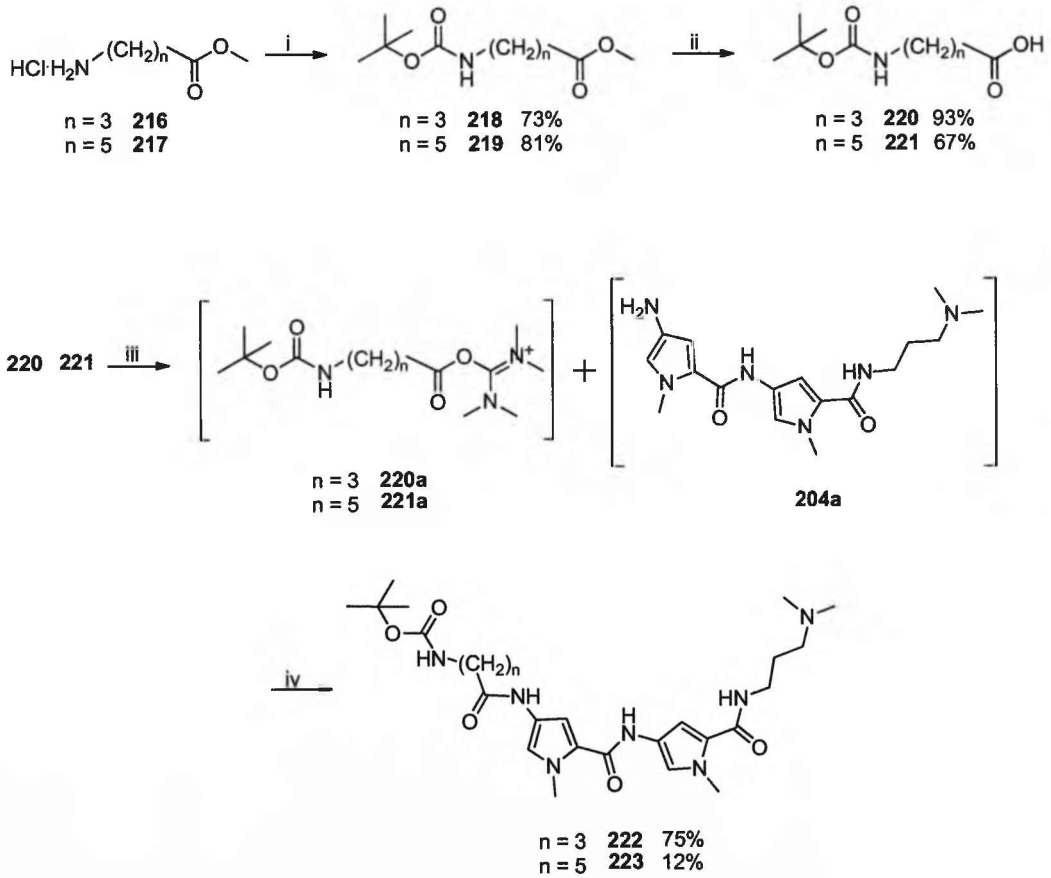

Scheme 5.7 *Reagents and conditions:* i) Boc_2O, NEt_3, MeOH, r.t., 1 hr: ii) 2M NaOH/MeOH, r.t., 16 hr: iii) HBTU, EDIPA, DMF, 0 °C, 30min: iv) DMF, 0 °C → r.t., 3 hr.

Coupling to the artemisinin carboxylic acid derivatives **190** and **199** was achieved by removal of the Boc group of **222** or **223** using trifluoroacetic acid (TFA) followed by *in situ* addition of the relevant HBTU activated artemisinin carboxylic acid (Scheme 5.8).

Again, coupling of the *O*-aryl linked artemisinin **199** with dipyrroles **222** and **223** was successful and purification by HPLC provided **224** and **225** for biological testing (Scheme 5.8).

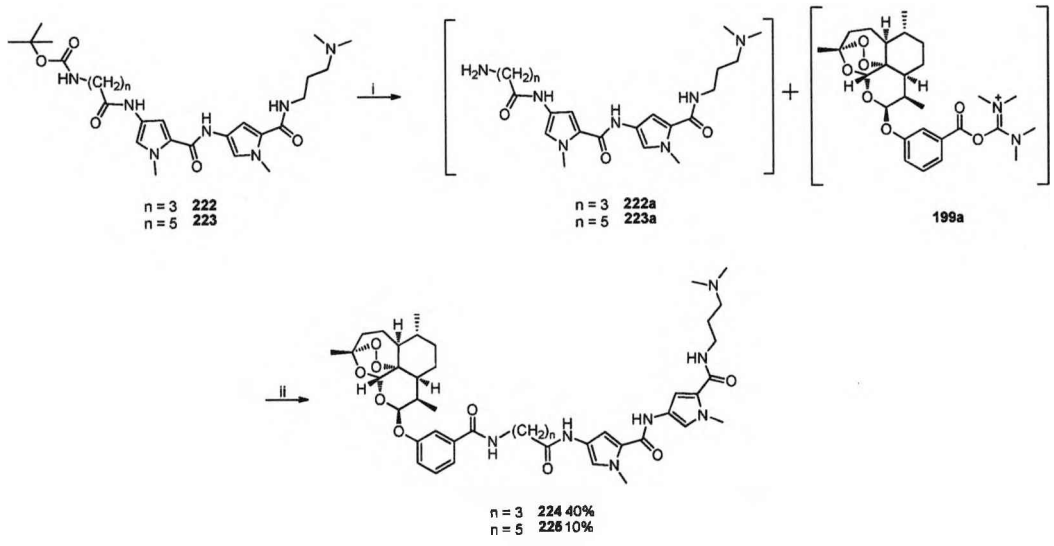

Scheme 5.8 *Reagents and conditions:* i) TFA, r.t., 2 hr: ii) DMF, r.t., 16 hr: ii) DMF, 0 °C → r.t., 3 hr.

We had hoped that the extended primary amine of **223** would assist in a clean amide coupling with artemisinin derivative **190**, due to the removal some of the steric interference. However, similar results were obtained as before with a large amount of polar by-products being formed making purification difficult. The presence of the

desired product **226** was confirmed by HRMS and a poorly resolved ^{1}H NMR spectra indicated the expected structure, nevertheless the data again proved inconclusive.

An additional area of SAR we wished to examine was the effect of the number of pyrrole units on the DNA binding affinity of the conjugates. As outlined above (Section 5.2), we synthesised a tripyrrole carboxamide unit **205** in moderate yield. We attempted the peptide coupling of **205** with artemisinin derivative **199** using HBTU conditions, however no reaction was observed.

In an effort to facilitate the coupling we synthesised a tripyrrole chain incorporating a three carbon linker **227**: nonetheless the amide coupling reaction was still unsuccessful. This was disappointing as there are numerous literature examples where an increase in pyrrole unit length, facilitates an increase in DNA binding affinity, and we had hoped to exploit this property.[8,15]

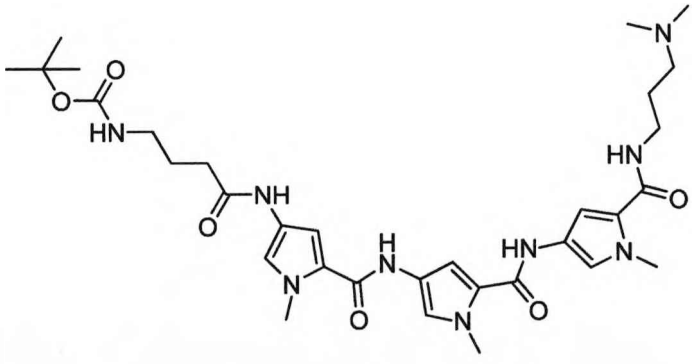

227

5.4.1 Synthesis of Conjugates via the Modified Curtius Reaction

In addition to flexible methylene linkers of varying lengths, we wished to incorporate more rigid spacers such as aromatic or piperazine linkers. However, we found that the choice of commercially available aminoesters of the type required was limited. In

an effort to expand our options we looked at a modified Curtius reaction[31] as a means of coupling that would allow the use of a carboxylic acid-alcohol linker.

The reaction proceeds through the interaction of the carboxylate anion with diphenylphosphoryl azide (DPPA) to give a carboxylic acid azide **228**, which undergoes thermal rearrangement to give an isocyanate **229** which in turn reacts with the alcohol to give the required carbamate **230** (Figure 5.9).

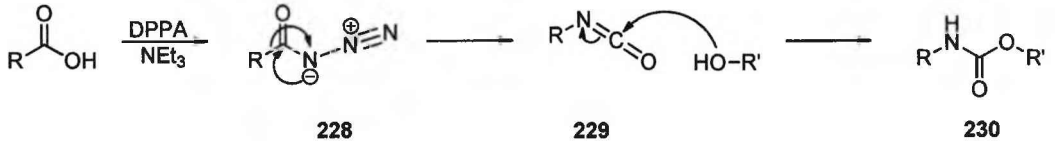

Figure 5.9 *Pathway of the modified Curtius rearrangement using DPPA.*

We were unsure whether an aromatic carboxylic acid, of the type shown in **199**, would freely undergo the proposed rearrangement to form the carbamate. We therefore carried out a model study with a protected alcohol-ester chain **231** shown in Scheme 5.9.

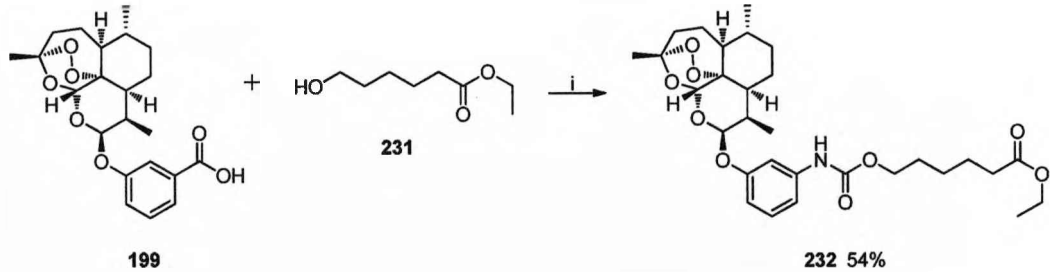

Scheme 5.9 *Reagents and conditions:* i) DPPA, NEt_3, MeCN, 55 °C, 24 hr.

The expected carbamate product **232** was obtained in 54% yield, so we continued with the addition of the alcohol linked dipyrrole **234** to the artemisinin phenoxy derivative **199** (Scheme 5.10).

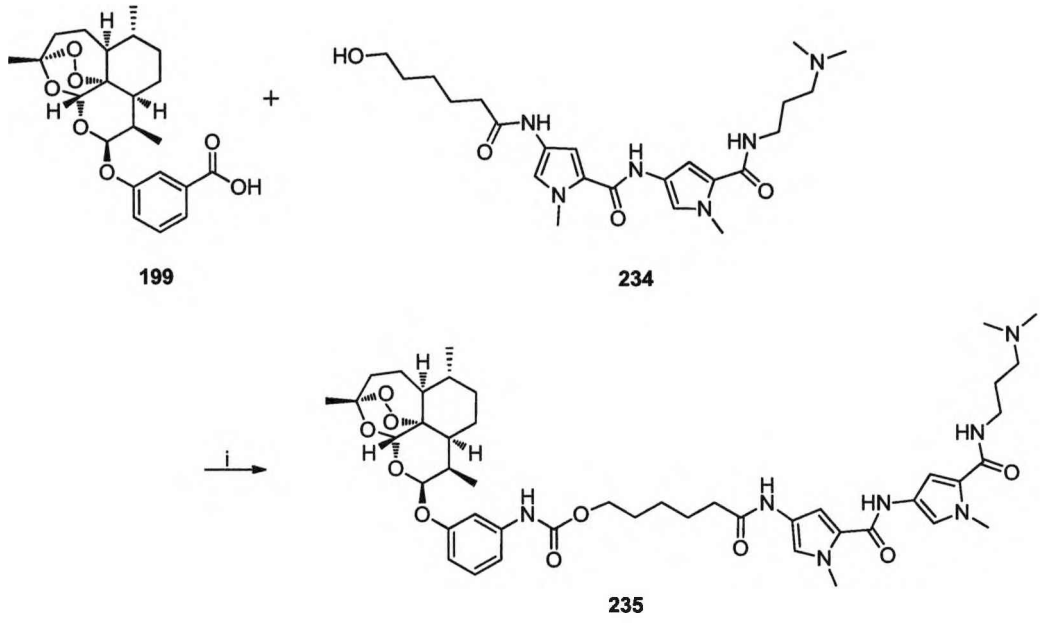

Scheme 5.10 *Reagents and conditions:* i) DPPA, NEt_3, MeCN, 55 °C, 24 hr.

Using the same conditions followed by purification by column chromatography, we obtained crude material that gave a weak but promising ^{1}H NMR spectrum. Analysis by HRMS indicated the presence of a small amount of the desired product accompanied by a high proportion of unwanted impurities making further purification of the product problematic. Optimisation of this reaction sequence could involve the hydrolysis of compound **232** (Scheme 5.9), followed by activation of the resulting carboxylic acid by HBTU and coupling to the dipyrrole moiety to furnish compound **235**. Regrettably we decided to discard this synthetic route as time pressures dictated that the work should continue to biological evaluation of the products we had in hand.

5.5 Future Routes for the Synthesis of Minor Groove Binding-Artemisinin Conjugates

The use of an alternative *O*-benzyl linker has been identified as a promising route to structural variation of the conjugates we have in hand.

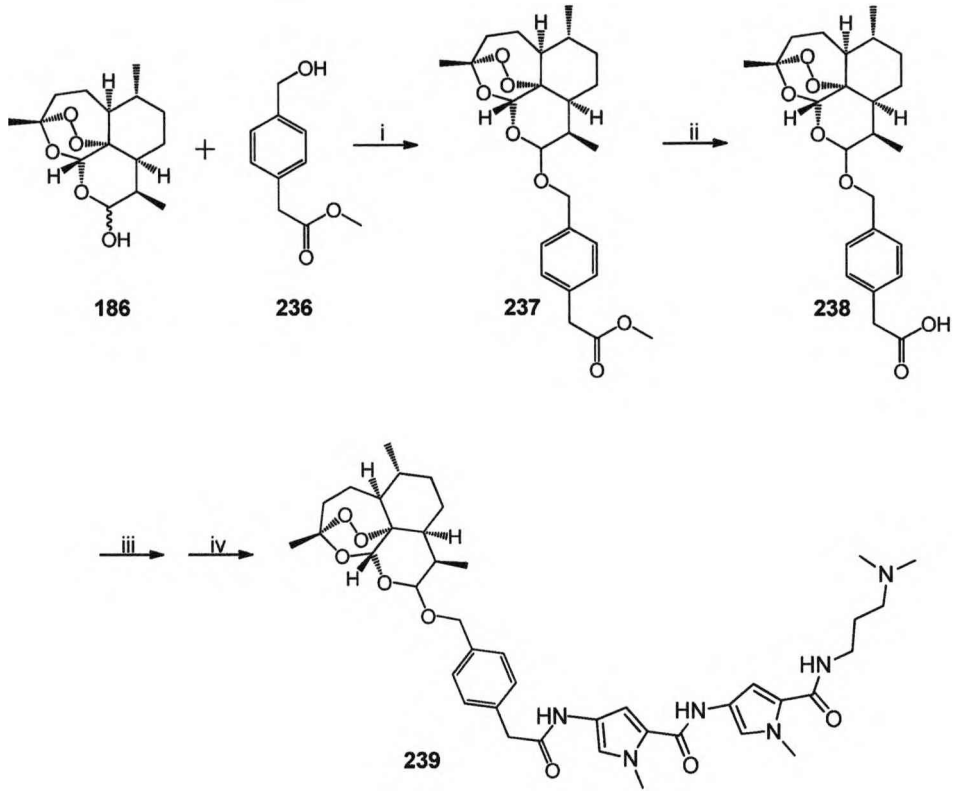

Figure 5.10 *Proposed route to incorporate an extended phenoxy linker at the C-10 position of artemisinin. Reagents and conditions: i) TMSOTf, $AgClO_4$, NEt_3; ii) KOH/MeOH; iii) HBTU, EDIPA; iv)* ***204a****.*

In the proposed synthesis shown in Figure 5.10, alcohol **236** can be used to provide an extended phenoxy linker **237** with two additional methylene groups. Ester hydrolysis and activation of the resulting carboxylic acid **238** should enable efficient coupling with a dipyrrole carboxamide unit to furnish the novel conjugate **239**. The extended benzyl linker also provides additional rigidity which may have an effect on the DNA binding affinity of **239**. It is anticipated that the coupling of dipyrrole chains fitted with methylene tethers, *e.g.* **222** and **223**, to artemisinin derivative **238**

will proceed smoothly to furnish a library of conjugates suitable for biological testing.

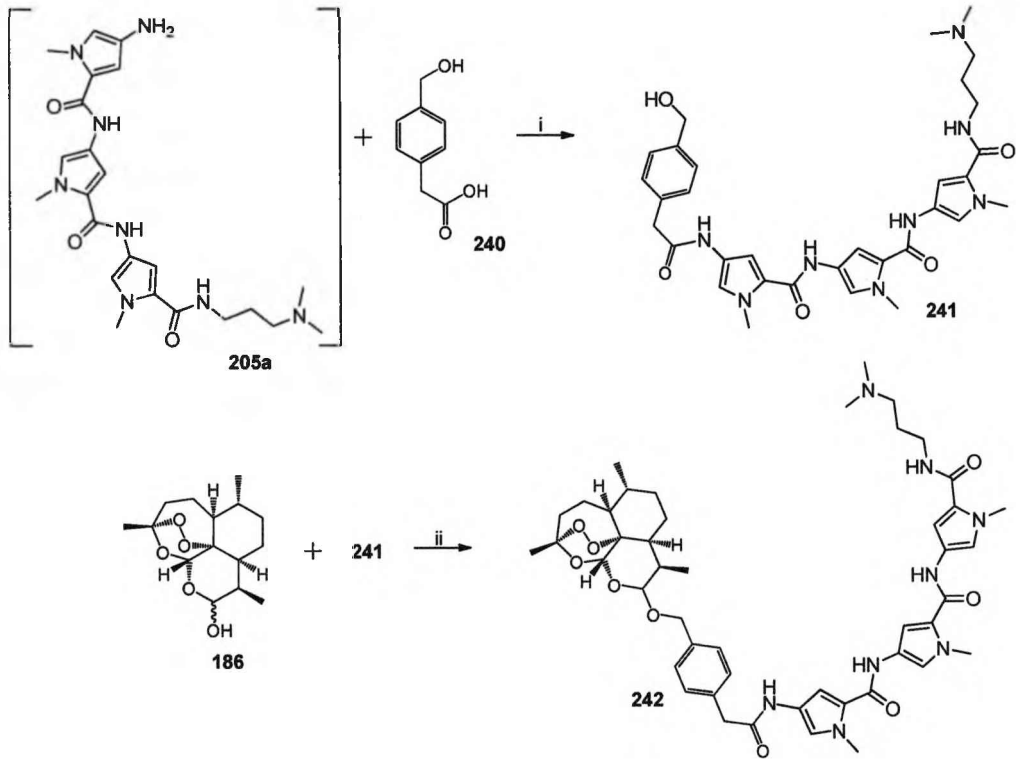

Figure 5.11 *Proposed route to allow the coupling of artemisinin to tri- and tetrapyrrole units. Reagents and conditions: i) HBTU, EDIPA; ii) TMSOTf, $AgClO_4$, NEt_3.*

In an attempt to facilitate the synthesis of artemisinin conjugates incorporating tri- and tetrapyrrole carboxamide chains, we propose a synthesis whereby the *O*-aryl carboxylic acid **240** can be first coupled to the pyrrole portion, **205a**, and thereafter the free alcohol **241** can be coupled to DHA *via* an ether linkage to give **242** (Figure 5.11).

5.6 Determination of DNA Binding Affinity by Thermal Denaturation Studies

After the successful synthesis of three artemisinin-minor groove binder conjugates **213**, **224** and **225**, we then wanted to evaluate their DNA binding affinity. If the conjugates can successfully bind to double-stranded DNA, the duplex should be stabilised when exposed to the conjugates, which can be determined by thermal melting studies. The hybrids were compared to the potent minor groove binder netropsin to a) determine the effect of the additional artemisinin portion on the binding affinity of the minor groove binding unit, and b) determine if the linker length of the hybrids had an effect on DNA binding.

5.6.1 Hypochromicity and DNA Melting Curves

Double-stranded DNA demonstrates a 30% lower molecular absorbance than denatured single-strand DNA due to an effect termed hypochromicity. The close proximity of the bases in the duplex state, results in the π-electrons of neighbouring bases interacting, thereby reducing the transition dipoles of the bases and a reduced ability to absorb light and a reduced UV absorbance for the duplex.

This effect can be used to observe the transition of duplex to single-strand DNA. By measuring the UV absorbance whilst increasing the temperature, one can produce a thermal melting curve (Figure 5.12). The stability of the duplex in solution can be determined by the mid-point of the curve and is termed the thermal melting stability (T_m).

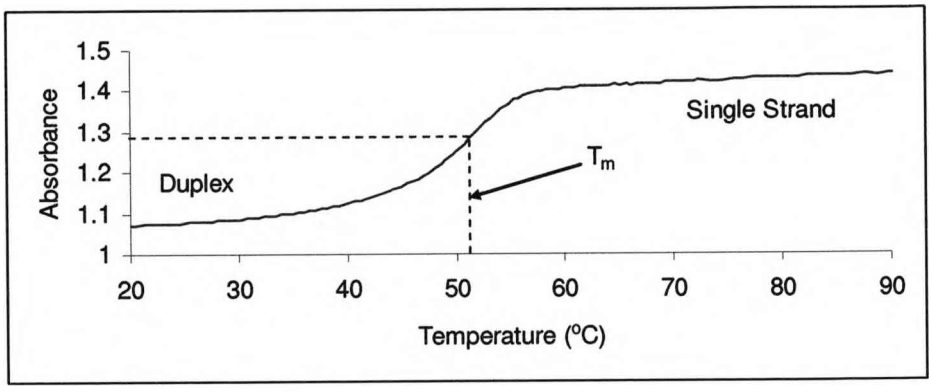

Figure 5.12 *A typical melting curve for a dodecamer duplex, where T_m is the transition from the duplex to single strand DNA.*

5.6.2 The d(CGCGAATTCGCG) Dodecamer

The duplex we chose, to study the effects of our conjugates, was a synthetic dodecamer d(CGCGAATTCGCG), often called the Dickerson-Drew dodecamer. This sequence has been a popular choice to observe the binding of netropsin and distamycin to the AT tract using X-ray crystallography and NOE experiments. Netropsin has been shown to bind tightly at the centre of the AATT tract at a duplex:drug ratio of 1:1.[32,33] The general use of this sequence as a model for the binding of netropsin to DNA, and reported thermal denaturation studies of this duplex, indicated its suitability for thermal melting studies with the artemisinin-dipyrrole conjugates.[34]

This system also allowed us to control the stoichiometry of the number of drug molecules per duplex to a 1:1 ratio as opposed to using natural double-stranded DNA where the stoichiometry of binding is more variable. This stoichiometric control would give a more meaningful comparison of the T_m values between the three conjugates.

All drug:duplex solutions were prepared in a 1:1 ratio. The samples were heated from 19-90°C and the UV absorption recorded approximately twice per 1°C to produce a melting curve.

5.6.3 Thermal Denaturation of d(CGCGAATTCGCG)

The curves produced from thermal denaturation of the d(CGCGAATTCGCG) duplex alone (series 1; control), the duplex with netropsin (series 2), the duplex with conjugate **213** (series 3), the duplex with conjugate **224** (series 4) and the duplex with conjugate **225** (series 5), are shown in Figure 5.13.

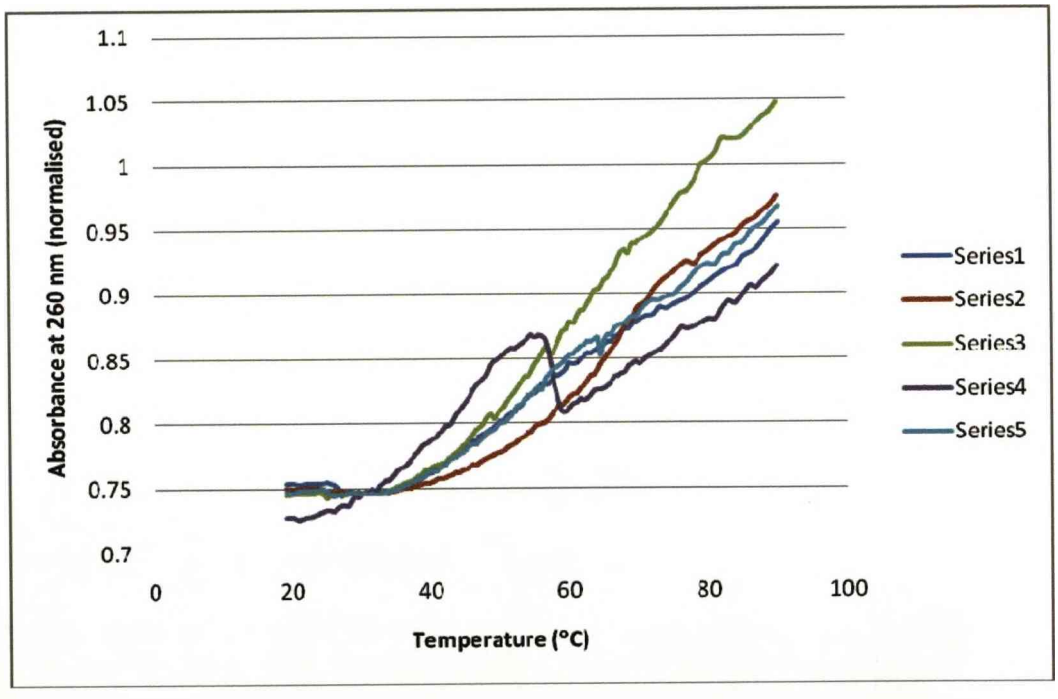

Figure 5.13 *Melting curves produced for the d(CGCGAATTCGCG)duplex alone and when exposed to netropsin, conjugate **213**, conjugate **224** and conjugate **225**.*

The curves shown in Figure 5.13 are normalised to 30 °C regarding the duplex control. One can clearly see the stabilisation provided to the duplex by netropsin

(series 2), shown by the shift of the curve to the right of the control indicating denaturation at a higher temperature.

However, when the duplex is exposed to conjugate **225** (series 5), incorporating a 5-carbon tether, the curve matches closely with that of the control, indicating no additional stabilisation of the duplex. When the duplex is exposed to conjugate **213**, with no tether (series 3), the duplex actually appears to be destabilised, the curve shifting to the left.

An anomalous result was produced from the thermal denaturation of the duplex in the presence of conjugate **224** (series 4), incorporating a 3-carbon tether. Repetition of the experiment produced the same result giving what could be described as a biphasic melting curve.

The most accurate method of comparing the stability of the duplex in the various conditions described, is in terms of the T_m which is calculated from the maximum point of the first derivative of the melting curve produced (Figure 5.12). However the curves produced from our experiments, including the control, did not show typical melting behaviour *i.e.* none of the curves formed a plateau at higher temperatures to give a classic sigmoidal shape. As a result no maximum point could be determined form the first derivative of the curves. The curves were also quite shallow, not showing a sharp transition from the duplex to the denatured single-strand. Disappointingly, the outcome of this poor melt behaviour is that we cannot, at this point, draw definite conclusions from this preliminary testing. However, it does appear that none of the drug conjugates show comparable binding to that of netropsin.

The Dickerson sequence (d(CGCGAATTCGCG)) was chosen because of previously reported studies (mainly NMR) with minor groove binders and the predictable stoichiometry of binding. However, self-complementary sequences of this type do have the potential to form hairpin structures **243** (Figure 5.14) that can complicate the T_m studies and could explain the biphasic melting of the duplex when exposed to conjugate **224**. A better approach for future work may be to use a non-self-complementary sequence *e.g.* **245**, which is likely to have better behaved melting properties.

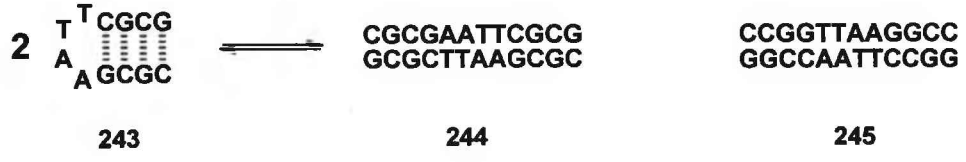

Figure 5.14 *Potential hairpin structures formed by the self-complementary d(CGCGATATCGCG) oligomer.*

5.7 Conclusion

In conclusion, we have highlighted a successful route to the coupling of artemisinin to a synthetic dipyrrole. Use of an *O*-aryl linked carboxylic acid at the C-10 position of artemisinin, allows for facile coupling to amine-functionalised dipyrrole chains using HBTU/EDIPA amide coupling conditions.

The coupling of a C-10 carba linked carboxylic acid to the dipyrrole portion, however, proved problematic, with side reactions evident, making purification difficult. The coupling of artemisinin to a synthetic tripyrrole was also unproductive both with and without an extended linker.

Diversification of the C-10 *O*-aryl conjugates was successfully achieved by the incorporation of a flexible tether linking the two portions. It was proposed that the

flexibility and length of said linker would allow more freedom of movement for both portions of the conjugate thereby optimising interactions with the DNA duplex.

The use of alternative *O*-benzyl linkers has been proposed as a route to a series of more structurally rigid hybrids that may demonstrate an altered affinity for the minor groove of DNA.

Thermal denaturation studies of the d(CGCGAATTCGCG) duplex in the presence of netropsin and conjugates **213**, **224** and **225** have been carried out. However the selected duplex did not produce the classic sigmoidal denaturation curve, even under control conditions. Early comparisons of the curves obtained, indicate that the conjugates tested may not demonstrate DNA binding affinity comparable with netropsin. Work is ongoing to improve the curves produced so as to define a value for T_m, and to allow accurate evaluation of the artemisinin-dipyrrole conjugates.

5.8 Acknowledgements

The dodecamer d(CGCGAATTCGCG) was synthesised by Dr James Gaynor by kind permission of Dr Rick Cosstick at the University of Liverpool. Thermal denaturation experiments were performed at the University of Leeds under the kind supervision of Dr Julie Fisher.

5.9 References

(1) Woerdenbag, H. J., Moskal, T. A., Pras, N., Malingre, T. M., El-Feraly, F. S., Kampinga, H. H., Konings, A. W. T., *J. Nat. Prod.* **1993**, *56*, 849-856.

(2) Lai, H., Singh, N. P., *Cancer Lett.* **1995**, *91*, 41-46.

(3) Moore, J. C., Lai, H., Li, J., Ren, R., McDougall, J. A., Singh, N. P., Chou, C., *Cancer Lett.* **1995**, *98*, 83-87.

(4) Singh, N. P., Lai, H., *Life Sciences* **2001**, *70*, 49-56.

(5) Lai, H., Sasaki, T., Singh, N. P., Messay, A., *Life Sciences* **2005**, *76*, 1267-1279.

(6) Li, P. C. H., Lam, E,. Roos, W. P., Zdzienicka, M. Z., Kaina, B., Efferth, T., *Cancer Res.* **2008**, *68*, 4347-4351.

(7) Bailly, C., Chaires, J. B., *Bioconjug. Chem.* **1998**, *9*, 513-538.

(8) Baraldi, P. G., Bovero, A., Fruttarolo, F., Preti, D., Tabrizi, M. A., Pavani, M. G., Romagnoli, R., *Med. Res. Rev.* **2004**, *24*, 475-528.

(9) Wemmer, D. E., Dervan, P. B., *Curr. Opin. Struct. Biol.* **1997**, *7*, 355-361.

(10) Jeon, R., Wender, P., *Arch. Pharmacol. Res.* **2001**, *24*, 39-43.

(11) Tokuda, M., Fujiwara, K., Gomibuchi, T., Hirama, M., Uesugi, M., Sugiura, Y., *Tet. Lett.* **1993**, *34*, 669-672.

(12) Wittman, M. D., Kadow, J. F., Langley, D. R., Vyas, D. M., Rose, W. C., Solomon, W., Zein, N., *Bioorg. Med. Chem. Lett.* **1995**, *5*, 1049-1052.

(13) Semmelhack, M. F., Gallagher, J. J., Ding, W. D., Krishnamurthy, G., Babine, R., Ellestad, G. A., *J. Org. Chem.* **1994**, *59*, 4357-4359.

(14) Banfi, L., Basso, A., Bevilacqua, E., Gandolfo, V., Giannini, G., Guanti, G., Musso, L., Paravidino, M., Riva, R., *Bioorg. Med. Chem.* **2008**, *16*, 3501-3518.

(15) Baraldi, P. G., Preti, D., Fruttarolo, F., Tabrizi, M. A., Romagnoli, R., *Bioorg. Med. Chem.* **2007**, *15*, 17-35.

(16) O'Neill, P. M., Pugh, M., Stachulski, A. V., Ward, S. A., Davies, J., Park, B. K., *J Chem Soc, Perkin Trans.* **2001**, 2682-2689.

(17) O'Neill, P. M., Miller, A., Bishop, L. P. D., Hindley, S., Maggs, J. L., Ward, S. A., Roberts, S. M., Scheinmann, F., Stachulski, A. V., Posner, G. H., Park, B. K., *J. Med. Chem.* **2000**, *44*, 58-68.

(18) Chadwick, J. Ph.D. Thesis, University of Liverpool, 2006.

(19) Pu, Y. M., Ziffer, H., *J. Med. Chem.* **1995**, *38*, 613-616.

(20) Toshima, K., Matsuo, G., Tatsuta, K., *Tet. Lett.* **1992**, *33*, 2175-2178.

(21) Zhao, R., Lown, W., *Heterocycles* **1995**, *41*, 337-344.

(22) Barker, P., Gendler, P., Rapoport, H., *J. Org. Chem.* **1978**, *43*, 4849-4853.

(23) Hotzel, C., Marotto, A., Pindur, U., *Eur. J. Med. Chem.* **2003**, *38*, 189-197.

(24) David-Cordonnier, M., Hildebrand, M., Baldeyrou, B., Lansiaux, A., Keuser, C., Benzschawel, K., Lemster, T., Pindur, U., *Eur. J. Med. Chem.* **2007**, *42*, 752-771.

(25) Damayanthi, Y., Praveen Reddy, B. S., Lown, J. W., *J. Org. Chem.* **1999**, *64*, 290-292.

(26) Baraldi, P. G., Cacciari, B., Guiotto, A., Leoni, A., Romagnoli, R., Spalluto, G., Mongelli, N., Howard, P. W., Thurston, D. E., Bianchi, N., Gambari, R., *Bioorg. Med. Chem. Lett.* **1998**, *8*, 3019-3024.

(27) Baraldi, P. G., Romagnoli, R., Guadix, A. E., Pineda de las Infantas, M. J., Gallo, M. A., Espinosa, A., Martinez, A., Bingham, J. P., Hartley, J. A., *J. Med. Chem.* **2002**, *45*, 3630-3638.

(28) Dourtoglou, V., Gross, B., *Synthesis* **1984**, 572.

(29) Valeur, E., Bradley, M., *Chem. Soc. Rev.* **2009**, *38*, 606-631.

(30) Montalbetti, C. A. G. N., Falque, V., *Tetrahedron* **2005**, *61*, 10827-10852.

(31) Ninomiya, K., Shioiri, T., Yamada, S., *Tetrahedron* **1974**, *30*, 2151-2157.

(32) Kopka, M. L., Yoon, C., Goodsell, D., Pjura, P., Dickerson, R. E., *Proc. Natl. Acad. Sci. USA.* **1985**, *82*, 1376-1380.

(33) Kopka, M. L., Yoon, C., Goodsell, D., Pjura, P., Dickerson, R. E., *J. Biol. Chem.* **1985**, *183*, 553-563.

(34) Wilson, W. D., Zuo, E. T., Jones, R. L., Zon, G. L., Baumstark, B. R., *Nucl. Acids Res.* **1987**, *15*, 105-118.

6.0 Experimental Procedure - Synthesis and Biological Activity of Minor Groove Binding-Artemisinin Conjugates

6.1 Chemical Procedures

Reaction procedure: Air- and moisture-sensitive reactions were carried out in oven-dried glassware sealed with rubber septa under a positive pressure of dry nitrogen from a balloon, unless otherwise indicated. Similarly, sensitive liquids and solutions were transferred *via* syringe or stainless steel cannula. Reactions were stirred using Teflon coated magnetic stir bars. Organic solutions were concentrated using a Buchi rotary evaporator with a diaphragm vacuum pump.

Purification of reagents and solvents: Anhydrous solvents were either obtained from commercial sources or dried and distilled immediately prior to use under a constant flow of dry nitrogen. THF, diethyl ether were distilled from Na/Ph_2CO, and dichloromethane from CaH_2. All other reagents were used as received from commercial sources unless otherwise indicated.

Purification of products: Analytical thin layer chromatography was performed with 0.25 mm silica gel plates (Merck 60 F_{254}). Plates were visualised by ultraviolet light or by treatment with iodine, *p*-anisaldehyde, ninhydrin or potassium permanganate followed by gentle heating. Chromatographic purification of products was accomplished by flash chromatography performed on silica gel (BDH 60 230-400 mesh). High pressure liquid chromatography (HPLC) was performed using a Gilson 321-pump coupled to a Gilson UV/Vis-151 spectrophotometer on a reverse phase, semi-preparative column. Preparative traces were plotted using Clarity - Chromatography software.

Analysis: Melting points were determined on a Gallenkamp apparatus and are uncorrected. NMR spectra were measured on a Bruker AMX 400 (^{1}H, 400 MHz and ^{13}C, 100 MHz) nuclear magnetic resonance spectrometer. Solvents are indicated in the text. Solids and liquids were used directly without any further treatment to record IR spectra using a JASCO FT/IR-4100 spectrometer. Mass spectra (MS) and high resolution mass spectra (HRMS) were recorded on a VG analytical 7070E machine and a Fisons Trio 1000 quadrupole GC mass spectrometer using electron ionisation (EI) or chemical ionisation (CI) respectively. Microanalyses were determined by the University of Liverpool Microanalysis Laboratory.

^{1}H NMR signals corresponding to artemisinin have been assigned using the following numbering system:

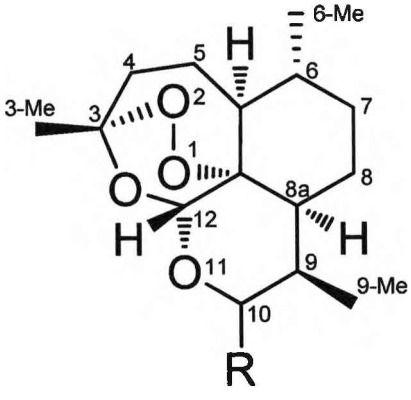

Dihydroartemisinin 10α-benzoate[1] 187

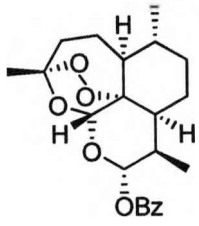

Benzoyl chloride (3.2 mL, 27.6 mmol) was added to a stirring solution of DHA **186** (5.00 g, 17.6 mmol) in anhydrous CH_2Cl_2 (60 mL) and anhydrous pyridine (9 mL) at 0 °C. After stirring at room temperature for 16 hours, the solvents and pyridine were removed *in vacuo* and the residue dissolved in EtOAc. This was then washed successively with 7% aq. citric acid solution (2 × 50 mL), sat. $NaHCO_3$ (50 mL) and water (50 mL). The organic extracts were dried over $MgSO_4$ and the solvents removed under reduced pressure to give a yellow oil. Purification by flash column chromatography (10:90 EtOAc: Hexane) gave **187** (6.25 g, 92%) as a white crystalline solid.

187: m.p. 110-112 °C Lit. 111-112 °C; IR ν_{max} 2929 (ν_{C-H}), 1736 ($\nu_{C=O}$), 1452 ($\nu_{C=C}$), 877, 831 (ν_{O-O}) cm^{-1}; ^1H NMR (400 MHz, $CDCl_3$) δ 8.14 (2H, m, Ar-H), 7.64-7.55 (1H, m, Ar-H), 7.50-7.26 (2H, m, Ar-H), 6.03 (1H, d, *J*=9.9 Hz, H-10β), 5.53 (1H, s, H-12), 2.81 (1H, ddq, *J* =9.8, 7.1, 4.5 Hz, H-9), 2.43 (1H, td, *J*=13.5, 4.0 Hz, H-4α), 2.08-0.94 (19H, m) (including 1.43 (3H, s, 3-Me), 0.99 (3H, d, *J*=5.9 Hz, 9-Me), 0.94 (3H, d, *J*=7.2 Hz, 6-Me)) ppm; ^{13}C NMR (100 MHz, $CDCl_3$) δ 165.7, 133.7, 130.5, 130.0, 128.7, 104.9, 92.9, 92.0, 80.6, 52.1, 45.8, 37.7, 36.7, 34.5, 32.4, 26.3, 25.0, 22.5, 20.7 and 12.7; *m/z* (EI) 411.1766 ($[M + Na]^+$) requires 411.1784; Anal. $C_{22}H_{28}O_6$ requires C 68.02%, H 7.27%, found C 67.70%, H 7.11%.

10β-Allyldeoxoartemisinin[1] 188

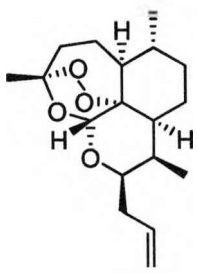

A solution of **187** (0.40 g, 1.03 mmol) in anhydrous 1,2-dichloroethane (4 mL) was added dropwise *via* cannula to a stirring mixture of allyltrimethylsilane (0.76 mL, 4.80 mmol), anhydrous $ZnCl_2$ (0.16 g, 1.20 mmol) and powdered 4 Å molecular sieves in anhydrous 1,2-dichloroethane (5 mL) at 0 °C. After stirring at 0 °C for 3 hours, the reaction mixture was diluted with EtOAc (150 mL) and washed with 5% aq. citric acid (50 mL), saturated aq. $NaHCO_3$ (50 mL), and brine (50 mL). The organic extracts were dried over $MgSO_4$ and the solvents removed *in vacuo*. Purification by flash column chromatography (10:90 EtOAc:Hexane) afforded **188** (0.19 g, 60%) as a white crystalline solid.

188: m.p. 73-75 °C Lit. 76-78 °C; IR ν_{max} 2991, 2958, 2918, 2873 (ν_{C-H}), 1643 ($\nu_{C=C}$), 879, 840, 823 (ν_{O-O}) cm^{-1}; ^1H NMR (400 MHz, $CDCl_3$) 5.98 (1H, m, -C<u>H</u>=CH_2), 5.32 (1H, s, H-12), 5.15 (2H, m, -CH=C<u>H</u>$_2$), 4.32 (1H, m, H-10), 2.73 (1H, m, H-9), 2.45-2.18 (3H, m), 2.06-1.58 (5H, m), 1.53-0.90 (14H, m) (including 1.42 (3H, s, 3-Me), 0.97 (3H, d, *J*=6.1 Hz, 6-Me), 0.90 (3H, d, *J*=7.6 Hz, 9-Me)) ppm; ^{13}C NMR (100 MHz, $CDCl_3$) δ 136.9, 116.5, 103.5, 89.5, 81.1, 75.1, 52.8, 44.7, 37.9, 37.0, 34.9, 34.6, 30.6, 26.5, 25.3, 25.1, 20.6 and 13.4; *m/z* (ES) 331.1878 ($[M + Na]^+$) requires 331.1385; Anal. $C_{18}H_{28}O_4$ requires C 70.10%, H 9.15%, found C 70.29%, H 9.19%.

10β-(2-Oxoethyl)deoxoartemisinin[2] 189

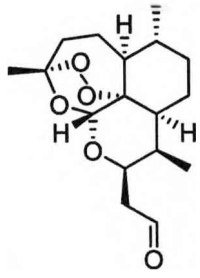

Ozone was bubbled through a solution of **188** (0.80 g, 2.60 mmol), in anhydrous MeOH (45 mL) at -78 °C for 60 minutes until the solution became saturated with ozone and appeared blue. Nitrogen was then bubbled through the solution to purge excess ozone. PPh_3 (2.04 g, 7.79 mmol) was added to the stirring solution at -78 °C. The mixture was allowed to warm to room temperature and stirred overnight. The solvent was removed *in vacuo* and the residue purified by flash column chromatography (15:85 EtOAc:Hexane) to give **189** (0.74 g, 92%) as a white solid.

189: m.p. 95-96 °C; IR ν_{max} 2933 (ν_{C-H}), 1718 ($\nu_{C=O}$), 877, 825 (ν_{O-O}) cm^{-1}; ^1H NMR (400 MHz, $CDCl_3$) 9.80 (1H, dd, *J*=3.1, 1.5 Hz, -C<u>H</u>O), 5.32 (1H, s, H-12), 4.98 (1H, m, H-10), 2.79-2.61 (2H, m, -C<u>H</u>$_2$CHO), 2.47-2.41 (1H, m), 2.37 (1H, td, *J*=14.6, 4.0 Hz, H-4α), 2.07 -2.01 (1H, m), 1.97-1.91 (1H, m), 1.82-1.76 (1H, m), 1.71-1.66 (2H, m), 1.55-0.88 (14H, m) (including 1.41 (3H, s, 3-Me), 0.98 (3H, d, *J*=6.0 Hz, 6-Me), 0.88 (3H, d, *J*=7.6 Hz, 9-Me)) ppm; ^{13}C NMR (100 MHz, $CDCl_3$) δ 202.2, 103.6, 89.7, 81.3, 69.8, 52.5, 44.8, 44.4, 37.9, 36.9, 34.7, 30.1, 26.4, 25.1, 25.0, 20.5 and 13.4; *m/z* (CI) 328.21328 ($[M + NH_4]^+$) requires 328.21240; Anal. $C_{17}H_{26}O_5$ requires C 65.78%, H 8.44 %, found C 65.69 %, H 8.47 %.

10β-(2-Carboxyethyl)deoxoartemisinin[2] 190

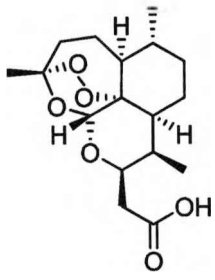

NaH_2PO_4 (0.40 g, 3.38 mmol) was added to a stirring solution of **189** (0.70 g, 2.26 mmol) in *t*-BuOH (31 mL) and water (6 mL). 2-Methyl-2-butene (13.0 mL, 26.00 mmol) was then added, followed by $NaClO_2$ (0.61 g, 6.80 mmol). The resulting pale yellow solution was stirred at room temperature for 2 hours and then concentrated *in vacuo*. 1.0 M aq. NaOH (50 mL) was added and the resulting solution washed with CH_2Cl_2 (3 × 50 mL). The aqueous phase was acidified with 1.0 M aq. HCl and extracted with CH_2Cl_2 (3 × 50 mL). The combined organic extracts were dried over $MgSO_4$, filtered and concentrated under reduced pressure to give **190** (0.66 g, 90%) as a white brittle foam.

190: m.p. 150-152 °C; IR ν_{max} 3423 (ν_{O-H}), 2939 (ν_{C-H}), 1590 ($\nu_{C=O}$), 877, 845 (ν_{O-O}) cm^{-1}; ^1H NMR (400 MHz, $CDCl_3$) 5.36 (1H, s, H-12), 4.88 (1H, ddd, *J*=9.9, 6.1, 3.4 Hz, H-10), 2.75-2.62 (2H, m, H-9 and -CH_2CO_2H), 2.52 (1H, dd, *J*=15.7, 3.6 Hz, -CH_2CO_2H), 2.37 (1H, td, *J*=13.4, 4.1 Hz, H-4α), 2.06 (1H, m), 1.96 (1H, m), 1.83 (1H, m), 1.71 (2H, m), 1.59-0.89 (15H, m) (including 1.42 (3H, s, 3-Me), 0.98 (3H, d, *J*=6.0 Hz, 6-Me), 0.89 (3H, d, *J*=7.6 Hz, 9-Me)) ppm; ^{13}C NMR (100 MHz, $CDCl_3$) δ 176.2, 103.7, 100.0, 89.8, 81.2, 71.3, 52.5, 44.2, 37.9, 36.8, 36.2, 34.7, 30.2, 26.2, 25.1, 20.5 and 13.1; *m/z* (ES) 349.1615 ($[M + Na]^+$) requires 349.1627.

HBTU activated 10β-(2-Carboxyethyl)deoxoartemisinin 190a

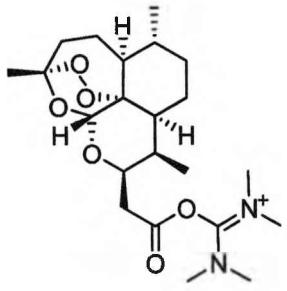

EDIPA (0.27 g, 2.13 mmol) and HBTU (0.51 g, 1.36 mmol) were added sequentially to a stirring solution of **190** (0.35 g, 1.06 mmol) in DMF (10 mL) at 0 °C under nitrogen. This was allowed to stir for up to an hour before addition of the desired amine at 0 °C.

***O*-Methyl-3-benzoate dihydroartemisinin[3] 198**

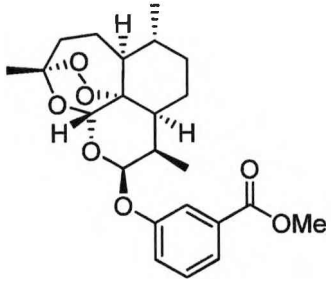

TMSOTf (1.5 mL, 8.32 mmol) was added to a stirring solution of DHA **186** (1.69 g, 5.94 mmol), methyl 3-hydroxybenzoate (2.71 g, 17.82 mmol) and $AgClO_4$ (0.25 g, 1.19 mmol) in anhydrous CH_2Cl_2 (50 mL) at -78 °C. After 3 hours NEt_3 (7.5 mL) was added. The reaction mixture was allowed to warm to room temperature and the solvent removed *in vacuo* to give a brown oil. Purification by flash chromatography (15:85 EtOAc:Hexane) gave **198** (2.00 g, 80%) as a white solid.

198: m.p. 60-62 °C; IR ν_{max} 3359 ($\nu_{C\text{-}H,\ Ester}$), 2933 ($\nu_{C\text{-}H}$), 1712 ($\nu_{C=O}$), 874, 819 ($\nu_{O\text{-}O}$) cm^{-1}; ^1H NMR (400 MHz, $CDCl_3$) 7.69 (2H, m, Ar-H), 7.38 (2H, m, Ar-H), 5.57

(1H, d, *J*=2.7 Hz, H-10), 5.48 (1H, s, H-12), 3.91 (3H, s, -OMe), 2.85 (1H, m, H-9), 2.42 (1H, td, *J*=14.2, 3.8 Hz, H-4α), 2.09-0.97 (19H, m) (including 1.44 (3H, s, 3-Me), 1.04 (3H, d, *J*=7.3, 6-Me), 0.97 (3H, d, *J*=6.1, 9-Me)) ppm; ^{13}C NMR (100 MHz, $CDCl_3$) δ 167.2, 158.0, 131.9, 130.0, 123.6, 121.4, 118.3, 104.7, 100.8, 88.7, 81.4, 52.9, 52.6, 44.7, 37.8, 36.7, 35.0, 31.3, 26.5, 25.0, 24.9, 20.7 and 13.4; *m/z* (ES) 441.1905 ($[M + Na]^+$) requires 441.1889.

_O_-carboxy-3-phenyl dihydroartemisinin[3] 199

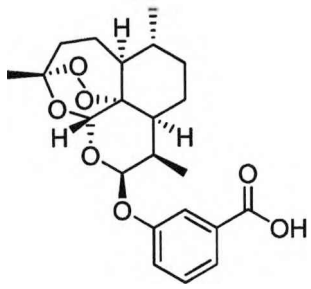

A solution of **198** (1.65 g, 3.95 mmol) in 5% w/v KOH/MeOH (50 mL) was stirred at room temperature for 4 days at which point complete consumption of the starting material was observed. The solution was acidified to neutral pH with 3.0 M aq. HCl and the solvent removed *in vacuo*. The resulting aqueous solution was extracted with EtOAc (4 × 50 mL), the organic extracts dried over $MgSO_4$ and concentrated *in vacuo* to give **199** (1.21 g, 76%) as a white solid.

199: m.p. 128-130 °C; IR ν_{max} 3535 (ν_{O-H}), 2924 (ν_{C-H}), 1687 ($\nu_{C=O}$), 874, 825 (ν_{O-O}) cm^{-1}; ^{1}H NMR (400 MHz, $CDCl_3$) 7.80 (2H, m, Ar-H), 7.42 (2H, m, Ar-H), 5.59 (1H, d, *J*=2.8 Hz, H-10), 5.50 (1H, s, H-12), 2.89 (1H, m, H-9), 2.43 (1H, td, *J*=14.2, 3.8 Hz, H-4α), 2.10-0.97 (19H, m) (including 1.45 (3H, s, 3-Me), 1.05 (3H, d, *J*=7.3 Hz, 6-Me), 0.97 (3H, d, *J*=6.1 Hz, 9-Me)) ppm; ^{13}C NMR (100 MHz, $CDCl_3$) δ 172.2, 157.8, 131.1, 130.1, 124.1, 122.2, 118.9, 104.7, 100.8, 88.7, 81.4, 52.9, 44.8,

37.8, 36.8, 35.0, 31.3, 26.5, 25.1, 24.9, 20.7 and 13.4; *m/z* (ES) 427.1740 ([M + Na]$^+$) requires 427.1733.

HBTU activated *O*-carboxy-3-phenyl dihydroartemisinin 199a

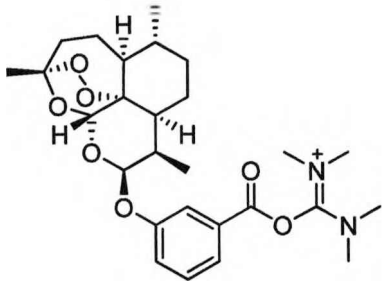

EDIPA (0.27 g, 2.07 mmol) and HBTU (0.59 g, 1.56 mmol) were added sequentially to a stirring solution of **199** (0.42 g, 1.04 mmol) in DMF (10 mL) at 0 °C under nitrogen. This was allowed to stir for up to an hour before addition of the desired amine at 0 °C.

1-Methyl-2-trichloroacetylpyrrole[4] 201

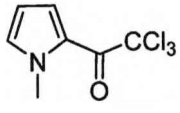

A solution of *N*-methyl-pyrrole **200** (1.62 g, 20.00 mmol) in CH_2Cl_2 (8 mL) was added dropwise to a solution of trichloroacetyl chloride (3.65 g, 20.10 mmol) in CH_2Cl_2 (12 mL) over 3 hours. During this time, the reaction mixture was stirred vigorously and a stream of N_2 was passed over the reaction mixture into a Drechsel flask containing 1 M NaOH to remove HCl as it was formed. Once all the trichloroacetyl chloride was added, the system was sealed under nitrogen and the solution stirred overnight. The solvent was removed *in vacuo* and resultant dark red residue was dissolved in chloroform and filtered through a short column of silica gel.

Removal of chloroform under reduced pressure gave analytically pure pale yellow needles of **201** (4.50 g, 100%).

201: m.p. 62-63 °C, Lit. 64-65 °C;[4] IR ν_{max} 3126 (ν_{Py-H}), 2954 (ν_{C-H}), 2811 (ν_{C-N}), 1653 ($\nu_{C=O}$), 806, 741, 685, 609 (ν_{C-Cl}) cm^{-1}; ^1H NMR (400 MHz, $CDCl_3$) 7.51 (1H, dd, *J*=4.4, 1.6 Hz, Py-H5), 6.98 (1H, t, *J*=2.2 Hz, Py-H3), 6.23 (1H, dd, *J*=4.5, 2.5 Hz, Py-H4), 3.97 (3H, s, Py-$C\underline{H}_3$) ppm; ^{13}C NMR (100 MHz, $CDCl_3$) δ 173.3, 134.0, 124.4, 122.2, 109.3, 96.7 and 39.0; *m/z* (CI) 225.96014 ($[M + H]^+$) requires 225.95932; Anal. $C_7H_6Cl_3NO$ requires C 37.12%, H 2.67%, N 6.18; found C 37.13%, H 2.62%, N 6.09%.

1-Methyl-2-trichloroacetyl-4-nitropyrrole[4] 202

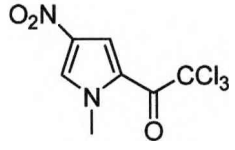

A suspension of **201** (2.00 g, 8.81 mmol) in acetic anhydride (20 mL) was cooled to -40 °C and to it was added 70% HNO_3 (1.0 mL, 1.8 eq) over a period of five minutes. The reaction vessel was allowed to warm to room temperature over a period of 3 hours and stirred at ambient temperature overnight. The mixture was cooled to -20 °C and a few drops of cold isopropyl alcohol added until a precipitate formed. The precipitate was collected by filtration, washed with cold isopropyl alcohol and dried under reduced pressure to give **202** (0.98 g, 41%) as a white solid.

202: m.p. 133-135 °C, Lit. 135-140 °C;[4] IR ν_{max} 3145 (ν_{Py-H}), 2968 (ν_{C-H}), 1691 ($\nu_{C=O}$), 1514, 1311 (ν_{C-N}), 812, 798, 748, 684, 609 (ν_{C-Cl}) cm^{-1}; ^1H NMR (400 MHz, $CDCl_3$) 7.96 (1H, d, *J*=1.7 Hz, Py-H5), 7.77 (1H, d, *J*=1.8 Hz, Py-H3), 4.06 (3H, s, Py-$C\underline{H}_3$) ppm; ^{13}C NMR (100 MHz, $CDCl_3$) δ 174.1, 135.2, 130.6, 122.6, 118.0,

100.0 and 40.2; *m/z* (ES) 324.9510 ([M + Na]$^+$) requires 324.9526; Anal. $C_7H_5Cl_3N_2O_3$ requires C 30.97%, H 1.86%, N 10.32%, found C 30.89%, H 1.85%, N 10.35%.

_N_-(3-(Dimethylamino)propyl)-1-methyl-4-nitro-1H-pyrrole-2-carboxamide[4] 203

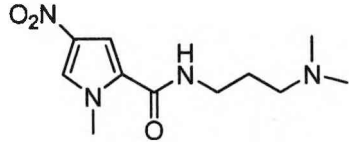

A solution of 3-dimethylaminopropylamine (0.41 g, 4.00 mmol) in THF (10 mL) was stirred at 0 °C. A solution of compound **202** (0.90 g, 3.33 mmol) in THF (10 mL) was added dropwise and stirred at 0 °C for a further 5 minutes. After removal of solvent *in vacuo*, the residue was purified by flash column chromatography (10:90 MeOH:CH_2Cl_2) to give **203** as a yellow crystalline solid (0.73 g, 86%).

203: m.p. 106-108 °C; IR ν_{max} 3248 ($\nu_{N\text{-}H,\ Amide}$), 3126 ($\nu_{Py\text{-}H}$) , 2947, 2860, 2819, 2769 ($\nu_{C\text{-}H}$), 1649 ($\nu_{C=O}$), 1545, 1340 ($\nu_{N=O}$) cm^{-1}; ^{1}H NMR (400 MHz, $CDCl_3$) 7.55 (1H, d, *J*=1.9 Hz, Py-H5), 7.04 (1H, d, *J*=2.0 Hz, Py-H3), 4.00 (3H, s, Py-C$\underline{H}_3$), 3.49 (2H, m, -NC$\underline{H}_2$-), 2.54 (2H, t, *J*=6.0 Hz, -NC$\underline{H}_2$-), 2.34 (6H, s, -N(C$\underline{H}_3$)$_2$), 1.80 (2H, quin, *J*=6.2 Hz, -$CH_2C\underline{H}_2CH_2$-) ppm; ^{13}C NMR (100 MHz, $CDCl_3$) δ 160.8, 135.3, 127.3, 126.8, 107.1, 59.1, 51.0, 45.5, 40.1, 38.3 and 25.3; *m/z* (CI) 255.14607 ([M + H]$^+$) requires 255.14572.

_N_-(3-(Dimethylamino)propyl)-1-methyl-4-(1-methyl-4-nitro-1H-pyrrole-2-carboxamido)-1H-pyrrole-2-carboxamide[4] 204

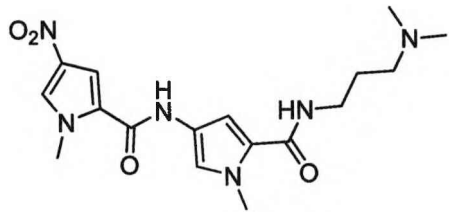

A solution of **203** (1.00 g, 4.16 mmol) in MeOH (40 mL) was hydrogenated at atmospheric pressure over PtO_2 overnight. The catalyst was removed by filtration through celite and the solvent removed *in vacuo*. The residual oil was dissolved in DMF (20 mL) and concentrated to half its original volume under reduced pressure to completely remove MeOH. A solution of **202** (1.12 g, 4.16 mmol) in DMF (8 mL) was added with stirring at 0 °C. The reaction mixture was then allowed to return to ambient temperature and stirred overnight. The solvent was removed *in vacuo* and the residue purified by flash column chromatography (10:90 MeOH:CH_2Cl_2 + NH_3 0.25% v/v) to give **204** as an orange crystalline solid (0.90g, 60%).

204: m.p. 189-191 °C, Lit. 190-191 °C;[4] IR ν_{max} 3587, 3297 ($\nu_{N\text{-}H,\ Amide}$), 3124 ($\nu_{Py\text{-}H}$), 2945, 2861, 2822, 2779 ($\nu_{C\text{-}H}$), 1647 ($\nu_{C=O}$), 1500, 1308 ($\nu_{N=O}$) cm^{-1}; ^1H NMR (400 MHz, MeOD) 7.89 (1H, d, *J*=1.9 Hz, Py-H5), 7.41 (1H, d, *J*=2.0 Hz, Py-H5), 7.22 (1H, d, *J*=1.9 Hz, Py-H3), 6.90 (1H, d, *J*=2.0 Hz, Py-H3), 4.00 (3H, s, Py-$C\underline{H}_3$), 3.89 (3H, s, Py-$C\underline{H}_3$), 3.42 (2H, t, *J*=6.4 Hz, -$NC\underline{H}_2$-), 3.19 (2H, m, -$NC\underline{H}_2$-), 2.92 (6H, s, -$N(C\underline{H}_3)_2$), 2.03 (2H, quin, *J*=6.5 Hz, -$CH_2C\underline{H}_2CH_2$-) ppm; ^{13}C NMR (100MHz, $CDCl_3$) δ 164.5, 160.0, 136.6, 129.1, 128.2, 125.2, 123.3, 120.8, 109.1, 106.2, 58.8, 45.8, 39.0, 38.4, 37.2 and 28.6; *m/z* (ES) 377.1931 ($[M + H]^+$) requires 377.1937.

_N_-(3-(Dimethylamino)propyl)-1-methyl-4-(1-methyl-4-(1-methyl-4-nitro-1H-pyrrole-2-carboxamido)-1H-pyrrole-2-carboxamido)-1H-pyrrole-2-carboxamide[4] 205

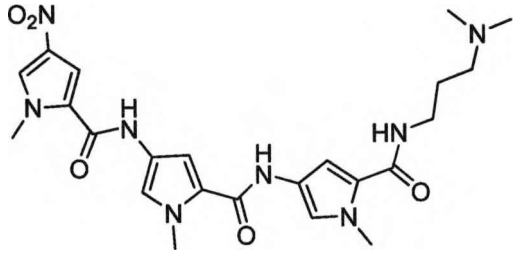

A solution of **204** (0.90 g, 2.40 mmol) in MeOH (40 mL) was hydrogenated at atmospheric pressure over PtO_2 overnight. The catalyst was removed by filtration through celite and the solvent removed *in vacuo*. The residual oil was dissolved in DMF (20 mL) and concentrated to half its original volume under reduced pressure to completely remove MeOH. A solution of **202** (0.63 g, 2.40 mmol) in DMF (8 mL) was added with stirring at 0 °C. The reaction mixture was then allowed to return to ambient temperature and stirred overnight. The solvent was removed *in vacuo* and the residue purified by flash column chromatography (10:90 MeOH/CH_2Cl_2 + NH_3 0.25% v/v) to give **205** (0.53 g, 44%) as an orange crystalline solid.

205: m.p. 188-190 °C; IR ν_{max} 3275 ($\nu_{N\text{-}H,\ Amide}$) , 3128 ($\nu_{Py\text{-}H}$), 2947 ($\nu_{C\text{-}H}$), 1641 ($\nu_{C=O}$), 1500, 1308 ($\nu_{N=O}$) cm^{-1}; ^1H NMR (400 MHz, MeOD) 7.71 (1H, d, *J*=1.8 Hz, Py-H5), 7.57 (1H, d, *J*=1.6 Hz, Py-H5), 7.31 (1H, d, *J*=1.7 Hz, Py-H5), 7.06 (1H, d, *J*=1.7 Hz, Py-H3), 6.51 (1H, d, *J*=1.9 Hz, Py-H3), 6.29 (1H, d, *J*=1.7 Hz, Py-H3), 4.03 (3H, s, Py-C$\underline{H}_3$), 3.89 (3H, s, Py-C$\underline{H}_3$), 3.80 (3H, s, Py-C$\underline{H}_3$), 3.54 (2H, q, *J*=5.8 Hz, -NC$\underline{H}_2$-), 2.47 (2H, t, *J*=6.2 Hz, -NC$\underline{H}_2$-), 2.28 (6H, s, -N(C$\underline{H}_3$)$_2$), 1.78 (2H, quin, *J*=6.1 Hz, -$CH_2C\underline{H}_2CH_2$-) ppm; ^{13}C NMR (100 MHz, MeOD) δ 162.5, 159.6, 158.2, 135.4, 127.4, 126.6, 124.9, 123.2, 121.8, 121.5, 120.1, 119.8, 108.5, 104.3, 103.4,

59.2, 45.8, 40.2, 38.6, 37.1, 36.8 and 26.0; *m/z* (ES) 499.2426 ($[M + H]^+$) requires 499.2417.

General Procedure 1

Carboxamide-Artemisinin Coupling Conditions

A solution of **204** (ca. 0.50 mmol) in MeOH (20 mL) was hydrogenated at atmospheric pressure over PtO_2 until complete consumption of the starting material was observed. The catalyst was removed by filtration through celite and the solvent removed *in vacuo*. The residual oil was dissolved in DMF (20 mL) and concentrated to half its original volume under reduced pressure to completely remove MeOH. The remaining solution was then transferred to a flask containing a stirring solution of the pre-activated artemisinin with carboxylic acid linker **199a** (ca. 1.00 mmol). This was allowed to stir overnight and the solvent then removed *in vacuo*. The residue was dissolved in EtOAc and washed with water (3 × 50 mL). The combined aqueous washings were then reduced *in vacuo* and the crude mixture purified by flash column chromatography (5:95 MeOH:CH_2Cl_2) to give the desired conjugate. Further purification by reverse phase HPLC (MeOH:H_2O, 50:50 to 100:0 over 1 hr) was performed.

Artemisinin-Dipyrrole Conjugate with a Phenoxy-Linker 213

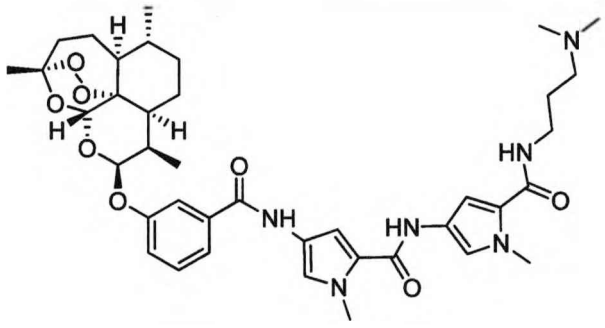

A solution of **204** (0.26 g, 0.69 mmol) in MeOH (20 mL) was hydrogenated and added to a prepared solution of **199a** (0.42 g, 1.03 mmol) as outlined in General Procedure 1. This was allowed to stir overnight and the solvent then removed *in vacuo*. The residue was dissolved in EtOAc and washed with water (3 × 50 mL). The combined aqueous washings were then reduced *in vacuo* and the crude mixture purified by flash column chromatography (5:95 MeOH:CH_2Cl_2) to give **213** (0.10 g, 20%) as an orange crystalline solid.

213: IR ν_{max} 3408 ($\nu_{N\text{-}H,\ Amide}$), 2939 ($\nu_{C\text{-}H}$), 1639 ($\nu_{C=O,\ Amide}$), 921, 835 ($\nu_{O\text{-}O}$), 746 ($\nu_{C=C}$) cm^{-1}; ^1H NMR (400 MHz, MeOD) 7.70-7.20 (5H, m, Ar-H and Py-H5), 7.18 (1H, d, *J*=1.7 Hz, Py-H5), 7.04 (1H, d, *J*=2.0 Hz, Py-H3), 6.89 (1H, d, *J*=1.9 Hz, Py-H3), 5.60 (1H, d, *J*=3.3 Hz, H-10), 5.51 (1H, s, H-12), 3.95 (3H, s, Py-CH_3), 3.89 (3H, s, Py-CH_3), 3.42 (2H, t, *J*=6.5 Hz, -NCH_2-), 3.13 (2H, t, *J*=7.2 Hz, -NCH_2-), 2.86 (6H, s, -$N(CH_3)_2$), 2.85 (1H, m, H-9), 2.37 (1H, td, *J*=14.3, 3.8 Hz, H-4α), 2.08-0.99 (21H, m) (including 1.36 (3H, s, 3-Me), 1.08 (3H, d, *J*=7.3 Hz, 6-Me), 0.99 (3H, d, *J*=6.3 Hz, 9-Me)) ppm; ^{13}C NMR (100 MHz, MeOD) δ167.4, 165.3, 161.8, 159.3, 131.3, 129.9, 125.1, 124.3, 123.8, 123.7, 122.8, 122.6, 121.9, 121.6, 121.5, 121.4, 117.1, 107.1, 90.2, 82.4, 57.0, 50.3, 46.1, 43.9, 39.0, 37.7, 37.4, 37.3, 37.0, 36.2, 32.7, 31.5, 26.8, 26.5, 21.1, 19.7 and 13.7; *m/z* (ES) 733.3915 ($[M + H]^+$)

requires 733.3925.

Methyl 4-(*tert*-butoxycarbonylamino)butanoate[5] 218

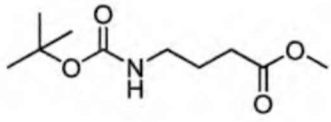

To a stirred solution of methyl 4-aminobutanoate **216** (1.00 g, 6.51 mmol) in MeOH (60 mL), triethylamine (6.3 mL, 45.6 mmol) and subsequently di-*tert*-butyldicarbonate (2.13 g, 9.75 mmol) were added. The reaction was stirred for 1 hour at ambient temperature. MeOH was removed *in vacuo* and the residue purified by column chromatography to give **218** (1.03 g, 73%) as a clear oil.

218: IR ν_{max} 3592, 3356 ($\nu_{N\text{-}H,\ Amide}$), 2976 ($\nu_{C\text{-}H}$), 1730 ($\nu_{C=O,\ Ester}$), 1691 ($\nu_{C=O,\ Amide}$) cm^{-1}; ^1H NMR (400 MHz, $CDCl_3$) 4.96 (1H, brs, NH), 3.68 (3H, s, $-OCH_3$), 3.20 (2H, q, *J*=6.5 Hz, $-HNCH_2-$), 2.38 (2H, t, *J*=7.3 Hz, $-CH_2CO-$), 1.85 (2H, quin, *J*=7.1 Hz, $-CH_2CH_2CH_2-$), 1.44 (9H, s, *t*-Bu) ppm; ^{13}C NMR (100 MHz, $CDCl_3$) δ 174.2, 156.4, 79.6, 52.1, 40.3, 31.7, 28.8 and 25.7; *m/z* (CI) 218.13938 ($[M + H]^+$) requires 218.13923.

4-(*tert*-Butoxycarbonylamino)butanoic acid[6] 220

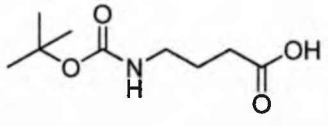

A methanolic solution of NaOH (2 M, 70 mL) was added to a stirring solution of methyl 4-(*tert*-butoxycarbonylamino)butanoate **218** (1.00 g, 4.61 mmol) in CH_2Cl_2/MeOH (9:1 v/v, 20 mL). The solution was stirred until complete consumption of the starting material was observed. The solvents were then removed

in vacuo and the residue diluted with water. The aqueous solution was cooled and acidified to pH 2-3 with HCl (2 M, 10 mL). The acidified mixture was then extracted with diethyl ether (2 × 50 mL) and dried over Na_2SO_4. The ether was removed *in vacuo* to yield **220** (0.88 g, 93%) as a clear oil with no need for further purification.

220: IR ν_{max} 3590, 3347 ($\nu_{N\text{-}H,\ Amide}$), 2978 ($\nu_{C\text{-}H}$), 1691 ($\nu_{C=O}$) cm^{-1}; ^1H NMR (400 MHz, $CDCl_3$) 4.75 (1H, brs, NH), 3.20 (2H, t, *J*=6.2 Hz, -HNCH_2-), 2.41 (2H, t, *J*=7.3 Hz, -CH_2CO-), 1.86 (2H, quin, *J*=7.1 Hz, -$CH_2CH_2CH_2$-), 1.44 (9H, s, *t*-Bu) ppm; ^{13}C NMR (100 MHz, $CDCl_3$) δ 178.7, 156.6, 79.9, 40.2, 31.7, 28.8 and 25.6; *m/z* (CI) 204.12325 ($[M + H]^+$) requires 204.12358.

HBTU Activated 4-(*tert*-Butoxycarbonylamino)butanoic acid 220a

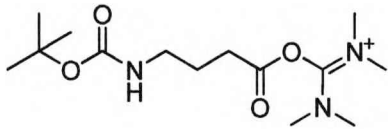

EDIPA (0.45 g, 3.51 mmol) and HBTU (1.00 g, 2.63 mmol) were added sequentially to a stirring solution of **220** (0.36 g, 1.76 mmol) in DMF (10 mL) at 0 °C under nitrogen. This was allowed to stir for up to an hour before addition of the desired amine at 0 °C.

tert-butyl 4-(5-(5-(3-(dimethylamino)propylcarbamoyl)-1-methyl-1H-pyrrol-3-yl carbamoyl)-1-methyl-1H-pyrrol-3-ylamino)-4-oxobutylcarbamate 222

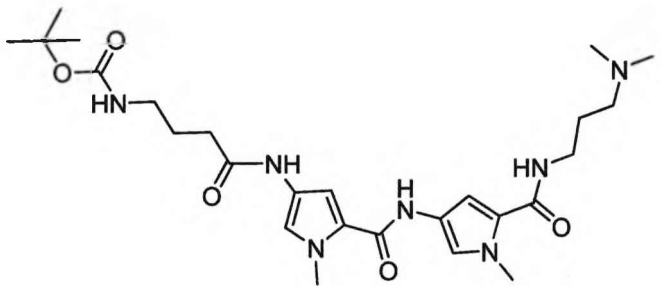

A solution of **204** (0.33 g, 0.88 mmol) in MeOH (20 mL) was hydrogenated and added to a prepared solution of **220a** (0.36 g, 1.76 mmol) as outlined in General Procedure 1. This was allowed to stir overnight and the solvent then removed *in vacuo*. The residue was dissolved in EtOAc and washed with water (3 × 50 mL). The combined aqueous washings were then reduced *in vacuo* and the crude mixture purified by flash column chromatography (20:80 MeOH:CH_2Cl_2 + NH_3 0.25% v/v) to give **222** (0.35 g, 75%) as an orange crystalline solid.

222: IR ν_{max} 3291 ($\nu_{N\text{-}H,\ Amide}$), 2977, 2937 ($\nu_{C\text{-}H}$), 1646 ($\nu_{C=O}$) cm^{-1}; ^1H NMR (400 MHz, MeOD) 7.24 (1H, d, *J*=1.7 Hz, Py-H5), 7.21 (1H, d, *J*=1.4 Hz, Py-H5), 6.91 (1H, d, *J*=1.8 Hz, Py-H3), 6.84 (1H, m, Py-H3), 3.87 (3H, m, Py-C$\underline{H}_3$), 3.84 (3H, m, Py-C$\underline{H}_3$), 3.38 (2H, t, *J*=6.2 Hz, -NC$\underline{H}_2$-), 3.13-3.08 (4H, m, -NC$\underline{H}_2$-), 2.82 (6H, s, -N(C$\underline{H}_3$)$_2$), 2.42 (2H, m, -C$\underline{H}_2$C=O), 1.99 (2H, m, -$CH_2C\underline{H}_2CH_2$-), 1.86 (2H, m, -$CH_2C\underline{H}_2CH_2$-), 1.42 (9H, s, *t*-Bu) ppm; ^{13}C NMR (100 MHz, MeOD) δ 173.1, 165.0, 161.7, 159.0, 129.3, 124.9, 124.5, 123.8, 123.7, 121.3, 117.6, 111.1, 80.5, 57.2, 44.1, 37.4, 35.0, 34.7, 31.6, 29.4 and 26.9; *m/z* (ES) 532.3266 ($[M + H]^+$) requires 532.3247.

Artemisinin-dipyrrole conjugate with a 3C-extended phenoxy linker 224

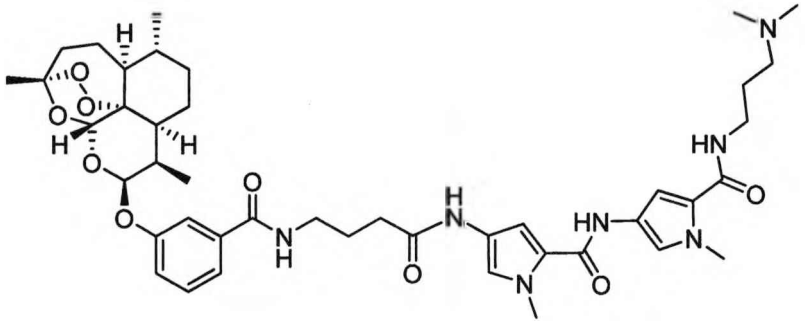

The Boc-protected linker **222** (0.33 g, 0.61 mmol) was stirred in TFA (10 mL) for 2 hours or until complete consumption of the starting material was observed. The TFA was removed *in vacuo* and the residue dissolved in DMF (10 mL) which was then added to a prepared solution of **199a** (0.25 g, 0.61 mmol) as outlined in General Procedure 1. This was allowed to stir overnight and the solvent then removed *in vacuo*. The residue was dissolved in EtOAc and washed with water (3 × 50 mL). The combined aqueous washings were then reduced *in vacuo* and the crude mixture purified by flash column chromatography (10:90 MeOH:CH_2Cl_2) to give **224** (0.20 g, 40%) as an orange crystalline solid.

224: IR ν_{max} 3302 ($\nu_{N\text{-}H,\ Amide}$), 2929 ($\nu_{C\text{-}H}$), 1639 ($\nu_{C=O,\ Amide}$), 867, 815 ($\nu_{O\text{-}O}$), 746 ($\nu_{C=C}$) cm^{-1}; ^1H NMR (400 MHz, MeOD) 7.48-7.17 (4H, m, Ar-H) ,7.09 (1H, d, *J*=1.9 Hz, Py-H5), 7.05 (1H, d, *J*=1.9 Hz, Py-H5), 6.73 (1H, d, *J*=1.8 Hz, Py-H3), 6.72 (1H, d, *J*=1.9 Hz, Py-H3), 5.50 (1H, d, *J*=3.3 Hz, H-10), 5.43 (1H, s, H-12), 3.79 (6H, s, Py-C$\underline{H}_3$), 3.39 (2H, m, -NHC$\underline{H}_2$-), 3.30-3.26 (4H, m, -NHC$\underline{H}_2$-), 2.74 (1H, m, H-9), 2.38-2.25 (3H, m, -NHC$\underline{H}_2$- and H-4α), 2.22 (6H, s, -N(C$\underline{H}_3$)$_2$), 1.99-0.90 (23H, m) (including 1.26 (3H, s, 3-Me) and 0.99 (3H, d, *J*=7.3 Hz, 6-Me), 0.90 (3H, d, *J*= 6.4 Hz, 9-Me)) ppm; ^{13}C NMR (100 MHz, MeOD) δ 173.0, 170.3, 164.6, 161.7, 159.2, 137.5, 131.2, 125.0, 123.7, 123.6, 122.5, 121.4, 121.0, 120.8, 117.1, 113.0, 106.3, 106.0, 90.1, 82.4, 58.7, 54.3, 46.1, 45.8, 41.0, 39.0, 37.8, 37.2, 37.3,

36.2, 36.2, 35.2, 32.7, 28.7, 27.2, 26.5, 26.2, 26.1, 21.2 and 13.7; *m/z* (ES) 818.4485 ($[M + H]^+$) requires 818.4453.

Methyl 6-(*tert*-butoxycarbonylamino)hexanoate 219

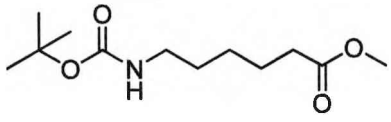

To a stirred solution of methyl 6-aminohexanoate.HCl **217** (2.50 g, 13.76 mmol) in MeOH (150 mL), triethylamine (13.4 mL, 96.32 mmol) and subsequently di-*tert*-butyldicarbonate (4.50 g, 20.64 mmol) were added. The reaction was stirred for 1 hour at ambient temperature. MeOH was removed *in vacuo* and the residue purified by column chromatography to give **219** (2.73 g, 81%) as a clear oil.

219: IR ν_{max} 3369 ($\nu_{N-H,\ Amide}$), 2933 (ν_{C-H}), 1732 ($\nu_{C=O,\ Ester}$), 1693 ($\nu_{C=O,\ Amide}$); ^{1}H NMR (400 MHz, $CDCl_3$) 4.53 (1H, brs, NH), 3.64 (3H, s, -OC$\underline{H}_3$), 3.14 (2H, q, *J*=6.3 Hz, -HNC$\underline{H}_2$-), 2.33 (2H, t, *J*=7.4 Hz, -C$\underline{H}_2$CO-), 1.68 (2H, quin, *J*=7.6 Hz, -HNCH$_2$C$\underline{H}_2$-), 1.53 (2H, q, *J*=7.2, -C$\underline{H}_2$CH$_2$CO-), 1.44 (9H, s, *t*-Bu), 1.38 (2H, m, -(CH$_2$)$_2$C$\underline{H}_2$(CH$_2$)$_2$-) ppm; ^{13}C NMR (100 MHz, $CDCl_3$) δ 174.5, 156.4, 79.5, 51.9, 40.8, 34.3, 30.2, 28.8, 26.7 and 25.0; *m/z* nominal mass (CI) 246 ($[M + H]^+$) requires 246.

6-(*tert*-Butoxycarbonylamino)hexanoic acid 221

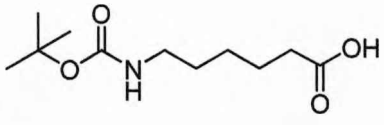

A methanolic solution of NaOH (2 M, 122 mL) was added to a stirring solution of methyl 6-(*tert*-butoxycarbonylamino)hexanoate **219** (2.00 g, 8.16 mmol) in

CH_2Cl_2/MeOH (9:1 v/v, 40 mL). The solution was stirred until complete consumption of the starting material was observed. The solvents were then removed *in vacuo* and the residue diluted with water. The aqueous solution was cooled and acidified to pH 2-3 with HCl (2 M, 10 mL). The acidified mixture was then extracted with diethyl ether (2 × 50 mL) and dried over Na_2SO_4. The ether was removed *in vacuo* to yield **221** (1.26 g, 67%) as a clear oil with no need for further purification.

221: IR ν_{max} 3364 ($\nu_{N\text{-}H,\ Amide}$), 2948, 2872 ($\nu_{C\text{-}H}$), 1687 ($\nu_{C=O}$) cm^{-1}; ^1H NMR (400 MHz, $CDCl_3$) 9.80 (1H, brs, -OH) 4.64 (1H, brs, -NH), 3.13 (2H, m, -$HNCH_2$-), 2.37 (2H, t, *J*=7.4 Hz, -CH_2CO-), 1.69 (2H, quin, *J*=7.4 Hz, -$HNCH_2CH_2$-), 1.54 (2H, quin, *J*=7.3 Hz, -CH_2CH_2CO-), 1.44 (9H, s, *t*-Bu), 1.40 (2H, m, -$(CH_2)_2CH_2(CH_2)_2$-) ppm; ^{13}C NMR (100 MHz, $CDCl_3$) δ 179.5, 156.5, 79.6, 40.7, 34.3, 30.1, 28.8, 26.6 and 24.7; *m/z* (CI) 232.15475 ($[M + H]^+$) requires 232.15488.

HBTU activated 6-(*tert*-butoxycarbonylamino)hexanoic acid 221a

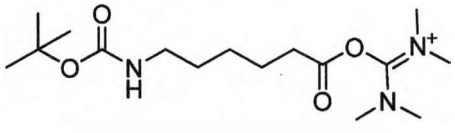

EDIPA (1.03 g, 7.97 mmol) and HBTU (2.25 g, 5.98 mmol) were added sequentially to a stirring solution of **221** (0.92 g, 3.99 mmol) in DMF (10 mL) at 0 °C under nitrogen. This was allowed to stir for up to an hour before addition of the desired amine at 0 °C.

tert-Butyl 6-(5-(5-(3-(dimethylamino)propylcarbamoyl)-1-methyl-1H-pyrrol-3-ylcarbamoyl)-1-methyl-1H-pyrrol-3-ylamino)-6-oxohexylcarbamate 223

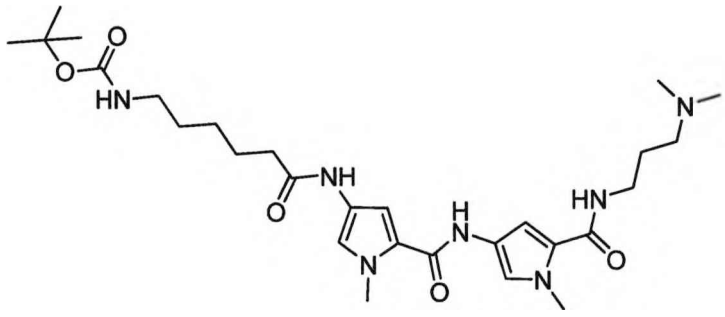

A solution of **204** (0.75 g, 1.99 mmol) in MeOH (20 mL) was hydrogenated and added to a prepared solution of **221a** (0.36 g, 1.76 mmol) as outlined in General Procedure 1. This was allowed to stir overnight and the solvent then removed *in vacuo*. The residue was dissolved in EtOAc and washed with water (3 × 50 mL). The combined aqueous washings were then reduced *in vacuo* and the crude mixture purified by flash column chromatography (20:80 MeOH:CH_2Cl_2 + NH_3 0.25% v/v) to give **223** (0.14 g, 12%) as an orange crystalline solid.

223: ^{1}H NMR (400 MHz, MeOD) 7.21 (1H, m, Py-H5), 7.18 (1H, d, *J*=1.6 Hz, Py-H5), 6.91 (1H, s, Py-H3), 6.87 (1H, s, Py-H3), 3.90 (3H, s, Py-C$\underline{H}_3$), 3.89 (3H, s, Py-C$\underline{H}_3$), 3.43 (2H, t, *J*=6.4 Hz, -OCNHC$\underline{H}_2$-), 3.18 (2H, t, *J*=7.0 Hz, -OCNHC$\underline{H}_2$-), 3.08 (2H, m, -C$\underline{H}_2$N(CH$_3$)$_2$), 2.90 (6H, s, -N(C$\underline{H}_3$)$_2$), 2.40 (2H, quin, *J*=7.4 Hz, -C$\underline{H}_2$CONH-), 2.02 (2H, m, -CH$_2$C$\underline{H}_2$CH$_2$-) 1.76 (2H, m, -NCH$_2$C$\underline{H}_2$(CH$_2$)$_3$-), 1.55-1.36 (4H, m, -OCCH$_2$C$\underline{H}_2$C$\underline{H}_2$(CH$_2$)$_2$-), 1.44 (9H, s, *t*-Bu) ppm; ^{13}C NMR (100 MHz, MeOD) δ 176.3, 165.2, 161.7, 159.0, 129.7, 125.8, 125.7, 123.8, 121.3, 121.2, 119.3, 113.0, 80.5, 57.2, 44.1, 37.4, 35.0, 34.7, 31.6, 29.4 and 26.9; *m/z* (ES) 560.3548 ([M + H]$^+$) requires 560.3560.

Artemisinin-dipyrrole conjugate with a 5C-extended phenoxy linker 225

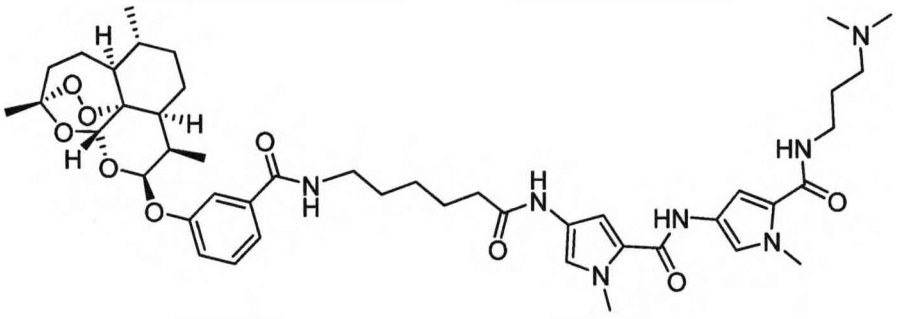

The Boc-protected linker **223** (0.13 g, 0.24 mmol) was stirred in TFA (10 mL) for 2 hours or until complete consumption of the starting material was observed. The TFA was removed *in vacuo* and the residue dissolved in DMF (10 mL) which was then added to a prepared solution of **199a** (0.20 g, 0.48 mmol) as outlined in General Procedure 1. This was allowed to stir overnight and the solvent then removed *in vacuo*. The residue was dissolved in EtOAc and washed with water (3 × 50 mL). The combined aqueous washings were then reduced *in vacuo* and the crude mixture purified by flash column chromatography (10:90 MeOH:CH_2Cl_2) to give **225** (0.02 g, 14%) as an orange crystalline solid.

225: IR ν_{max} 3301 ($\nu_{N\text{-}H,\ Amide}$), 2939 ($\nu_{C\text{-}H}$), 1639 ($\nu_{C=O,\ Amide}$), 867, 809 ($\nu_{O\text{-}O}$), 746 ($\nu_{C=C}$) cm^{-1}; ^1H NMR (400 MHz, MeOD) 7.69-7.25 (4H, m, Ar-H), 7.18 (1H, d, *J*=1.7 Hz, Py-H5), 7.12 (1H, d, *J*=2.0 Hz, Py-H5), 6.90 (1H, d, *J*=1.7 Hz, Py-H3), 6.85 (1H, d, *J*=2.0 Hz, Py-H3), 6.45 (1H, s, H-12), 5.43 (1H, m, H-10), 3.92 (3H, s, Py-CH_3), 3.89 (3H, s, Py-CH_3), 3.42 (2H, m, -NHCH_2-), 3.17 (2H, m, -NHCH_2-), 2.97-2.80 (9H, m) (including 2.89 (6H, s, -$N(CH_3)_2$), 2.86 (1H, m, H-9)), 2.55 (2H, m, -CH_2C(O)NH-), 2.38 (1H, m, H-4α), 2.04-0.99 (27H, m) (including 1.30 (3H, s, 3-Me) and 1.09 (3H, d, *J*=7.2 Hz, 6-Me), 0.99 (3H, d, *J*= 6.0 Hz, 9-Me)) ppm; ^{13}C NMR (100 MHz, MeOD) δ 171.1, 169.1, 165.1, 161.7, 159.3, 137.5, 131.1, 130.0, 128.9, 124.7, 124.4, 123.4, 123.0, 122.0, 121.8, 119.8, 117.5, 113.3, 110.6, 109.3,

103.7, 90.2, 57.3, 53.1, 48.5, 43.9, 41.4, 40.8, 39.3, 38.6, 36.3, 35.8, 35.1, 32.4, 30.6, 29.0, 28.1, 27.2, 26.7, 26.4, 21.2 and 13.3 ppm; *m/z* (ES) 846.4786 ($[M + H]^+$) requires 846.4766.

6.2 Appendix

tert-Butyl 4-(5-(5-(5-(3-(dimethylamino)propylcarbamoyl)-1-methyl-1H-pyrrol-3-ylcarbamoyl)-1-methyl-1H-pyrrol-3-ylcarbamoyl)-1-methyl-1H-pyrrol-3-ylamino)-4-oxobutylcarbamate 227

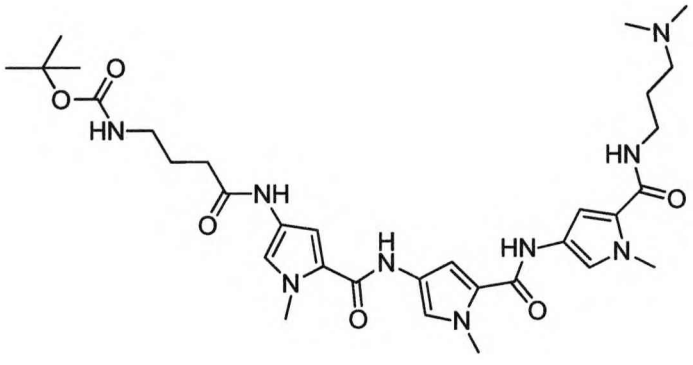

A solution of **205** (0.65 g, 1.30 mmol) in MeOH (20 mL) was hydrogenated and added to a prepared solution of **220a** (0.40 g, 1.95 mmol) as outlined in General Procedure 1. This was allowed to stir overnight and the solvent then removed *in vacuo*. The residue was dissolved in EtOAc and washed with water (3 × 50 mL). The combined aqueous washings were then reduced *in vacuo* and the crude mixture purified by flash column chromatography (20:80 MeOH:CH_2Cl_2 + NH_3 0.25% v/v) to give **227** (0.40 g, 47%) as an orange crystalline solid.

227: ^{1}H NMR (400 MHz, MeOD) 7.24-7.19 (3H, m, Py-H), 6.97-6.87 (3H, m, Py-H), 3.90 (3H, s, Py-C$\underline{H}_3$), 3.89 (3H, s, Py-C$\underline{H}_3$), 3.87 (3H, s, Py-C$\underline{H}_3$), 3.46 (2H, m, -

OCNHC$\underline{H}_2$-), 3.18-3.10 (4H, m, -NHC$\underline{H}_2$-), 2.89 (6H, s, -N(C$\underline{H}_3$)$_2$), 2.42 (2H, quin, *J*=7.6 Hz,-C$\underline{H}_2$CONH-), 2.00 (2H, quin, *J*=6.9 Hz, -CH$_2$C$\underline{H}_2$CH$_2$-) 1.87 (2H, quin, *J*=7.2 Hz, -CH$_2$C$\underline{H}_2$CH$_2$-), 1.43 (9H, s, *t*-Bu) ppm; ^{13}C NMR (100 MHz, MeOD) δ 173.2, 170.6, 165.2, 161.8, 144.7, 129.4 124.9, 124.4, 123.8, 123.7, 121.3, 121.1, 109.2, 107.1, 106.4, 80.5, 57.1, 43.9, 41.3, 38.5, 37.3, 31.4, 29.2, 27.8 and 26.8; *m/z* (ES) 461.2874 ([M + H]$^+$); requires 461.2876.

Artemisinin-Dipyrrole Conjugate with a Carba-Linker 206

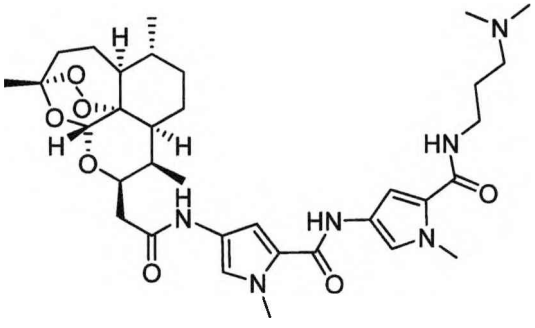

A solution of **204** (0.20 g, 0.53 mmol) in MeOH (20 mL) was hydrogenated and added to a prepared solution of **190a** (0.35 g, 1.06 mmol) as outlined in General Procedure 1. This was allowed to stir overnight and the solvent then removed *in vacuo*. The residue was dissolved in EtOAc and washed with water (3 × 50 mL). The combined aqueous washings were then reduced *in vacuo* and the crude mixture purified by flash column chromatography (5:95 MeOH:CH$_2$Cl$_2$) to give **206** (0.12 g, 33%) as an orange crystalline solid.

206: ^{1}H NMR (400 MHz, CDCl$_3$) 7.43 (1H, s, Py-H5), 7.31 (1H, d, *J*=1.8 Hz, Py-H5), 6.97 (1H, d, *J*=1.8 Hz, Py-H3), 6.64 (1H, s, Py-H3), 6.01 (1H, s, H-12), 3.99 (6H, s, Py-CH$_3$), 2.98 (6H, s, -N(CH$_3$)$_2$), 2.57-2.33 (3H, m, H-9 and -C$\underline{H}_2$C(O)NH-), 2.10-1.25 poorly resolved, 1.31 (3H, s, 3-Me), 0.99 (3H, m, 6-Me), 0.87 (3H, m, 9-

Me) ppm; ^{13}C NMR (100 MHz, $CDCl_3$) δ 172.7, 165.4, 161.8, 130.0, 124.3, 123.5, 107.0, 106.5, 106.4, 105.5, 101.5, 93.3, 90.6, 82.9, 56.8, 54.3, 47.2, 46.3, 37.4, 37.0, 28.6, 19.7 and 12.3; *m/z* (ES) 655.3834 $[M + H]^+$) requires 655.3819.

Artemisinin-dipyrrole Conjugate with a 5C-extended carba-linker 226

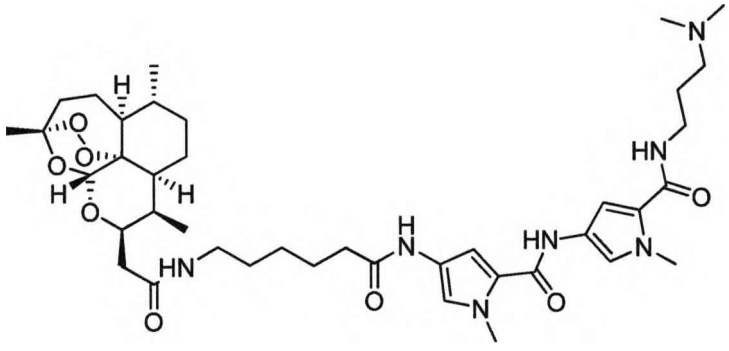

The Boc-protected linker **223** (0.35 g, 0.62 mmol) was stirred in TFA (10 mL) for 2 hours or until complete consumption of the starting material was observed. The TFA was removed *in vacuo* and the residue dissolved in DMF (10 mL) which was then added to a prepared solution of **190a** (0.20 g, 0.61 mmol) as outlined in General Procedure 1. This was allowed to stir overnight and the solvent then removed *in vacuo*. The residue was dissolved in EtOAc and washed with water (3 × 50 mL). The combined aqueous washings were then reduced *in vacuo* and the crude mixture purified by flash column chromatography (10:90 MeOH:CH_2Cl_2) to give **226** as an orange crystalline solid.

226: ^1H NMR (400 MHz, $CDCl_3$) δ 7.18 (1H, d, *J*=1.6 Hz, Py-H5), 7.15 (1H, d, *J*=2.0 Hz, Py-H5), 6.89 (1H, d, *J*=1.6 Hz, Py-H3), 6.86 (1H, d, *J*=1.3 Hz, Py-H3), 6.01 (1H, s, H-12), 3.91 (3H, s, Py-CH_3), 3.90 (3H, s, Py-CH_3), 3.45 (2H, m, -NCH_2-), 3.25 (2H, m, -NCH_2-), 3.07 (2H, m, -NCH_2-), 2.82 (6H, s, -$N(CH_3)_2$), 2.46-2.20

(3H, m, H-9 and -C<u>H</u>$_2$C(O)NH-), 2.10-1.25 poorly resolved, 0.99 (3H, m, 6-Me), 0.87 (3H, m, 9-Me) ppm; ^{13}C NMR (100 MHz, $CDCl_3$) δ 173.7, 163.7, 163.4, 163.0, 128.6, 127.7, 120.1, 118.9, 117.2, 112.1, 98.1, 57.0, 43.9, 40.7, 19.4 and 13.4; *m/z* (ES) 768.4614 ([M + H]$^+$) requires 768.4660.

Artemisinin phenoxy linker with extended 5C-linker *via* modified Curtius rearrangement 232

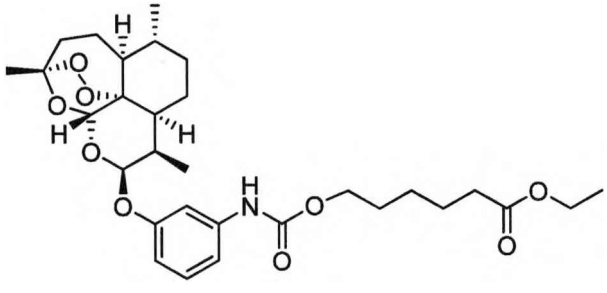

A solution of **190** (0.20 g, 0.49 mmol), ethyl 6-hydroxyhexanoate **231** (0.04 g, 0.25 mmol), DPPA (0.14 mg, 0.49 mmol) and triethylamine (0.05 g, 0.49 mmol) in anhydrous MeCN (10 mL) was stirred at 55 °C for 24 hours. The solvent was then removed *in vacuo* and the residue taken up in EtOAc (50 mL). The solution was washed successively with 5% citric acid, H_2O, $NaHCO_3$ and brine and the combined organic extracts dried over Na_2SO_4. Purification by column chromatography (10:90 MeOH:CH_2Cl_2) afforded **232** (0.08 g, 54%) as a white crystalline solid.

232: IR ν_{max} 3343 ($\nu_{N\text{-}H,\ Amide}$), 2941, 2869 ($\nu_{C\text{-}H}$), 1735 ($\nu_{C=O}$), 873, 826 ($\nu_{O\text{-}O}$) cm^{-1}; ^{1}H NMR (400 MHz, MeOD) δ 7.21 (2H, m, Ar-H), 7.01 (1H, m, Ar-H), 6.86 (1H, m, Ar-H), 5.74 (1H, d, *J*=5.7 Hz, H-10α), 5.49 (1H, s, H-12), 4.16 (2H, t, *J*=6.6 Hz, -HNC(O)OC<u>H</u>$_2$-), 4.15 (2H, q, *J*=7.2 Hz, -C(O)OC<u>H</u>$_2$CH$_3$), 2.83 (1H, m, H-9), 2.42 (1H, td, *J*=14.3, 3.9 Hz, H-4α), 2.34 (2H, t, *J*=7.4 Hz, -C<u>H</u>$_2$C(O)OEt), 2.07-1.84 (5H,

m), 1.79-1.47 (8H, m) (including (4H, m, -$CH_2\underline{CH_2}CH_2\underline{CH_2}CH_2$-)), 1.46-0.97 (15H, m) (including 1.43 (3H, s, 3-Me), 1.31 (2H, m, -Et$\underline{CH_2}$Et-) and 1.27 (3H, t, *J*=7.2 Hz, -C(O)O$CH_2\underline{CH_3}$), 1.02 (3H, d, *J*=7.3 Hz, 6-Me), 0.97 (3H, d, *J*=6.1 Hz, 9-Me)) ppm; ^{13}C NMR (100 MHz, MeOD) δ 174.1, 158.5, 154.0, 139.5, 130.2, 120.4, 112.6, 111.6, 107.9, 104.6, 100.8, 88.7, 65.4, 60.7, 52.9, 44.8, 37.8, 36.7, 35.0, 34.6, 31.4, 29.0, 26.4, 25.8, 25.0, 24.8, 20.7, 14.7 and 13.4; *m/z* (ES) 584.2834 ([M + Na]$^+$) requires 584.2836.

6-Hydroxyhexanoic acid 233

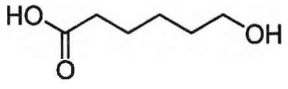

A methanolic solution of NaOH (2 M, 187 mL) was added to a stirring solution of ethyl 6-hydroxyhexanoate **231** (2.00 g, 12.48 mmol) in CH_2Cl_2/MeOH (9:1 v/v, 20 mL). The solution was stirred until complete consumption of the starting material was observed. The solvents were then removed *in vacuo* and the residue diluted with water. The aqueous solution was cooled and acidified to pH 2-3 with HCl (2 M, 10 mL). The acidified mixture was then extracted with diethyl ether (2 × 50 mL) and dried over Na_2SO_4. The ether was removed *in vacuo* to yield **233** (1.57 g, 95%) as a clear oil with no need for further purification.

233: IR ν_{max} 3332 (ν_{O-H}), 2937, 2866 (ν_{C-H}), 1706 ($\nu_{C=O}$) cm^{-1}; ^{1}H NMR (400 MHz, $CDCl_3$) δ 5.00 (1H, br, -O$\underline{H}$), 3.68 (2H, t, *J*=6.5 Hz, -$C\underline{H_2}$OH), 2.39 (2H, t, *J*=7.4 Hz, -C(O)$C\underline{H_2}$-), 1.70 (2H, quin, *J*=7.4 Hz, -$CH_2C\underline{H_2}(C_3H_6)$-), 1.63 (2H, quin, *J*=7.0 Hz, -$CH_2C\underline{H_2}(C_3H_6)$-), 1.46 (2H, m, -$(CH_2)_2C\underline{H_2}(CH_2)_2$-) ppm; ^{13}C NMR (100 MHz, $CDCl_3$) δ 179.3, 62.9, 34.3, 32.5, 25.6 and 24.8 ppm; *m/z* (CI) 150.11334 ([M + NH_4]$^+$); requires 150.11302.

HBTU-activated 6-Hydroxyhexanoic acid 233a

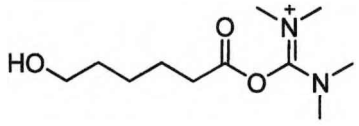

EDIPA (0.26 g, 2.00 mmol) and HBTU (0.57 g, 1.50 mmol) were added sequentially to a stirring solution of **233** (0.13 g, 1.0 mmol) in DMF (10 mL) at 0 °C under nitrogen. This was allowed to stir for up to an hour before addition of the desired amine at 0 °C.

***N*-(3-(Dimethylamino)propyl)-4-(4-(6-hydroxyhexanamido)-1-methyl-1H-pyrrole-2-carboxamido)-1-methyl-1H-pyrrole-2-carboxamide 234**

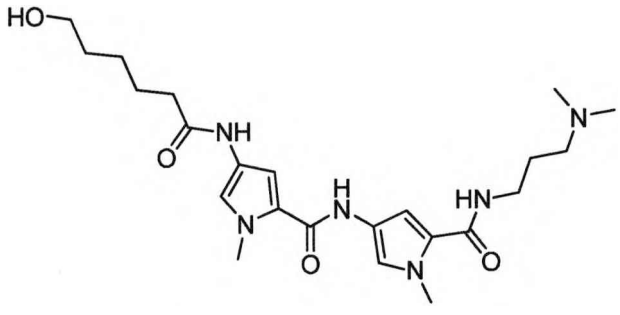

A solution of **204** (0.26 g, 0.68 mmol) in MeOH (20 mL) was hydrogenated and added to a prepared solution of **233a** (0.13 g, 1.00 mmol) as outlined in General Procedure 1. This was allowed to stir overnight and the solvent then removed *in vacuo*. The residue was dissolved in EtOAc and washed with water (3 × 50 mL). The combined aqueous washings were then reduced *in vacuo* and the crude mixture purified by flash column chromatography (20:80 MeOH/CH_2Cl_2) to give **234** (0.14 g, 45%) as an orange crystalline solid.

234: IR ν_{max} 3128 (ν_{O-H}), 2935 (ν_{C-H}), 1639 ($\nu_{C=O}$) cm^{-1}; ^1H NMR (400 MHz, $CDCl_3$) δ 7.20 (1H, d, *J*=1.8 Hz, Py-H), 7.18 (1H, d, *J*=1.8 Hz, Py-H), 6.89 (1H, d, *J*=1.8,

Py-H), 6.88 (1H, d, *J*=1.8 Hz, Py-H), 3.92 (3H, s, Py-C$\underline{H}_3$), 3.86 (3H, s, Py-C$\underline{H}_3$), 3.59 (2H, t, *J*=6.6 Hz, -C$\underline{H}_2$OH), 3.39 (2H, t, *J*=6.5 Hz, -NC$\underline{H}_2$-), 3.08 (2H, t, *J*=7.2 Hz, -NC$\underline{H}_2$-), 2.81 (6H, s, -N(CH_3)$_2$), 2.35 (2H, t, *J*=7.7 Hz, -C(O)C$\underline{H}_2$-), 1.98 (2H, m, -NCH$_2$C$\underline{H}_2$-), 1.73 (2H, quin, *J*=7.2 Hz, -CH$_2$C$\underline{H}_2$(C_3H_6)-), 1.60 (2H, quin, *J*=7.1 Hz, -CH$_2$C$\underline{H}_2$(C_3H_6)-), 1.45 (2H, m, -(CH_2)$_2$C$\underline{H}_2$(CH_2)$_2$-) ppm; ^{13}C NMR (100 MHz, $CDCl_3$) δ 173.7, 165.1, 161.8, 125.0, 124.5, 123.8, 123.7, 121.3, 121.1, 107.0, 106.4, 63.2, 57.2, 44.1, 37.7, 37.4, 37.3, 33.8, 27.3 and 27.1.

6.2 Biological Testing

Melting curves were measured using a Hewlett Packard HP8452a spectrophotometer coupled to a Peltier thermostat. The measurements were performed in buffer, pH 7 (10 mM NaH_2PO_4, 100 mM NaCl), with a drug–DNA ratio of 1:1. The DNA-dodecamer used, d(CGCGAATTCGCG), was kindly provided by Dr J. Gaynor and Dr R. Cosstick of the Department of Chemistry, University of Liverpool. Solutions of conjugates **213**, **224** and **225** were made up in RNAase free H_2O with approximately 1% v/v DMSO.

The temperature inside the cuvette was increased over the range 19–90 °C with a heating rate of 1.0 °C min^{-1} for 19-25 °C, 0.5 °C min^{-1} for 25-80 °C and returning to 1.0 °C min^{-1} for 80-90 °C. The absorption data were registered and plotted against the temperature. The melting curve was analysed using Microsoft Excel for data analysis and technical graphics.

6.3 References

(1) Hindley, S., Ward, S. A., Storr, R. C., Searle, N. L.., Bray, P. G., Park, B. K., Davies, J., O'Neill, P. M., J. Med. Chem. **2002**, 45, 1052-1063.

(2) Chadwick, J., Mercer, A. E., Park, B. K., Cosstick, R., O'Neill, P. M., Bioorg. Med. Chem. **2009**, 17, 1325-1338.

(3) Chadwick, J. Ph.D. Thesis, University of Liverpool, 2006.

(4) Nishiwaki, E., Tanaka, S., Lee, H., Shibuya, M., Heterocycles **1988**, 27, 1945-1952.

(5) Barbayianni, E., Fotakopoulou, I., Schmidt, M., Constantinou-Kokotou, V., Bornscheuer, U. T., Kokotos, G., The Journal of Organic Chemistry **2005**, 70, 8730-8733.

(6) Theodorou, V., Skobridis, K., Tzakos, A. G., Ragoussis, V., Tetrahedron Letters **2007**, 48, 8230-8233.